

## RESPONSE OF MAMMALIAN CELLS TO OXIDATIVE DNA DAMAGE

AN EXAMINATION OF THE RESPONSE OF MAMMALIAN CELLS TO  
OXIDATIVE DNA DAMAGE IN RELATION TO AGEING AND  
NEURODEGENERATION USING RECOMBINANT ADENOVIRUS VECTORS

By DERRIK M. LEACH B.Sc (Hon)

A Thesis Submitted to the School of Graduate Studies in Partial Fulfilment of the  
Requirements for the Degree Doctor of Philosophy

McMaster University © Copyright by Derrik M. Leach, March. 2012

McMaster University DOCTOR OF PHILOSOPHY (2012) Hamilton, Ontario (Science)

TITLE: An examination of the response of mammalian cells to oxidative DNA damage in relation to ageing and neurodegeneration using recombinant adenovirus vectors

PAGES: xvii, 251

## Abstract

Ageing is associated with a progressive decline in cognitive and physical function, as well as neurodegeneration. The DNA damage theory of ageing postulates that phenotypes associated with chronological ageing result from a time dependent accumulation of DNA damage caused by endogenously generated reactive oxygen species (ROS). In this work, we have used a host cell reactivation (HCR) technique to examine base excision repair (BER), the major pathway for removal of ROS generated damage, in fibroblasts from normal individuals and from patients with Cockayne syndrome (CS). The HCR assay utilizes an adenovirus encoded  $\beta$ -galactosidase ( $\beta$ -gal) reporter gene treated with methylene blue plus visible light (MB+VL) to measure BER of 7,8-dihydro-8-oxoguanine (8-oxoG). The results presented here demonstrate that host cell repair mechanisms remove MB+VL generated 8-oxoG from viral DNA and that reactivation of gene expression correlates with cellular repair capacity and requires CSA and CSB. Using the HCR assay, we demonstrate that culturing of primary human fibroblasts in media containing low levels of MB increases BER, suggesting increased DNA repair capacity may play a role in the therapeutic application of MB in Alzheimer's disease treatment. We also demonstrate that BER decreases *in vitro* with increasing number of cell divisions, and that HCR of the damaged reporter gene is lower in fibroblasts from older donors. Using a second  $\beta$ -gal reporter gene assay, the enhanced expression assay, we were unable to show a relationship between the degree of decreased BER in CS and severity of clinical phenotype. However, we identified an interaction between CSB and the telomere protein TRF2. Overexpression of TRF2 leads to decreased nucleotide excision repair of UVC induced damage in a CSB dependent manner. We also

demonstrate defective telomeres in the absence of functional CSB. The data presented in this work provide additional support for the DNA damage theory of ageing.

It is not how long it takes to get to the end; it is what happens in between that is the bases for  
everything

## **Acknowledgments**

I would like to thank my supervisor Dr. Andrew J. Rainbow for providing me the opportunity to do graduate work and for his continued support and direction throughout the duration of my graduate experience. I would also like to thank the other members of my supervisory and defence committee Dr. Andre Bedard, Dr. Suleiman A. Igdoura and Dr. Rebecca Laposa.

I would like to thank all the members of the Rainbow Lab that I had a chance to get to know and work with over the years including Diana Dregoesc, Rob Cowan, Adrian Rybak, Shaqil Kassam, Shari Yasin and Prachi Sharma. I would especially like to thank ‘The’ Natalie Zacal for all of her help and friendship, without which I may not have survived. Café 411 will be missed.

I would also like to thank all of my friends who have always been there and have always been able to make me smile. From LSB/The Phoenix I would like to thank Megan McKerlie, Taylor Mitchell, Lulu Vazquez-Paz, Alicia Pepper, Dejan Kristan, Simon Livermore, Phil Cumbo, Aidan Dineen, Kaja Jeyanthan and Bart Maslikowski for all the great times; I will never forget them. To Nixon’s Hitmen, thank you for the good company and my first Hockey Championship. I would also like to thank Fargol Firouzhian for her constant support and friendship through everything.

Finally, I would like to thank my family, my brother Damian (Stephanie), my sister Kimi (Kevin), and my adorable nephew and niece Benjamin and Jillian. I would especially like to thank my parents Darryl and Irene for always putting up with me and supporting me in everything I have decided to do. Without them there is no way I would have been able achieve any of my goals.

## Table of Contents

<b>Abstract</b>	<b>iii</b>
<b>Acknowledgments</b>	<b>vi</b>
<b>Table of Contents</b>	<b>vii</b>
<b>List of Figures</b>	<b>xi</b>
<b>List of Tables</b>	<b>xiv</b>
<b>Preface</b>	<b>xv</b>
<b>Abbreviations</b>	<b>xvi</b>
<b>Chapter 1: Literature review</b>	<b>1</b>
Ageing	2
The DNA damage theory of Ageing	4
Oxidative DNA damage: 8-oxoguanine	7
Base excision repair (BER)	11
BER of 8-oxoguanine	14
Base excision repair, ageing and neurodegeneration	16
Cockayne syndrome (CS)	17
Use of recombinant adenovirus vectors to study DNA repair	21
Project summary	37
<b>Chapter 2: Early host cell reactivation of an oxidatively damaged adenovirus-encoded reporter gene requires Cockayne syndrome proteins CSA and CSB. Published as: Derrick M. Leach and Andrew J. Rainbow, Mutagenesis 26(2): 315-321, 2011, (reproduced with permission)</b>	<b>39</b>
Preface	40
Abstract	41
Introduction	41
Materials and Methods	42
<i>Cells, virus and culture conditions</i>	42
<i>Treatment of the virus with MB+VL</i>	42
<i>Treatment of the virus with UVC</i>	42
<i><math>\beta</math>-Galactosidase reporter gene expression assay (HCR)</i>	42
<i>graphing and statistical analysis</i>	42
Results	42
<i>Normal HCR of the MB+VL damaged reporter gene in SV40-transformed human skin fibroblasts requires CSA and CSB</i>	42
<i>Reactivation of expression from a MB+VL –damaged <math>\beta</math>-gal reporter gene in rodent cells</i>	43
Discussion	43

Funding	46
Acknowledgements	46
References	46
<b>Chapter 3: Host Cell repair of UVC and methylene blue plus visible light induced DNA damage in an adenovirus encoded reporter gene correlates with reactivation of gene expression.</b>	<b>48</b>
Preface	49
Abstract	50
Introduction	52
Materials and methods	54
<i>Cells, virus and culture conditions</i>	54
<i>Treatment of the virus with UVC</i>	55
<i>Treatment of the virus with MB+VL</i>	55
<i>Selective (Hirt) extraction of Adenovirus DNA from infected cells</i>	56
<i>Restriction digestion and Endonuclease treatment of selectively extracted adenovirus DNA</i>	57
<i>Separation of adenovirus DNA by alkaline gel electrophoresis and detection by southern blotting</i>	57
<i>Preparation of a radiolabeled probe for detection of the adenovirus encoded LacZ gene</i>	58
<i>Graphing and statistical analysis</i>	60
Results	61
<i>Loss of T4 pyrimidine-DNA glycosylase sensitive sites over time in human and Chinese hamster ovary cells</i>	61
<i>Host cell reactivation of UVC-irradiated AdCA35 in GM637F and CHO-AA8 cells</i>	62
<i>Loss of formamidopyrimidine (Fapy)-DNA glycosylase sensitive sites over time in human and Chinese hamster ovary cells</i>	66
<i>Host cell reactivation of the MB+VL treated adenovirus encoded <math>\beta</math>-gal gene in human and Chinese hamster ovary cells</i>	67
<i>Calculation of the surviving fraction of the 3kb lacZ fragment from southern blot experiments.</i>	71
Discussion	74
Acknowledgements	79
<b>Chapter 4: Increased host cell reactivation of an oxidatively damaged reporter gene in human primary lung fibroblasts cultured in media containing a low concentration of methylene blue.</b>	<b>80</b>
Preface	81
Abstract	82
Introduction	84
Materials and Methods	87
<i>Cells, virus and culture conditions</i>	87
<i>Host cell reactivation assay</i>	87
<i>Treatment of the virus with methylene blue plus visible light (MB+VL)</i>	88
<i>2.4 HCR of MB+VL-treated AdCA35</i>	88
<i>Graphing and Statistical Analysis</i>	89

<i>Immunoblotting</i>	90
Results	90
<i>Increased host cell reactivation of MB+VL damaged AdCA35 in IMR90 human normal primary lung fibroblasts cultured in 100 nM methylene blue.</i>	90
<i>Host cell reactivation of MB+VL damaged AdCA35 in human normal primary skin fibroblasts cultured in 100 nM methylene blue.</i>	91
<i>Western blot analysis of proteins involved in base excision repair of oxidative DNA damage in IMR90 fibroblasts cultured in 100nM methylene blue</i>	92
<i>Effects of growth in 100nM MB on expression of the undamaged reporter gene.</i>	92
4. Discussion	101
<b>Chapter 5: Oxidative DNA damage leads to greater expression of an undamaged reporter gene driven by the cytomegalovirus immediate early promoter in Cockayne syndrome fibroblasts.</b>	<b>105</b>
Preface	106
Abstract	107
Introduction	109
Materials and Methods	113
<i>Cell Lines and Viruses.</i>	113
<i>The enhanced expression assay</i>	114
<i>Immunoblotting</i>	115
<i>Graphing and Statistical Analysis</i>	116
Results	116
<i>Enhanced expression of the CMV driven <math>\beta</math>-galactosidase reporter gene in primary human fibroblasts following cellular pre-treatment with methylene blue plus visible light. .</i>	116
<i>Enhanced expression of the AdCA35 reporter in primary human fibroblasts from patients with Cockayne syndrome following cellular pre-treatment with UVC</i>	118
<i>Western blot analysis of CSB expression in human primary skin fibroblasts from normal and Cockayne syndrome individuals.</i>	119
Discussion	124
Acknowledgements	129
<b>Chapter 6: TRF2 interacts with the Cockayne syndrome group B protein and over expression of TRF2 reduces repair of UV damaged DNA</b>	<b>130</b>
Preface	131
Abstract	133
Introduction	134
Materials and Methods	137
<i>Cell lines</i>	137
<i>Host Cell Reactivation (HCR)</i>	137
<i>Immunoblotting and immunoprecipitation</i>	138
<i>Metaphase chromosome spreads and FISH</i>	139
Results	140
<i>Overexpression of the shelterin component TRF2 reduces HCR of the UVC treated reporter gene in primary fibroblasts</i>	140
<i>Overexpression of TRF2 has no effect on HCR of the MB+VL treated reporter gene</i>	142

<i>CSB is required for the TRF2 mediated decrease in HCR</i>	144
<i>The transcription coupled repair factor CSB interacts with TRF2</i>	146
<i>FISH analysis of metaphase cells lacking functional CSB suggests increased telomere instability</i>	148
Discussion	151
<b>Chapter 7: Discussion</b>	<b>157</b>
8-oxoG, transcription and repair	158
MB increased BER capacity and Alzheimer's disease	162
Oxidative DNA damage in telomeres	164
Oxidative DNA damage and ageing	169
<b>Appendix I: Host cell reactivation of the MB+VL treater reporter gene in primary fibroblasts from patients with Alzheimer's disease.</b>	<b>171</b>
<b>Appendix II: Further examination of enhanced expression from the undamaged adenovirus based reporter construct in primary fibroblasts following cellular MB+VL treatment</b>	<b>179</b>
<b>Appendix III: Examination of CSB deficient fibroblasts for complementation of UVC sensitivity after expression of wild type CSB</b>	<b>190</b>
<b>Appendix IV: Examination of the response of primary fibroblasts from patients with Cockayne syndrome to oxidative damage and metal exposure</b>	<b>197</b>
<b>Appendix V: Examination of the response of fibroblasts from patients with Ataxia telangiectasia to oxidative damage and metal exposure</b>	<b>219</b>
<b>References</b>	<b>230</b>

## List of Figures

<b>Figure 1:</b> Types of DNA damage, DNA repair mechanisms and the consequences of DNA damage.	6
<b>Figure 2:</b> Mechanisms of redox homeostasis.	9
<b>Figure 3:</b> Structure of 7,8-dihydro-8-oxoguanine	10
<b>Figure 4:</b> The BER pathways	13
<b>Figure 5:</b> The GO pathway.	15
<b>Figure 6:</b> Structure of the adenovirus virion.	23
<b>Figure 7:</b> Schematic representation of the human adenovirus 5 genome	25
<b>Figure 8:</b> Schematic representation of the adenoviral constructs used in this work	26
<b>Figure 9:</b> Schematic representation of the HCR assay employed in this work	32
<b>Figure 10:</b> Structure and reactions of methylene blue.	36
<b>Figure 2-1:</b> Reduced HCR of the MB+VL-treated reporter in SV40-transformed CSA and CSB fibroblasts compared to the SV40-transformed normal fibroblast GM637F	43
<b>Figure 2-2:</b> Time course of gene reactivation for MB+VL or UVC-damaged AdCA35 in SV40-transformed normal and CS fibroblasts	44
<b>Figure 2-3:</b> Time course of gene reactivation for MB+VL-damaged AdCA35 in WT MEFs	45
<b>Figure 2-4:</b> Time course of gene reactivation for MB+VL -damaged AdCA35 in repair-proficient and repair-deficient CHO cells	45
<b>Figure 3-1:</b> Repair of UVC induced CPDs from the Ad encoded lacZ gene in human and rodent cells measured by loss of T4pdg sensitive sites.	64
<b>Figure 3-2:</b> Host cell reactivation of UVC treated AdCA35 in human and rodent cells	65
<b>Figure 3-3:</b> Repair of MB+VL induced 8-oxoG from the Ad encoded lacZ gene in human and rodent cells measured by loss of Fpg sensitive sites.	69
<b>Figure 3-4:</b> Host cell reactivation of MB+VL treated AdCA35 in human and rodent cells.	70

<b>Figure 4-1:</b> Increased host cell reactivation of MB+VL treated AdCA35 in IMR90 fibroblasts cultured in 100nM methylene blue.	94
<b>Figure 4-2:</b> Absolute D <sub>37</sub> values for reporter gene reactivation in normal lung and skin fibroblasts over time.	95
<b>Figure 4-3:</b> Host cell reactivation of MB+VL treated AdCA35 in GM8400 and GM9503 primary skin fibroblasts cultured in 100nM methylene blue.	96
<b>Figure 4-4:</b> Western blot analysis of proteins associated with repair of oxidative DNA damage in IMR90 fibroblasts.	97
<b>Figure 4-5:</b> Proposed mechanism for the development and progression of Alzheimer's disease and the potential targets of MB.	98
<b>Figure 5-1:</b> Expression of the undamaged reporter gene in normal and CS primary fibroblasts pre-treated with MB+VL.	120
<b>Figure 5-2:</b> Expression of the undamaged reporter gene in normal primary fibroblasts pre-treated with increasing concentrations of MB plus 10 min VL (protocol A).	121
<b>Figure 5-3:</b> Enhanced expression of the undamaged AdCA35 reporter following cellular pretreatment with UVC.	122
<b>Figure 5-4:</b> Western Blot analysis of CSB expression in normal, CSA and CSB primary fibroblasts.	123
<b>Figure 6-1:</b> HCR of the UVC treated reporter gene in primary human fibroblasts overexpressing shelterin proteins.	141
<b>Figure 6-2:</b> Normal HCR of the MB+VL treated reporter gene in IMR90 fibroblasts overexpressing TRF2.	143
<b>Figure 6-3:</b> The TRF2 mediated decrease in HCR requires CSB.	145
<b>Figure 6-4:</b> CSB interacts with TRF2 <i>in vivo</i> .	147
<b>Figure 6-5:</b> Analysis of metaphase chromosomes from CSB deficient CS7SE fibroblasts.	149
<b>Figure 6-6:</b> Analysis of metaphase chromosomes from CSA deficient CS3BE fibroblasts.	150
<b>Figure AII-1:</b> Enhanced expression of the undamaged β-gal reporter in normal primary fibroblasts.	184

<b>Figure AII-2:</b> Time course for $\beta$ -gal expression in normal and CS primary fibroblasts pre-treated with MB+VL.	185
<b>Figure AII-3:</b> Enhanced expression of the undamaged reporter in normal and CS primary fibroblasts following pre-treatment with MB+VL.	186
<b>FigureAII-4:</b> Enhanced expression of the undamaged reporter in CSA and CSB primary fibroblasts pre-treated with MB+VL.	187
<b>Figure AIII-1:</b> Coimmunoprecipitation (coIP) of CSB and TRF2.	194
<b>Figure AIII-2:</b> Expression of wild type CSB rescues the UV-repair defect in CSB deficient fibroblasts.	195
<b>Figure AIII-3:</b> Complementation of the SV40 transformed GM16095 fibroblasts with WT and mutant CSB.	196
<b>Figure AIV-1:</b> Normal and CS primary skin fibroblasts were infected with MB+VL treated AdCA35 (MOI 100) and $\beta$ -gal was scored at 3, 12, 24 and 44 hours after infection.	203
<b>Figure AIV-2:</b> Normal and CS primary skin fibroblasts were infected with MB+VL treated AdCA17 (MOI 160) and $\beta$ -gal was scored 12hrs after infection.	205
<b>Figure AIV-3:</b> HCR of the MB+VL treated $\beta$ -gal reporter in CSA primary fibroblasts compared to the normal primary fibroblast GM9503.	206
<b>Figure AIV-4:</b> HCR of the MB+VL treated $\beta$ -gal reporter in CSB primary fibroblasts compared to the normal primary fibroblast GM9503.	207
<b>Figure AIV-5:</b> The effect of $Al_2(SO_3)_4$ (left), $CdCl_2$ (middle) and $Pb(CH_3COO)_4$ (left) on metabolic activity/cell viability in normal and CS deficient fibroblasts.	211
<b>Figure AIV-6:</b> The effect of aluminum, cadmium and lead on HCR of the MB+VL treated AdCA35 reporter gene	213
<b>Figure AV-1:</b> The effect of $Al_2(SO_3)_4$ (left), $CdCl_2$ (middle) and $Pb(CH_3COO)_4$ (left) on metabolic activity/cell viability in normal AT and fibroblasts.	223
<b>Figure AV-2:</b> The effect of aluminum, cadmium and lead on HCR of the MB+VL treated AdCA35 reporter gene.	225

## List of Tables

<b>Table 1:</b> Comparison of $D_0$ and $D_{37}$ values from southern blot and HCR experiments.	73
<b>Table 4-1:</b> Expression of the untreated reporter gene in cells grown in the presence of 100nM MB relative to control cells.	100
<b>Table AI-1:</b> Age, race and sex of control cell lines isolated from apparently healthy individuals and from individuals affected with familial Alzheimer's disease Type III.	174
<b>Table AI-2:</b> HCR capacity of AD primary skin fibroblasts measured by $D_{37}$ relative to normal control primary fibroblasts.	175
<b>Table AI-3:</b> HCR capacity of AD primary skin fibroblasts measured by $D_{37}$ relative to normal control primary fibroblasts.	176
<b>Table AII-1:</b> Summary of mutations, clinical symptoms and cellular characteristics of normal, CSA and CSB primary fibroblasts.	188
<b>Table AIV-1:</b> The effect of 4mM $Al_2(SO_3)_4$ on HCR of the MB+VL treated reporter in normal and CS primary fibroblast strains.	214
<b>Table AIV-2:</b> The effect of 4mM Aluminum sulfate on HCR of the MB+VL treated reporter gene in normal and CS primary fibroblasts.	215
<b>Table AV-1:</b> The effect of 4mM $Al_2(SO_3)_4$ on HCR of the MB+VL treated reporter in normal and AT primary fibroblast strains.	226

## **Preface**

This thesis is presented as a collection of Chapters in the form of journal articles or manuscripts for submission to peer reviewed journals for publication. Chapter 2 has already been published (*Mutagenesis* (2011) 26(2) 315-321). Chapters 3, 4 and 5 on which I will be listed as first author are prepared for submission. Chapter 6 forms the basis for the beginning of a collaborative project which is to be prepared as a manuscript and submitted with me as a co-author. The appendices present: preliminary work done by myself and T.R.H. Mitchell (Dr. X.D. Zhu's Lab, Department of Biology, McMaster University, Hamilton, Ontario, Canada) leading to the discovery of an interaction between CSB and TRF2 and telomere dysfunction in Cockayne syndrome. Expression of different viral constructs in cells pretreated with a DNA damaging agent and data for the survival and reactivation of gene expression in primary fibroblasts from patients with Cockayne syndrome, Alzheimer's disease and Ataxia telangiectasia are presented in appendices.

The presentation of this thesis as a collection of manuscripts has resulted in some overlap in the discussion of certain topics. In an attempt to avoid repetition, the reader will be referred to various Chapters of the thesis for additional information or discussion on a certain topic. Each chapter contains its' own materials and methods section. I have written all Chapters presented in this thesis.

## Abbreviations

<sup>1</sup> MB	singlet state methylene blue
<sup>3</sup> MB	triplet state methylene blue
<sup>1</sup> O <sub>2</sub>	singlet oxygen
6-4pp	6-4 photoproduct
Aβ	amyloid beta
AD	Alzheimer's disease
Ad	adenovirus
Al	aluminum
ATM	ataxia telangiectasia mutated
BER	base excision repair
BSA	bovine serum albumin
C	cytosine
Cd	cadmium
CPD	cyclobutane pyrimidine dimer
CMV	cytomegalovirus
CS	Cockayne syndrome
CSA	Cockayne syndrome group A
CSB	Cockayne syndrome group B
coIP	coimmunoprecipitation
dsDNA	double strand DNA
ESS	endonuclease sensitive site
ETC	electron transport chain
FEN-1	flap endonuclease-1
FISH	fluorescence <i>in situ</i> hybridization
Fpg	formamidopyrimidine [fapy]-DNA glycosylase
G	guanine
GGR	global genome repair
GSH	glutathione
HCR	host cell reactivation
HCMV	human cytomegalovirus
HGPS	Hutchinson-Gilford's progeria
HNE	HeLa nuclear extract
HPV	human papillomavirus
IE	immediate early
IP	immunoprecipitation
ITR	inverted terminal repeat
LigIII	[DNA] ligase IIIα
LP	long patch
LT	large T
MB	methylene blue

MB+VL	methylene blue plus visible light
MCI	mild cognitive impairment
MCMV	murine cytomegalovirus
mtDNA	mitochondrial DNA
MEF	mouse embryonic fibroblast
NLS	nuclear localization signal
O <sup>•</sup> <sub>2</sub>	superoxide radical
Pb	lead
PAGE	polyacrylamide gel electrophoresis
polβ	[DNA] polymerase β
RNA polIII	RNA polymerase II
ROS	reactive oxygen species
SDS	sodium dodecyl sulfate
SOD	superoxide dismutase
SP	short patch
ssDNA	single strand DNA
SV40	simian virus 40
T4pdg	T4 pyrimidine dimer glycosylase
T	thymine
TCR	transcription coupled repair
TP	terminal protein
TRF2	telomere repeat binding factor 2
UV	ultraviolet
VL	visible light
WCE	whole cell extract
WT	wild type
XP	xeroderma pigmentosum

**Chapter 1:**  
**Literature review**

## **Ageing**

Ageing is a progressive process in which there is an overall decline in the functional capacity of an organism leading to an increased risk of injury from the surrounding environment, the development of disease, and increased mortality (Kirkwood and Austad 2000). Additionally, increasing age is accompanied by a decrease in Darwinian fitness. Darwinian fitness also decreases with age as the reproductive capacity of an individual is reduced as a result of declining physical capacity and reduced fertility. While some animals such as Hydra and certain turtles and fish do not display any detectable ageing (Finch 2009), it is a nearly universal process. In species that do age, it is a multidimensional process that affects different organ systems and tissues to different extents over time within an individual. Furthermore, the effects of ageing are not uniform among individuals of a specific population or species as a whole, likely because of genetic differences and environmental factors. The greatest risk factor for a large number of diseases/disorders, including most forms of cancer, is increasing age. For this reason, understanding the underlying mechanisms of the ageing process are of great importance. Although we have made tremendous gains, the process of ageing remains poorly understood and is still a topic of vigorous debate.

The use of model organisms such yeast, nematodes, fruit flies, rats and mice have proven to be powerful tools in ageing research. For instance, it was first recognized in rats that decreasing dietary food intake (caloric restriction(CR)/dietary restriction (DR)) increases longevity (Osborne et al. 1917) and subsequent studies in yeast, nematodes, flies, spiders and mammals have demonstrated increases in lifespan as great as 50% (Klass 1977; Weindruch and Walford 1988; Austad 1989; Chippindale et al. 1993; Chapman and Partridge 1996; Lin et al. 2000; Masoro 2005; Tatar 2007). To date, CR/DR is the only known method for extending the

lifespan of a number of species. Understanding the mechanism(s) leading to increased longevity by CR/DR may provide targets for treating or slowing age related conditions/disorders including neurodegeneration and cancer.

It is difficult to study human ageing directly for a number of reasons including the ethics of using human subjects experimentally and our long generation time which makes less invasive/more ethical and observational studies difficult to perform and hard to interpret. While the data regarding ageing gained from the study of model organisms is invaluable in the quest for understanding the process, the fact remains that these systems are not human. A wealth of information regarding human ageing has come from the study of rare human premature aging/progeroid syndromes including Hutchinson-Gilford progeria (HGPS), Werner syndrome (WS), Bloom syndrome (BS), ataxia-telangiectasia (AT), Rothmund-Thomson syndrome (RTS), trichothiodystrophy (TTD), xeroderma pigmentosum (XP) and Cockayne syndrome (CS) (Pesce and Rothe 1996; Martin and Oshima 2000; Capell et al. 2009). The study of the molecular mechanisms underlying these disorders has provided a better understanding of the processes of DNA metabolism such as transcription, replication and repair. In fact, most of these disorders are caused by mutations in genes involved in DNA repair (Martin and Oshima 2000; Hasty et al. 2003; Arking 2006). The relationship between defective DNA repair in these syndromes with phenotypes of premature/accelerated ageing provides strong support that genome integrity plays a vital role in the ageing process.

## **The DNA damage theory of Ageing**

Unlike other biological molecules found in the cell, DNA relies entirely on the maintenance and repair of an existing molecule with no precursor to maintain its fidelity. In 1958 it was suggested that ageing may result from mutations in DNA (Failla 1958), two years after the free radical theory of aging was proposed by Denham Harman postulating that endogenously generated radical species resulting in accumulation of cellular damage was the basis of ageing (Harman 1956). The DNA damage theory of ageing hypothesizes that the age associated decline in the functional capacity of an organism is caused by the accumulation of DNA damage causing cellular dysfunction that is eventually manifested at the tissue/organ level (Szilard 1959; Arking 2006). An association between the accumulation of DNA damage in cells and organs with a gradual decline in the function of tissues and overall aging of an organism has indeed been recognized (Kirkwood 2005). For more discussion on the accumulation of DNA damage in cells and organs see Chapters 4 and 5.

DNA damage has been implicated as a major causative factor in the processes of mutagenesis, carcinogenesis and ageing. Damage to DNA, the cell's most important macromolecule, can occur by spontaneous hydrolysis or through interaction with endogenous and exogenous/environmental agents. One of the most important and greatest sources of DNA damage in terms of relative abundance is reactive oxygen species (ROS) generated by the metabolic processes of the cell. Environmental elements such as x-rays, ultraviolet (UV) radiation and countless chemical agents can also alter the chemical and physical structure of DNA (see Figure 1). ROS themselves can cause single strand DNA (ssDNA breaks) and over 70 different oxidative base lesions (Hoeijmakers 2001). Furthermore, it has been estimated that greater than  $1 \times 10^5$  oxidative lesions occur in the genomic DNA of a cell per day (Fraga et al.

1990). Depending on the type of DNA damage and the effect it has on processes such as transcription and DNA replication, lesions are classified as cytotoxic or mutagenic. Lesions such as ssDNA and double strand DNA (dsDNA) breaks and certain base alterations that interfere with transcription and replication are considered cytotoxic and can lead to cell cycle arrest, permanent senescence or cell death (Hoeijmakers 2009). Mutagenic lesions are those that can lead to permanent changes in a cell's DNA sequence by either causing improper replication or aberrant chromosome segregation. In other words, cytotoxic lesions have an immediate effect on the cell, while the consequences of mutagenic lesions are long term.

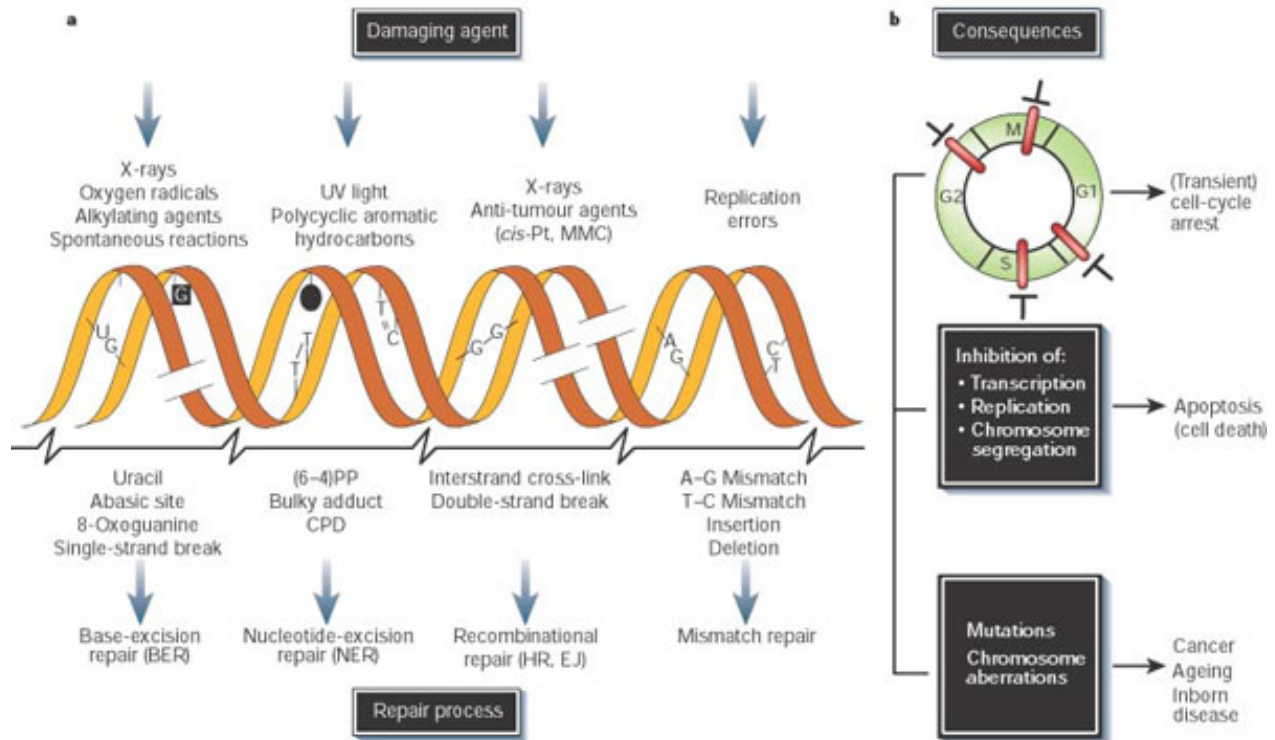


**Figure 1:** Types of DNA damage, DNA repair mechanisms and the consequences of DNA damage. a) The most common DNA damaging agents are shown at the top, with the types of DNA damage generated shown in the middle and the DNA repair mechanism responsible for removal of the lesion at the bottom. b) Cellular consequences of DNA damage. Acute affects of damage on cell cycle progression causing transient arrest in the G1, S, G2 and M phases (top) and on DNA metabolism (middle). The long term consequences of DNA damage shown at the bottom permanent changes in the DNA sequence (point mutations affecting single genes or chromosome aberrations which may involve multiple genes) and their biological effects. Abbreviations: cis-Pt and MMC, cisplatin and mitomycin C, respectively (both DNA-crosslinking agents); (6-4)PP and CPD, 6-4 photoproduct and cyclobutane pyrimidine dimer, respectively (both induced by UV light); BER and NER, base- and nucleotide-excision repair, respectively; HR, homologous recombination; EJ, end joining. Reproduced from Hoeijmakers 2001 with permission from Nature Publishing group (license number: 2853091298384).

### **Oxidative DNA damage: 8-oxoguanine**

In addition to causing DNA damage and being linked to the initiation and progression of cancer (Klaunig and Kamendulis 2004), ROS function as essential intracellular signaling molecules (Finkel and Holbrook 2000) and are a component of the inflammatory response. The essential functions of ROS in the cell are well recognized and occur when they are present at low to moderate concentrations. Once the intracellular level of ROS exceeds the amount required, a cell is considered to be in a state of oxidative stress (Kovacic and Jacintho 2001). A number of enzymatic and non-enzymatic antioxidants exist in the cell to deal with the overproduction of ROS and maintain redox homeostasis (Droge 2002). Redox homeostasis is achieved by maintaining a balance between the rate of ROS production and their clearance by these antioxidant compounds or enzymes. Enzymes involved in these processes include superoxide dismutase (SOD), glutathione peroxidase and catalase and non-enzymatic compounds include vitamin E ( $\alpha$ -tocopherol),  $\beta$ -carotene, vitamin C (ascorbate) and glutathione (Halliwell and Gutteridge 1989). When the balance of ROS and antioxidants is perturbed and shifted towards higher levels of ROS, the result is increased levels of macromolecular damage (see Figure 2).

DNA bases are highly susceptible to the harmful effects of ROS, in particular guanine (G) due to its low redox potential (Neeley and Essigmann 2006). One of the most commonly formed mutagenic lesions is the guanine oxidation product 7,8-dihydro-8-oxoguanine (8-oxoG, 8-oxoguanine, 8-hydroxyguanine) (Park et al. 1992) which is commonly used as a biomarker for the level of oxidative stress and damage in a cell. 8-oxoG is a highly mutagenic lesion due to its ability to functionally mimic thymine (T), which during DNA replication can result in an improper pairing with adenine (A) (David et al. 2007) (See Figure 3; See also Chapter 4 for

further discussion on 8-oxoG and its relation to ageing). Following a subsequent round of replication and failure to recognize and repair the 8-oxoG:A pairing can lead to a stable G:cytosine (C) to T:A transversion (Neeley and Essigmann 2006), which are found in many mutated oncogenes and tumor suppressor genes (Shibutani et al. 1991; Moriya 1993; Hussain and Harris 1998). The structure of 8-oxoG differs from many other types of DNA lesions in that replicative DNA polymerases can efficiently bypass the lesion (Shibutani et al. 1991). (For a discussion of the effect of 8-oxoG on transcription by RNA polymerase II (polII) see Chapter 2, 5 and 7). In addition to the formation of 8-oxoG in dsDNA, ROS can react with dGTP in the nucleotide pool to form 8-oxodGTP, making it possible during DNA replication to insert the damaged nucleotide opposite C or A on the template strand potentially resulting in A:T to C:G transversions (Cheng et al. 1992; Demple and Harrison 1994).

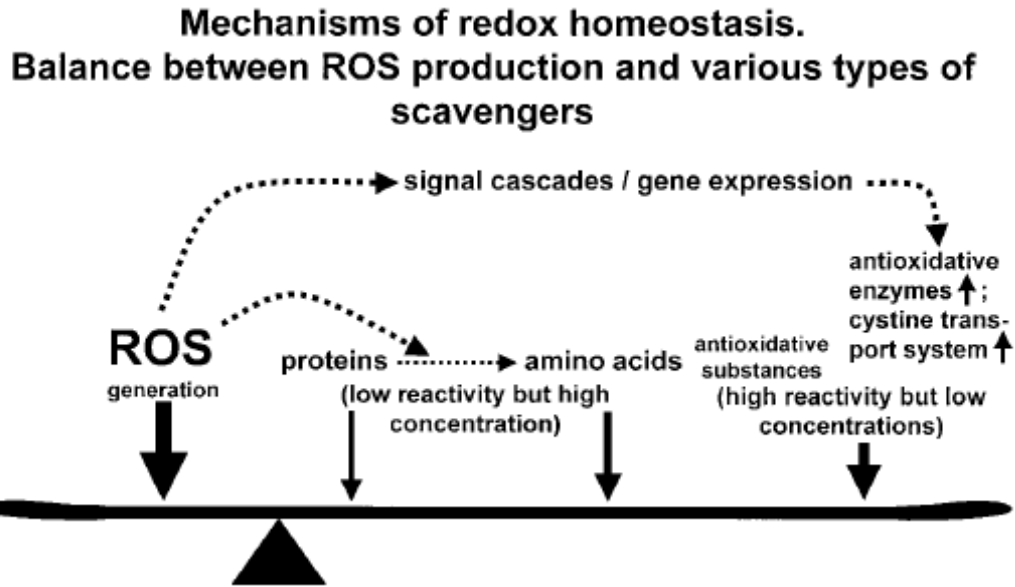


**Figure 2:** Mechanisms of redox homeostasis. Balance between ROS production and various types of scavengers. The steady-state levels of ROS are determined by the rate of ROS production and their clearance by scavenging mechanisms. Certain antioxidative enzymes including superoxide dismutase (SOD), glutathione peroxidase, catalase and thioredoxin are potent ROS scavengers but occur in cells only at relatively low concentrations. The same is true for nonenzymatic antioxidants. Amino acids and proteins are also ROS scavengers, but are less effective than classical antioxidants (Droge 2002).

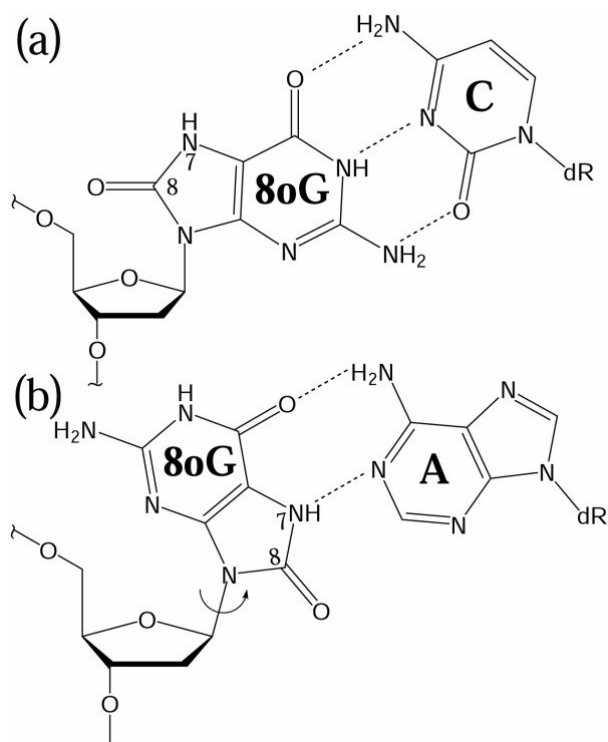


**Figure 3:** Structure of 7,8-dihydro-8-oxoguanine (8-oxoG) and its ability to base pair properly with cytosine (C) and improperly with adenine (A) (Wang and Schlick 2007).

## **Base excision repair (BER)**

Cells are equipped with a battery of DNA repair mechanisms to combat DNA damage and prevent its negative effects (Friedberg et al. 1995; Hoeijmakers 2001) (see Figure 1). A major component of DNA repair pathways is the ability to induce temporary cell cycle arrest in order to efficiently repair damage (Bartek and Lukas 2001). Base excision repair (BER) is the major repair pathway for protecting the cell against DNA lesions caused by cellular metabolism including nucleotides altered by oxidation, methylation, deamination, hydroxylation and ssDNA breaks (Wilson and Bohr 2007; Maynard et al. 2009). BER is initiated by a class of enzymes known as DNA glycosylases that recognize and remove the altered base. While these enzymes display some overlap in substrate specificity, the cell's set of glycosylases allows it to detect and remove a wide variety of minor base alterations (Wilson and Bohr 2007; Maynard et al. 2009). BER can be broken down into two sub-pathways: short patch (SP) repair where a single nucleotide is replaced and long patch (LP) repair where 2-8 nucleotides are replaced (Dianov 2011). BER is initiated by recognition of a lesion by a DNA glycosylase which catalyzes the hydrolysis of the N-glycosidic bond between the DNA base and the sugar phosphate backbone (see Figure 4; for a review of BER see Wilson and Bohr 2007 and Dianov 2011). Release of the corrupted base results in the formation of an apurinic/apyrimidinic (AP) site (also known as an abasic site) that is cleaved on its 5' side by AP-endonuclease 1 (APE1) generating a ssDNA break. The resulting ssDNA break possesses a 5' sugar phosphate that is removed by DNA polymerase  $\beta$  ( $\text{pol}\beta$ ) prior to repair synthesis to add a single nucleotide to the 3' end of gap. Following repair synthesis, DNA ligase III $\alpha$  (LigIII) with XRCC1 completes repair by ligating the gap. This describes the short patch sub-pathway and is used to achieve the majority of repair in the cell (Dianov et al. 1992; Dianov et al. 1998; Dianov et al. 2000). A switch to long patch

repair occurs if the 5' sugar phosphate left after APE1 processing is resistant to the lyase activity of DNA pol $\beta$ . Following the addition of the first nucleotide by DNA pol $\beta$ , repair synthesis is switched to DNA pol $\delta/\epsilon$  where an additional 2-8 nucleotides are added. The additional nucleotides result in a flap that is processed/removed in a PCNA-dependent manner by flap endonuclease-1 (FEN-1) followed by DNA ligase I sealing of the nick to complete repair (Frosina et al. 1996). (For discussion of the effect of transcription on BER of oxidative DNA Chapter 7)

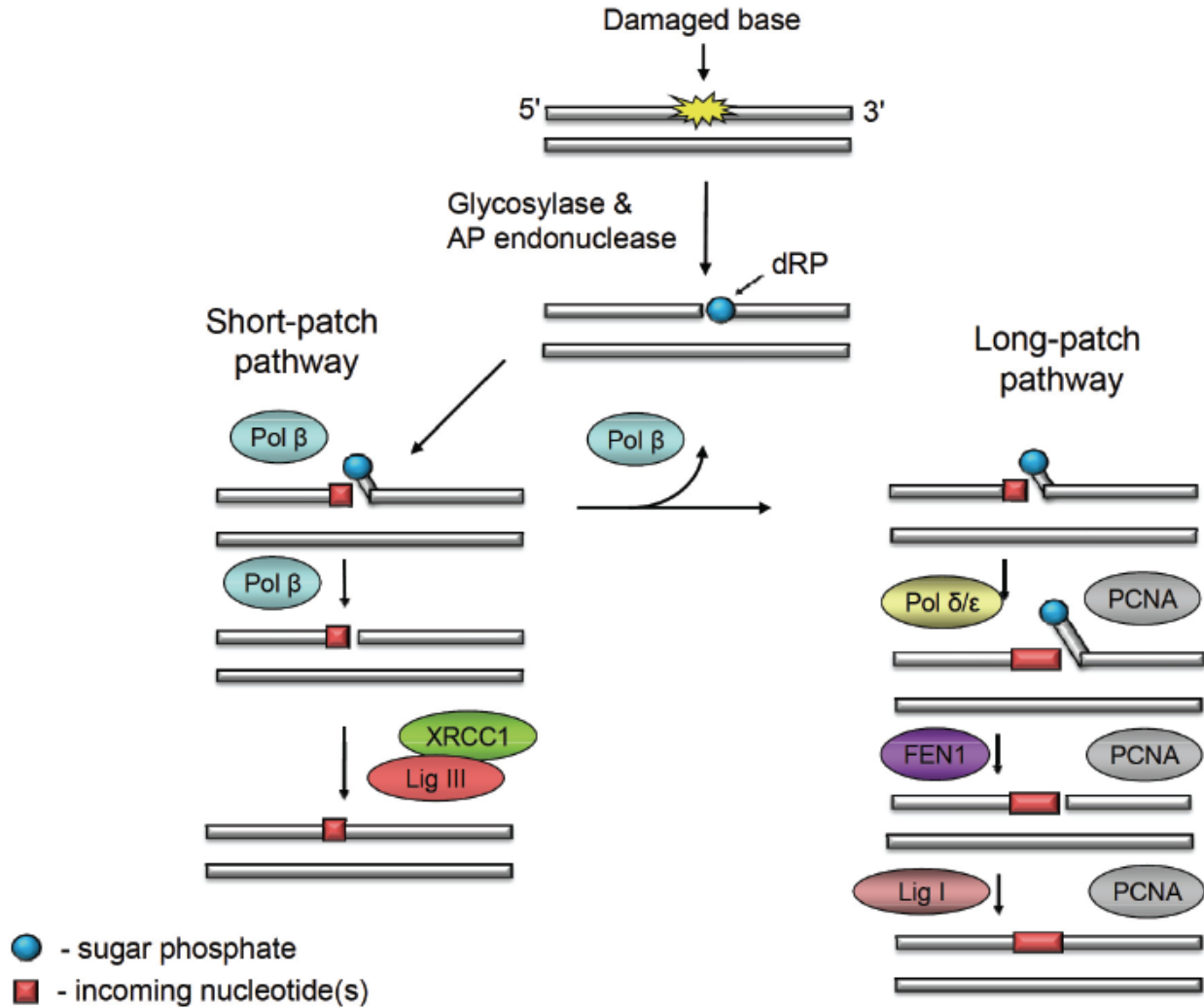


**Figure 4:** The BER pathways. BER is initiated by a damage specific DNA glycosylase and APE1 that excise the damaged base and incise the arising abasic site, respectively generating a DNA single strand break with a 5'-sugar phosphate. Pol  $\beta$  removes the 5'-sugar phosphate and also adds one nucleotide into the single-nucleotide gap. Finally, XRCC1-Lig III complex seals the remaining DNA ends. This pathway is commonly referred to as the short patch BER pathway (left branch). However, if the 5'- sugar phosphate is resistant to cleavage by Pol  $\beta$ , then Pol  $\delta/\epsilon$  adds 2-8 more nucleotides into the repair gap, generating a flap structure that is removed by FEN-1 in a PCNA-dependent manner. Lig I then seals the remaining DNA ends. This pathway is commonly referred to as long patch BER (right branch). This figure was reproduced from Dianov 2011 by the Creative Commons Attribution Noncommercial License agreement which allows unrestricted use of this figure in non-commercial works provided it is properly cited.

## **BER of 8-oxoguanine**

The steady state level of 8-oxoG in eukaryotic DNA has been estimated at several per  $10^6$  guanine bases (Gedik and Collins 2005). The similarity in structure between 8-oxoG and G, the negligible effect of 8-oxoG on distortion of the DNA helix and its relatively low frequency present a difficult task for the cell to detect and repair the lesion. The unique qualities of 8-oxoG have driven the evolution of a pathway for dealing with 8-oxoG in most organisms sometimes referred to as the GO repair pathway (see Figure 5). In humans this pathway consists of three enzymes 8-oxoG DNA glycosylase 1 (OGG1), MutT homolog 1 (MTH1), and MutY homolog (MUTYH) (Barnes and Lindahl 2004). OGG1 is the specific glycosylase that recognizes and removes 8-oxoG:C base pairs in DNA for repair by SP-BER (Dianov et al. 1998). Should an 8-oxoG lesion go undetected or unrepaired and DNA replication results in the improper insertion of A creating an 8-oxoG:A pairing, the glycosylase MUTYH recognizes and removes the A leaving an AP site. Repair synthesis occurs by DNA pol $\beta$ , which unlike replicative polymerases has a much higher probability of inserting C opposite 8-oxoG, to regenerate the original 8-oxoG:C pairing (Krahn et al. 2003). This allows another opportunity for OGG1 to detect and remove the 8-oxoG and restore the DNA to its original state. Finally, MTH1 hydrolyzes 8-oxodGTP from the nucleotide pool to prevent its incorporation in newly synthesized DNA during replication (for a review of BER of 8-oxoG see David et al. 2007).

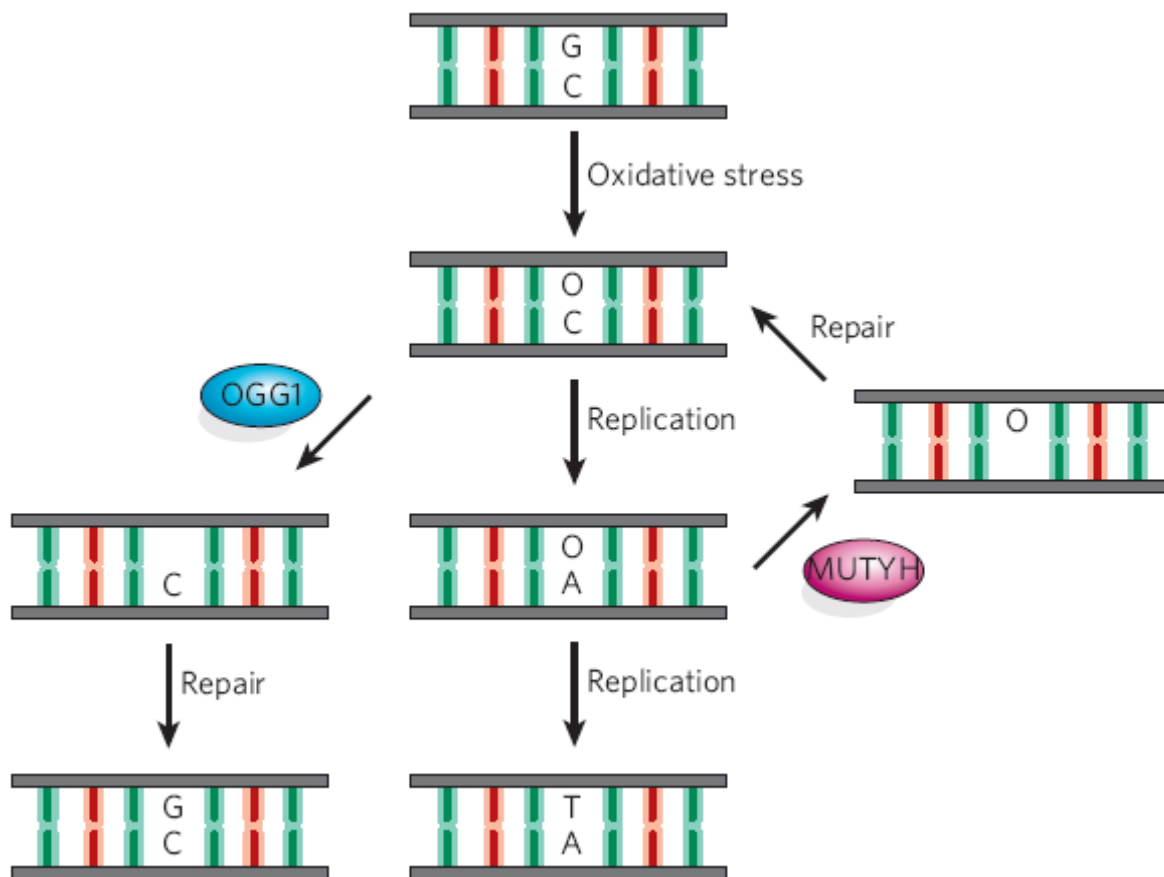


**Figure 5:** The GO pathway. The presence of 8-oxoG (O) in DNA causes G-to-T transversions, as illustrated in the central pathway. The human DNA glycosylases OGG1 and MUTYH are involved in excision of bases from the DNA. OGG1 removes 8-oxoG from 8-oxoG•C base pairs, and MUTYH removes A from 8-oxoG•A base pairs, both generating AP sites in the DNA. The corresponding bacterial enzymes are MutM and MutY. The steps labelled ‘repair’ summarize the actions of AP endonuclease, deoxyribosephosphate lyase, DNA polymerase and DNA ligase. Notably, OGG1 also has AP lyase activity. MutT and its human homologue MTH1 (not shown) have an important role in preventing the incorporation of 8-oxoG, through hydrolysis of free 8-oxo-dGTP. Reproduced from David et al. 2007 with permission from NPG (license number 2853101181500).

### **Base excision repair, ageing and neurodegeneration**

The majority of the human nervous system is made up of the central nervous system (CNS) which is comprised of the brain and the spinal cord. A major manifestation of the ageing process is cognitive decline and reduced motor functions as a result of neurodegeneration. This neurodegeneration is caused by defects in the non-dividing neuronal population of the CNS. Because neurons are terminally differentiated post-mitotic cells, replication associated repair cannot occur (Hanawalt 2008) meaning repair occurs by general genome surveillance and transcription coupling. Neurons have a weak antioxidant defense system and are subjected to higher amounts of ROS due to their high metabolic rate and associated O<sub>2</sub> consumption (Liu et al. 2002). The role of DNA damage and repair can be linked to neurodegeneration by a number of human disorders with mutations in DNA repair factors such as the Cockayne syndrome (CS) genes, the xeroderma pigmentosum (XP) genes, ATM, NBS1, Bloom's syndrome (BLM) and the Fanconi anemia (FANC) genes. Individuals with disorders caused by mutations in these genes exhibit (to differing severities) premature ageing, progressive neurodegeneration, ataxia and mental retardation (Rolig and McKinnon 2000). The brain is a very metabolically active organ resulting in a high level of ROS production making BER a highly relevant, if not the most important pathway for DNA repair in neurons (Fishel et al. 2007). The brain is not exposed to environmental agents such as UV radiation, rendering NER less important. The ageing and/or neurodegenerative phenotype of individuals affected by disorders combined with their association with decreased BER of oxidative DNA provides support for the DNA damage theory of ageing (Jackson and Bartek 2009). For additional discussion about the relationship of oxidative DNA damage with ageing and neurodegeneration see Chapters, 4 and 5.

### **Cockayne syndrome (CS)**

As discussed above, the DNA damage theory of ageing is one of the major hypotheses for explaining the mechanisms behind ageing at the cellular and molecular level. A causal role of DNA damage in the ageing process of humans is supported by a number of progeroid syndromes with inherited defects in DNA repair pathways (de Boer et al. 2002; Martin 2005). The use of progeroid syndromes to study human ageing has been challenged (Miller 2004). Miller's point of contention with the use of progeroid syndromes (specifically HGPS) as models for accelerated ageing including the lack of characteristics observed in the elderly and the presence of some that are not observed during natural ageing. The counter argument to this position is that these disorders model ageing in a 'segmental' fashion (Hasty and Vijg 2004; Miller 2004), meaning that some tissues and organs show ageing phenotypes as a result of the mutation(s) causing the disorder, making that gene relevant to that specific segment of the aging organism. It is due to this imperfect ability of these disorders to mimic natural ageing that they have been classified as segmental progeroid syndromes. Miller argues that we cannot know that two matching phenotypes, one caused at an accelerated pace by an altered gene and the other 'naturally' through ageing, are truly the same and have the same root. Hasty and Viig (Hasty and Vijg 2004) have rebutted Miller's arguments pointing out that every normal individual exhibits a segmental ageing phenotype when considering all possible ageing phenotypes. It is true that no progeroid or segmental progeroid syndrome perfectly displays all phenotypes of ageing, however the ability of single gene mutations to accelerate the appearance of many different features associated with ageing provides support for their use in studying the mechanisms behind these phenotypic changes. Further support for the use of segmental progeroid syndromes as ageing models comes

from their association with DNA repair defects, accumulation of DNA damage and decreased repair capacity observed in association with natural ageing (See Chapter 4 additional discussion).

Cockayne syndrome (CS) is a rare segmental progeroid syndrome with typically affected individuals appearing normal at birth followed by severe postnatal growth failure resulting in cachectic dwarfism (Nance and Berry 1992, Natale 2011; CS is also discussed in Chapters 2, 5 and 6). CS is an autosomal recessive disorders caused by mutations in genes that are best characterized for their involvement in the nucleotide excision repair (NER) pathway which detects and removes bulky helix distorting lesions such as those generated by ultraviolet (UV)-light (Nospikel 2009). A second disorder, xeroderma pigmentosum (XP), is also caused by mutations in genes involved in the NER pathway (Nospikel 2009). NER functions via two subpathways, transcription coupled repair (TCR) which removes RNA polymerase II (polII) blocking lesions from the transcribed strand of active genes, and global genomic repair (GGR) which is responsible for removing lesions throughout the entire genome (For a review of NER see Nospikel 2009).

In addition to the characteristics already mentioned, CS individuals display cutaneous photosensitivity but do not have the increased incidence of skin cancer observed in XP, exhibit premature ageing, developmental abnormalities, ocular abnormalities/retinal degeneration, severe neurodegeneration (Nance and Berry 1992; Natale 2011). The average lifespan of severely affected individuals is 5 years and those mildly affected by the disorder live to an average of 30.3 years (Natale 2011). A hallmark characteristic of skin fibroblasts from CS patients is a failure to recover RNA synthesis following exposure to UV-light (Mayne and Lehmann 1982) resulting from defective removal of UV-induced cyclobutane pyrimidine dimers (CPDs) via TCR-NER (Venema et al. 1990). The CSA (MIM 216400) and CSB (MIM 133540)

proteins are required to couple repair of UV-induced lesions to RNA polIII transcription (Venema et al. 1990). Approximately 80% of reported CS cases are caused by mutations in the *CSB* gene (Nance and Berry 1992; Natale 2011) with mutations in *CSA* found to a lesser extent and an even smaller number of cases resulting from specific mutations in *XPB*, *XPD*, and *XPG* genes (Rapin et al. 2000). Mutations in the latter three genes result in a disorder with a combined XP/CS phenotype (Rapin et al. 2000).

The *CKNI/CSA/ERCC8* gene encodes a 396 amino acid protein whose predicted amino acid sequence indicates it is a WD40 repeat protein (Henning et al. 1995). WD40-repeat proteins form stable  $\beta$ -propeller platforms that serve as rigid scaffolds to which other proteins can bind to in a stable or reversible manner and are commonly involved in co-ordination of multi-protein complex assemblies (Li and Roberts 2001). The *ERCC6/CSB* gene encodes the 1493 residue CSB protein (Ensembl transcript: ENST00000355832) as well as 3 additional protein coding transcripts (Ensembl transcripts: ENST00000374129, ENST00000342592, ENST00000374127).

Based on sequence similarity, CSB has been classified as a member of the SWI/SNF2 family of proteins (Matson et al. 1994) and exhibits ATPase activity (Selby and Sancar 1997; Citterio et al. 2000; Beerens et al. 2005). CSB contains seven consecutive ATPase domains conserved in DNA and RNA helicases, two nuclear localization signals and a highly acidic region (Troelstra et al. 1992). CSB is a phosphoprotein with an N-terminal proline-rich region and is phosphorylated by the oxidative stress activated tyrosin kinase c-Abl (Sun et al. 2000; Sun et al. 2000) at tyrosine 932 (Imam et al. 2007). The CSB-PGBD3 fusion protein generated from the splice isoform (Ensembl transcript: ENST00000374127) of *ERCC6/CSB* containing the first five *ERCC6/CSB* exons and the PiggyBac transposable element *PGBD3* found within intron 5 of *CSB* is as abundantly expressed as CSB in normal fibroblasts (Newman et al. 2008).

Despite the large body of research into the function of the CS proteins, specifically CSB, the molecular mechanism(s) behind the pathophysiology of CS remains poorly understood. In addition, phenotype/genotype relationships with respect to CS severity and mutation location within CSA or CSB have not been established and the reason for the highly variable nature of CS clinical features remains poorly understood. The difficulty in explaining CS pathology through a defect in TCR-NER led to the hypothesis that the CS proteins have additional functions, specifically that they were involved in the repair of oxidative DNA damage. A substantial amount of evidence now supports a role for CSA and CSB in repair of oxidative DNA damage. In earlier work from our laboratory we reported the defective removal of UV induced CPDs by CS cells is only partially corrected by T4 endonuclease V (*denV*) (Francis et al. 1997). DenV is a DNA glycosylase that removes CPDs and generates an apurinic/apyrimidinic site (AP site) that requires further processing by BER. This suggested that CS cells are deficient in BER processes as well as NER (Francis et al. 1997). Defective repair of 8-oxoG, one of the most prominent endogenously formed oxidative base lesions (Kasai and Nishimura 1984; Ames 1989; Shigenaga et al. 1989) has been demonstrated in SV40 transformed CS-A and CS-B fibroblasts (Spivak and Hanawalt 2006; Leach and Rainbow 2011). Reduced repair of 8-oxoG was also demonstrated in mitochondrial DNA from CS-A and CS-B cells (Stevnsner et al. 2002). A number of CS-A and CS-B skin fibroblasts have been shown to accumulate greater background levels as well as induced levels of 8-oxoG when compared to normal fibroblasts (Tuo et al. 2003; D'Errico et al. 2007). Background levels of 8-oxoG are returned to that of wild type (WT) cells in CSA fibroblasts by expression of WT CSA (D'Errico et al. 2007). Demonstration that exposure to ionizing radiation (IR) leads to retinal degeneration, a hallmark phenotype of classical CS, in *CSA*<sup>-/-</sup> and *CSB*<sup>-/-</sup> but not normal mice supports a role for the CS proteins in the response to

oxidative damage in mice and provides a link between defective repair and a clinical symptom (Gorgels et al. 2007). Although a substantial amount of evidence supports a role for the CS proteins in repair of oxidative DNA damage, the mechanism of their involvement is presently not understood. In addition to the role CSB has been found to play in repair of oxidative DNA damage, additional functions have been discovered including the ability to actively wrap DNA resulting in local topological changes in chromatin (Beerens et al. 2005), general chromatin remodelling capabilities (Newman et al. 2006), strand exchange capabilities (Muftuoglu et al. 2006), strand annealing (Muftuoglu et al. 2006; Berquist and Wilson 2009) and a role in general transcription (Licht et al. 2003).

### **Use of recombinant adenovirus vectors to study DNA repair**

Adenoviruses are double-stranded DNA (dsDNA) viruses with a genome of approximately 36kb (Csaky 2001). More than 100 serotypes in the adenovirus family have been identified with all members sharing a number of identical antigens and other molecular aspects (Levy et al. 1994; Csaky 2001). The most extensively studied adenoviruses, serotypes 2 and 5 are of human origin and are able to efficiently infect human cells (Shenk 1996). Research into the structure and function of these two serotypes has been driven largely by their promise as vectors for use in gene therapy. This promise arises from the ability of the adenoviruses to infect a large variety of cell types from a number of vertebrate species and subsequently drive high levels of expression of an inserted transgene (Addison et al. 1997; Kovesdi et al. 1997; Yeh and Perricaudet 1997) The stability of adenoviruses allows for the maintenance and expression of inserted transgenes for long periods of time and up to 72 hours in this work (Levy et al. 1994; Csaky 2001; Palmer and Ng 2005). In addition to the study and use of adenoviruses in gene

therapy, they have also been developed as a research tool for use in cellular and molecular biology. The ease and efficiency with which the adenovirus can infect both quiescent and replicating cells in culture (Horwitz 1990; Hitt et al. 1999) makes it an excellent system for introduction and transient expression of a transgene or for use as a reporter.

### *Structure of the Adenovirus*

The adenovirus virion is an icosahedral non-enveloped capsid containing the viral DNA bound and organized by a number of virally encoded proteins (see Figure 6). The viral particle consists of proteins designated pI to pX and DNA all of which are encoded by the viral genome. The viral capsid is made up of 240 homotrimeric hexons (pII) forming the faces and edges of the capsid and 12 penton bases capping each vertex of the adenovirus icosahedron (Levy et al. 1994; Medina-Kauwe 2003; Vellinga et al. 2005). Trimers of pIV extend from the penton bases at each the vertices to form fibers (San Martin and Burnett 2003) with a C-terminal globular domain required for binding of adenovirus particles to host cell receptors (Henry et al. 1994). Proteins IIIa, VI, VIII and IX are considered minor components of the capsid with the remaining six viral proteins contained within (Vellinga et al. 2005). Five of the six internal proteins (V, VII, X(Mu), IVa2 and the terminal protein (TP)) are associated with the dsDNA genome and function to organize and anchor it (Goncalves and de Vries 2006). The final protein, the viral p23 protease is contained inside the capsid and is involved in assembly of the viral particle (Goncalves and de Vries 2006).

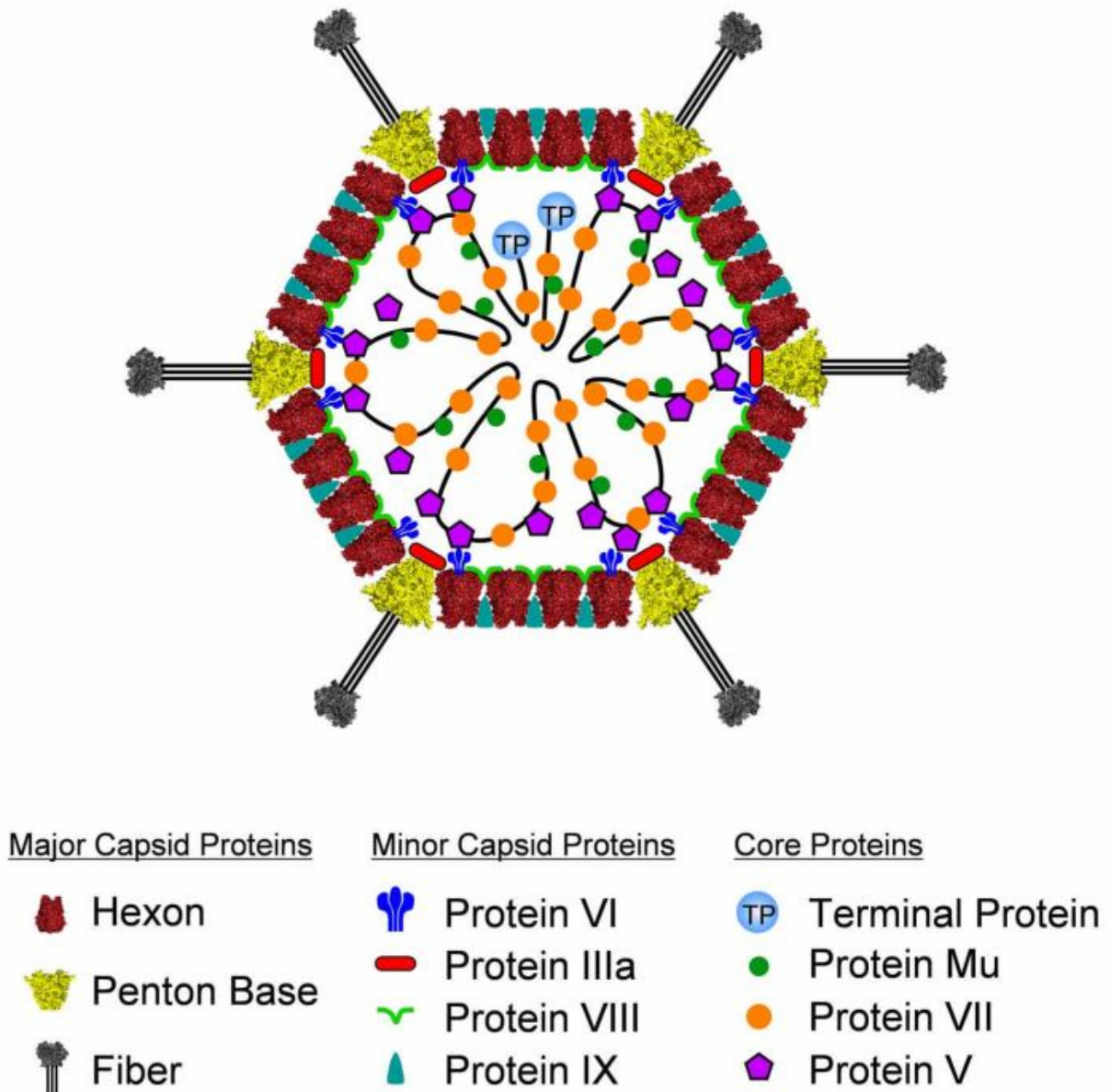


**Figure 6:** Structure of the adenovirus virion. The cross-section of the virion structure shown above is mainly theoretical and is based results from cryo-electron (cryoEM) microscopy and x-ray crystallography and shows the eleven structural proteins of the virion.. The size of each viral component is not to scale. Protein IX stabilizes the capsid on the outside an although only a small number of hexons are shown associated with pVI, cryoEM data shows every hexon is associated (Saban et al. 2006) For a detailed review of the current knowledge on the structure and function of each viral component see Russel 2009. The above diagram is used with permission from Nemerow et al. 2009

*The recombinant non-replicating adenovirus*

The linear dsDNA genome of the adenovirus contains a 103 nucleotide inverted terminal repeat (ITR) sequence at each end. The viral genome is divided into early and late transcriptional units based on the timing of gene transcription (see Figure 7). The transcription of the early genes (*E1A*, *E1B*, *E2A*, *E2B*, *E3* and *E4*) occurs prior to DNA replication, which marks the transition to late gene expression. All virally encoded genes are transcribed by host RNA polII with the exception the small virus-associated I and II RNAs that are transcribed by host RNA polymerase III (Goncalves and de Vries 2006). Following infection, early region 1 (E1) is the first to be transcribed. The *E1A* and *E1B* gene products are required to transactivate the downstream early transcription units and complete viral gene expression and replication (Flint and Shenk 1989). The most extensively used adenovirus vectors are the recombinant viruses with the E1 region deleted. Deletion of the E1 region prevents expression of downstream (temporal) genes and provides approximately 5kb of space for the insertion of foreign DNA. Construction and subsequent replication of E1 deleted adenoviruses is generally achieved by infection of human cell lines expressing the E1 gene products such as 293 cells (Graham et al. 1977).

In this work we have used the recombinant non-replicating adenoviruses AdCA17, AdCA35, Ad5HCMVSp1*lacZ* and AdCA18 (Addison et al. 1997) from serotype 5 (Ad5) to study DNA in tissue culture (see Figure 8). The HCMV IE enhancer/promoter is one of the most frequently used promoters to drive expression of transgenes inserted into viral vectors (Addison et al. 1997). Its use is based on the fact that it can drive high levels of transgene expression in a number of different types of cells (Boshart et al. 1985; Schmidt et al. 1990). The viral enhancer region contains a number of imperfect repeats that binds a number of different transcription factors including NF- $\kappa$ B, AP1 and cAMP responsive binding protein (CREB)

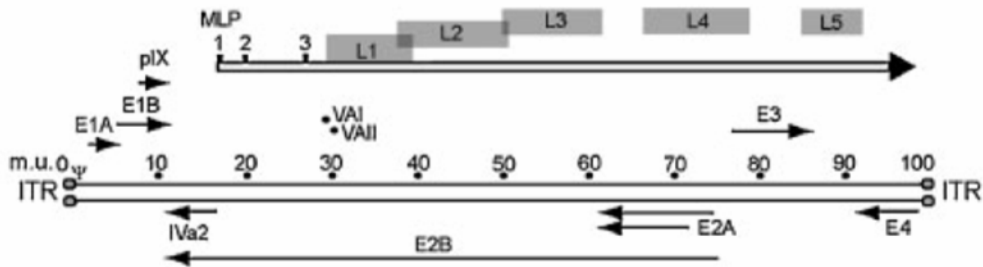


**Figure 7:** Schematic representation of the human adenovirus 5 genome. The location and orientation of transcribed genes are indicated by arrows with the gene name above. The ITR sequences at both ends of the linear genome are depicted as circles and  $\psi$  represents the packaging domain. The early (E) genes located in the early region 1 (E1A and E1B), 2 (E2A and E2B), 3 (E3) and 4 (E4) encode for the most part proteins involved in regulation of viral and host cell gene expression as well as adenovirus DNA replication. The late (L) genes are regulated by the major late promoter (MLP). A large primary mRNA transcript is generated which through alternative splicing and differential polyadenylation leads to the mRNA species (L1-L5) that code for the majority of the structural components of the virus. (m.u. – map units). The above figure is from (Goncalves and de Vries 2006) Reproduced with permission from Wiley and Sons (licence number 2853110726947)

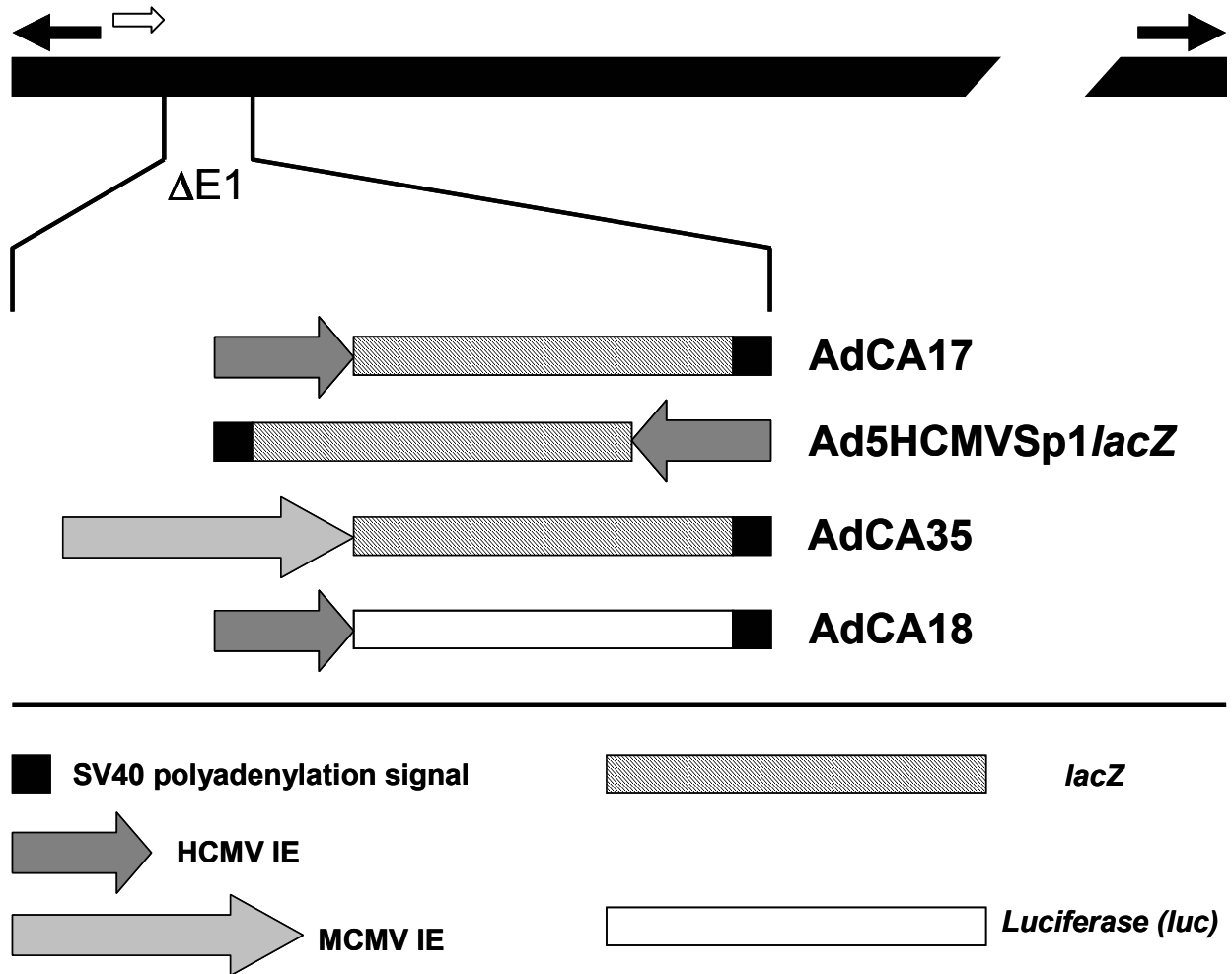


**Figure 8:** Schematic representation of the adenoviral constructs used in this work. The above diagram depicts the promoter/enhancer gene combinations as well as their orientation of insertion into the deleted E1 region of adenovirus 5. All of these viral constructs have the E1 region deleted and replaced with a transgene. AdCA17, AdCA35 and Ad5HCMVSp1*lacZ* all express *E. coli LacZ* whose gene product is the  $\beta$ -galactosidase ( $\beta$ -gal) enzyme while AdCA18 expresses luciferase (Addison et al. 1997). The three viral constructs expressing *LacZ* differ in the promoter used to drive expression or promoter-transgene orientation. All constructs use either the human or murine cytomegalovirus (HCMV or MCMV, respectively) immediate early (IE) promoter/enhancer to express the transgene (Addison et al. 1997). Solid arrows above the adenovirus backbone represent the ITRs. The open arrow to the left of the deleted E1 region represents the E1a enhancer that remains in the E1 deleted backbone. The direction of the arrow represents the direction that the enhancer drives expression. The above figure is adapted from Addison et al. 1997.

(Hennighausen and Fleckenstein 1986; Fickenscher et al. 1989; Sambucetti et al. 1989; Stamminger et al. 1990; Niller and Hennighausen 1991). While the HCMV IE promoter is able to drive expression of transgenes in cells derived from both humans and mice, expression in mouse cells is 10-50 fold lower (Addison et al. 1995; Addison et al. 1995a). The AdCA17 virus drives expression of the transgene by insertion of the HCMV IE enhancer element in the forward/rightward direction upstream of the *lacZ* transcriptional start site of the  $\beta$ -gal reporter into the deleted E1 region (Addison et al. 1997). The Ad5HCMVSp1*lacZ* reporter construct, is similar to AdCA17 except the reporter cassette (HCMV IE upstream of the *lacZ* transcriptional start site) is inserted into the deleted E1 region in the opposite/leftward orientation, which results in less transcription of the reporter compared to AdCA17. This difference in expression may result from the E1a enhancer, which remains in the vector backbone, acting synergistically with the HCMV IE enhancer/promoter in AdCA17 to increase transcription (Addison et al. 1997). The AdCA35 construct contains the MCMV IE promoter/enhancer upstream of the  $\beta$ -gal reporter inserted in the forward/rightward direction and drives higher levels expression compared to both AdCA17 and Ad5HCMVSp1*lacZ* (Addison et al. 1997). Finally, AdCA18 is similar to AdCA17, but instead of  $\beta$ -gal, luciferase (*luc*) is expressed by the HCMV IE enhancer/promoter (Addison et al. 1997).

### *Infection of cells by the Adenovirus virion*

The initial event of the adenovirus infection process is binding of the C-terminal globular end of the capsid fiber to host cell receptors. Although the virus is capable of binding a number of cell surface receptors (Zhang and Bergelson 2005), the coxsakie virus B adenovirus receptor (CAR) is the major receptor for binding and infection (Bergelson et al. 1997; Mayr and Freimuth

1997; Tomko et al. 1997; Roelvink et al. 1998). In addition to CAR binding by the capsid fibers, arginine-glycine-aspartic acid (RGD) motifs located on the penton base interact with cell surface co-receptors of the integrin family to trigger internalization by clathrin-coated vesicles and signaling that results in cytoskeletal reorganization and an increase in microtubule mediated trafficking towards the nucleus (Salone et al. 2003; Meier and Greber 2004; Goncalves and de Vries 2006).

Once the adenovirus has been internalized, the exact mechanism of lysosomal escape is not known, although lack of the p23 protease or use of protease inhibitors yields viral particles that are noninfectious (Cotten and Weber 1995). The released nucleocapsid subsequently binds to microtubule motor proteins and is transported to the nuclear pore complex (NPC) for entry into the nucleus (Trotman et al. 2001). Disassembly of the nucleocapsid begins enroute to the NPC through the activity of the p23 protease (Cotten and Weber 1995). Targeting of the viral core, consisting of pVII wrapped viral DNA covalently linked to TP (Chatterjee et al. 1986) to the nucleus and nucleolus is mediated by signals from pVII and the nuclear localization signal (NLS) of the TP (Zhao and Padmanabhan 1988; Greber et al. 1997; Lee et al. 2004; Wodrich et al. 2006). The condensed pVII condensed viral core inhibits expression of the adenovirus encoded genes (Haruki et al. 2006). It was previously proposed that active transcription of viral DNA is required for removal of pVII (Chen et al. 2004), however it has recently been shown that transcription independent degradation of pVII occurs within a few hours after infection. Protein VII also appears to inhibit cell cycle checkpoint signaling by preventing recognition of viral DNA as damage (Karen and Hearing 2011). Following nuclear entry, viral DNA associates with the nuclear matrix through the covalently attached TP (Bodnar et al. 1989; Schaack et al. 1990; Fredman and Engler 1993). DNA from both wild type and E1 deleted adenovirus 5 is organized

into a chromatin like state very similar to genomic DNA by association with all nucleosome components, histone H2A/H2B, H3 and H4 (Komatsu et al. 2011). This chromatinization of adenovirus DNA is required for efficient transcription of adenovirus encoded genes (Ross et al. 2011). While nuclear organization of the viral DNA into a chromatin like structure is necessary for gene transcription, it also provides the cell with a template for epigenetic downregulation of gene expression (Ross et al. 2009). These features of the adenovirus contribute to its usefulness as a vector for gene delivery and also as a tool for examining DNA repair mechanisms of cells in tissue culture.

#### *Use of the adenovirus to study DNA repair*

The introduction of foreign DNA particles (plasmids and viral DNA) containing externally generated damage into cells has been used for some time to study cellular DNA repair function and capacity (Rainbow and Mak 1973; Lytle et al. 1976; Protic et al. 1988; Colicos et al. 1991; Smith et al. 1995; Valerie and Singhal 1995; Johnson and Latimer 2005). Host cell reactivation (HCR) of viral gene expression is used to measure cellular repair capacity. The specific repair pathway examined is determined by the agent used to damage the DNA of the reporter construct. The HCR assay currently used in our lab utilizes a recombinant non-replicating adenovirus (Ad) expressing the *E. coli*  $\beta$ -galactosidase ( $\beta$ -gal) under control of the cytomegalovirus (CMV) immediate early (IE) enhancer region (Addison et al. 1997). The rationale behind the HCR assay is that in the absence of DNA damage, host cell transcription of the reporter gene by RNA polymerase II (polII) is uninterrupted and efficiently generates full mRNA transcripts which lead to the production of functional  $\beta$ -gal. Upon introduction of DNA damage into the Ad encoded reporter gene, transcription by RNA polII is blocked and DNA

repair must first detect, remove and repair the DNA before proper transcription and production of the  $\beta$ -gal protein can occur (see Figure 9 for a schematic representation of the HCR assay). The result is reduced expression of the reporter gene in comparison to the undamaged control. The inability of the recombinant adenovirus to replicate allows the system to examine DNA repair activity that is not associated with replication. This feature is important when examining repair in relationship to aging, as the majority of tissues and cells in a developed organism are differentiated and no longer replicate. The HCR assay measures the ability of an untreated cell to reactivate gene expression from a damage template, which may be more relevant when examining the so called basal capacity for repair in cells in relation to ageing. For a discussion of the effect of cellular treatment on global or transcription coupled repair mechanisms see Chapter 5 and 7.

The Ad based HCR assay has been used extensively by our lab to examine repair of UVC induced lesions (CPDs) by the nucleotide excision repair (NER) pathway in primary and transformed cell types under various conditions (Francis et al. 1997; Boszko and Rainbow 1999; Francis and Rainbow 1999; Dregoesc et al. 2007; Wu et al. 2007; Ghodgaonkar et al. 2008; Dregoesc and Rainbow 2009). Exposure of DNA to UVC radiation results in the formation of 6-4 pyrimidine-pyrimidone dimers as well as cyclobutane pyrimidine dimers (Friedberg et al. 1995). These lesions act as a strong block to transcription by RNA polII, thus requiring removal by DNA repair mechanisms to resume efficient transcription (Donahue et al. 1994). Removal of transcription blocking lesions is achieved by the transcription coupled repair (TCR) sub-pathway of NER (Friedberg et al. 1995). Using a PCR based approach our lab has verified that UVC induced lesions are in fact removed from the Ad encoded *lacZ* gene and that the removal strongly correlates with reactivation of gene expression (Boszko and Rainbow 1999). These

results demonstrated that HCR of UVC induced lesions in the adenovirus reporter gene measures NER. More recently we have used the HCR assay to examine base excision repair (BER) of oxidative DNA damage generated by exposure of the virus to methylene blue plus visible light (MB+VL) prior to infection of cells (Kassam and Rainbow 2007; Pitsikas et al. 2007; Rainbow and Zagal 2008; Kassam and Rainbow 2009; Leach and Rainbow 2011; Rainbow et al. 2011). MB is a photosensitizer that upon exposure to VL generates singlet oxygen ( $^1\text{O}_2$ ) which through interaction with DNA leads mainly to the formation of 7,8-dihydro-8-oxoguanine (8-oxoG) and a small number of additional single base modifications (Floyd et al. 1989; Tuite and Kelly 1993). Studies examining the ability of 8-oxoG to block transcription by RNA polII have shown conflicting results and have demonstrated transcription blockage is dependent on a number of factors including the sequence context surrounding the lesion as well as the strength of the promoter driving transcription (Kitsera et al.; Kuraoka et al. 2003; Kathe et al. 2004; Tornaletti et al. 2004; Charlet-Berguerand et al. 2006; Pastoriza-Gallego et al. 2007). It was also suggested that the observed decrease in expression from a reporter gene containing 8-oxoG lesions results from gene inactivation by the 8-oxoG DNA glycosylase (OGG1) and that this inactivation is increased in the absence of the Cockayne syndrome (CS) group B (CSB) protein (Spivak and Hanawalt 2006; Khobta et al. 2009).

For additional discussion on the HCR assay see Chapter 2 and 3. We have also reported a second  $\beta$ -gal assay, the enhanced expression assay for examining the response of cells following cellular treatment with a damaging agent (Francis and Rainbow 2000; Zagal et al. 2005; Pitsikas et al. 2007). For a discussion on the enhanced expression assay see chapter 5.

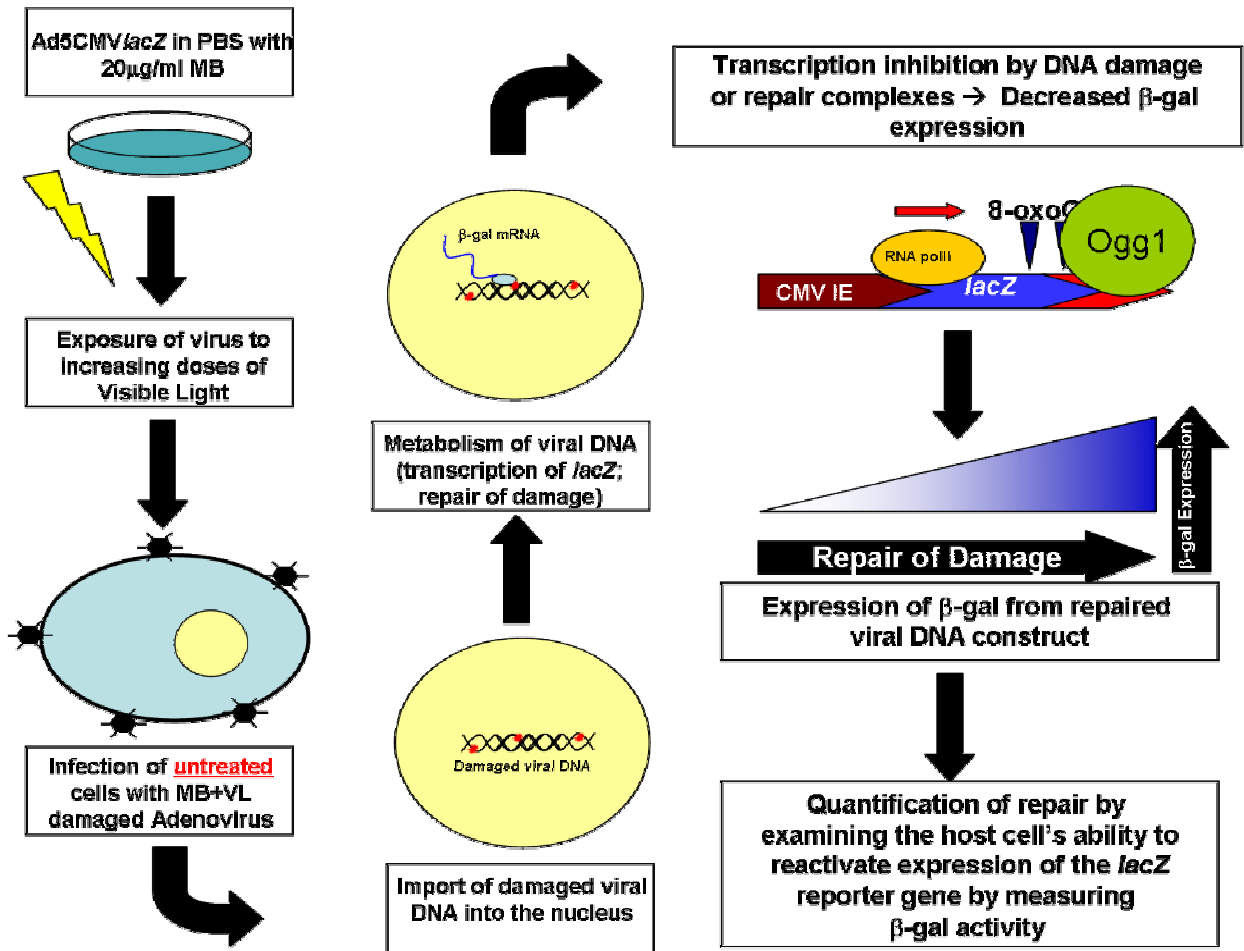


**Figure 9:** Schematic representation of the HCR assay employed in this work. The capacity of fibroblasts to repair MB+VL induced 8-oxoG lesions was examined using an adenovirus based HCR assay. 8-oxoG lesions were introduced to the adenovirus encoded  $\beta$ -gal reporter gene using MB+VL prior to infection of cells. HCR curves representing relative survival of  $\beta$ -gal were generated by measuring the change in absorbance caused by cleavage of the  $\beta$ -gal substrate chlorophenolred- $\beta$ -D-galactopyranoside (CPRG). Absorbance for each dose was normalized to the observed for untreated control cells. Different methods to plot and analyze the resulting  $\beta$ -gal survival curves were used throughout this work and are described in each section.

*Methylene blue*

Methylene Blue (MB, swiss blue, aniline violet, methionine hydrochloride, tetramethionine hydrochloride) was originally developed as a dye for the textile industry but was quickly recognized for its uses in the biological sciences as a stain for cell structures and selective staining and inactivation of bacterial species (Oz et al. 2009). MB was first used in medicine as an antiseptic and is currently being investigated in 30 clinical trials in the United States (January 2012; clinical trials.gov; NIH). (For a discussion on the use of MB in the treatment of Alzheimer's disease see Chapter 4). In this work, we have used MB as a photosensitizer to induce oxidative damage in DNA of both the adenovirus reporter and genomic DNA of cells.

MB ( $C_{16}H_{18}ClN_3S$ , Figure 10) is a thiazine dye that absorbs light in the 600-700nm region of the VL spectrum, gaining its blue colour by the transmission of 350-600nm VL. The photosensitizing properties of MB are derived from its ability to directly absorb energy from visible light (VL). The absorbed light energy can then act through two mechanisms to produce damage in biological systems. Light excitation of MB can induce singlet ( $^1MB$ ) or triplet ( $^3MB$ ) states of the molecule causing energy transfer via electrons (Type I) or energy (Type II) to reaction intermediates or biological molecules directly. The excited  $^1MB$  state has an equal probability of returning to the ground state or being further excited to the  $^3MB$  state (Foote 1976). The type II mechanism occurs in the presence of molecular oxygen ( $O_2$ ) where it interacts with  $^3MB$  to generate singlet oxygen ( $^1O_2$ ) and ground state MB (Figure 10B), and with a much lower yield due to its slow reaction rate, superoxide ( $O_2^{\bullet-}$ ) and reduced MB (MB) (Floyd et al. 2004). The result of the type II mechanism is oxidative damage to DNA, mainly the formation of 7,8-dihydro-8-oxoguanine (8-oxoG) (Floyd et al. 1989; Wainwright 2003). For type I reactions,

<sup>3</sup>MB can lead to the formation of hydroxide radicals by transfer of an electron from a hydrogen (H) atom (Floyd et al. 2004). In addition to the nucleic acid damage induced by MB, alterations to proteins and lipids also occur, in particular lipid peroxidation affecting membrane integrity and alteration in the function of ion channels, receptors and transporters (Tuite and Kelly 1993).

The ability of MB to accept and donate electrons to a variety of compounds allows it to function as both a prooxidant and an antioxidant (McCord and Fridovich 1970; Kelner et al. 1988; Salaris et al. 1991; Riedel et al. 2003). MB can cycle between the oxidized (MB) and reduced (MBH<sub>2</sub>/leucoMB) states and is capable of being reduced *in vivo* by numerous NAD(P)H-dependent enzymes (Kelner et al. 1988, Figure 10A). As mentioned above, reduction of MB to MBH<sub>2</sub> results in the production of <sup>1</sup>O<sub>2</sub>. Cytochrome c, a subunit of the electron transport chain (ETC) complex IV carries electrons from the ETC complex III to complex IV and normally transfers an electron to O<sub>2</sub> to form H<sub>2</sub>O, is capable of oxidizing MBH<sub>2</sub> back to MB (McCord and Fridovich 1970; Kelner et al. 1988). Interestingly, the presence of low levels of MB in tissue culture media has been shown to delay senescence *in vitro* replicative in human IMR90 primary lung fibroblasts (Atamna et al. 2008). Normal primary fibroblasts have a finite *in vitro* replicative lifespan known as their Hayflick limit (Hayflick and Moorhead 1961). After reaching this limit, cells enter a state of senescence, where the cell remains metabolically active but is no longer capable of dividing. The study of *in vitro* lifespan or aging using cell culture as a model often uses population doubling level (PDL) as a measure of cellular longevity. The optimal lifespan extension of IMR90 cells maintained in culture with 100nM MB at 20% O<sub>2</sub> was an increase of greater than 20 PDL (greater than 80 total PDL with 100nM MB compared to less than 60 total PDL without 100nM MB; with culturing beginning at PDL=9). Extension of cellular lifespan was observed regardless of the PDL at which MB was introduced to the culture

media, however with decreasing effectiveness as the starting PDL increased. A significant 70% increase in cellular oxygen consumption by cells grown in MB as well as the ability of MB to protect against the toxic effects of cadmium and hydrogen peroxide ( $H_2O_2$ ) were also observed (Atamna et al. 2008). The presence of MB also increased the levels of cytochrome c by approximately 30% compared to the ETC complex I and III subunits (Atamna et al. 2008).

In addition to the upregulation of cytochrome c, an increase in phase II antioxidant defense enzymes (TrxR1 and NQO1) was also observed in MB treated IMR90 human primary lung fibroblasts (Atamna et al. 2008). Phase II antioxidant defense enzymes act downstream of major cellular redox sensors such as glutathione (GSH) to boost the cellular defense against oxidative stress and related damage (Hayes and McLellan 1999; Griffiths 2000). Phase II enzymes are regulated by a common transcription factor and gene expression pathway requiring promoter binding by the antioxidant response element (ARE) (Nguyen et al. 2003). These data suggest that culturing cells in the presence of MB increases the level of oxidative stress, leading to a cellular response that includes upregulation of pathways involved in protecting against downstream oxidation of cellular macromolecules such as DNA. Mitochondrial dysfunction, oxidative DNA damage and telomere shortening are all proposed mechanisms to explain cellular senescence and can be explained by the free radical theory of aging (Harman 1981). In addition to primary defense mechanisms directly acting against ROS, base excision repair (BER) is the major excision repair pathway involved in protecting cells from the damaging effects of ROS on DNA.

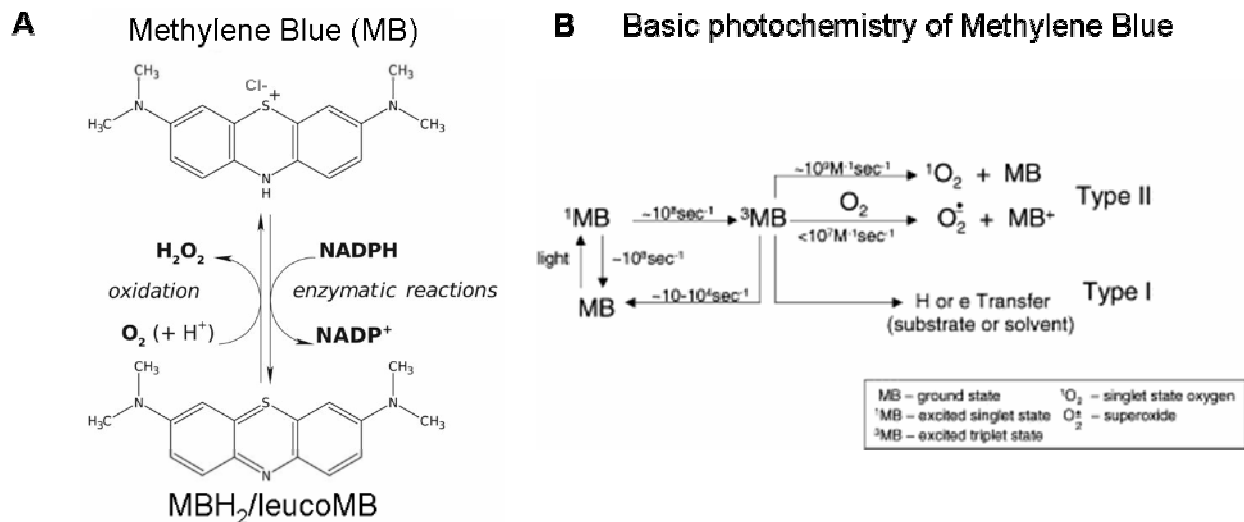


**Figure 10:** Structure and reactions of methylene blue. A) Molecular structure of oxidized MB (top) and reduced MBH<sub>2</sub> (bottom). MB is a redox cycling molecule and has various substrates within the cell. NADPH through enzymatic reactions can reduce MB to MBH<sub>2</sub>, which through interaction with O<sub>2</sub> can be oxidized back to MB. This oxidation step results in the production of ROS, mainly hydrogen peroxide (H<sub>2</sub>O<sub>2</sub>). Adapted from Oz et al. 2009 with permission. B) Photochemical reactions of MB. MB is excited by light to the singlet state ( $^1\text{MB}$ ). Once excited to  $^1\text{MB}$ , the probability of decay back to ground state or further excitement to  $^3\text{MB}$  is equal.  $^3\text{MB}$  can react with O<sub>2</sub> to generate singlet oxygen ( $^1\text{O}_2$ ) in a type II process. Downstream effects of MB production of  $^1\text{O}_2$  include interaction with DNA and the formation of 8-oxoG.  $^3\text{MB}$  can also react via type I processes where a H atom or electron transfer occurs with a substrate molecule. Adapted from Floyd et al. 2004 with permission.

## **Project summary**

In this work, we have utilized adenovirus-based reporter gene assays to study repair of MB+VL induced oxidative DNA damage in human fibroblasts from patients with ageing and neurodegenerative disorders. From the DNA damage theory of ageing, we hypothesized that intrinsic defects in base excision repair are the main cause of increased DNA damage in these cells rather than defects in other cellular processes leading to increased oxidative stress by increased exposure to ROS.

Skin fibroblasts were used to study repair of oxidative DNA damage in cells from patients with ageing and neurodegenerative phenotypes. In contrast to neurons, skin fibroblasts are mitotically active which requires justification for their use in studying DNA repair and its relation to the neurodegenerative pathology of human disorders such as CS and Alzheimer's disease (AD). Although epigenetic modifications lead to differential expression patterns in different cell types, the genetic code of an individual is identical in every cell type whether it is a dividing skin fibroblast or a neuron. It is therefore reasonable to assume that processes affected by inherent mutations in neurons from patients with ageing/neurodegenerative diseases will also be affected in other cell types as long as they remain active. Due to their high metabolic rate, oxidative DNA damage is most likely to occur in neurons, suggesting BER is likely the most important repair pathway. Defective incision activity of the OGG1 glycosylase has been observed in brain tissue from a number of AD patients (Mao et al. 2007) consistent with observations of defects in repair of oxidative damage in non-neuronal tissue such as leukocytes from AD patients using the comet assay (Kadioglu et al. 2004; Migliore et al. 2005) and in skin fibroblasts using the micronucleus assay (Trippi et al. 2001). This demonstrates that BER defects

in a pathologically affected cell type (neurons) can be detected in other cell types including skin fibroblasts that are not clinically affected.

## **Chapter 2**

### **Early host cell reactivation of an oxidatively damaged adenovirus-encoded reporter gene requires Cockayne syndrome proteins CSA and CSB.**

**Published as: Derrick M. Leach and Andrew J. Rainbow, *Mutagenesis* 26(2): 315-321, 2011, (reproduced with permission)**

## **Preface**

Host cell reactivation (HCR) of gene expression from exogenously damaged DNA has long been used as a technique to study the capacity of different cell types to repair DNA lesions. Fibroblasts isolated from individuals with Cockayne syndrome are defective in HCR of UVC and methylene blue plus visible light (MB+VL) treated reporter constructs (Francis and Rainbow 1999; Spivak and Hanawalt 2006). Studies examining expression of a MB+VL treated plasmid based green fluorescent protein (GFP) in mouse embryonic fibroblasts (MEFs) suggested that the observed deficiency in HCR of MB+VL induced damage in CS fibroblasts was the result of transcriptional inactivation rather than a failure to reactivate expression (Khobta et al. 2009).

The results presented in this Chapter demonstrate that expression of an MB+VL treated reporter gene is in fact reactivated over time and that the reactivation requires both the CSA and CSB proteins.

The work presented in this Chapter has been published (*Mutagenesis* 26(2): 315-321, 2011) and is reproduced with permission in this work. My contributions include writing of the manuscript and all data presented within it. Dr. Rainbow provided critical insight into the experiments and writing of the manuscript as well as guidance throughout.

## Early host cell reactivation of an oxidatively damaged adenovirus-encoded reporter gene requires the Cockayne syndrome proteins CSA and CSB

Derrick M. Leach and Andrew J. Rainbow\*

Department of Biology, McMaster University, 1280 Main Street West, Hamilton, Ontario L8S 4K1, Canada.

\*To whom correspondence should be addressed. Department of Biology, McMaster University, 1280 Main Street West, Hamilton, Ontario L8S 4K1, Canada. Tel: +1 905 525 9140 ext. 23544; Fax: +1 905 522 6066; Email: rainbow@mcmaster.ca

Received on April 29, 2010; revised on August 22, 2010;  
accepted on September 20, 2010

**Reduced host cell reactivation (HCR) of a reporter gene containing 8-oxoguanine (8-oxoG) lesions in Cockayne syndrome (CS) fibroblasts has previously been attributed to increased 8-oxoG-mediated inhibition of transcription resulting from a deficiency in repair. This interpretation has been challenged by a report suggesting reduced expression from an 8-oxoG containing reporter gene occurs in all cells by a mechanism involving gene inactivation by 8-oxoG DNA glycosylase and this inactivation is strongly enhanced in the absence of the CS group B (CSB) protein. The observation of reduced gene expression in the absence of CSB protein led to speculation that decreased HCR in CS cells results from enhanced gene inactivation rather than reduced gene reactivation. Using an adenovirus-based  $\beta$ -galactosidase ( $\beta$ -gal) reporter gene assay, we have examined the effect of methylene blue plus visible light (MB + VL)-induced 8-oxoG lesions on the time course of gene expression in normal and CSA and CSB mutant human SV40-transformed fibroblasts, repair proficient and CSB mutant Chinese hamster ovary (CHO) cells and normal mouse embryo fibroblasts. We demonstrate that MB + VL treatment of the reporter leads to reduced expression of the damaged  $\beta$ -gal reporter relative to control at early time points following infection in all cells, consistent with *in vivo* inhibition of RNA polIII-mediated transcription. In addition, we have demonstrated HCR of reporter gene expression occurs in all cell types examined. A significant reduction in the rate of gene reactivation in human SV40-transformed cells lacking functional CSA or CSB compared to normal cells was found. Similarly, a significant reduction in the rate of reactivation in CHO cells lacking functional CSB (CHO-UV61) was observed compared to the wild-type parental counterpart (CHO-AA8). The data presented demonstrate that expression of an oxidatively damaged reporter gene is reactivated over time and that CSA and CSB are required for normal reactivation.**

### Introduction

The correct chemical structure of DNA bases allows the specific pairing of adenine with thymine and guanine with

cytosine, forming the basis by which accurate transmission of hereditary information through DNA replication and functional information through transcription occurs. The chemical properties of the bases leave them susceptible to alteration by a number of factors including reactive oxygen species (ROS) generated endogenously by metabolic processes of the cell, from environmental sources including ultraviolet (UV) radiation, ionising radiation and dietary sources. Due to its low redox potential, guanine is particularly susceptible to oxidation by ROS and can form a large number of oxidised products (1). Of the many oxidised guanine products formed, 7,8-dihydro-8-oxoguanine (8-oxoguanine; 8-oxoG) is one of the most frequent forms of oxidative DNA lesions generated in living cells (2). 8-oxoG can functionally mimic T, allowing it to easily base pair with either A or C during replication and transcription. Failure to recognise and repair an improper 8-oxoG:A following replication results in G to T transversions during replication and mutant transcripts during transcription of nascent mRNAs (1). The base excision repair (BER) pathway is responsible for removing oxidised bases, including 8-oxoG from chromosomal DNA and relies on DNA glycosylases to recognise specific lesions and initiate the repair process (3). 8-oxoguanine DNA glycosylase (hOGG1 in humans; OGG1 in mice) recognises 8-oxoG lesions base-paired with C and catalyses excision of the damaged base, initiating its repair (for a review of BER, see ref. 3). In addition, the Cockayne syndrome group B protein (CSB) has been shown to be involved in processing of the lesion (4–6). Among the many functions of CSB, the best studied to date is the role it plays in conjunction with the Cockayne syndrome group A (CSA) protein in coupling transcription by RNA polymerase II (polII) to repair of nucleotide excision repair (NER) substrates in actively transcribed genes via the transcription-coupled repair (TCR) subpathway of NER (7). Mutations in CSA and CSB in humans normally causes Cockayne syndrome, a segmental progeroid syndrome characterised by premature ageing and neurodegeneration beginning in early childhood (8). Using a plasmid-based  $\beta$ -galactosidase ( $\beta$ -gal) reporter gene treated with the photosensitiser methylene blue (MB) activated by visible light (VL) to generate 8-oxoG lesions, Spivak and Hanawalt (9) showed a reduced level of expression in SV40-transformed human fibroblasts deficient for CSA and CSB compared to normal. This observation was interpreted as defective host cell reactivation (HCR) of the reporter gene in CSA and CSB cells resulting from impaired removal of 8-oxoG, with the persistent 8-oxoG lesions hindering reporter gene transcription by RNA polIII. The interpretation of this observation as an inability of cells lacking CSA and CSB to properly process methylene blue plus visible light (MB + VL)-induced 8-oxoG and reactivate gene expression has recently been challenged. Using a plasmid-based reporter construct, Khobta *et al.* (10) examined the expression of a MB + VL-treated green fluorescent protein (GFP) reporter gene in

D. M. Leach and A. J. Rainbow

spontaneously transformed mouse embryo fibroblasts (MEFs) between 8 and 48 h after transfection. Compared to the non-damaged control vector, the 8-oxoG containing reporter demonstrated the same level of transcription at 8 h with ~50% reduction in transcription over a subsequent 40-h period (10). In addition to wild-type (WT) MEFs, reporter gene expression was also examined in *Csb<sup>mi/m</sup>*, *Ogg1<sup>-/-</sup>* and *Csb<sup>mi/m</sup> Ogg1<sup>-/-</sup>*-immortalised MEFs. The authors suggest that *Ogg1* mediates inactivation of the reporter gene and that the effect is considerably enhanced by the absence of functional CSB (10). Based on their finding of no difference in reporter gene expression from damaged and undamaged plasmids at 8 h after infection, Khobta *et al.* (10) also conclude that 8-oxoG does not impede RNA polIII. In addition, they conclude that the decreased expression levels of the oxidatively damaged reporter gene in CSB-deficient cells compared to normal cells (9,11) are not due to the lack of CSB-mediated repair/reactivation of the reporter construct, but rather *Ogg1/hOGG1* mediated inactivation that is enhanced in the absence of functional CSB. Recently presented data by the same group (12) demonstrated decreased acetylation of histone H4 in oxidatively damaged plasmid DNA introduced into HeLa cells, suggesting gene silencing may be mediated by chromatin alterations in the 8- to 48-h period following transfection of the plasmid.

To further study the effect of 8-oxoG on gene expression, we have examined expression of a recombinant adenovirus-encoded  $\beta$ -gal reporter gene damaged by MB + VL in normal and CSA and CSB mutant SV40-transformed human fibroblasts; WT MEFs and repair-proficient and repair-deficient CHO cells with a mutation in the hamster CSB homologue. We demonstrate that MB + VL treatment of the reporter gene leads to reduced expression relative to control at early time points following infection in all cells examined and that HCR of reporter gene expression occurs in all cell types examined by a mechanism requiring CSA and CSB.

## Materials and methods

### Cells, virus and culture conditions

The SV40-transformed fibroblasts GM637F (normal), CSA-SV40 (CS3BE.S3.G1) and CSB-SV40 (CS1AN.S3.G2) were obtained from NIGMS (Camden, NJ, USA). The spontaneously transformed MEF line WT MEF (ERCC1<sup>+/+</sup>; referred to as WT MEF hereafter) (13) was obtained from Dr X-D Zhu McMaster University, Hamilton, Ontario, Canada. The SV40-transformed mouse embryo fibroblast cell line BC1-6 was from Dr S.E. Andrew University of Alberta, Edmonton, Alberta and has been previously described (14). The Chinese hamster ovary (CHO) cell lines CHO-AA8 (repair proficient parental) and CHO-UV61 (repair deficient) were provided by Dr Larry Thompson, Lawrence Livermore National Laboratory, Livermore, CA with the help of Dr Gordon Whitmore, Physics Division, Ontario Cancer Institute, Toronto, Ontario. Cell cultures were grown at 37°C in a humidified incubator in 5% CO<sub>2</sub> and cultured in Eagle's  $\alpha$ -minimal essential media ( $\alpha$ -MEM) supplemented with 10% foetal bovine serum and antimycotic antibiotic (100  $\mu$ g/ml penicillin, 100  $\mu$ g/ml streptomycin and 250 ng/ml amphotericin B). The recombinant adenoviruses Ad5HCMVlacZ (AdCA17) and Ad5MCMVlacZ (AdCA35) were obtained from The Robert E. Fitzhenry Vector Laboratory, McMaster University, Hamilton, Ontario. The viruses were propagated, collected and titered as described previously (15).

### Treatment of the virus with MB + VL

Preparation of MB was carried out under minimal ambient light conditions as described previously (16). Treatment of the virus was performed under minimal ambient light conditions as described previously (17). Briefly, a 4 ml volume of 20  $\mu$ g/ml (53.5  $\mu$ M) MB solution was prepared by diluting the MB stock in cold phosphate-buffered saline (PBS) (4°C) in a 35-mm Petri dish and subsequently shielded from any ambient light. An appropriate volume of stock

Ad5MCMVlacZ was added to the Petri dish containing the MB solution in order to obtain the desired multiplicity of infection (MOI) upon infecting cells. Prior to exposing the virus to VL, an aliquot was removed for use as the undamaged control. The solution was then exposed to VL using a 1000 W bulb (General Electric, GE R1000) at a distance of 82 cm from the source for a defined period of time while being kept on ice with continuous stirring. After each defined VL exposure, aliquots were removed for use in infecting cells. The aliquots were diluted in unsupplemented  $\alpha$ -MEM and used to infect cells.

### Treatment of the virus with UVC

UV irradiation of the virus was carried out as previously described (18). Briefly, the virus was resuspended in a 35-mm Petri dish in cold PBS at the appropriate dilution to achieve an MOI of 100 pfu/ml upon infection of cells. Using a General Electric germicidal lamp (model G8T5) emitting predominantly at 254 nm, the virus was irradiated with stirring on ice with an incident fluence rate of 2 J/m<sup>2</sup>/sec. After each UV exposure, 200  $\mu$ l aliquots were removed from the viral preparation and appropriately diluted using unsupplemented  $\alpha$ -MEM.

### $\beta$ -Galactosidase reporter gene expression assay (HCR)

We have previously reported a HCR assay for examining BER of MB + VL-induced 8-oxoG lesions in a number of different cell strains (16,17,19). The HCR assay utilises a recombinant non-replicating adenovirus (Ad) expressing the  $\beta$ -gal reporter gene under control of (16,17,19) the murine cytomegalovirus immediate early promoter (20) to examine the ability of different cell types to remove damage and reactivate reporter gene expression. Upon exposure to VL, MB leads to the formation of 8-oxoG lesions with a small number of other single-base oxidative lesions occurring (21,22). Cells were seeded for confluence (SV40-transformed cells at  $3.5 \times 10^4$  cells per well; MEFs and CHO cells at  $4 \times 10^4$  cells per well) in 96-well plates (Falcon, Franklin Lakes, NJ, USA). After seeding, cells were incubated for 18–24 h and subsequently infected with 40  $\mu$ l of untreated or MB + VL-treated virus for 90 min at a MOI of 100 pfu/cell. Following the 90-min viral absorption period, the infection medium was aspirated and cells were overlaid with 200 ml of complete  $\alpha$ -MEM and incubated for a further 1, 2, 3, 6, 12, 24 or 44 h before harvesting for measurement of  $\beta$ -gal activity. For the time course experiments, cells from the same pool were seeded into separate 96-well plates for each time point and infected with virus from the same preparation. A single HCR experiment consisted of triplicate wells for each treatment of the virus and triplicate wells of non-infected cells were used to obtain background levels of  $\beta$ -gal activity.  $\beta$ -Gal activity was scored as previously described (23).

### Graphing and statistical analysis

All curves for inactivation of  $\beta$ -gal activity following MB + VL treatment of the virus were plotted using Origin Laboratory software. Each point on the graphs represents an arithmetic mean  $\pm$  standard error of triplicate determinations of the  $\beta$ -gal activity at each VL exposure to the virus relative to the untreated control for single representative experiments.  $D_{37}$  values for each cell line were obtained by extrapolation from the HCR survival curves from each independent experiment.  $D_{37}$  values for each cell type were then calculated relative to the indicated repair-proficient cell line used within the same experiment and used as a measure of relative HCR capacity. For individual time course experiments, the  $D_{37}$  values for each cell line at each time point were calculated relative to the indicated repair proficient normal at 12 h after infection. The data calculated in this manner were pooled from independent experiments to construct the  $D_{37}$  reactivation time course curves. Statistical analysis of differences between relative  $D_{37}$  values was carried out using a one-sample two-tailed *t*-test with a confidence interval of 0.05. The  $\chi^2$  goodness of fit test was used to quantify how well the  $D_{37}$  reactivation time course curves for repair-deficient cell lines matched the curves for the appropriate repair-proficient control cell line over the range of time points examined (24). For comparison of two cell types,  $\chi^2$  values were obtained for each time point and summed over the indicated ranges to obtain *P*-values representing the goodness of fit between the two  $D_{37}$  reactivation curves.

## Results

### Normal HCR of the MB + VL-damaged reporter gene in SV40-transformed human skin fibroblasts requires CSA and CSB

In the present work, we first examined expression from a MB + VL-damaged reporter gene using our recombinant adenovirus-based  $\beta$ -gal gene. In agreement with the results of Spivak and Hanawalt (9) using a plasmid-based reporter gene, we find a significant deficiency in reporter gene expression

from CSA-SV40 and CSB-SV40 fibroblasts compared to the normal GM637F fibroblasts 44 h following infection with the MB + VL-treated adenovirus (Figure 1). Similar results were obtained at 24 h following infection with the MB + VL-treated adenovirus (data not shown). To investigate whether reactivation of reporter gene expression was taking place, we examined the expression of the MB + VL-treated reporter gene at various times after infection with the MB + VL-treated adenovirus. To facilitate examining expression at very early time points following infection, we used the AdCA35 virus, which drives higher levels of transgene expression than AdCA17 (20). The expression of the MB + VL-treated reporter gene was reduced compared to the non-treated reporter at early times after infection and expression of the damaged reporter gene increased when  $\beta$ -gal expression was assayed at later times (Figure 2A). The  $D_{37}$  time course curve (Figure 2B) was plotted using  $D_{37}$  values obtained from HCR plots. Expression of the  $\beta$ -gal reporter is reactivated by the host cell reaching a maximum level by 12 h in both normal and CS-deficient SV40-transformed fibroblasts. The rate of reactivation was significantly reduced in CSA-SV40 and CSB-SV40 compared to GM637F as measured by the  $\chi^2$  goodness of fit test ( $P < 0.05$ ).

It has been reported that repair of UV-induced cyclobutane pyrimidine dimers in plasmids results in a time dependant recovery of transcription from damaged genes resulting from the gradual removal of UV-induced transcription blocking lesion (9,10,25,26). In contrast to the levelling off of reactivation by 12 h after infection for the MB + VL-treated reporter gene, infection of cells with a UVC-treated reporter

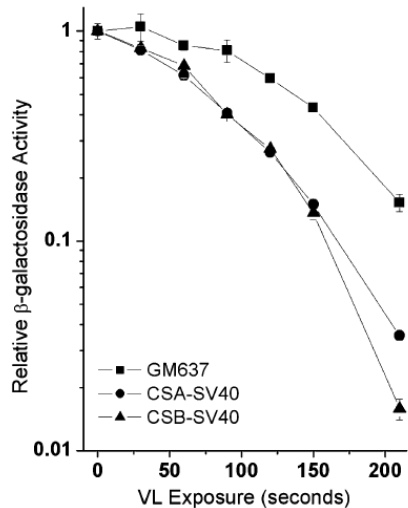


**Fig. 1.** Reduced HCR of the MB + VL-treated reporter in SV40-transformed CSA and CSB fibroblasts compared to the SV40-transformed normal fibroblast GM637F. CSA-SV40 and CSB-SV40 fibroblasts demonstrate a reduced capacity to reactivate  $\beta$ -gal expression from the MB + VL-treated reporter gene (AdCA17) 44 h after infection compared to the normal SV40-transformed fibroblast GM637F. The above  $\beta$ -gal survival curve is from a representative experiment done in triplicate. Each point represents  $\beta$ -gal expression for the given VL dose  $\pm$  standard error. The average relative  $D_{37}$  values compared to G637F for CSA-SV40 and CSB-SV40 at 44 h (0.70 and 0.71, respectively) for three independent experiments were significantly decreased by one-sample two-tailed  $t$ -test ( $P < 0.05$ ). A similar significant decrease in relative  $D_{37}$  was observed for CSA-SV40 and CSB-SV40 compared to GM637F at 24 h after infection (data not shown).

gene resulted in a continual increase in reporter gene expression from 1 to 72 h after infection of GM637F cells (Figure 2C). Expression from the UVC-damaged virus increased at a significantly slower rate in CSA-SV40 and CSB-SV40 ( $P < 0.05$  by  $\chi^2$  goodness of fit test), consistent with defective TCR-NER and proficient global genome repair-NER in these cells.

#### Reactivation of expression from a MB + VL-damaged $\beta$ -gal reporter gene in rodent cells

The experiments showing inactivation of a reporter gene containing oxidative DNA damage were carried out using normal and CSB-deficient MEFs (10). To address the possibility of a difference between human and rodent cells, we next examined expression of the MB + VL-damaged adenovirus-based reporter gene in MEFs and CHO cells. Expression of the MB + VL-treated reporter gene was measured in two different MEF lines. It can be seen that expression of the MB + VL-treated reporter gene increased over time reaching a maximum at 12 h in both WT MEF and BC1-6 (Figure 3A and B). Reporter gene expression was found to be significantly increased between 3 and 12 h for both WT MEF ( $P = 0.02$ ) and BC1-6 ( $P = 0.009$ ) by a two-sample  $t$ -test. At time points from 12 to 44 h after infection, we observed a slight decrease in the relative  $D_{37}$  value consistent with results published for the expression of a plasmid-based reporter gene during this time period (10,12). However, in the current work, the difference in the relative  $D_{37}$  value at 24 or 44 h compared to 12 h was not significant.

We also examined the time course of  $\beta$ -gal expression in repair-proficient and repair-deficient CHO cells to determine if the observed reactivation was specific to mice or if it occurred in other rodent species and to examine the role of CSB in gene reactivation. Figure 4A shows typical inactivation curves for  $\beta$ -gal activity in the repair-proficient parental line CHO-AA8 and the repair-deficient line CHO-UV61 carrying a mutation in the hamster homologue of CSB (27) and Figure 4B shows the time course of gene reactivation. These results demonstrate that the expression of the  $\beta$ -gal reporter was reactivated by the host cell in both CHO-AA8 and CHO-UV61 cells. This reactivation was significant by two-sample  $t$ -test from 3 to 6 h for CHO-AA8 ( $P = 0.009$ ) and 3 to 12 h in CHO-UV61 ( $P = 0.001$ ). In addition, the increase in reactivation over time (3–44 h) was significantly reduced in the CSB mutant CHO-UV61 compared to CHO-AA8 as determined by the  $\chi^2$  goodness of fit test ( $P = 0.0439$ ).

## Discussion

The data presented here demonstrate that expression of a reporter gene containing oxidative DNA lesions is reactivated over time (1–12 h) by host cell mechanisms and that a normal level of reactivation in human fibroblasts requires the CSA and CSB gene products. The previous report by Khobta *et al.* examined the time course of expression from a plasmid-based reporter containing low levels of 8-oxoG in MEFs beginning 8–12 h after introduction through to 48 h. A reduction in gene expression with time was observed in repair-proficient WT MEFs, repair-deficient *Ogg1*<sup>-/-</sup> MEFs and to a greater extent in *Csb*<sup>ml/m</sup> MEFs expressing a mutated copy of CSB mimicking the mutation in the human patient CS1AN (10,28). Based on their results, they suggested that oxidative DNA damage led to *Ogg1/CSB*-mediated reporter gene inactivation (10).

D. M. Leach and A. J. Rainbow

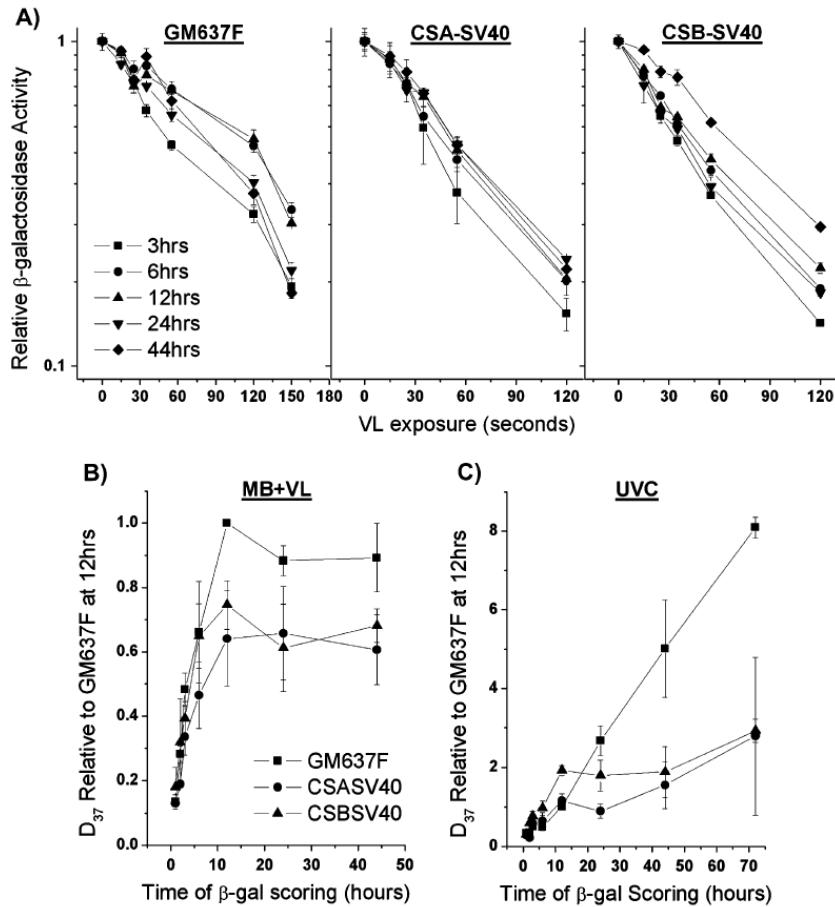


**Fig. 2.** Time course of gene reactivation for MB + VL or UVC-damaged AdCA35 in SV40-transformed normal and CS fibroblasts. (A) HCR curves for  $\beta$ -gal expression from MB + VL-treated AdCA35 over time (3–44 h) in SV40-transformed human skin fibroblasts. Cells were infected with the MB + VL-treated (or mock treated) AdCA35 at an MOI of 100 pfu/cell and subsequently harvested for  $\beta$ -gal expression at 3, 6, 12, 24 and 44 h following infection. Representative survival curves for  $\beta$ -gal expression in SV40-transformed cells are shown. Each point is an average  $\pm$  standard error (SE) of triplicate determinations. (B) Time course of gene reactivation (relative  $D_{37} \pm$  SE) for MB + VL-damaged AdCA35 in SV40-transformed normal and CS-deficient fibroblasts shows reduced reactivation of reporter gene expression in CSA- and CSB-deficient fibroblasts. The increase in gene reactivation is significantly reduced in CSA-SV40 (6–44 h,  $P = 0.04$  and 12–44 h,  $P = 0.02$ ) and CSB-SV40 (3–44 h,  $P = 0.03$ ; 6–44 h,  $P = 0.03$ ; 12–44 h,  $P = 0.01$ ; 24–44 h,  $P = 0.009$ ) compared to GM637F as determined by the  $\chi^2$  goodness of fit test. (C) Time course of gene reactivation (relative  $D_{37} \pm$  SE) of UV damaged AdCA35 in SV40-transformed normal and CS-deficient fibroblasts. The increase in gene reactivation is significantly reduced in CSA-SV40 (6–72 h,  $P = 0.03$ ; 12–72 h,  $P = 0.01$ ; 24–72 h,  $P = 0.006$  and 44–72 h,  $P = 0.02$ ) and CSB-SV40 (for all time ranges: 3–72 h, 6–72 h, 12–72 h, 24–72 h, 44–72 h,  $P < 0.0001$ ) compared to GM637F as determined by the  $\chi^2$  goodness of fit test. For both (B and C), each point on the curves is the arithmetic average of at least three independent experiments done in triplicate determinations  $\pm$  SE.

In the current work, we show that the change in relative  $D_{37}$  for expression of the MB + VL-treated adenovirus-encoded reporter gene slows and levels off from 12 to 44 h; however, no significant differences were observed between pooled relative  $D_{37}$  values over that time period. More importantly, compared to early times after infection (1–3 h), expression from the MB + VL-treated reporter was significantly increased at the later time points consistent with gene reactivation.

While the ability of 8-oxoG to block RNA polIII transcription has been disputed (29–32), the observation that CSB can improve RNA polIII elongation through 8-oxoG lesions suggests that at the very least, 8-oxoG leads to transient stalling of the RNA polIII transcription complex (29). We demonstrate here that at early times after infection (1–3 h) with the reporter gene containing MB + VL-induced oxidative damage, gene expression is inhibited compared to the

undamaged control in all cell types examined. The decrease in expression from the MB + VL-damaged adenovirus reporter compared to the undamaged control for all VL doses is consistent with an *in vivo* decrease of RNA polIII transcription due to 8-oxoG lesions on the template strand. Reactivation of gene expression is consistent with BER and/or bypass of 8-oxoG lesions.

It has been shown that repair of 8-oxoG in MEF genomic DNA, as measured by loss of formamidopyrimidine-DNA glycosylase-sensitive sites (FSS) is  $\sim 50\%$  complete 4 h after induction by a photosensitizer (*Ro 19-8022*) and VL,  $>80\%$  complete by 8 hrs and nearly 100% complete at 16 h (33). In the current work, expression of the MB + VL-damaged reporter gene in MEFs, CHO cells and human fibroblasts was found to be significantly increased between 1 and 12 h, but levelled off by 12 h after infection. This suggests that

Reduced HCR of oxidatively damaged DNA in CS cells

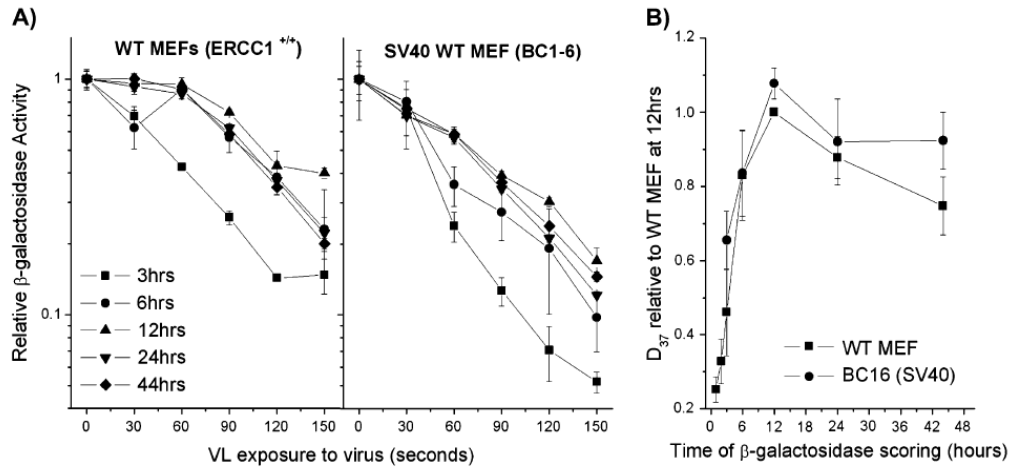


**Fig. 3.** Time course of gene reactivation for MB + VL-damaged AdCA35 in WT MEFs (A) HCR curves for  $\beta$ -gal expression over time in MEFs. The spontaneously transformed MEFs WT MEF and the SV40-transformed MEFs BC1-6 were infected with MB + VL-damaged (or mock treated) AdCA35 at an MOI of 100 pfu/cell and subsequently harvested for  $\beta$ -gal expression at 1, 2, 3, 6, 12, 24 and 44 h after infection. Representative survival curves for  $\beta$ -gal expression for both MEF cell lines examined 3–44 h after infection are shown. Each point is an average  $\pm$  standard error (SE) of triplicate determinations. (B) Change in the  $D_{37}$  value for each cell line at each time point were normalised to the  $D_{37}$  value obtained for WT MEF at 12 h for at least three independent experiments each done in triplicate. Each point is the average of the pooled results  $\pm$  SE.

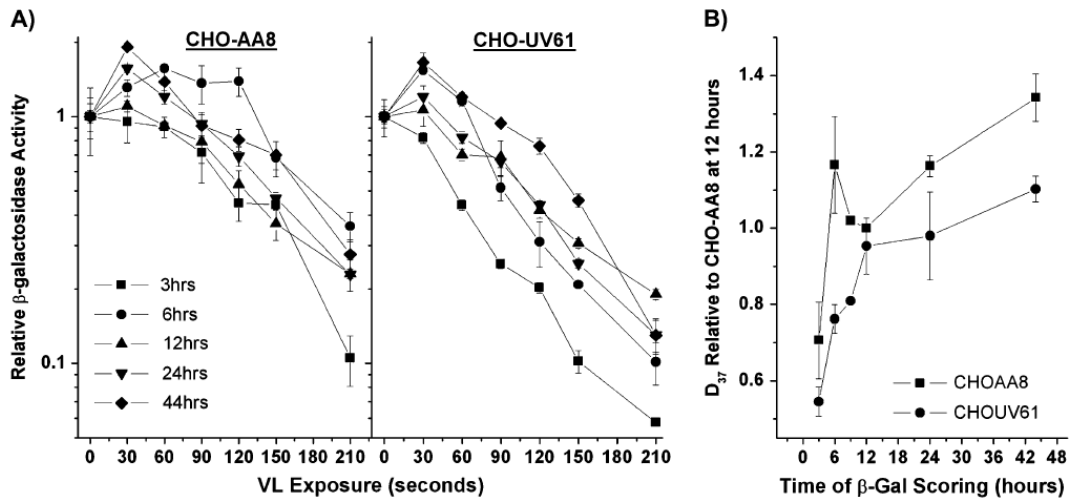


**Fig. 4.** Time course of gene reactivation for MB + VL-damaged AdCA35 in repair-proficient and repair-deficient CHO cells. (A) HCR curves for  $\beta$ -gal expression over time in CHO cells. CHO-AA8 and the CHO-UV61 cells were infected with MB + VL-damaged (or mock treated) AdCA35 at an MOI of 100 pfu/cell and subsequently harvested for  $\beta$ -gal expression at 3, 6, 9, 12, 24 and 44 h after infection. Representative survival curves for  $\beta$ -gal expression for both CHO cell lines examined 3–44 h after infection are shown. Each point is an average  $\pm$  standard error (SE) of triplicate determinations. (B) Change in the  $D_{37}$  value for each cell line at each time point were normalised to the  $D_{37}$  value obtained for CHO-AA8 at 12 h for at least three independent experiments each done in triplicate ( $n = 1$  for 9-h time point,  $n = 2$  for 24 and 44 h). Each point is the average of the pooled results  $\pm$  SE. The increase in gene reactivation is significantly reduced in CHO-UV61 compared to CHO-AA8 cells of the time points examined (3–44 h,  $P = 0.0439$ ; 6–44 h,  $P = 0.025$ ; 12–44 h,  $P = 0.0301$ ; 24–44 h,  $P = 0.0085$ ) as determined by the  $\chi^2$  goodness of fit test.

reactivation of the reporter gene is near completion by 12 h after infection, consistent with the time course for removal of 8-oxoG lesions from cellular DNA. In contrast, reactivation of the UVC-damaged reporter gene in the GM637F normal human fibroblasts continued to increase from 1 to 72 h after infection, consistent with the longer time course for removal of UVC-induced DNA damage in human cellular DNA (34,35).

Similar to human fibroblasts and MEFs, we observed a significant increase in reporter gene expression relative to

control in WT CHO-AA8 cells and mutant CHO-UV61. The results presented are consistent with a role for the CSB homologue in hamsters in repair and/or bypass of MB + VL-induced 8-oxoG. The rate of change in relative  $D_{37}$  over time in CHO cells slows between 12 and 24 h; however, the continuous increase in gene expression over the time points examined suggests reactivation of MB + VL-induced 8-oxoG continues over a longer period of time in CHO cells compared to MEFs. Hamster cells do indeed repair 8-oxoG, as measured by loss of FSS at a slower rate than mouse cells with only 56%

D. M. Leach and A. J. Rainbow

of FSS removed at 8 h (36) compared to >80% in mouse cells at the same time point (33). The hamster homologue of CSB, which is involved in repair of UV-induced damage (27) and oxidative damage (36), shows no significant involvement in RNA polIII-mediated transcription (27). This suggests that CSB-stimulated lesion bypass and/or coupling of repair to transcription may be absent in hamster cells, possibly accounting for slower repair and subsequent gene reactivation.

It is possible that the decreased level of gene expression seen in MEFs lacking functional CSB compared to WT MEFs, as previously reported (10), could result from a failure of cells lacking CSB to reactivate gene expression from a damaged reporter to WT levels prior to 12 h. In the current work, we were unable to detect a significant change in expression of the MB + VL-treated reporter between 12 and 44 h after infection, whereas Khobta *et al.* (10) demonstrated a significant decrease in reporter gene expression over this time period. This difference could result from differences in the experimental conditions and the reporter gene employed.

Both studies employed MB + VL to generate 8-oxoG lesions in the reporter gene. MB + VL induces high yields of 8-oxoG, while oxidative pyrimidine modifications, sites of base loss and single-strand breaks (SSBs) are rare (37). The generation of SSBs by MB + VL has been shown to occur at a rate of ~0.1 modifications per 10 000 bp, while 8-oxoG occurs at a rate of 2.7 modifications per 10 000 bp in supercoiled plasmid DNA (37). A similar ratio of SSBs to 8-oxoG lesions was observed in DNA isolated from treated bacteria (37) suggesting the mechanism and profile of DNA damage is independent of the system in which it is treated. Khobta *et al.* (10) employed MB + VL treatment of covalently closed plasmids of 0.8  $\mu$ M MB + VL exposures resulting in the induction of an average of three FSS per plasmid, corresponding to an average of ~0.5 FSS per transcribed strand of their GFP-encoding reporter gene. In the present work, we employed 53.5  $\mu$ M MB plus from 10 to 150 sec VL treatment to the recombinant adenovirus-encoding lacZ reporter gene. Previous reports have shown that treatment of adenovirus with MB + VL has negligible effects on the protein capsid and subsequent infectivity of viral particles (38). Preliminary results indicate that VL exposures to the virus of 10–150 sec would result in an average of about one to six FSS per transcribed strand of the lacZ reporter gene (data not shown). This indicates that the 8-oxoG lesion frequency from VL exposures to the virus of 10–150 sec used in the HCR experiments reported here were somewhat greater those used in the study by Khobta *et al.*, although of a similar order of magnitude.

In the work presented here, we utilised an adenovirus-based reporter system with confluent cultures, whereas Khobta *et al.* used a plasmid-based system with exponentially growing cultures (10,39). Regardless of the level of DNA damage, p53 upregulation, transcriptional activation and p53-dependant apoptosis are attenuated in confluent cultures compared to sparse growing cultures lacking cell–cell contacts (40). The higher cell density of the confluent cultures used in the current work may more closely reproduce the microenvironment in a living organism and account for the observed difference in gene inactivation. Differences in the level of expression and stability of the adenovirus encoded compared to the plasmid encoded reporter gene may account for the difference in the level of gene inactivation observed. Differences in the degree of chromatin association/modification between the two systems may also contribute to the difference (12).

## Funding

National Cancer Institute of Canada with funds from the Canadian Cancer Society (16066).

## Acknowledgements

We thank Robert W. Cowan, Faculty of Health Sciences, McMaster University and Shaqil Kassam, Faculty of Science, McMaster University, for performing initial experiments showing reduced HCR of the MB + VL-treated adenovirus-encoded reporter gene in CHO-UV61 compared to CHO-AA8 cells and in CSB-SV40 fibroblasts compared to GM637F, respectively.

Conflict of interest statement: None declared.

## References

- Neeley, W. L. and Essigmann, J. M. (2006) Mechanisms of formation, genotoxicity, and mutation of guanine oxidation products. *Chem. Res. Toxicol.*, **19**, 491–505.
- Park, E. M., Shigenaga, M. K., Degan, P., Kom, T. S., Kitzler, J. W., Wehr, C. M., Kolachana, P. and Ames, B. N. (1992) Assay of excised oxidative DNA lesions: isolation of 8-oxoguanine and its nucleoside derivatives from biological fluids with a monoclonal antibody column. *Proc. Natl. Acad. Sci. U.S.A.*, **89**, 3375–3379.
- David, S. S., O'Shea, V. L. and Kundu, S. (2007) Base-excision repair of oxidative DNA damage. *Nature*, **447**, 941–950.
- Dianov, G., Bischoff, C., Sunesen, M. and Bohr, V. A. (1999) Repair of 8-oxoguanine in DNA is deficient in Cockayne syndrome group B cells. *Nucleic Acids Res.*, **27**, 1365–1368.
- Osterod, M., Larsen, E., Le Page, F., Hengstler, J. G., Van Der Horst, G. T., Boiteux, S., Klungland, A. and Epe, B. (2002) A global DNA repair mechanism involving the Cockayne syndrome B (CSB) gene product can prevent the in vivo accumulation of endogenous oxidative DNA base damage. *Oncogene*, **21**, 8232–8239.
- Tuo, J., Jaruga, P., Rodriguez, H., Bohr, V. A. and Dizdaroğlu, M. (2003) Primary fibroblasts of Cockayne syndrome patients are defective in cellular repair of 8-hydroxyguanine and 8-hydroxyadenine resulting from oxidative stress. *FASEB J.*, **17**, 668–674.
- Cleaver, J. E., Lam, E. T. and Revet, I. (2009) Disorders of nucleotide excision repair: the genetic and molecular basis of heterogeneity. *Nat. Rev. Genet.*, **10**, 756–768.
- Nance, M. A. and Berry, S. A. (1992) Cockayne syndrome: review of 140 cases. *Am. J. Med. Genet.*, **42**, 68–84.
- Spivak, G. and Hanawalt, P. C. (2006) Host cell reactivation of plasmids containing oxidative DNA lesions is defective in Cockayne syndrome but normal in UV-sensitive syndrome fibroblasts. *DNA repair*, **5**, 13–22.
- Khobta, A., Kitsera, N., Speckmann, B. and Epe, B. (2009) 8-Oxoguanine DNA glycosylase (Ogg1) causes a transcriptional inactivation of damaged DNA in the absence of functional Cockayne syndrome B (Csb) protein. *DNA repair*, **8**, 309–317.
- Pastoriza-Gallego, M., Amier, J. and Sarasin, A. (2007) Transcription through 8-oxoguanine in DNA repair-proficient and Csb(-)/Ogg1(-) DNA repair-deficient mouse embryonic fibroblasts is dependent upon promoter strength and sequence context. *Mutagenesis*, **22**, 343–351.
- Khobta, A., Anderhub, S., Kitsera, N. and Epe, B. (2010) Gene silencing induced by oxidative DNA base damage: association with local decrease of histone H4 acetylation in the promoter region. *Nucleic Acids Res.*, **38**, 4285–4295.
- Zhu, X. D., Niedernhofer, L., Kuster, B., Mann, M., Hoeijmakers, J. H. and de Lange, T. (2003) ERCC1/XPF removes the 3' overhang from uncapped telomeres and represses formation of telomeric DNA-containing double minute chromosomes. *Mol. Cell*, **12**, 1489–1498.
- Fritzell, J. A., Narayanan, L., Baker, S. M. *et al.* (1997) Role of DNA mismatch repair in the cytotoxicity of ionizing radiation. *Cancer Res.*, **57**, 5143–5147.
- Graham, F. L. and Prevec, L. (eds.) (1991) *Methods in Molecular Biology*. Humana Press, Clifton, NJ, USA.
- Pitsikas, P., Lee, D. and Rainbow, A. J. (2007) Reduced host cell reactivation of oxidative DNA damage in human cells deficient in the mismatch repair gene hMSH2. *Mutagenesis*, **22**, 235–243.
- Kassam, S. N. and Rainbow, A. J. (2007) Deficient base excision repair of oxidative DNA damage induced by methylene blue plus visible light in xeroderma pigmentosum group C fibroblasts. *Biochem. Biophys. Res. Commun.*, **359**, 1004–1009.

18. Bennett, C. B. and Rainbow, A. J. (1988) Enhanced reactivation and mutagenesis of UV-irradiated adenovirus in normal human fibroblasts. *Mutagenesis*, **3**, 157–164.
19. Kassam, S. N. and Rainbow, A. J. (2009) UV-inducible base excision repair of oxidative damaged DNA in human cells. *Mutagenesis*, **24**, 75–83.
20. Addison, C. L., Hitt, M., Kunsken, D. and Graham, F. L. (1997) Comparison of the human versus murine cytomegalovirus immediate early gene promoters for transgene expression by adenoviral vectors. *J. Gen. Virol.*, **78**, 1653–1661.
21. Floyd, R. A., West, M. S., Eneff, K. L. and Schneider, J. E. (1989) Methylene blue plus light mediates 8-hydroxyguanine formation in DNA. *Arch. Biochem. Biophys.*, **273**, 106–111.
22. Tuite, E. M. and Kelly, J. M. (1993) Photochemical interactions of methylene blue and analogues with DNA and other biological substrates. *J. Photochem. Photobiol.*, **21**, 103–124.
23. Pitsikas, P., Francis, M. A. and Rainbow, A. J. (2005) Enhanced host cell reactivation of a UV-damaged reporter gene in pre-UV-treated cells is delayed in Cockayne syndrome cells. *J. Photochem. Photobiol.*, **81**, 89–97.
24. Bevington, P. R. and Robinson, D. K. (eds.) (2003) *Data Reduction and Error Analysis for the Physical Sciences*. McGraw-Hill, Boston, MA, USA.
25. Ganesan, A. K., Hunt, J. and Hanawalt, P. C. (1999) Expression and nucleotide excision repair of a UV-irradiated reporter gene in unirradiated human cells. *Mutat. Res.*, **433**, 117–126.
26. Johnson, J. M. and Latimer, J. J. (2005) Analysis of DNA repair using transfection-based host cell reactivation. *Methods Mol. Biol.*, **291**, 321–335.
27. Orren, D. K., Dianov, G. L. and Bohr, V. A. (1996) The human CSB (ERCC6) gene corrects the transcription-coupled repair defect in the CHO cell mutant UV61. *Nucleic Acids Res.*, **24**, 3317–3322.
28. van der Horst, G. T., van Steeg, H., Berg, R. J. *et al.* (1997) Defective transcription-coupled repair in Cockayne syndrome B mice is associated with skin cancer predisposition. *Cell*, **89**, 425–435.
29. Charlet-Berguerand, N., Feuerhahn, S., Kong, S. E., Zisman, H., Conaway, J. W., Conaway, R. and Egly, J. M. (2006) RNA polymerase II bypass of oxidative DNA damage is regulated by transcription elongation factors. *EMBO J.*, **25**, 5481–5491.
30. Kathe, S. D., Shen, G. P. and Wallace, S. S. (2004) Single-stranded breaks in DNA but not oxidative DNA base damages block transcriptional elongation by RNA polymerase II in HeLa cell nuclear extracts. *J. Biol. Chem.*, **279**, 18511–18520.
31. Kuraoka, I., Endou, M., Yamaguchi, Y., Wada, T., Handa, H. and Tanaka, K. (2003) Effects of endogenous DNA base lesions on transcription elongation by mammalian RNA polymerase II. Implications for transcription-coupled DNA repair and transcriptional mutagenesis. *J. Biol. Chem.*, **278**, 7294–7299.
32. Tornaletti, S., Maeda, L. S., Kolodner, R. D. and Hanawalt, P. C. (2004) Effect of 8-oxoguanine on transcription elongation by T7 RNA polymerase and mammalian RNA polymerase II. *DNA repair*, **3**, 483–494.
33. Klungland, A., Rosewell, I., Hollenbach, S., Larsen, E., Daly, G., Epe, B., Seeberg, E., Lindahl, T. and Bames, D. E. (1999) Accumulation of premutagenic DNA lesions in mice defective in removal of oxidative base damage. *Proc. Natl. Acad. Sci. U.S.A.*, **96**, 13300–13305.
34. Kantor, G. J. and Setlow, R. B. (1981) Rate and extent of DNA repair in nondividing human diploid fibroblasts. *Cancer Res.*, **41**, 819–825.
35. Konze-Thomas, B., Levinson, J. W., Maher, V. M. and McCormick, J. J. (1979) Correlation among the rates of dimer excision, DNA repair replication, and recovery of human cells from potentially lethal damage induced by ultraviolet radiation. *Biophys. J.*, **28**, 315–325.
36. Sunesen, M., Stevnsner, T., Brosh, R. M., Jr., Dianov, G. L. and Bohr, V. A. (2002) Global genome repair of 8-oxoG in hamster cells requires a functional CSB gene product. *Oncogene*, **21**, 3571–3578.
37. Epe, B., Pflaum, M. and Boiteux, S. (1993) DNA damage induced by photosensitizers in cellular and cell-free systems. *Mutat. Res.*, **299**, 135–145.
38. Schagen, F. H., Moor, A. C., Cheong, S. C., Cramer, S. J., van Ommond, H., van der Eb, A. J., Dubbelman, T. M. and Hoeber, R. C. (1999) Photodynamic treatment of adenoviral vectors with visible light: an easy and convenient method for viral inactivation. *Gene Ther.*, **6**, 873–881.
39. Kitsera, N., Khobta, A. and Epe, B. (2007) Destabilized green fluorescent protein detects rapid removal of transcription blocks after genotoxic exposure. *Biotechniques*, **43**, 222–227.
40. Bar, J., Cohen-Noyman, E., Geiger, B. and Oren, M. (2004) Attenuation of the p53 response to DNA damage by high cell density. *Oncogene*, **23**, 2128–2137.

### **Chapter 3**

**Host Cell repair of UVC and methylene blue plus visible light induced DNA damage in an adenovirus encoded reporter gene correlates with reactivation of gene expression.**

## **Preface**

Reactivation of gene expression from the adenovirus encoded *lacZ* reporter gene is a well established technique used in our laboratory. It has been used extensively to examine the ability of cells to process UVC induced lesions (Rainbow and Mak 1973; Francis and Rainbow 1999; Dregoes et al. 2007; Dregoes and Rainbow 2009). Experiments using southern blot techniques have demonstrated removal of UVC induced lesions in genomic DNA of cells in culture (Spivak et al. 2006) and our lab has demonstrated using a PCR based assay that these lesions are removed from the adenovirus encoded reporter gene by host cell repair machinery.

Experiments suggesting that MB+VL induced oxidative damage caused transcriptional inactivation of introduced reporter genes was addressed in the previous Chapter. The transcription blocking potential of 8-oxoG (Kitsera et al.; Kuraoka et al. 2003; Kathe et al. 2004; Tornaletti et al. 2004; Charlet-Berguerand et al. 2006; Pastoriza-Gallego et al. 2007), the major base lesion generated by treatment of DNA with MB+VL and the finding that CSB can act as an elongation factor to stimulate lesion bypass (Charlet-Berguerand et al. 2006) made it necessary to determine if MB+VL induced 8-oxoG lesions were being repaired in the viral DNA.

In order to examine this, we have used a southern blot technique to measure the loss of endonuclease sensitive sites over time to measure lesion removal. Presented in this Chapter is work done by Natalie Zacal and I. All experiments with UVC treatment were conducted by Natalie Zacal and all MB+VL treatment experiments were conducted by me. All figures presented in this Chapter were constructed by me. The Chapter is presented in the form of a manuscript, written by me and is intended for submission to a peer reviewed journal. Dr. Andrew J. Rainbow provided critical insight into experimental design and writing of the manuscript.

## **Abstract**

Host cell reactivation (HCR) for the expression of a damaged reporter gene is a simple and quick method of examining cellular DNA repair capacity. Previously we have reported the use of a recombinant adenovirus (Ad) based HCR assay to examine nucleotide excision repair (NER) of UVC-induced DNA lesions in several mammalian cell types. The recombinant non-replicating Ad expresses the *E. coli*  $\beta$ -galactosidase ( $\beta$ -gal) reporter gene under control of the cytomegalovirus (CMV) immediate early (IE) enhancer. Using a PCR based approach we have shown previously that HCR for expression of the UVC-damaged Ad reporter gene reflects the removal of UVC induced cyclobutane pyrimidine dimers (CPDs) by NER. More recently we have used methylene blue plus visible light (MB+VL) to induce the major oxidative lesion 7,8-dihydro-8-oxoguanine (8-oxoG) in the recombinant adenovirus encoded reporter gene in order to study base excision repair (BER). The reported variability regarding 8-oxoG's potential to block transcription by RNA polIII, and data demonstrating that a number of factors play a role in transcriptional bypass of the lesion, led us to examine the repair of 8-oxoG in the Ad reporter and its relationship to HCR for expression of the reporter gene. In this work we have used a southern blot technique to examine removal of UVC and MB+VL induced DNA damage by loss of endonuclease sensitive sites from the Ad encoded  $\beta$ -gal reporter gene in human and rodent cells. We show that repair of UVC induced CPDs via NER as well as MB+VL induced 8-oxoG via BER is substantially greater in human SV40 transformed GM637F skin fibroblasts compared to hamster CHO-AA8 cells. We show also that HCR for expression of the UVC-damaged as well as the MB+VL-damaged reporter gene is substantially greater in human SV40 transformed GM637F skin fibroblasts compared to hamster CHO-AA8 cells. The difference between the human and rodent cells in the removal of both CPDs and 8-oxoG from the damaged reporter

gene correlated with the difference in HCR for expression of the damaged reporter gene. These results suggest that the major factor for HCR of the MB+VL treated reporter gene in human cells is DNA repair in the adenovirus rather than lesion bypass.

## Introduction

Host cell reactivation (HCR) of damaged reporter genes has long been used to examine the DNA repair capacity of different cell types (Rainbow and Mak 1973; Lytle et al. 1976; Protic et al. 1988; Colicos et al. 1991; Smith et al. 1995; Valerie and Singhal 1995; Johnson and Latimer 2005). The specific repair pathway examined is determined by the agent used to damage the DNA of the reporter construct. One HCR assay used in our lab utilizes a recombinant non-replicating adenovirus (Ad) expressing the *E. coli*  $\beta$ -galactosidase ( $\beta$ -gal) under control of the cytomegalovirus (CMV) immediate early (IE) enhancer region (Addison et al. 1997). The rationale behind this HCR assay is that in the absence of DNA damage, host cell transcription of the reporter gene by RNA polymerase II (polII) is uninterrupted and efficiently generates full mRNA transcripts which lead to the production of functional  $\beta$ -gal. Upon introduction of DNA damage into the Ad encoded reporter gene, transcription by RNA polII is blocked and DNA repair must first detect, remove and repair the DNA before proper transcription and production of the  $\beta$ -gal protein can occur. The result is reduced expression of the reporter gene in comparison to the undamaged control.

The Ad based HCR assay has been used extensively by our lab to examine repair of UVC induced lesions (CPDs) by the nucleotide excision repair (NER) pathway in primary and transformed cell types under various conditions (Francis et al. 1997; Boszko and Rainbow 1999; Francis and Rainbow 1999; Dregoes et al. 2007; Wu et al. 2007; Ghodgaonkar et al. 2008; Dregoes and Rainbow 2009). Exposure of DNA to UVC radiation results in the formation of 6-4 pyrimidine-pyrimidone dimers as well as cyclobutane pyrimidine dimers (Friedberg et al. 1995). These lesions act as a strong block to transcription by RNA polII, thus requiring removal by DNA repair mechanisms to resume efficient transcription (Donahue et al. 1994). Removal of

transcription blocking lesions from cellular DNA can be achieved by the transcription coupled repair (TCR) sub-pathway of NER (Friedberg et al. 1995). Using a PCR based approach our lab verified that UVC induced lesions are in fact removed from the Ad encoded *lacZ* gene and that the removal strongly correlates with reactivation of gene expression (Boszko and Rainbow 1999). These results demonstrated that HCR of UVC induced lesions in the adenovirus reporter gene measures NER. More recently we have used the HCR assay to examine base excision repair (BER) of oxidative DNA damage generated by exposure of the virus to methylene blue plus visible light (MB+VL) prior to infection of cells (Kassam and Rainbow 2007; Pitsikas et al. 2007; Rainbow and Zacal 2008; Kassam and Rainbow 2009; Leach and Rainbow 2011; Rainbow et al. 2011). MB is a photosensitizer that upon exposure to VL generates singlet oxygen ( $^1O_2$ ) which through interaction with DNA leads mainly to the formation of 7,8-dihydro-8-oxoguanine (8-oxoG) and a small number of additional single base modifications (Floyd et al. 1989; Tuite and Kelly 1993). Studies examining the ability of 8-oxoG to block transcription by RNA polII have shown conflicting results and have demonstrated transcription blockage is dependent on a number of factors including the sequence context surrounding the lesion as well as the strength of the promoter driving transcription (Kitsera et al.; Kuraoka et al. 2003; Kathe et al. 2004; Tornaletti et al. 2004; Charlet-Berguerand et al. 2006; Pastoriza-Gallego et al. 2007). It was also suggested that the observed decrease in expression from a reporter gene containing 8-oxoG lesions (Spivak and Hanawalt 2006) results from gene inactivation by the 8-oxoG DNA glycosylase (OGG1) and that this inactivation is increased in the absence of the Cockayne syndrome (CS) group B (CSB) protein (Spivak and Hanawalt 2006; Khobta et al. 2009). We have since shown that the MB+VL treated reporter gene is significantly reactivated over time

and that reactivation requires the CS group A (CSA) and CSB proteins (Leach and Rainbow 2011).

In this study we have directly examined removal of UVC and MB+VL generated damage from the Ad encoded *lacZ* gene in human and rodent cells by examining the loss of endonuclease sensitive sites by southern blot. Consistent with our previous results demonstrating removal of UVC induced CPD by the PCR based technique (Boszko and Rainbow 1999), we show by southern blot that CPDs are repaired in Ad DNA and that HCR of reporter gene expression correlates with lesion removal. Similarly, we show removal of MB+VL induced lesions was greater in human GM637F cells compared to hamster CHO-AA8 cells, which also correlated with HCR for reporter gene expression. Taken together, the results presented here strongly support the conclusion that actual removal of UVC and MB+VL induced lesions from the reporter gene are major factors leading to HCR for expression of the damaged reporter gene.

## **Materials and methods**

### *Cells, virus and culture conditions*

The SV40 transformed repair proficient human skin fibroblast GM637F was obtained from NIGMS (Camden, NJ, USA). The repair proficient Chinese hamster ovary (CHO) cells CHO-AA8 were provided by Dr Larry Thompson, Lawrence Livermore National Laboratory, Livermore, CA with the help of Dr Gordon Whitmore, Physics Division, Ontario Cancer Institute, Toronto, Ontario. Cell cultures were grown at 37°C in a humidified incubator in 5% CO<sub>2</sub> and cultured in Eagle's  $\alpha$ -minimal essential media ( $\alpha$ -MEM) supplemented with 10% fetal bovine serum (FBS) and antimycotic/ antibiotic 100 $\mu$ g/ml penicillin, 100 $\mu$ g/ml streptomycin and

250ng/ml amphotericin B. The recombinant adenovirus Ad5MCMVlacZ with the murine CMV IE enhancer (AdCA35) was obtained from The Robert E. Fitzhenry Vector Laboratory, McMaster University, Hamilton, Ontario. The virus was propagated, collected and titred as described previously (Graham and Prevec 1991).

#### *Treatment of the virus with UVC*

UV irradiation of the virus was carried out as previously described (18). Briefly, the virus was resuspended in a 35-mm Petri dish in cold PBS at the appropriate dilution to achieve the desired MOI. Using a General Electric germicidal lamp (model G8T5) emitting predominately at 254 nm, the virus was irradiated on ice with stirring with an incident fluence rate of 2 J/m<sup>2</sup>/sec. For southern blot experiments examining the loss of endonuclease sensitive sites, a 250µl aliquot of untreated virus was removed as a control and the remaining virus was exposed to a total dose of 240 J/m<sup>2</sup> of UVC-irradiation. For selective extraction of Ad used for detecting lesion removal cells were infected with AdCA35 at a multiplicity of infection (MOI) of 100 plaque forming units (pfu)/ml. A greater MOI was used for the southern blot experiments compared to HCR experiments to ensure enough copies of the gene were present for efficient detection by probe hybridization. For HCR experiments, after each UV exposure, 200µl aliquots were removed from the viral preparation and appropriately diluted using unsupplemented a-MEM.

#### *Treatment of the virus with MB+VL*

Preparation of MB was as described previously (Pitsikas et al. 2007). Treatment of the virus was performed as described previously (Kassam and Rainbow 2007). Briefly, virus

suspended in cold phosphate buffered saline (PBS) (4°C,) with 20µg/ml MB and exposed to VL. For southern blot experiments examining the loss of endonuclease sensitive sites, a 250µl aliquot of untreated virus was removed as a control and the remaining virus was exposed to visible light using a 1000-W bulb (General Electric, GE R1000) at a distance of 75 cm, on ice with stirring for a total exposure of 480 seconds. For selective extraction of Ad used for detecting lesion removal cells were infected with AdCA35 at a MOI of 100 pfu/ml. For HCR experiments, the same conditions were used for treatment of the virus and 200µl aliquots of exposed virus was collected after each sequential visible light exposure was subsequently used to infect cells.

*Selective (Hirt) extraction of Adenovirus DNA from infected cells*

Adenovirus DNA was selectively isolated from infected cells by the Hirt extraction protocol (Hirt 1967). Following the repair incubation period, growth media was aspirated from the infected (or mock infected) monolayer of cells and subsequently overlaid with 0.5ml of lysing solution (10mM Tris (pH 7.4), 10mM EDTA, 05% SDS, 100mM NaCl, 100mg/ml proteinase K (Roche)). Cells were lysed for 8hrs 37°C and the sample was subsequently transferred to a 1.5ml Eppendorf tube using a wide bore pipette tip. 0.25ml of 3M sodium acetate (pH 7) was added to the samples and mixed gently by inversion and allowed to precipitate overnight on ice. Following precipitation, the samples were centrifuged at 17 500g for 30 minutes at 4°C. After centrifugation, the supernatant from each sample was extracted with phenol, phenol:chloroform and chloroform and the final aqueous phase was ethanol precipitated overnight with 20µg/ml glycogen (Roche) as a DNA carrier. Following ethanol precipitation, the

resulting pellet was redissolved in 40-100µl ddH<sub>2</sub>O in preparation for restriction enzyme digestion.

*Restriction digestion and Endonuclease treatment of selectively extracted adenovirus DNA*

Prior to treatment of Ad DNA with either T4pdg (New England Biolabs (NEB) M0308S) or Fpg (NEB M02040), all samples were digested overnight by 40 units of EcoRI (New England Biolabs R0101) in a total reaction volume of 50µl in 1x NEB Buffer 1. After digestion, the enzyme was heat inactivated at 65°C for 20min. For subsequent treatment of UVC damaged DNA by T4pdg, the digested samples were extracted by phenol:chloroform and the resulting aqueous phase was ethanol precipitated and resuspended in ddH<sub>2</sub>O. Samples were then divided in two and digested or mock digested overnight with 10 units T4pdg in (1x T4pdg reaction buffer, 100ug/ml bovine serum albumin (BSA)). Following T4pdg treatment, samples were loaded into a 8% alkaline agarose gel and separated by electrophoresis. For endonuclease treatment of MB+VL damaged DNA, the EcoRI digested samples were divided in half and incubated with or without 16 units of Fpg (1xNEB buffer 1, 100µg/ml BSA) for 5 hours. Following incubation the samples were loaded directly into an 8% alkaline agarose gel and separated by electrophoresis.

*Separation of adenovirus DNA by alkaline gel electrophoresis and detection by southern blotting*

Alkaline agarose gel electrophoresis and southern blot detection of Ad *lacZ* DNA was performed essentially as described in (Sambrook and Russel: Molecular Cloning: A laboratory

manual. Third edition). Briefly, Ad DNA was separated on denaturing 8% alkaline agarose gels run at 10V for 24 hours. Following gel electrophoresis, two 30 min washes in neutralization buffer (1.5M Tris (pH 7.4), 1.5M NaCl) were performed after which DNA was transferred to a neutral nylon membrane (Hybond N, Amersham) by upward capillary transfer of 10x SSC. After transfer, the membrane was washed with 6x SSC and the DNA was UV crosslinked to the membrane (UV stratalinker). Prior to hybridization with the radioactive probe specific to the Ad encoded *lacZ* gene, membranes were prehybridized with church mix (0.5M NaPi (pH 7.2), 1mM EDTA, 7% SDS, 1%BSA) in roller bottles at 65°C in a rotating hybridization oven.

*Preparation of a radiolabeled probe for detection of the adenovirus encoded LacZ gene*

The radioactive probe used for detection of Ad *lacZ* DNA was generated by klenow (Invitrogen) extension of primers (primer 1: 5'-GATCTTGCTATGGATCCC-3'; primer 2: 5'-CAACTGGTAATGGTAGCG-3') flanking an 835bp portion of the Ad encoded *lacZ* gene. The same primers were used to PCR amplify the 835bp fragment for use in klenow extension and probe generation. The probe used in this study is a double stranded probe which measures overall repair in the viral reporter gene. Klenow extension of primers 1 and 2 using the 835bp PCR product as a template was carried out using  $\alpha$ -<sup>32</sup>P dATP,  $\alpha$ -<sup>32</sup>P dCTP,  $\alpha$ -<sup>32</sup> dGTP and  $\alpha$ -<sup>32</sup>P dTTP (3000Ci/mmol 10mCi/ml, Perkin Elmer). Klenow extension was carried out for 90 min in a total volume of 50 $\mu$ l in 1x OLB (40mM NaPi (pH 7.2), 1mM EDTA, 1% SDS) with 50  $\mu$ Ci of each radioactive  $\alpha$ -<sup>32</sup>P dNTP (200ng template DNA, 5ng each primer, 9 units Klenow). The reaction was stopped by the addition of 50ml TNES (10mM Tris (pH 7.4), 100mM NaCl, 10mM EDTA, 1% SDS) and incubation at 65°C for 10 min. Unincorporated nucleotides were separated

from the labeled probe by elution through a sephadex G-50 column with 1ml TNES. Immediately before hybridization with the nylon membrane the was boiled for 5 min and added to 25ml of prewarmed (65°C) church mix and filtered through a 0.2µm syringe filter. The prehybridization solution was removed from the roller bottles containing the membranes and the 25ml sterile church mix containing the probe was immediately added. Hybridization was carried out at 65°C with rotation for 18-24 hours. Following hybridization, three 15 min washes in 25ml church wash (40mM NaPi (pH 7.2), 1mM EDTA (pH 8) 1% SDS) were performed at 65°C. The membrane was then sealed in plastic and intensifying phosphor screens were used for visualization of the radioactive signal from the hybridized membrane. Phosphor screens were scanned using a phosphorimager (Storm scanner 8200) and quantified using ImageQuant software.

#### β-galactosidase reporter gene expression assay (HCR)

The HCR assay was performed as previously described (Leach and Rainbow 2011). Briefly, the HCR uses the recombinant Ad (AdCA35) expressing *β-gal* under control of the MCMV IE enhancer. GM637F and CHO-AA8 cells were seeded for confluence ( $3.5 \times 10^4$  cells/well) in 96 well plates (Falcon, Franklin Lakes, NJ, USA). Cells were then incubated for 18-24 hrs and subsequently infected with UVC or MB+VL treated AdCA35 at an MOI of 100 plaque forming units (pfu)/cell. After 90 min of viral adsorption, the infection media was aspirated and replaced with 200ml of complete α-MEM. After an additional 24 hours of repair incubation cells were harvested for measurement of β-gal activity by addition chlorophenolred-β-D-galactopyranoside (CPRG). β-gal activity was scored as previously described (Pitsikas et al. 2005).

*Graphing and statistical analysis*

The counts per pixel for images obtained by scanning the phosphor screens with the phosphorimager were quantified using ImageQuant software. The surviving fraction (SF) of the endonuclease treated sample relative to its respective control was calculated (counts from endonuclease treated sample corresponding to the 3kb *lacZ* fragment/ counts from mock treated sample corresponding to the 3kb *lacZ* fragment). The SF was then used to calculate the number of endonuclease induced ssDNA breaks at each (#ssDNA breaks =  $-\ln(\text{SF})$ ). These numbers were converted to the percentage of endonuclease induced ssDNA breaks for graphical representation and statistical analysis. Statistical analysis of the percent removal of endonuclease sensitive sites at each time point compared to  $t=0$  was done using a one sample two tailed t-test with a confidence interval of 0.05. Statistical analysis of the percent removal at each time point between GM637F and CHO-AA8 cells was done using a two sample independent t-test with a confidence interval of 0.05. The HCR  $\beta$ -gal survival curves for UVC and MB+VL treatment were plotted using Origin Lab software. The absolute  $D_{37}$  values (VL dose to virus required to reduce  $\beta$ -gal expression to 37% of the untreated virus) used for statistical analysis for each cell line were obtained by extrapolation from the HCR survival curves of each independent experiment. A two sample independent t-test with a confidence interval of 0.05 was used to compare absolute  $D_{37}$  values from GM637F and CHO-AA8 cells.

## Results

### *Loss of T4 pyrimidine-DNA glycosylase sensitive sites over time in human and Chinese hamster ovary cells*

The purpose of this study was to determine if repair of MB+VL induced 8-oxoG occurs in the Ad encoded reporter gene and if it does whether or not it correlates with HCR. Using a quantitative PCR approach, we have previously demonstrated that UVC induced lesions are removed from the adenovirus encoded *lacZ* reporter gene and that this removal correlates with HCR capacity (Boszko and Rainbow 1999). To confirm the use of southern blotting to examine loss of endonuclease sensitive sites and the correlation with HCR we first examined removal of UVC induced lesions by loss of T4 pyrimidine-DNA glycosylase (T4pdg) sensitive sites. T4pdg recognizes cyclobutane pyrimiding dimers (CPDs) and through its glycosylase activity cleaves the glycosyl bond on the 5' side of the CPD generating an abasic (AP) site. The AP site is converted into a single strand break after cleavage of the phosphodiester bond at the AP site by the endonuclease activity of T4pdg. GM637F and CHO-AA8 seeded in 6cm dishes cells were infected with UVC treated (or mock treated) AdCA35 and incubated to allow for repair. Cells were harvested for Hirt extraction of Ad DNA at 0, 1.5, 3, 6 and 24 hours. Following phenol:chloroform extraction and ethanol precipitation, Ad DNA was digested with EcoRI to generate a 3kb *lacZ* fragment. Samples were then purified and divided and half the sample was digested with T4pdg to induce single strand breaks at sites of UVC induced CPDs and the other half mock digested for control. Following digestion with T4pdg the samples were run on a denaturing 8% alkaline agarose gel at 10V for 24 hours. The DNA was transferred to a neutral nylon membrane and a radioactively labeled probe specific to a 835bp portion of the Ad encoded *lacZ* gene was used to detect the reporter gene DNA. Figure 1A shows the results of a southern

blot examining the loss of T4pdg sensitive sites over time in both GM637F and CHO-AA8 cells. In the human SV40 transformed GM637F fibroblasts, considerable recovery of the 3kb *lacZ* fragment is evident after 24hrs of repair incubation whereas only a small amount was detected for Ad DNA extracted from CHO-AA8 cells. For both cell lines, the surviving fraction of the T4pdg treated sample at each time point was used to calculate the percent removal of T4pdg induced ssDNA breaks and is shown in Figure 1B. A significant removal of T4pdg sensitive sites was observed in GM637F cells after 24 hours of repair incubation while significantly less removal was detected following any of the time points in CHO-AA8. After 24 hours of repair incubation a significant difference in the percent of T4pdg sensitive sites removed was observed between GM637F (~ 60%) and CHO-AA8 (~ 20%) cells. These results demonstrate that repair of UVC induced CPDs in the Ad encoded *lacZ* gene occurs in human SV40 transformed GM637F fibroblasts and occurs at a much slower rate in CHO-AA8 cells.

#### *Host cell reactivation of UVC-irradiated AdCA35 in GM637F and CHO-AA8 cells*

UVC induced CPDs act as a strong block to transcription by RNA polII and are thought to require removal for reactivation of gene expression from the UVC treated reporter gene. The significantly increased removal of T4pdg sensitive sites in GM637F compared to CHO-AA8 cells after 24 hours of repair incubation suggested that if lesion removal is required for gene reactivation, HCR of  $\beta$ -gal expression would be greater in GM637F compared to CHO-AA8 cells. To test this, we examined HCR of the UVC-irradiated reporter gene 24 hours after infection in both cell types. Levels of  $\beta$ -gal activity from UVC treated AdCA35 were normalized to the untreated control. The pooled results from 3 independent experiments are shown in Figure

2.  $\beta$ -gal survival curves were fitted to the linear quadratic equation  $\ln SF = -(\alpha x + \beta x^2 + \gamma)$  with error used for weighting. Absolute  $D_{37}$  values were extrapolated from the resulting curves for survival of  $\beta$ -gal expression from the UVC treated AdCA35. Consistent with this, HCR as measured by the  $D_{37}$  value (the dose required to reduce expression of the reporter gene to 37% of the control expression) was significantly greater in GM637F compared to CHO-AA8 cells. Overall these data demonstrate that repair of UVC induced CPDs are removed from the Ad encoded *lacZ* gene and that HCR of  $\beta$ -gal expression correlates with repair.

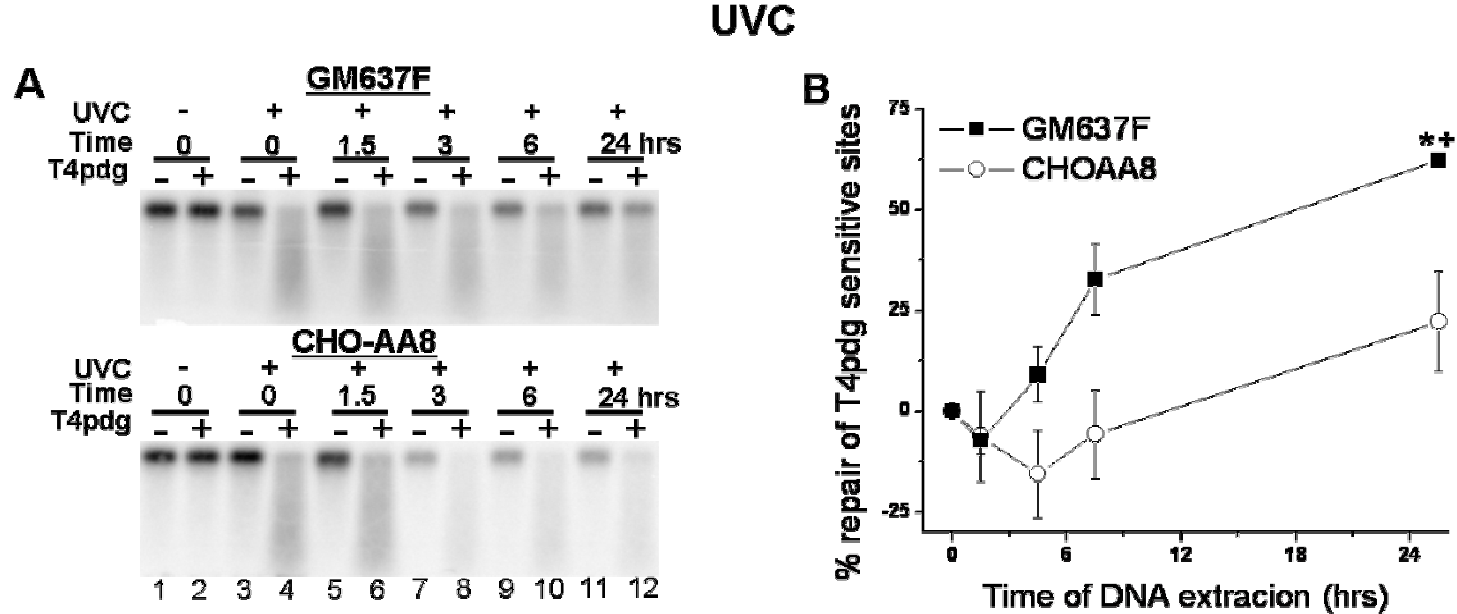


**Figure 1:** Repair of UVC induced CPDs from the Ad encoded *lacZ* gene in human and rodent cells measured by loss of T4pdg sensitive sites. A) Southern blot analysis of the repair of UVC induced CPDs in the Ad *lacZ* gene. Shown here is a representative blot. Lanes 1 and 2 contain untreated Ad DNA while lanes 3 and 4 contain Ad DNA exposed to  $240 \text{ J/m}^2$  UVC. Lanes 1-4 have not undergone any repair incubation. T4pdg treatment demonstrates that prior to UVC exposure there are no detectable endonuclease sensitive sites but a small number of ssDNA breaks and following exposure a large number of sites are generated (compare lanes 2 and 4). During repair incubation NER removes CPDs resulting in the loss of T4pdg sensitive sites and recovery of the full length 3kb *lacZ* fragment. As long as CPDs persist in the *lacZ* DNA, T4pdg will induce a ssDNA break resulting in less full length signal compared to the control. Recovery the 3kb *lacZ* fragment can be seen in GM637F cells 24hrs after infection while no recovery is seen in CHO-AA8 cells. B) Quantification of the percent removal of CPDs from the Ad encoded *lacZ* gene in GM637F and CHO-AA8 cells. Each point on the graphs represents an arithmetic mean  $\pm$  SE of the percent removal of UVC induced T4pdg sensitive sites from 3 independent experiments. A significant increase in the percent removal of UCV induced T4pdg sensitive sites was observed in GM637F (0-24hrs,  $p=0.0004$ , one sample two tailed t-test, indicated by an asterisk) significant removal was not detected in CHO-AA8 cells. A significant difference in the percent removal of T4pdg sensitive sites was observed between GM637F and CHO-AA8 24 hours after infection ( $p=0.033$ , two sample independent t-test, indicated by a cross/plus sign)

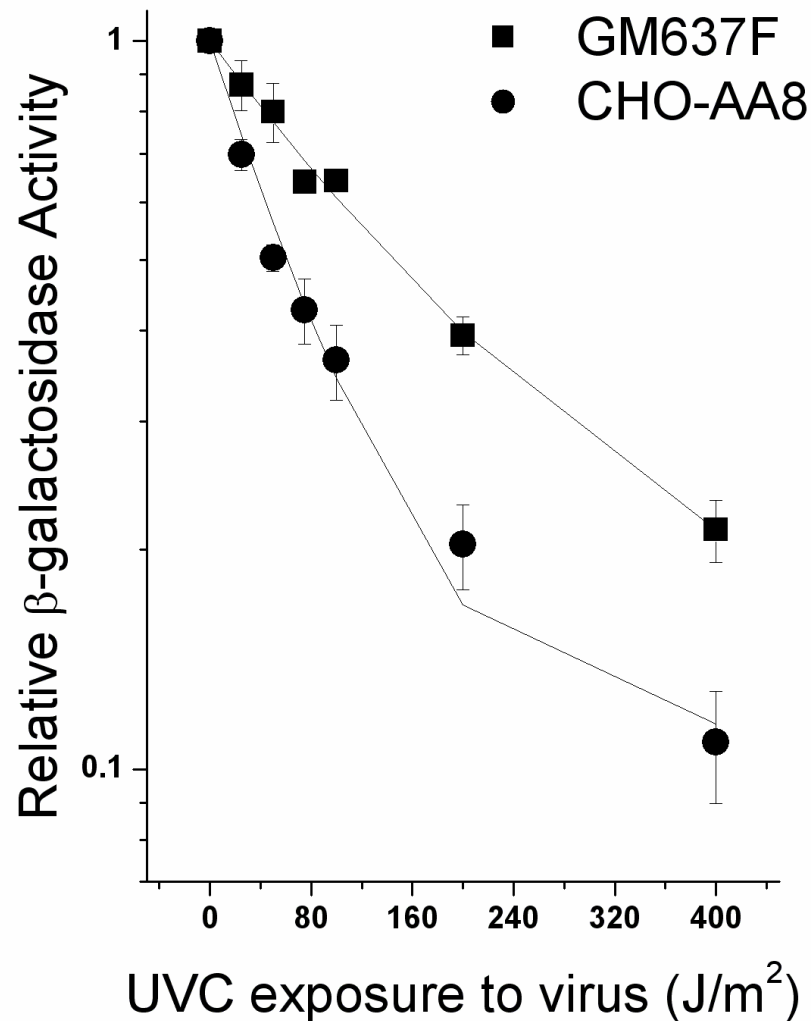


**Figure 2:** Host cell reactivation of UVC treated AdCA35 in human and rodent cells. Cells seeded in 96 well plates were infected with UVC-irradiated (or mock-irradiated) AdCA35 at an MOI of 100 and incubated for 24hrs to allow for repair and reactivation of expression from the Ad encoded  $\beta$ -gal reporter gene. Each point on the graphs represents an arithmetic mean  $\pm$  SE of the  $\beta$ -gal activity at each UVC exposure to the virus relative to the untreated control. The curves are fitted to a linear quadratic equation using error for weight and the equation was used to determine the  $D_{37}$  value for each cell line. Average absolute  $D_{37}$  ( $\pm$ SE) values calculated using the linear quadratic equation were 224.23 J/m<sup>2</sup> for GM637F and 91.74 J/m<sup>2</sup> for CHO-AA8. HCR capacity was 2.4 times greater in GM637F compared to CHO-AA8 for the UVC treated reporter gene. This increased was significant by two sample independent t-test ( $p=0.0057$ ) using absolute  $D_{37}$  values calculated from each individual experiment.

*Loss of formamidopyrimidine (Fapy)-DNA glycosylase sensitive sites over time in human and Chinese hamster ovary cells*

We have previously demonstrated significant reactivation of reporter gene expression following MB+VL and UVC treatment over time in human SV40 transformed fibroblasts and CHO cells (Leach and Rainbow 2011). To determine if repair of MB+VL induced 8-oxoG occurs in the Ad encoded *lacZ* gene we examined lesion removal by loss of formamidopyrimidine (Fapy)-DNA glycosylase sensitive sites. Treatment of the virus with MB+VL leads to the formation of 8-oxoG lesions and a small amount of other single base lesions (Floyd et al. 1989; Tuite and Kelly 1993). The *E. coli* Fpg enzyme is an endonuclease that catalyzes the excision of oxidative guanine lesions including 8-oxoG generating an abasic/apurinic (AP) site that is further processed into a single strand break by the enzyme's AP lyase activity (Klungland and Bjelland 2007). To assess if host cell repair machinery removes MB+VL induced 8-oxoG lesions from the adenovirus encoded  $\beta$ -gal reporter gene, cells seeded in 6cm dishes were infected with AdCA35 treated or mock treated with MB+VL and incubated for 24 hours. Cells were harvested for selective Hirt extraction of adenovirus DNA following repair incubation periods of 0, 1.5, 3, 6, 12 and 24 hours. Following phenol:chloroform extraction and ethanol precipitation, Ad DNA was digested with EcoRI to generate a 3kb *lacZ* fragment. Samples were then divided and half the sample was digested with Fpg to induce single strand breaks at sites of MB+VL induced 8-oxoG and the other half mock digested as a control. Following the Fpg digestion, samples were separated on a denaturing 8% alkaline agarose gel at 10V for 24 hours. The DNA was transferred to a neutral nylon membrane and hybridized with a radioactively labeled probe specific to a 835bp portion of the Ad encoded *lacZ* gene. Figure 3A shows the results of a southern blot examining the loss of Fpg sensitive sites over time in both

GM637F and CHO-AA8 cells. In the human SV40 transformed GM637F fibroblasts, recovery of the 3kb *lacZ* fragment is obvious after 24hrs of repair incubation while very little repair was detected in Ad DNA extracted from CHO-AA8 cells. For both cell lines, the surviving fraction of the Fpg treated sample at each time point was used to calculate the percent removal of Fpg induced ssDNA breaks and is shown in Figure 3B. Similar to removal of T4pdg sensitive sites, a significant removal of Fpg sensitive sites was observed in GM637F cells after 24 hours of repair incubation while only low levels of removal were detected following any of the time points in CHO-AA8. Following 24 hours of repair incubation a significant difference in the percent of Fpg sensitive sites removed was observed between GM637F (~80%) and CHO-AA8 cells. These results demonstrate that repair of MB+VL 8-oxoG in the Ad encoded *lacZ* gene is greater in human SV40 transformed GM637F fibroblasts compared to CHO-AA8 cells.

*Host cell reactivation of the MB+VL treated adenovirus encoded  $\beta$ -gal gene in human and Chinese hamster ovary cells*

We have previously demonstrated significant reactivation of reporter gene expression following MB+VL treatment over time in human SV40 transformed GM637F fibroblasts and CHO cells (Leach and Rainbow 2011). Consistent with *in vivo* inhibition of transcription by RNA polIII by 8-oxoG, treatment of the Ad encoded reporter gene with MB+VL led to reduced expression of the reporter gene compared to control. Levels of  $\beta$ -gal activity from MB+VL treated AdCA35 were normalized to the untreated control. The pooled results from 3 independent experiments are shown in Figure 3.  $\beta$ -gal survival curves were fitted to the linear quadratic equation  $\ln SF = -(\alpha x + \beta x^2 + y)$  with error used for weighting. Absolute  $D_{37}$  values were extrapolated from the resulting curves for survival of  $\beta$ -gal expression from the MB+VL treated reporter. Similar to the

results observed with UVC, the significantly increased removal of Fpg sensitive sites in GM637F compared to CHO-AA8 cells after 24 hours suggested HCR of  $\beta$ -gal expression would be greater in GM637F compared to CHO-AA8 cells if lesion removal is a requirement of gene reactivation. We examined HCR of the MB+VL treated reporter gene 24 hours after infection in both cell types to determine if a correlation exists between the rate of lesion removal and HCR (Figure 4). Similar to the UVC results, HCR was significantly greater in GM637F compared to CHO-AA8 cells. Taken together, these data demonstrate that repair of MB+VL induced 8-oxoG are removed from the Ad encoded *lacZ* gene and that HCR of  $\beta$ -gal expression correlates with repair.

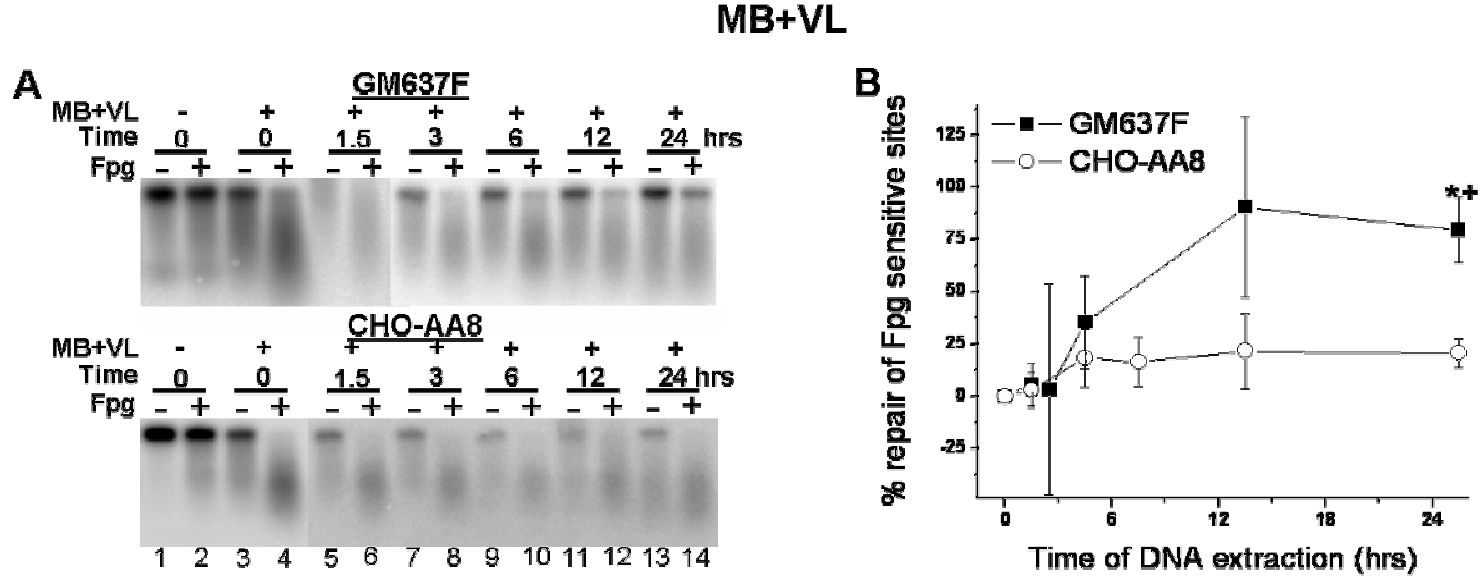


**Figure 3:** Repair of MB+VL induced 8-oxoG from the Ad encoded lacZ gene in human and rodent cells measured by loss of Fpg sensitive sites. A) Southern blot analysis of the repair of MB+VL induced 8-oxoG in the Ad lacZ gene. Shown here is a representative blot. Lanes 1 and 2 contain untreated Ad DNA while lanes 3 and 4 contain Ad DNA exposed to 480 seconds VL in PBS with 20 $\mu$ g/ml MB. Lanes 1-4 have not undergone any repair incubation. We can see some ssDNA breaks and a small amount of oxidative lesions are present prior to treatment with MB+VL. Following VL exposure, a large number of endonuclease sensitive sites are generated (compare lanes 2 and 4). During repair incubation BER removes 8-oxoG resulting in the loss of Fpg sensitive sites and recovery of the full length 3kb lacZ fragment. As long as 8-oxoG lesions persist in the lacZ DNA, Fpg will induce ssDNA breaks resulting in fewer full length fragments and less signal compared to the control. Recovery the 3kb lacZ fragment can be seen in GM637F can be seen beginning at 6 hrs and increasing until 24hrs after infection. In contrast no recovery is seen in CHO-AA8 cells. B) Quantification of the percent removal of Fpg sensitive sites from the Ad encoded lacZ gene in GM637F and CHO-AA8 cells. Each point on the graphs represents an arithmetic mean  $\pm$  SE of the percent removal of MB+VL induced Fpg sensitive sites from 3 independent experiments. A significant increase in the percent removal of MB+VL induced Fpg sensitive sites was observed in GM637F (0-24hrs,  $p=0.036$ , one sample two tailed t-test, indicated by an asterisk) significant removal was not detected in CHO-AA8 cells. A significant difference in the percent removal of Fpg sensitive sites was observed between GM637F and CHO-AA8 24 hours after infection ( $p=0.025$ , two sample independent t-test, indicated by a cross/plus sign)

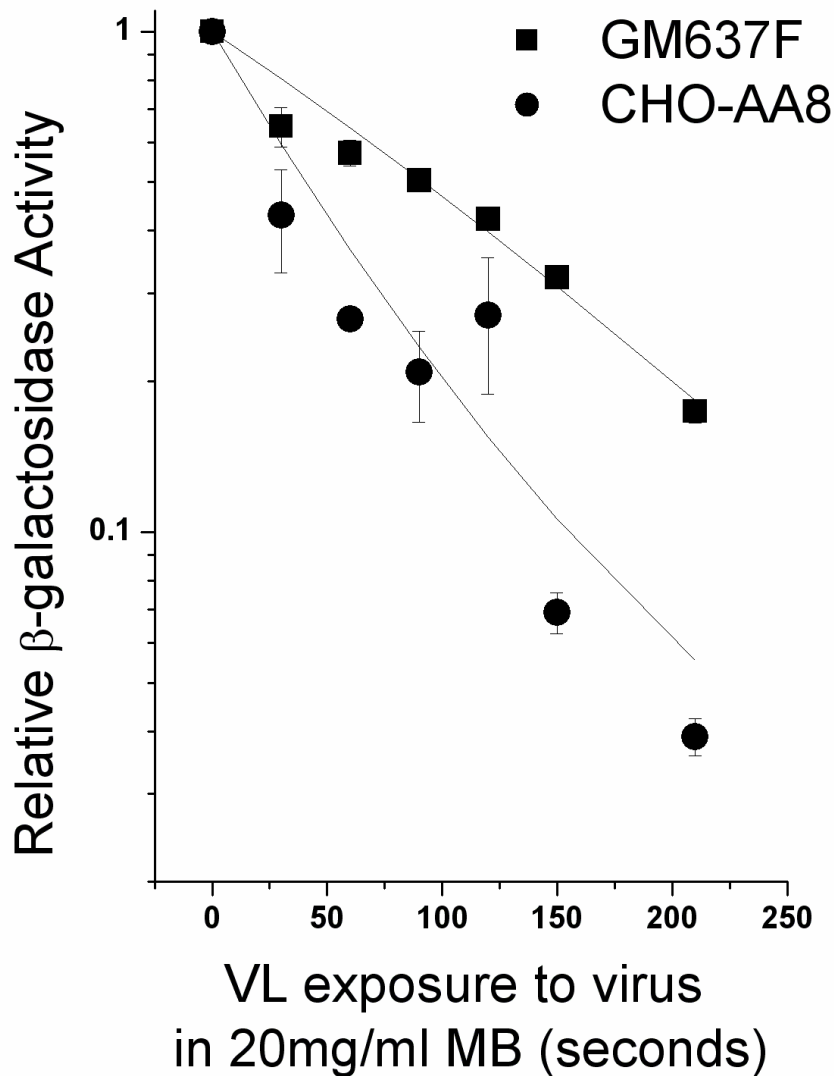


**Figure 4:** Host cell reactivation of MB+VL treated AdCA35 in human and rodent cells. Cells seeded in 96 well plates were infected with MB+VL treated (or mock treated) AdCA35 at an MOI of 100 and incubated for 24hrs to allow for repair and reactivation of expression from the Ad encoded  $\beta$ -gal reporter gene. Each point on the graphs represents an arithmetic mean  $\pm$  SE of the  $\beta$ -gal activity at each MB+VL exposure to the virus relative to the untreated control. The curves are fitted to a linear quadratic equation using error for weight and the equation was used to determine the  $D_{37}$  value for each cell line. Average absolute  $D_{37}$  ( $\pm$ SE) values calculated using the linear quadratic equation were 120.56s for GM637F and 47.69s  $J/m^2$  for CHO-AA8. Similar to UVC induced damage, HCR capacity was 2.5 times greater in GM637F compared to CHO-AA8 for the MB+VL treated reporter gene. Values were calculated by pooling data obtained from 3 independent experiments. This increased was significant by two sample independent t-test ( $p=0.0203$ ) using absolute  $D_{37}$  values calculated from each individual experiment.

*Calculation of the surviving fraction of the 3kb lacZ fragment from southern blot experiments.*

To determine how accurately HCR of gene expression in untreated cells represents removal of lesions from the *lacZ* transcriptional template we compared the ratios of the  $D_0$  values for  $\beta$ -gal expression between GM637F and CHO-AA8 (from HCR experiments) and the  $D_0$  values for the surviving fraction (SF) of the T4pdg/Fpg *lacZ* fragment from the southern blot experiments. The use of the  $D_{37}$  value is based on the single target single hit theory which states that a single event in the target (the *lacZ* gene) inactivates its function ( $\beta$ -gal expression for HCR or 3kb fragment for southern blot analysis of endonuclease sensitive sites). SF can be calculated using the poisson distribution:

$$SF=e^{-D/D_0}$$

Where  $D$  is the dose given and  $D_0$  is the dose required to induce on average a single event per target, therefore when  $D=D_0$ ,  $SF=0.37$ . From this, the term  $D_{37}$  refers to the dose that equals the  $D_0$ , generating on average a single event per target. In the case of measuring lesion removal by southern blot, the presence of a single endonuclease sensitive site in the *lacZ* gene results in the loss of one full 3kb ssDNA fragment. The  $D_{37}$  value calculated by solving for  $D_0$  using the SF data from the southern blots at time zero ( $t=0$ ), prior to any repair incubation represents the dose required to induce on average a single endonuclease sensitive site/lesion per *lacZ* gene. We can assume at  $t=0$  that an even distribution of induced lesions exists between both the transcribed and non-transcribed strand of the reporter gene. Therefore, when  $SF=0.37$ , we know that on average each strand contains one lesion.

Table 1 shows the  $D_0$  values calculated using the SF of the endonuclease treated 3kb *lacZ* fragment of the Ad genome isolated from GM637F and CHO-AA8 cells after both UVC and

MB+VL treatment. The absolute  $D_{37}$  values extrapolated from the average HCR curves fit to the linear quadratic equation are also shown. For UVC treatment of the virus, the increase in lesion removal (2.4 fold) and HCR (2.4 fold) for GM637F compared to CHO-AA8 at 24 hours are consistent and suggest the HCR assay correlates well with lesion removal. For MB+VL treatment, the increase in HCR (2.53 fold) capacity for GM637F compared to CHO-AA8 is similar to UVC, however the increase in lesion removal (19 fold) for GM637F compared to CHO-AA8 is much greater. These results suggest that MB+VL induced lesions are removed to a much greater extent in GM637F fibroblasts and that it is not reflected in the increase in HCR capacity observed compared to CHO-AA8.

**Table 1:** Comparison of  $D_0$  and  $D_{37}$  values from southern blot and HCR experiments.  $D_0$  values were calculated for the 3Kb lacZ fragment of the treated (UVC and MB+VL) AdCA35 using the surviving fraction (SF) at 0 and 24 hours after infection. Absolute  $D_{37}$  values for HCR experiments were extrapolated from the linear quadratic fit curves constructed using averaged points from 3 independent experiments for both UVC (Figure 2) and MB+VL (Figure 4) treatment of AdCA35. The bottom portion of the table shows the fold difference in  $D_0/D_{37}$  for GM637F compared to CHO-AA8 for each treatment at each time point.

	UVC				MB+VL			
	Time (hrs)	Abs $D_0$ from SB ( $J/m^2$ )		Abs $D_{37}$ from linear Quadratic ( $J/m^2$ )	Time (hrs)	Abs $D_0$ from SB (sec)		Abs $D_{37}$ from linear Quadratic (sec)
		Average	SE			Average	SE	
GM637F	0	148.3997	2.85864	-	0	343.342	59.79154	-
	24	397.0239	2.537956	224.23	24	5324.94	2726.786	120.56
CHO-AA8	0	126.6275	9.270553	-	0	220.5987	3.530441	-
	24	168.8055	8.588525	91.74	24	280.4338	9.208337	47.69
GM637F/CHO-AA8	0	1.171939				1.55641		
	24	2.351961		2.444190102		18.98823		2.52799329

## Discussion

In this study, we have examined repair of UVC and MB+VL induced lesions in the adenovirus encoded reporter gene in human and rodent cells using the repair proficient SV40 transformed human skin fibroblasts line GM637F and the hamster CHO-AA8 cell line. Transformation of cells with the SV40 large T (LT) antigen leads to a number of changes within the cell (Agarwal et al. 1998) and is dependent on binding of SV40 LT proteins to pRb and p53 (Cheng et al. 2009). SV40 LT directly binds and inactivates pRb and two related proteins p130 and p107, whose functions are to repress transcription factors that regulate the expression of downstream factors involved in cell cycle entry and progression (Cheng et al. 2009). Binding of p53 by SV40 LT interferes with the tumor suppressors ability to function as a sequence specific transcription factor (Cheng et al. 2009). The p53 tumor suppressor mediates recognition and repair of CPDs through upregulating expression of the global genome repair (GGR)-NER genes *XPC*, *XPE* and *gadd45* (Hwang et al. 1999; Smith et al. 2000; Adimoolam and Ford 2002; Tan and Chu 2002). It has been shown that p53 inactivation by SV40 LT in transformed human fibroblasts leads to significantly reduced GGR-NER of UVC induced CPDs in the absence of replication repair compared to the appropriate non-transformed control (Bowman et al. 2000). This suggests the majority of NER repair observed in the cellular DNA of SV40 transformed cells occurs predominantly via transcription coupled repair (TCR)-NER. However, in contrast to these observations other studies have shown similar levels and rates of removal of CDPs in SV40 transformed fibroblasts and their primary counterparts (Mori et al. 1993; Eveno et al. 1995; Yagi et al. 1998). Bowman et al. point out that the authors of the other studies did not take into

account whether or not the cells were replicating and therefore some of the observed repair may have been due to replication repair.

In all the studies discussed above, repair of UVC induced lesions was examined in genomic DNA of treated cells. The HCR assay measures the ability of an untreated cell to remove lesions from an actively transcribed gene and reactivate expression. Previous work from our lab examining HCR of the UVC treated adenovirus in normal and NER deficient CS and XP primary fibroblasts showed that GGR-NER is responsible for the majority of repair in the actively transcribed reporter gene in untreated cells with TCR-NER playing a smaller role. For HCR experiments, XP fibroblasts combined showed an average  $D_{37}$  relative to normal control cells of  $0.47 \pm 0.15(\text{SE})$  while CS fibroblasts combined showed a relative  $D_{37}$  of  $0.76 \pm 0.07(\text{SE})$  (Francis and Rainbow 1999). Data from our lab also shows that reactivation of the UVC treated reporter gene is lower in SV40 transformed XP and CS fibroblasts relative to normal compared to primary XP and CS fibroblasts relative to normal (Francis et al. 1997; Francis and Rainbow 1999; Francis et al. 2000). The recombinant adenovirus used in the HCR assay is non-replicating, so we are not observing any effects of replication repair. Together, this shows that in untreated cells, the majority of NER, even in the transcribing reporter gene is carried out by GGR-NER and that SV40 transformation affects this pathway.

Using a PCR based approach, our lab has previously demonstrated that UVC induced CPDs are removed from an Ad encoded  $\beta$ -gal reporter gene (*Ad5HCMVsp1lacZ*) (Boszko and Rainbow 1999). Greater removal of UVC induced lesions from the reporter gene correlated with increased HCR observed in NER proficient normal fibroblasts as well as increased HCR resulting from UVC pretreatment of cells compared to decreased removal in NER deficient XP and CS fibroblasts (Boszko and Rainbow 1999). We show that UVC induced CPDs in the virus

are repaired by host cell mechanism and that this repair occurs at a significantly greater rate in GM637F compared to CHO-AA8 cells. Similar to the difference observed for removal of T4pgd sensitive sites, we observed a significant increase in reactivation of the UVC damaged reporter gene in GM637F compared to CHO-AA8 cells. These results are consistent with the previously published HCR technique and suggest the HCR assay is a readout for repair. These results are also consistent with the reduced levels of GGR detected in rodent (CHO) compared to human cells (Mellon et al. 1987)

We have previously shown significant reactivation of gene expression from the adenovirus encoded *lacZ* gene over time following both UVC and MB+VL treatment in GM637F cells (Leach and Rainbow, 2011). To try and determine if HCR of the MB+VL treated adenovirus reporter represents repair or bypass of 8-oxoG lesions, we examined both lesion removal and HCR for gene expression. Similar to the results for UVC, we observed removal of Fpg sensitive sites from the *lacZ* gene, demonstrating DNA repair in the viral DNA. GM637F fibroblasts again demonstrated a significantly greater rate of removal compared to CHO-AA8. By 12 hours after infection, removal of MB+VL induced lesions appears to be complete with little change over the subsequent 12 hours. In comparison, only 60% of UVC induced damage is removed by 24 hours after infection. These data suggest that oxidative base damage is completed by BER at a much greater rate than UVC induced lesions by NER. The ratio of the fold increase in  $D_0$  for value for UVC treated AdCA35 from southern blot experiments (2.33; Table 1) to the fold increase of absolute  $D_{37}$  value extrapolated from the HCR (2.44) experiment shown in Figure 2 is 1:1.05 suggests that the increase in HCR of the UVC damaged reporter in GM637F compared to CHO-AA8 reflects a similar increase in the rate of lesion removal. For MB+VL treatment the values are 18.99 and 2.53 (respectively) with a ratio of 1:0.13. While the increase

in HCR observed for GM637F was significantly greater than CHO-AA8, the fold increase in gene reactivation did not reflect the fold increase in lesion removal. We have already demonstrated that reactivation of the MB+VL treated reporter reaches a maximum 12 hours after infection in GM637F while CHO-AA8 cells show reactivation continuing until 44 hours after infection (Leach and Rainbow 2011). In addition to maximal reactivation at 12 hours, we observed a decrease in expression from 12 to 24 hours (Chapter 2, Figure 2B). It is unclear why gene expression levels off or decreases at 12 hours, but the data presented in this Chapter suggest repair is complete by 12 hours. This decrease in expression at 24 hours coupled with the continued increase in reactivation seen in CHO-AA8 cells may explain why unlike UVC, the two assays do not correlate as well. The important observation is that the increase in lesion removal observed for GM637F was also reflected by significantly increased HCR in GM637F compared to CHO-AA8, suggesting that HCR of the MB+VL treated reporter represents repair.

When examining gene expression, the use of the  $D_{37}$  value assumes that a single lesion in the transcribed strand is capable of inhibiting gene expression and until that lesion is removed, gene reactivation cannot occur. Gene expression is not an instantaneous process as it requires transcription by RNA polIII, maturation of the resulting mRNA, translation, processing and shuttling of the final protein. This means, when measuring expression at a specific time (ie. 24hrs after infection) we are looking at the state of the DNA from an earlier time point. Because the HCR assay is measuring expression of a reporter gene, a minimum amount of time is required to allow for production of the  $\beta$ -gal enzyme.  $\beta$ -gal expression from the reporter gene at any given time in theory is related to the presence of transcription blocking events in the transcribed strand. While the data presented here does not examine repair in the viral reporter gene in a strand specific manner some speculation can be made. If repair were only occurring in one stand of the

*lacZ* gene, the maximum observable SF of the T4pdg/Fpg treated 3kb *lacZ* fragment after repair would be 0.5. For GM637F at 24 hours SF =  $0.55 \pm 0.0037$  (SE) for UVC and  $0.82 \pm 0.23$ (SE) for MB+VL. For MB+VL it is clear that repair is occurring overall at a faster rate than UVC and that repair is occurring in both strands of the reporter gene. The MB+VL data suggests that repair is occurring via a global repair mechanism rather than by coupling to transcription. The rapid rate of repair observed for the MB+VL treated reporter is consistent with the observation that OGG1 slides along and searches duplex DNA for 8-oxoG lesions at a rate of millions of base pairs per second (Blainey et al. 2006) and accumulates at sites of induced damage in less than two minutes (Zielinska et al. 2010). As mentioned above this increased rate of repair is consistent with our previously published results showing an earlier time for maximum gene reactivation following MB+VL treatment compared to UVC (Leach and Rainbow 2011). Based on our previous results demonstrating a greater role for GGR-NER in repair of UVC induced CPDs (discussed above) it is likely that the increase in SF for the UVC treated *lacZ* gene is the result of repair in both strands and that the value of SF= $0.55 \pm 0.0037$  (SE) is indicative of slower repair by GGR-NER rather than repair in the transcribed strand and none in the non-transcribed strand. The continual increase in expression from the UVC treated reporter gene to 72 hours after infection in GM637F (Chapter 2. Figure 2C; Leach and Rainbow 2011) suggests UVC induced CPDs are still being removed from 24 to 72 hours. This supports a greater role for GGR-NER in repair of the UVC damaged reporter in untreated cells. To support this, earlier experiments using a plasmid borne  $\beta$ -gal reporter gene did not find any evidence for TCR-NER in removal of lesions from the plasmid DNA (Ganesan et al. 1999).

The data presented here is consistent with our previous findings that HCR of the UVC treated reporter is consistent with removal of CPDs (Boszko and Rainbow 1999). It also

demonstrates that host cell repair mechanisms remove MB+VL induced 8-oxoG lesions from the adenovirus encoded reporter gene. Together with the data presented in Chapter 2, we demonstrate that HCR of  $\beta$ -gal expression correlates well with the kinetics of lesion removal and that increased HCR likely represents an increased rate or capacity of repair.

### **Acknowledgements**

Supported by the National Cancer Institute of Canada with funds from the Canadian Cancer Society.

## **Chapter 4**

**Increased host cell reactivation of an oxidatively damaged reporter gene in human primary lung fibroblasts cultured in media containing a low concentration of methylene blue.**

## **Preface**

Culturing of human primary fibroblasts in low levels of MB led to an increase in their *in vitro* replicative life span (Atamna et al. 2008). Experimental evidence, including work from our lab (Rainbow et al. 2011) demonstrates that repair of oxidative DNA damage decreases with increasing age. The increase in *in vitro* life span together with data from a clinical trial demonstrating that MB acts therapeutically in Alzheimer's disease to restore cognitive function led us to hypothesize that MB treatment has an effect on BER leading to increased *in vitro* lifespan of human primary fibroblasts in tissue culture.

The data presented in this Chapter show that BER is upregulated in fibroblasts cultured in low levels of MB, suggesting the DNA repair pathway plays a role in cellular longevity and in the therapeutic mechanism of MB action.

The work presented in this Chapter forms the basis of a manuscript that is to be submitted for peer review and publication. My contributions to this manuscript include all of the experiments, construction of all figures and writing of the manuscript. Dr. Andrew J. Rainbow provided critical insight into experimental design and writing of the manuscript as well as guidance throughout.

## Abstract

Alzheimer's disease (AD) is an age-related disease characterized by progressive neurodegeneration and dementia. Results from phase II clinical testing of methylene blue (MB) as a therapeutic agent for treatment of AD show that administration of MB significantly slowed disease progression in a large portion of individuals and improved cognitive function in AD patients after six months. MB has since been shown to mediate removal of amyloid-beta ( $A\beta$ ) peptides (senile plaques) in a mouse model by increasing activity of the proteasome. In addition MB extends *in vitro* replicative lifespan of IMR90 human primary lung fibroblasts when present at low levels in growth media. An increase in cytochrome c oxidase and in the expression of phase II anti-oxidant defence enzymes were associated with this MB mediated delay in senescence. Many reports have linked oxidative damage to DNA and the associated avoidance and/or repair processes to ageing and neurodegeneration. Amnesic mild cognitive impairment (MCI) and AD are both associated with decreased base excision repair (BER) and increased accumulation of unrepaired oxidative DNA damage. BER is the main pathway for the repair of oxidative DNA lesions and is a potential target for treatment and/or prevention of AD. MB acts as a photosensitizer and when exposed to visible light (VL) leads to the formation of 7,8-dihydro-8-oxoguanine (8-oxoG) oxidative DNA lesions that are repaired by BER. In the present work we have examined the effect of culturing IMR90 cells and primary human skin fibroblasts in 100nM MB on BER of oxidative DNA lesions using a host cell reactivation (HCR) assay. The HCR assay utilizes a non-replicating adenovirus (AdCA35) expressing the bacterial  $\beta$ -galactosidase ( $\beta$ -gal) gene and MB+VL to induced 8-oxoG lesions in the viral DNA. HCR was examined in cells grown in the presence of 100nM MB for 2 to 8 population doublings and

expression of the MB+VL-treated reporter gene was examined over a time course of 3 to 24 hours after infection with AdCA35. Consistent with an increase in BER capacity, a significant increase in expression of the oxidatively damaged  $\beta$ -gal reporter gene was observed in IMR90 fibroblasts grown in 100nM MB when scored at 12 hours after infection. However, Western blot analysis revealed no effect of growth in 100nM MB on the expression of the BER proteins APE1, CSB, DNA pol $\beta$  and p53. Although the growth of skin fibroblasts GM8400 and GM9503 in 100nM MB resulted in a small increase in expression of the oxidatively damaged  $\beta$ -gal reporter gene when scored at 12 hours after infection, this increase was not significant. The results presented here are consistent with increased BER in IMR90 lung fibroblasts due to growth in 100nM MB suggesting increased repair is involved in extension of their *in vitro* lifespan and may play a role in the positive outcome of AD patients treated with MB.

## Introduction

Alzheimer's disease (AD) is a progressive neurodegenerative disorder characterized by impaired thought and behavior as well as the inability to form new memories (Querfurth and LaFerla). AD is the most common cause of dementia (Selkoe 2001) and is found in 50% of individuals 85 years of age or older (Thies and Bleiler 2011). While the mechanisms that underlie the development and progression of AD are not fully understood a number of characteristics are pathologically associated with the disease including: extracellular deposition of amyloid-beta ( $A\beta$ ) (senile plaques), intracellular aggregation of hyperphosphorylated tau, the presence of neurofibrillary tangles, increased oxidative stress and DNA damage, a decline in cytochrome c oxidase, mitochondrial dysfunction and synaptic damage in the brain (Du et al.; Parker et al. 1990; Selkoe 2001; Mattson 2004; LaFerla et al. 2007; Reddy and Beal 2008; Coppede and Migliore 2009; Swerdlow and Khan 2009).

Strong evidence supports the accumulation of  $A\beta$  peptides in the brain as one of the major mechanisms of development and progression of AD (Haass and Selkoe 2007). The  $A\beta$  peptide is 39-43 amino acids in length and is generated by proteolytic cleavage of the  $A\beta$  precursor protein ( $A\beta$ PP), a cell surface receptor, by the  $\beta$ -secretase  $\beta$ -amyloid cleavage enzyme (BACE1) and subsequent action of a presenelin containing  $\gamma$ -secretase complex (Reddy et al.; Kang et al. 1987; Selkoe 1994; Selkoe 2001; Hardy 2006). The site of cleavage and the specific secretase catalyzing the reaction leads to the formation of either long ( $A\beta_{42,43}$ ) or short ( $A\beta_{39,40}$ ) species of  $A\beta$  (Atwood et al. 2002).  $A\beta_{42,43}$  peptides form aggregates more easily than the short  $A\beta_{39,40}$  species and are thought to act as a base for  $A\beta_{40}$  aggregation and formation of senile plaques (Atwood et al. 2002).  $A\beta$  peptides themselves stimulate the production of reactive

oxygen species (ROS) that can result in downstream DNA damage and subsequent neuronal cell death (Behl et al. 1994; Hensley et al. 1994; Varadarajan et al. 2000; Butterfield 2002). DNA nicking activity similar to nucleases has also been observed in A $\beta$ <sub>42</sub> peptides (Suram et al. 2007). In addition AD patients have significantly less active antioxidant defense systems (Vural et al. 2010), resulting in a greater amount of persistent cellular ROS and associated DNA damage.

Increasing evidence suggests that oxidative DNA damage, especially mitochondrial DNA (mtDNA) damage is an early event and is pivotal in AD progression and pathology (Gabbita et al. 1998; Wang et al. 2005; Wang et al. 2006; Coppede and Migliore 2009; Mao and Reddy 2011). Data from *postmortem* human brains, mouse and cell models have demonstrated that A $\beta$  results in the production of DNA damage in an age dependent manner in neurons (Hensley et al. 1995; Mattson 2004; Halliwell 2006; Coppede and Migliore 2009; Mao and Reddy 2011). It appears a strong feedback loop is formed between ROS, oxidative DNA damage and the formation of A $\beta$  peptides, resulting in a combined affect of all these factors leading to the development and progression of the AD neurodegeneration. Therapies that simultaneously target the multiple pathways and mechanisms thought to contribute to AD would be expected to be the most effective.

Methylene blue (MB, (tetra)methylthioninium chloride (MTC), C<sub>16</sub>H<sub>18</sub>ClN<sub>3</sub>S, rember<sup>TM</sup>) was initially developed for use in the textile industry and used in scientific research and medicine for over 100 years (Oz et al. 2009). Results from a recent clinical trial have shown that the administration of MB can significantly improve cognitive function in AD patients and slow progression of the disease by 81% (Gura 2008). Subsequent research showed that MB treatment reduces A $\beta$  levels and improves cognitive deficits in a mouse model of AD (Medina et al. 2011). Additionally, MB delays senescence and protects against the toxic affects of the DNA damaging

agents H<sub>2</sub>O<sub>2</sub> and cadmium in IMR90 human primary lung fibroblasts when present in growth media at a low concentration (Atamna et al. 2008). The MB mediated delay in cellular senescence was also associated with an upregulation of cytochrome c and antioxidant defense enzymes (Atamna et al. 2008).

MB is a thiazine dye that upon exposure to visible light (VL) is reduced to MBH<sub>2</sub> releasing highly reactive singlet oxygen (<sup>1</sup>O<sub>2</sub>) (Oz et al. 2009). When <sup>1</sup>O<sub>2</sub> generated by MB plus VL (MB+VL) interacts with DNA, the predominant lesion is of 8-oxoG with a small number of other single base oxidative lesions occurring (Floyd et al. 1989; Tuite and Kelly 1993). In addition to reduction of MB to MBH<sub>2</sub> by VL, numerous NAD(P)H-dependent enzymes can catalyze its reduction and the formation of <sup>1</sup>O<sub>2</sub> *in vivo* (Kelner et al. 1988). In its reduced MBH<sub>2</sub> state, it can accept an electron from a number of compounds allowing it to function as a prooxidant or an antioxidant depending on the conditions (McCord and Fridovich 1970; Kelner et al. 1988; Salaris et al. 1991; Riedel et al. 2003). These properties of MB allow it to cycle between its oxidized and reduced states in the proper environment.

In this work we present evidence that MB stimulates base excision repair (BER) of oxidative DNA damage, providing further information regarding the potential mechanism of action of MB in relation to AD pathology. BER is the major pathway responsible for detection and repair of oxidative DNA damage. Using a host cell reactivation (HCR) assay, we have examined the effect of 100nM MB in culture media on BER in normal human primary lung and skin fibroblasts (passage 9-21). We demonstrate a significant increase in HCR of the MB+VL treated adenovirus reporter in IMR90 primary lung fibroblasts grown in 100nM MB when reporter gene activity was scored at 12 hours after infection. An increase in HCR of the MB+VL treated adenovirus reporter was also detected in two primary skin fibroblasts grown in 100nM

MB when reporter gene activity was scored at 12 hours. However, the increase in HCR for the two primary skin fibroblasts was not significant. Our results suggest that growth of cells in 100nM MB results in increased BER of oxidative DNA damage. However, using Western blot analysis we were unable to detect a difference in the expression levels of several BER proteins in cells cultured with or without 100nM MB.

## **Materials and Methods**

### *Cells, virus and culture conditions*

The normal lung fibroblast IMR90 and the normal primary skin fibroblasts GM8400 and GM9503 were obtained from the Coriell Institute cell repository (Camden, NJ). Cell cultures were grown at 37°C in a humidified incubator in 5% CO<sub>2</sub> and cultured in Eagle's  $\alpha$ -minimal essential media ( $\alpha$ -MEM) supplemented with 10% fetal bovine serum (FBS) and antimycotic/antibiotic 100 $\mu$ g/ml penicillin, 100 $\mu$ g/ml streptomycin and 250ng/ml amphotericin B. Cell cultures grown in the presence of MB were cultured identically except the media contained 100nM MB (prepared fresh everytime). The recombinant adenoviruses Ad5MCMVlacZ with the murine CMV IE enhancer (AdCA35) was obtained from The Robert E. Fitzhenry Vector Laboratory, McMaster University, Hamilton, Ontario. The viruses were propagated, collected and titred as described previously (Graham and Prevec 1991).

### *Host cell reactivation assay*

We have previously reported a host cell reactivation (HCR) assay for examining base excision repair (BER) of methylene blue plus visible light (MB+VL) induced 8-oxoG lesions in a number of different cell strains including normal, CS and XPC fibroblasts (Kassam and

Rainbow 2007; Pitsikas et al. 2007; Leach and Rainbow 2011). The HCR assay utilizes a recombinant non-replicating adenovirus (Ad5CMVlacZ) expressing the  $\beta$ -galactosidase ( $\beta$ -gal) reporter gene under control of the murine cytomegalovirus (AdCA35) immediate early (IE) promoter (Addison et al. 1997) to examine the ability of different cell types to remove damage and reactivate reporter gene expression. Methylene blue (MB), a type II photosensitizer produces singlet oxygen ( $^1\text{O}_2$ ) upon exposure to visible light (VL) in the presence of oxygen (Slamenova et al. 2002) which through interaction with DNA predominately leads to the formation of 8-oxoG lesions with a small number of other single base oxidative lesions occurring (Floyd et al. 1989; Tuite and Kelly 1993).

#### *Treatment of the virus with methylene blue plus visible light (MB+VL)*

Preparation of methylene blue (MB) was as described previously (Pitsikas et al. 2007). Treatment of virus was performed as described previously (Kassam and Rainbow 2007). Briefly, virus suspended in cold phosphate buffered saline (PBS) (4°C,) with 20 $\mu\text{g}/\text{ml}$  MB was exposed to visible light using a 1000-W bulb (General Electric, GE R1000) at a distance of 75 cm, on ice with stirring for increasing amounts of time. The treated virus collected after each sequential visible light exposure was subsequently used to infect cells for the HCR assay.

#### *2.4 HCR of MB+VL-treated AdCA35*

Primary human fibroblasts (lung and skin) were seeded at a density of  $1.0 \times 10^4$  cells/well in 96 well plates (Falcon, Franklin Lakes, NJ). Control cells were seeded in media without MB while cells grown in MB were seeded in media containing 100nM MB. After seeding, cells were incubated for 18-24 hours and subsequently infected with 40 $\mu\text{l}$  of untreated or MB+VL treated virus for 90 minutes at a multiplicity of infection (MOI) of 200 plaque forming units (pfu)/cell.

Following the 90 minute viral adsorption period, the infection medium was aspirated and cells were washed with 200 $\mu$ l warmed PBS (37°C) and refed 200 $\mu$ l complete  $\alpha$ -MEM with or without 100nM MB and incubated for a further 3, 6, 12 or 24 hours before harvesting. A single HCR experiment consisted of triplicate wells for each treatment of the virus and triplicate wells of non-infected cells were used to obtain background levels of  $\beta$ -gal activity.  $\beta$ -gal activity was scored by measuring absorbance at 570nm as previously described (Pitsikas et al. 2005).

### *Graphing and Statistical Analysis*

The HCR  $\beta$ -gal survival curves were plotted using Origin Lab software. Each point on the graphs represents an arithmetic mean  $\pm$  SE of the  $\beta$ -gal activity at each VL exposure to the virus relative to the untreated control, calculated by pooling data obtained from multiple independent experiments. In contrast, absolute  $D_{37}$  values (VL dose to virus required to reduce  $\beta$ -gal expression to 37% of the untreated virus) for each cell line were obtained by extrapolation from the HCR survival curves of each independent experiment.  $D_{37}$  values of each cell type were then calculated relative to control (growth in media without 100nM MB) at each time point used in the same experiment and used as a measure of HCR capacity. The values from several independent experiments were used to obtain a mean absolute or relative  $D_{37} \pm$  SE. Statistical analysis of differences in  $\beta$ -gal expression at a given VL dose and absolute  $D_{37}$  values were done by two sample independent t-test using Origin Lab software. Statistical analysis of relative  $D_{37}$  values was done by one sample t-test using Origin Lab software. The  $\chi^2$ -goodness of fit test was used to determine if significant differences existed between entire curves or over specific portions of two curves.

### *Immunoblotting*

Whole cell extracts (WCE) were separated by SDS-PAGE (8% polyacrylamide) and transferred to a Hybond nitrocellulose membrane (Amersham Biosciences) in transfer buffer (25mM Tris, 0.2mM glycine, 15% Methanol, 0.01% SDS) for 2 hours. Following transfer, the membrane was blocked for 1 hour in PBST (3.2 mM Na<sub>2</sub>HPO<sub>4</sub>, 0.5 mM KH<sub>2</sub>PO<sub>4</sub>, 1.3 mM KCl, 135 mM NaCl, 0.05% Tween 20, pH 7.2) plus 20% nonfat dry milk at room temperature. The membrane was then incubated at 4°C overnight in PBST plus 5% nonfat dry milk and the indicated primary antibody at a dilution of 1:1000 (Abcam (ab3722) mouse anti-APE1 [2401]; Abcam (ab66598) mouse anti-CSB; Thermo Scientific mouse anti-DNA pol $\beta$  (DNA pol Ab-1(18s) cat# MS-669-P1; Cell Signalling rabbit anti-p53 #9282). Following incubation with the primary antibody the membrane was washed 3 times for 10 min in PBST and then incubated for 1 hour at room temperature with a 1:5000 dilution of the HRP conjugated secondary antibody (Amersham anti-rabbit NA934; Santa Cruz sc-2005 anti-mouse). The membrane was then washed 3 times for 15 min in PBST and then chemiluminescent detection was performed using the ECL Plus<sup>TM</sup> Western Blotting Detection System (GE Healthcare) and Amersham Hyperfilm ECL.

### **Results**

*Increased host cell reactivation of MB+VL damaged AdCA35 in IMR90 human normal primary lung fibroblasts cultured in 100 nM methylene blue.*

The previously published extension of *in vitro* lifespan by culturing cells with media containing 100nM MB was observed in IMR90 primary lung fibroblasts. To follow up on this finding and examine a potential role for BER in increasing maximum population doublings we first examined HCR of the MB+VL treated AdCA35 virus in IMR90 primary lung fibroblasts.

IMR90 fibroblasts were trypsinized and split 1:2 and allowed to adhere to the surface of the culture vessel. The media was then aspirated and cells were refed with fresh media with and without 100nM MB. The cells were then grown to confluence and passaged (one population doubling) at least one more time in media containing 100nM MB before beginning HCR experiments. HCR was examined in fibroblasts that had been maintained in growth media with 100nM MB for 2-8 passages/population doublings with MB being added to cells at passage 9-13.  $\beta$ -gal expression from the MB+VL treated AdCA35 (MOI 200 pfu/cell) in IMR90 fibroblasts was scored 3, 6, 12 and 24 hours after infection (Figure 1). It can be seen that HCR was significantly increased for scoring at 12 hours after infection in cells cultured in media containing 100nM MB compared to control (Figure 1, bottom left panel). From each individual HCR experiment, a  $D_{37}$  value (MB+VL dose to reduce expression of the damaged reporter to 37% expression compared to untreated control) was extrapolated from the curve for both conditions. Figure 2 shows the absolute  $D_{37}$  value at each time of  $\beta$ -gal scoring.

*Host cell reactivation of MB+VL damaged AdCA35 in human normal primary skin fibroblasts cultured in 100 nM methylene blue.*

We have previously reported a decrease in the capacity of normal human primary skin fibroblasts to reactivate expression of the MB+VL treated adenovirus reporter with increasing passage number. At high passage numbers a negative correlation exists between increasing age of donor and HCR capacity (Rainbow et al. 2011). The significant increase in HCR capacity observed in MB-treated IMR90 lung fibroblasts supports a role for increased DNA repair in the observed lengthening of *in vitro* lifespan (Atamna et al. 2008). We therefore also examined the effect of 100nM MB in the culture media in two primary skin fibroblasts; GM9503 and GM8400

to determine if growth in 100nM MB also results in increased HCR in skin fibroblasts. Consistent with results obtained using IMR90 fibroblasts, the skin fibroblasts GM9503 and GM8400 cultured in 100nM MB showed an increase in HCR capacity 12 hours after infection (Figure 3). However, this increase was non-significant. Figure 2 shows the absolute  $D_{37}$  value at each time of  $\beta$ -gal scoring for GM9503 and GM8400.

*Western blot analysis of proteins involved in base excision repair of oxidative DNA damage in IMR90 fibroblasts cultured in 100nM methylene blue*

The increased HCR observed in IMR90 fibroblasts cultured in 100nM MB is consistent with an increase in BER capacity. In an attempt to understand the mechanism behind the increased HCR in cells cultured in media containing 100nM MB we examined the expression of a number of proteins known to be involved in BER and the DNA damage response (APE1, Pol $\beta$ , p53, and CSB). Protein was harvested from IMR90 fibroblasts grown in 100nM MB and control cells not infected with AdCA35; infected with undamaged AdCA35; and infected with MB+VL treated AdCA35 (120 seconds VL exposure) 10 hours after infection. Figure 4 shows expression of APE1, DNA polymerase  $\beta$ , p53 and CSB. We were unable to detect any difference in the expression of any of these proteins suggesting any increase in BER is not the result of changes at the level of expression for these proteins.

*Effects of growth in 100nM MB on expression of the undamaged reporter gene.*

It has been reported that repair of DNA damage is greater in a cellular gene that is transcribing compared to the same gene in an uninduced state (Okumoto and Bohr 1987) and that BER enzymes assemble complexes on open chromatin regions associated with high levels of RNA polII and gene transcription following oxidative stress (Epe et al. 1993). In addition, we have reported that pretreatment of human fibroblasts with DNA damaging agents results in an

increased expression of the recombinant adenovirus encoded reporter gene (Francis and Rainbow 2000; Francis and Rainbow 2003; Zacal et al. 2005). Since a stalled transcription complex due to transcription blocking DNA lesions is thought to be a signal for the recruitment of the nucleotide excision repair (NER) DNA incision complex and subsequent removal and repair of the lesion (Francis and Rainbow 2000), increased transcription might be expected to lead to an enhanced rate of repair of DNA lesions in the transcribing strand. It was therefore possible that the increased HCR of the MB+VL-treated reporter gene in the 100nm MB treated compared to the untreated lung fibroblasts resulted from increased transcription of the reporter gene. We therefore examined the effect of 100nM MB treatment of cells on expression of the untreated reporter gene in primary lung fibroblasts. Table 1 shows the expression of the untreated reporter gene in cells grown in the presence of 100nM MB relative to control cells. It can be seen that growth in 100nM MB did not result in an increased expression of the undamaged reporter gene for any of the cells examined. Expression of the undamaged reporter gene in cells cultured in 100nM MB was decreased in IMR90 lung fibroblasts at 12 h after infection, whereas no other significant differences in expression of the undamaged reporter gene were detected between cells grown in 100nM MB and control in the IMR90 cells.

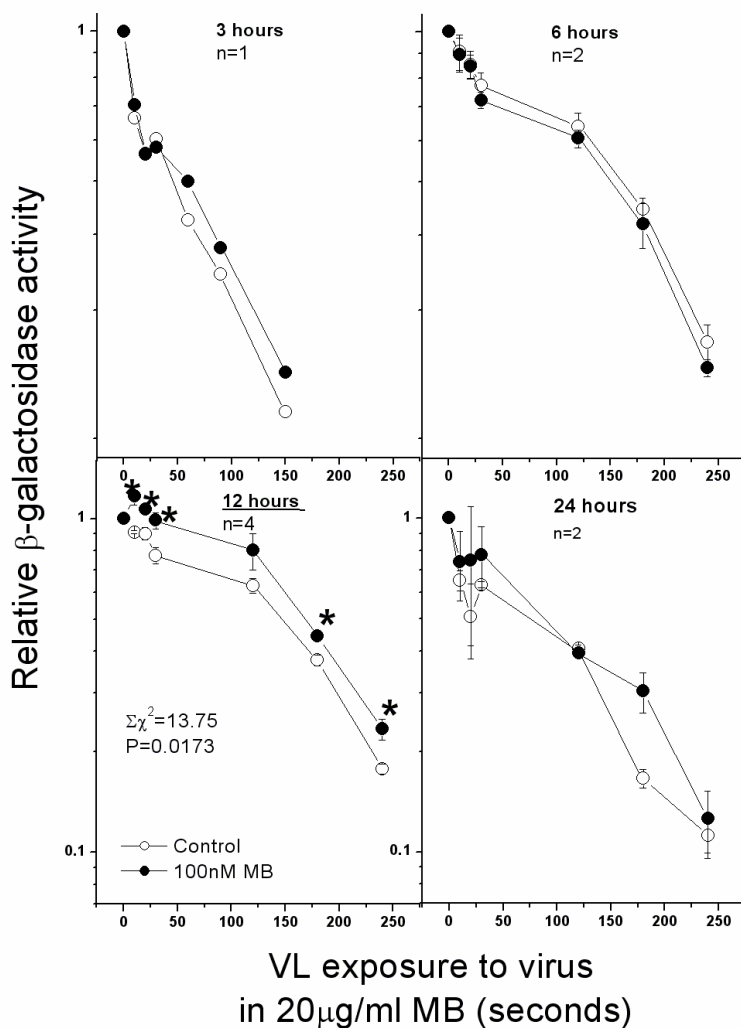


**Figure 1:** Increased host cell reactivation of MB+VL treated AdCA35 in IMR90 fibroblasts cultured in 100nM methylene blue. IMR90 primary lung fibroblasts were infected with MB+VL treated (or mock treated) AdCA35 (MOI 200) and allowed to repair and express the  $\beta$ -gal reporter gene for 3, 6, 12 and 24 hours before harvesting to measure gene expression. Time of harvesting and number of experiments (n) are indicated in the figure. Each point on the above curves is the arithmetic mean ( $\pm$ SE) of n experiments with each individual experiment done in triplicate determinations. HCR of  $\beta$ -gal expression from MB+VL treated AdCA35 was significantly increased at 12 hours for cells cultured in 100nM MB compared to control cells as measured by the  $\chi^2$ -goodness of fit test ( $p=0.0173$ ) for the entire HCR curve; by two sample independent t-test at VL doses of 10, 20, 30, 180 and 240 seconds to AdCA35 ( $p=0.01126$ ;  $p=0.00771$ ;  $0.0218$ ;  $0.0202$ ;  $0.0336$  respectively). Asterisks indicate points found to be significantly different compared to control.

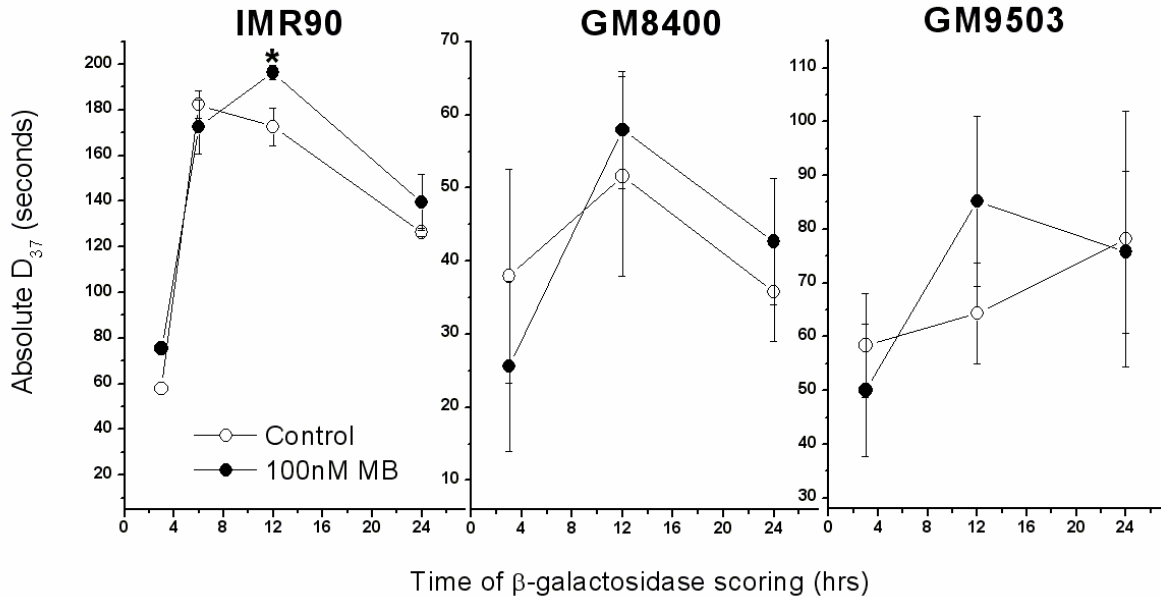


**Figure 2:** Absolute  $D_{37}$  values for reporter gene reactivation in normal lung and skin fibroblasts over time. For each individual HCR experiment an absolute  $D_{37}$  (seconds of visible light exposure to virus in  $20\mu\text{g/ml}$  MB to reduce  $\beta$ -gal expression to 37%) value was extrapolated from the resulting curve. Each curve shown above is the arithmetic mean ( $\pm$ SE) of all experiments conducted for each given fibroblast (n values for IMR90 are the same as Figure 2; n values for GM8400 and GM9503 are the same as Figure 3). Comparison of absolute  $D_{37}$  values for control cells and cells grown in 100nM MB at each time point was done using a two sample independent t-test. The absolute  $D_{37}$  for IMR90 fibroblasts cultured in 100nM MB was significantly increased compared to control ( $p=0.03199$ , indicated by an asterisk on the curve). For IMR90 lung fibroblasts, reactivation reached a maximum 6 hours after infection in control cells and 12 hours in cells grown in 100nM MB. Reactivation of the  $\beta$ -gal reporter gene in GM8400 and GM9503 reached a maximum absolute  $D_{37}$  12 hours after infection in cells cultured in 100nM MB. Control cells reached maximum reactivation at 12 hours in GM8400 and at 24 hours in GM9503. No significant differences in HCR were detected in GM8400 or GM9503 between control cells and those grown in 100nM MB.

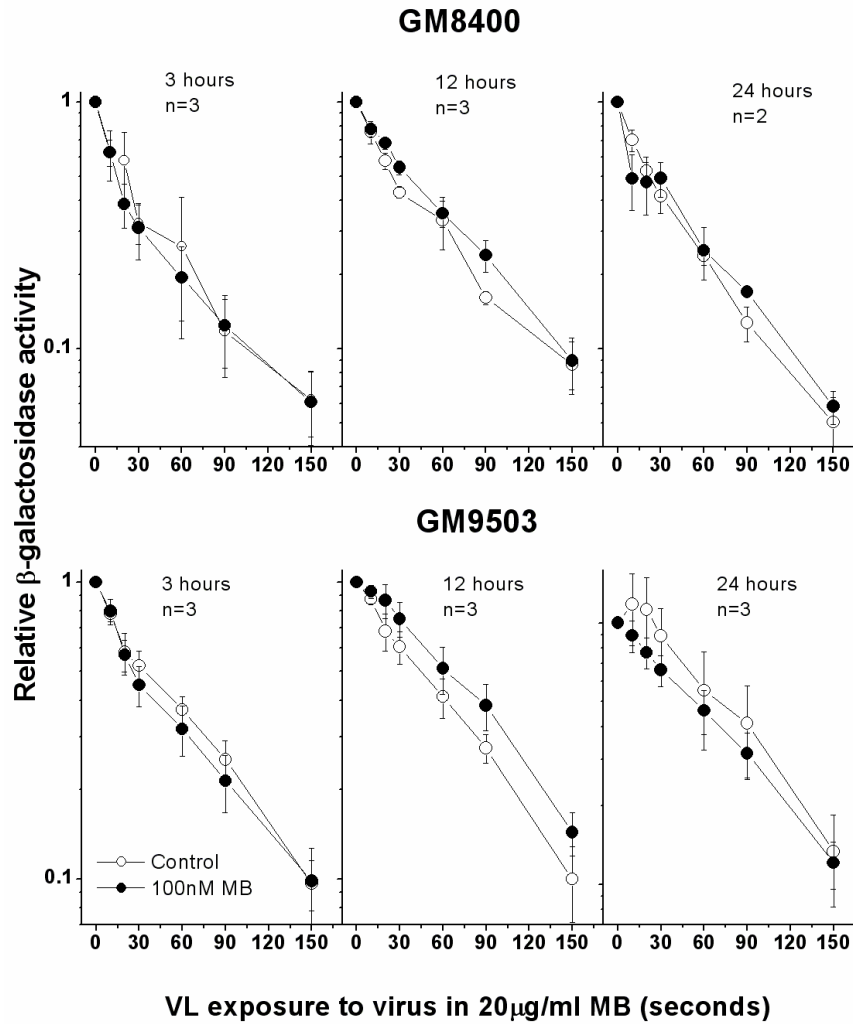


**Figure 3:** Host cell reactivation of MB+VL treated AdCA35 in GM8400 and GM9503 primary skin fibroblasts cultured in 100nM methylene blue. GM8400 and GM9503 primary skin fibroblasts were infected with MB+VL treated (or mock treated) AdCA35 (MOI 200) and allowed to repair and express the  $\beta$ -gal reporter gene for 3, 12 and 24 hours before harvesting to measure gene expression. Time of harvesting and number of experiments (n) is indicated in the figure. Each point on the above curves is the arithmetic mean ( $\pm$ SE) of n experiments with each individual experiment done in triplicate determinations. Similar to IMR90 fibroblasts, an increase HCR of MB+VL treated AdCA35 in skin fibroblasts grown in 100nM MB was observed at 12hrs. This difference was not found to be significant by analysis of absolute  $D_{37}$  values by two sample t-test (see Figure 2).

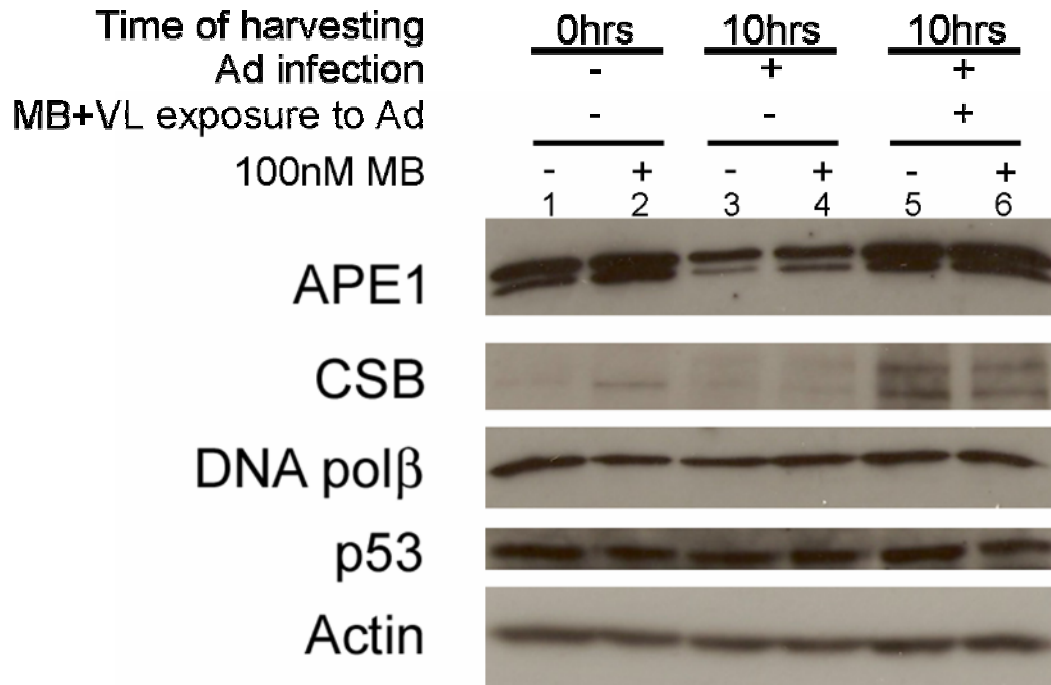


**Figure 4:** Western blot analysis of proteins associated with repair of oxidative DNA damage in IMR90 fibroblasts. Western blot analysis of BER protein expression was examined using whole cell extracts (WCE) from IMR90 primary lung fibroblasts. Control cells and cells grown in 100nM MB were mock infected, infected with untreated AdCA35 or MB+VL (120 seconds VL exposure) treated AdCA35 and incubated for 10 hours (Time of harvesting refers to the number of hours post infection with AdCA35). WCEs were collected and separated by SDS-PAGE on an 8% polyacrylamide gel and transferred to a nitrocellulose membrane. Actin was used as a loading control. No difference was detected between control cells or cells grown in 100nM MB for each condition. Expression of APE1 appears to be lower in cells infected with undamaged AdCA35. CSB expression is increased with infection by MB+VL damaged virus suggesting increased expression or stabilization following the introduction of oxidative DNA damage.

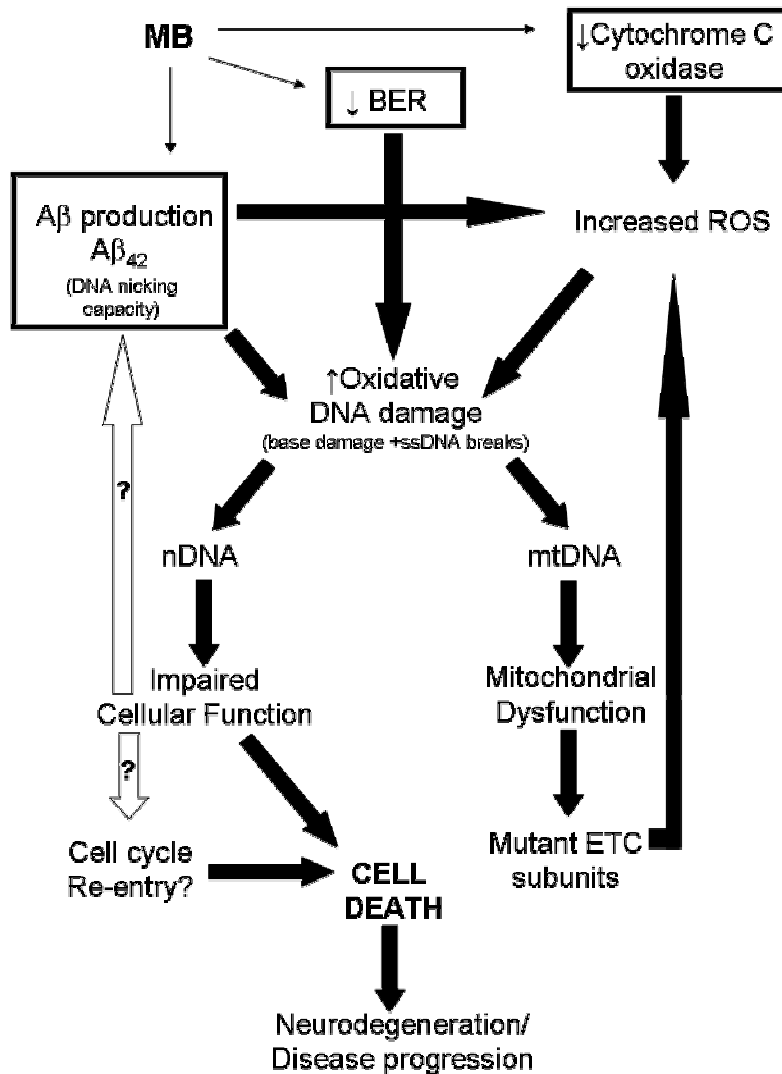


**Figure 5:** Proposed mechanism for the development and progression of Alzheimer’s disease and the potential targets of MB. Decreased BER capacity leads to the accumulation of oxidative DNA damage and low levels of neuronal cell death leading to MCI. Oxidative damage is unrepaired and accumulates in both nDNA and mtDNA as a result of lowered BER capacity. Accumulation of damage in nDNA leads to impaired cellular function and cell death. In addition, cellular dysfunction may trigger cell cycle re-entry that again results in cell death (Lopes et al. 2009) (represented by an open arrow containing a question mark as the exact cause and consequence of this response is not clear). Neuronal cell death results in neurodegeneration and the development and progression of AD. An additional consequence of impaired cellular function may be increased production of A $\beta$ . It is possible that A $\beta$  accumulation begins independently and works in conjunction with decreased BER during the early stages of disease development and later forms a feedback loop amplifying the process and driving the disease forward. Production of A $\beta_{42}$ , which has DNA nicking capabilities, directly adds to the accumulation of DNA damage through the generation of ssDNA breaks, while A $\beta$  peptides stimulate production of ROS. Mitochondrial dysfunction results from the accumulation of mtDNA damage and generates another feedback loop amplifying the attack on DNA.

Culturing of IMR90 lung fibroblasts in MB causes upregulation of cytochrome c and phase II antioxidant enzymes (Atamna et al. 2008). Cytochrome c oxidase is an electron carrier in the ETC and normally transfers an electron to O<sub>2</sub> generating H<sub>2</sub>O. Cytochrome c oxidase can transfer that electron to radical species such as the singlet oxygen radical (<sup>1</sup>O<sub>2</sub>) generated by *in vivo* reduction of MB by NAD(P)H-dependent enzymes (Kelner et al. 1988) thereby protecting the cell from their deleterious effects. The decline in cytochrome c oxidase observed in AD doesn't directly produce ROS, but rather decreases the cells capacity to get rid of them. In this study we have shown that culturing human fibroblasts in MB enhances HCR of oxidatively damaged DNA suggesting that the presence of MB decreases the amount of oxidative DNA damage in nDNA and mtDNA and prevents further accumulation as well as downstream cell death. MB increased BER combined with upregulation of cytochrome c oxidase and the reduction in Aβ accumulation makes this a promising compound for the treatment of AD as it appears to act on multiple pathways thought to be major contributors in the development and progression of the disease. Boxed portions of the proposed mechanism indicate the parts of the pathway that MB is likely acting on.

**Table 1:** Expression of the untreated reporter gene in cells grown in the presence of 100nM MB relative to control cells. Expression from cells cultured in 100nM MB was normalized to each expression in control cells (set to 1) for each individual experiment. The values contained in the table below are mean relative expression values ( $\pm$ SE) from the untreated virus. Growth of cells in 100nM MB did not lead to an increase in expression of the reporter gene for the untreated control virus suggesting that the increase in HCR for reporter gene expression is due to increased lesion removal rather than increased transcriptional bypass of the lesion.

Cell Type	Time of $\beta$ -gal scoring								
	3 hours		12 hours		24 hours				
IMR90	1.10	$\pm$ -	(1)	0.72	$\pm$ 0.0085*	(3)	0.66	$\pm$ 0.11	(2)
GM8400	1.17	$\pm$ 0.22	(3)	0.94	$\pm$ 0.14	(3)	0.92	$\pm$ 0.16	(2)
GM9503	0.90	$\pm$ 0.07	(3)	0.93	$\pm$ 0.20	(3)	1.16	$\pm$ 0.25	(3)

An asterisk (\*) indicates a value significantly different from 1 by two tailed one sample t-test. Numbers shown in brackets represent the number of experiments (n).

#### 4. Discussion

Cellular production of ROS increases with age leading to increased accumulation of oxidative DNA damage in older humans and mice (Kaneko et al. 1996; Hamilton et al. 2001; Sedelnikova et al. 2004; von Figura et al. 2009). Our lab has demonstrated a decrease in HCR of the MB+VL treated reporter in normal human primary skin fibroblasts with increasing passage number and that at high passage numbers a negative correlation exists between increasing age of donor and HCR capacity (Rainbow et al. 2011) supporting and *in vitro* decline in BER with age. It has been suggested that the impaired cellular function and neuronal cell death associated with normal ageing of the brain and pathological neurodegeneration results from the accumulation of oxidative DNA damage (Bohr et al. 1998; Schmitz et al. 1999). Consistent with this, a number of studies have shown increased levels of oxidative DNA damage in tissue samples from individuals with AD compared to control samples (Mecocci et al. 1994; Lyras et al. 1997; Gabbita et al. 1998; Lovell et al. 1999; Wang et al. 2005). Increased oxidative DNA damage has also been observed in samples from individuals with amnesic mild cognitive impairment (MCI) (Migliore et al. 2005; Wang et al. 2006), a phase considered the transition between normal ageing and the development of dementia (Coppede and Migliore 2009). Individuals affected by MCI and AD also demonstrate reduced BER (Lovell et al. 2000; Iida et al. 2002; Weissman et al. 2007; Shao et al. 2008; Mao and Reddy 2011); supporting the hypothesis that defective DNA repair is a major factor in development/progression of the disease. Together these observations suggest increasing the ability of cells to protect against the deleterious effects of oxidative DNA damage would provide an avenue for slowing the ageing process and preventing the progression or treating neurodegenerative disorders such as AD and MCI.

The use of MB as a therapeutic agent in the treatment of AD has shown promise in a recent clinical trial (Gura 2008) and both *in vitro* and *in vivo* studies have begun to elucidate potential mechanism(s) of action (Atamna et al. 2008; Medina et al. 2011). MB reduces A $\beta$  levels both *in vitro* and *in vivo* and culturing cells in growth media containing MB has delays cellular senescence in IMR90 human primary lung fibroblasts (Atamna et al. 2008). The presence of low levels of MB in growth media increased the levels of cytochrome c, a subunit of the electron transport chain (ETC) and is downregulated in AD (Parker et al. 1990). In addition to the upregulation of cytochrome c, an increase in phase II antioxidant defense enzymes was also observed in MB treated IMR90 human primary lung fibroblasts (Atamna et al. 2008). Phase II antioxidant defense enzymes act downstream of major cellular redox sensors such as glutathione (GSH) to boost the cellular defense against oxidative stress and related damage (Hayes and McLellan 1999; Griffiths 2000). The upregulation of pathways involved in protecting against downstream oxidation of cellular macromolecules including DNA by ROS suggests that culturing cells in the presence of MB increases the level of oxidative stress. Since an increase in oxidative stress and a decrease in BER are both associated with AD, the success of MB as a therapeutic drug combined with these observations prompted us to examine its effects on BER. We hypothesized that in addition to the upregulation of antioxidant defense mechanisms which would help to neutralize the deleterious effects of the drug itself as well as cellular ROS, MB may also stimulate BER.

Using the HCR assay our results demonstrate a significant increase in the ability of IMR90 primary lung fibroblasts cultured in 100nM MB to reactivate expression of the MB+VL treated reporter gene when measured 12 hours after infection. A similar but non-significant increase was observed in primary human skin fibroblasts. Previous work from our lab has shown

that reactivation of the MB+VL treated AdCA35 reporter gene reaches a maximum 12 hours after infection in normal SV40 transformed (Leach and Rainbow 2011). To address the possibility that changes in the level of transcription of the reporter gene in cells cultured in the presence of MB lead to the increase in HCR we compared expression of the untreated control virus in cells cultured in media containing 100nM MB and control cells. There was no significant increase in expression from the reporter gene in cells cultured in MB, in fact IMR90 fibroblasts showed a reduction. These data suggest that the significant increase in HCR observed in IMR90 and non-significantly in GM8400 and GM9503 were not the result of an MB stimulated increase in reporter gene expression and lesion bypass. Together these results strongly suggest that MB stimulates BER of 8-oxoG from an actively transcribed gene. Expression of a number of proteins involved in BER of 8-oxoG was examined to see if MB had an effect on their levels. No changes in expression were observed between cells cultured in growth media containing 100nM MB compared to control under any of the conditions examined. The increase in BER of 8-oxoG may be due changes in the level of BER factors that were not examined in this study or the activity of the proteins examined were increased by post-translational modifications that were not detectable under the conditions used.

In this study we have used pre-senescent mitotic fibroblasts to study the possible mechanism of action for MB in post-mitotic neuronal cells/tissues affected tissue in AD. DNA repair in post-mitotic cells and cells in G1 is mainly achieved by BER, which removes single base oxidative lesions and single strand DNA (ssDNA) breaks. The HCR assay examines repair in a non-replicating adenovirus in a confluent monolayer of cells. While the cells are not post-mitotic, the HCR assay measures repair in transcriptionally active DNA that is not being replicated.

The build up of oxidative DNA damage in nuclear DNA (nDNA) of post-mitotic cells such as neurons is believed to trigger cell death (Mao and Reddy 2011). Accumulation of DNA damage in mtDNA can lead to mutant transcripts encoding subunits of the ETC causing mitochondrial dysfunction, increased ROS production and related oxidative damage and ultimately cell death (Mao and Reddy 2011). The earliest detectable change in the progression towards dementia and AD, presumably caused by defective BER (Weissman et al. 2007; Shao et al. 2008), is the increase in oxidative DNA damage observed in MCI (Migliore et al. 2005; Wang et al. 2006). The results presented here suggest that part of the success of MB in preventing the progression of AD may be increased BER which prevents further accumulation of oxidative DNA damage, thereby preventing additional neuronal cell death. This combined with the upregulation of cytochrome c (Parker et al. 1990) and A $\beta$  reducing capabilities (Medina et al. 2011) of MB provides a strong explanation for its mechanism in treating AD (Figure 5). The ability of MB to simultaneously target multiple pathways thought to be key in AD pathology makes it a promising compound for continued study.

### **Acknowledgements**

Supported by the National Cancer Institute of Canada with funds from the Canadian Cancer Society.

## **Chapter 5**

**Oxidative DNA damage leads to greater expression of an undamaged reporter gene driven by the cytomegalovirus immediate early promoter in Cockayne syndrome fibroblasts.**

## **Preface**

Persistent DNA damage in an actively transcribed gene of cells treated with several DNA damaging agents leads to upregulation of gene expression from the untreated adenovirus reporter (Francis and Rainbow 2000; Francis and Rainbow 2003; Zacal et al. 2005; Pitsikas et al. 2007). This adenovirus based  $\beta$ -gal reporter gene assay is referred to as the enhanced expression assay. The upregulation is thought to occur by signalling resulting from stalled RNA polII complexes at sites of DNA damage. While defective BER is a general feature of cells from individuals with CS, a high degree of clinical variability is observed among patients (Nance and Berry 1992; Natale 2011). Primary fibroblasts isolated from CS patients also show variability in their accumulation of 8-oxoG following cellular exposure to ionizing radiation (Tuo et al. 2003). Using clinical and biochemical data collected for each patient/cell line (summarized in appendix II, Table 1) we examined primary skin fibroblasts from a number of different CS patients in order to determine if clinical severity had any correlation with the severity of the BER defect.

Results presented here demonstrate that all CS fibroblasts, regardless of clinical severity show greater expression of the undamaged reporter gene following cellular treatment with MB+VL. These observations support the conclusion that defective BER leads to the accumulation of 8-oxoG and that the lesion is capable of blocking transcription by RNA polII.

The work presented in this Chapter forms the basis of a manuscript that is to be submitted for peer review and publication. My contributions to this manuscript include all of the experiments, construction of all figures and writing of the manuscript. Dr. Andrew J. Rainbow provided critical insight into experimental design and manuscript writing as well as guidance throughout.

## Abstract

Cockayne syndrome (CS) is a rare genetic disease classified as a segmental progeroid syndrome with symptoms of accelerated aging and neurodegeneration. Many reports have linked oxidative damage to DNA and the associated avoidance and/or repair processes to ageing and neurodegeneration and it has been suggested that the accumulation of unrepaired DNA lesions plays a causal role in mammalian aging. Since base excision repair (BER) is the main pathway for the repair of oxidative DNA lesions, the relationship of BER to human aging is of considerable interest. In the present work we have used a reporter gene assay to examine BER of MB+VL induced 8-oxoG lesions in cells from CS patients. We have reported previously that pretreatment of cells with UVC irradiation leads to enhanced expression from the human cytomegalovirus immediate-early promoter of a  $\beta$ -galactosidase ( $\beta$ -gal) reporter gene at lower UV fluences and to higher levels in TCR-deficient cells (CS and xeroderma pigmentosum (XP) compared to TCR-proficient cells (normal and XPC). The induction of  $\beta$ -gal expression at low UV fluences was induced by persistent unrepaired cyclobutane pyrimidine dimers (CPDs) in actively transcribed regions of the genome and it is thought that stalled RNA polymerase II (polII) complexes at these unrepaired lesions lead to the increase in expression. Using this reporter gene assay we have examined the persistence (RNA polII blocking ability) of methylene blue plus visible light (MB+VL) induced 7,8-dihydroxy-8-oxoguanine/(8-oxoG) in primary skin fibroblasts from 7 CS patients with mutations in the *CSA* or *CSB* gene. Expression of the undamaged  $\beta$ -gal reporter was enhanced in all 7 CS fibroblasts relative to normal fibroblasts pretreated with MB+VL indicating the persistence of 8-oxoG in actively transcribed genes in cells from these CS individuals. These results support a role for the CSA and CSB proteins in the

repair of oxidative DNA damage and that 8-oxoG leads to inhibition of RNA polII progression during transcription of active genes.

## Introduction

Numerous endogenous and exogenous agents constantly interact with and alter the DNA of living organisms. To combat this and preserve the integrity of the genome, evolution has endowed cells with a repertoire of DNA repair mechanisms to detect and remove the large assortment of DNA modifications generated by these agents. The nucleotide excision repair (NER) pathway detects and removes bulky helix distorting lesions such as those generated by ultraviolet (UV) light. NER consists of two sub pathways; global genomic repair (GGR), which is responsible for removing lesions throughout the entire genome, and transcription coupled repair (TCR), which removes RNA polymerase II (polII) blocking lesions found within the transcribed strand of active genes (for a review of DNA repair pathways including NER see (Hoeijmakers 2009)). Base excision repair (BER) is responsible for repairing lesions with minor or non-helix distorting properties such as those generated by reactive oxygen species (ROS) (Dianov et al. 2001; Slupphaug et al. 2003). ROS are generated endogenously as a by-product of aerobic respiration in eukaryotic cells and have been estimated to cause  $10^5$  damaging events per genome per cell per day (Fraga et al. 1990). Detection of oxidized bases is accomplished by DNA glycosylases, a class of enzymes that catalyze cleavage of the N-glycosidic bond linking the oxidized base to the deoxyribose in the DNA backbone; a step which results in the formation of an apurinic/apyrimidinic (AP) site (Stivers and Jiang 2003; Dizdaroglu 2005; Huffman et al. 2005). Cells contain many different DNA glycosylases, each of which is responsible for recognizing a specific lesion or set of lesions (Dizdaroglu 2003) (For a review of BER and DNA glycosylase specificity see (Wilson and Bohr 2007)). Some glycosylases, such as the human 8-oxoguanine glycosylase (OGG1), which recognizes 7,8-dihydro-8-oxoguanine (8-oxoG), possess

AP-lyase activity which nicks the DNA backbone 3' to the AP site formed by its prior removal of the oxidized base, generating a single strand break (SSB) (Hazra et al. 2001). Lesions detected by DNA glycosylases lacking the associated AP-lyase activity, remain bound to the AP site to act as a docking site for an AP-lyase enzyme to subsequently generate the 3' incision in the DNA (Wilson and Bohr 2007). Following 3' incision by AP-lyase an AP endonuclease incises the DNA 5' to the abasic site, generating a nucleotide gap in place of the damaged base (Wilson and Barsky 2001). AP endonuclease 1 (APE1) is the major enzyme responsible for this step in human cells (Wilson and Barsky 2001). DNA polymerase  $\beta$  (pol  $\beta$ ) subsequently fills in the gap which in turn is joined by DNA ligase I on its own or in complex with x-ray cross-complementing 1 (XRCC1) protein to complete the repair process (Tomkinson et al. 2001).

Mutations in NER genes lead to a number of clinically distinct disorders including Cockayne syndrome (CS), xeroderma pigmentosum (XP), cerebro-ocular-facial syndrome (COFS) and UV sensitive syndrome (UV<sup>S</sup>S) (Itoh et al. 1995; Lehmann 2003). CS is a rare autosomal recessive disease classified as a segmental progeroid syndrome where affected individuals exhibit premature aging, developmental abnormalities and severe neurodegeneration (Nance and Berry 1992; Natale 2011). A hallmark characteristic of skin fibroblasts from CS patients is a failure to recover RNA synthesis following exposure to UV-light (Mayne and Lehmann 1982) resulting from defective removal of UV-induced cyclobutane pyrimidine dimers (CPDs) via TCR-NER (Venema et al. 1990). XP results from a genetic defect that abolishes both sub pathways of NER, excluding individuals with *XPC* or *XPE* mutations who retain functional TCR-NER. XP is caused by a mutation in one of seven XP genes (*XP-A* through *XP-G*) while CS is caused by mutations in the *CS-A* or *CS-B* gene or by specific mutations in *XP-B*, *XP-D*, *XP-G*, with the latter three resulting in a combined XP/CS phenotype (Hoeijmakers 2009). XP patients

show extreme photosensitivity with an incidence of skin cancer 1000 times greater than the normal population (de Boer and Hoeijmakers 2000). Approximately 20% of XP individuals and nearly 100% of those from the XP-A complementation group display neurological abnormalities (Kraemer et al. 1987; Sidwell et al. 2006). Poor growth and neurological abnormalities are considered hallmark symptoms for diagnosis of CS (Nance and Berry 1992; Natale 2011). Individuals affected with CS appear normal at birth but suffer from postnatal growth failure resulting in cachectic dwarfism, they are also photosensitive but do not have an increased incidence of skin cancer (Nance and Berry 1992; Natale 2011). Although CS and XP both arise from a defect in the same DNA repair pathway, it is difficult to resolve the differences in their clinical symptoms based solely on the affected NER sub-pathway.

Evidence from a number of studies have demonstrated that in addition to the lack of TCR-NER, CS cells have defective BER of oxidative lesions (Francis et al. 1997; Dianov et al. 1999; Osterod et al. 2002; de Waard et al. 2003; de Waard et al. 2004; Spivak and Hanawalt 2006; D'Errico et al. 2007; Gorgels et al. 2007). In earlier work from our laboratory we reported that the defective removal of UV induced cyclobutane pyrimidine dimers (CPDs) in CS cells is only partially corrected by T4 endonuclease V (denV) (Francis and Rainbow). DenV is a DNA glycosylase that removes CPDs and generates an apurinic/apyrimidinic site (AP site) that requires further processing by the BER pathway. This suggested that CS cells are deficient in BER processes as well as NER (Francis et al. 1997). Defective repair of 8-oxoG, one of the most prominent endogenously formed oxidative base lesions (Kasai and Nishimura 1984; Ames 1989), has been demonstrated in SV40 transformed CS-A and CS-B fibroblasts (Spivak and Hanawalt 2006; Leach and Rainbow 2011). Reduced repair of 8-oxoG was also demonstrated in mitochondrial DNA from CS-A and CS-B cells (Stevnsner et al. 2002). A number of CS-A and

CS-B skin fibroblasts have been shown to accumulate greater background levels (D'Errico et al. 2007) as well as induced levels (Tuo et al. 2003) of 8-oxoG when compared to normal fibroblasts. Background levels of 8-oxoG are returned to that of wild type (WT) cells in CSA fibroblasts by expression of WT CSA (D'Errico et al. 2007).

We have previously reported the use of an enhanced expression assay for detecting persistent unrepaired cellular DNA damage caused by cisplatin, N-acetoxy-acetylaminofluorine (Zacal et al. 2005), UVC irradiation (Francis and Rainbow 2000; Francis and Rainbow 2003; Zacal et al. 2005) and MB+VL (Pitsikas et al. 2007). In this assay, cells are pre-treated with a DNA damaging agent prior to the introduction of an undamaged adenovirus reporter construct. Using this assay we have reported that pretreatment of cells with UVC irradiation leads to enhanced expression from the human cytomegalovirus immediate-early promoter of a  $\beta$ -gal reporter gene at lower UV fluences and to higher levels in TCR-deficient cells (CS and XP) compared to TCR-proficient cells (normal and XPC) (Francis and Rainbow 2000; Zacal et al. 2005). The induction of  $\beta$ -gal expression at low UV fluences was induced by persistent unrepaired CPDs in actively transcribed regions of the genome (Francis and Rainbow 2000) and it is thought that stalled RNA polII complexes at these unrepaired lesions lead to the increase in expression. In addition, we have used this assay to show that pretreatment of cells defective in mismatch repair (LoVo cells; hMSH2<sup>-/-</sup>) with MB+VL results in enhanced expression of the undamaged reporter gene when compared to repair proficient cells (SW480) (Pitsikas et al. 2007). This latter report suggests that unrepaired MB+VL-induced 8-oxoG DNA lesions result in stalled RNA polII complexes and a subsequent increase in the expression of the reporter gene.

Using a host cell reactivation (HCR) assay, we and others (Spivak and Hanawalt 2006; Leach and Rainbow 2011) have shown that SV40 transformed human fibroblasts from patients

with mutations in CSA and CSB have reduced reactivation of the MB+VL treated reporter compared to SV40 transformed normal fibroblasts (Leach and Rainbow 2011). This reduction in HCR is consistent with RNA polII inhibition by unrepaired 8-oxoG lesions in SV40 transformed CS cells. The SV40 large T-antigen inhibits the function of pRb and p53 both of which have been shown to influence cellular DNA repair (Cheng et al. 2009). It was therefore considered important to also examine RNA polII inhibition by unrepaired 8-oxoG lesions in non-transformed CS cells.

In the present work we have used the enhanced expression assay to examine BER of MB+VL induced 8-oxoG lesions in primary skin fibroblasts from CS patients from complementation groups A and B as well as from normal individuals. The data support the conclusion that 8-oxoG lesions inhibit progression of actively transcribing RNA polII and that CSA and CSB fibroblasts are defective in BER of MB+VL induced 8-oxoG lesions.

## **Materials and Methods**

### *Cell Lines and Viruses.*

The normal fibroblasts GM9503, GM969C, GM38A and GM10901, the CSA fibroblasts CS3BE (GM1856), GM2965, the CSB fibroblasts, CS1AN (GM739), CS1BE (GM1629A), CS7SE (GM1428A), CS2BE (GM1098C) and GM10903 were obtained from NIGMS (Camden, NJ). The CSA primary fibroblast AG07076 was obtained from the Coriell Institute cell repository (Camden, NJ). The CSA, CS6BR and CSB CS3TAN primary fibroblasts were obtained from Dr. M. Stefanini Istituto di Genetica Molecolare CNR, Pavia, Italy. Table 1 in appendix II contains a list of CS fibroblasts used in this work with mutation and clinical data

Cell cultures were grown at 37°C in a humidified incubator in 5% CO<sub>2</sub> and cultured in Eagle's  $\alpha$ -minimal essential media ( $\alpha$ -MEM) supplemented with 15% fetal bovine serum and antimycotic antibiotic 100 $\mu$ g/ml penicillin, 100 $\mu$ g/ml streptomycin and 250ng/ml amphotericin B. The recombinant adenoviruses Ad5HCMVlacZ (AdCA17) and Ad5MCMVlacZ (AdCA35) was obtained from The Robert E. Fitzhenry Vector Laboratory, McMaster University, Hamilton, Ontario. The virus was collected and titered as described previously (Graham and Prevec 1991).

*The enhanced expression assay*

Primary human fibroblasts were seeded at a density of  $1.0 \times 10^4$  cells/well in 96 well plates (Falcon, Franklin Lakes, NJ) for pretreatment of cells with MB+VL, overlaying media was aspirated 12 hours after seeding and replaced in the dark with 100 $\mu$ l warmed complete  $\alpha$ -MEM containing MB (0, 2.5, 5, 7.5, 10, 12.5, 15, 17.5  $\mu$ g/ml) and incubated for a further 12 hours without exposure to light. Following the subsequent incubation period, media containing MB was aspirated, cells were washed with 100 $\mu$ l warmed PBS and overlaid with 40 $\mu$ l warmed PBS and exposed to visible light using a 1000-W bulb (General Electric, GE R1000) at a distance of 81cm for 10 min.

For pretreatment of cells with UVC, overlaying media was aspirated 24 hours after seeding and replaced with 40 $\mu$ l warmed PBS. A General Electric germicidal lamp (model G8T5) emitting predominately at 254nm was used to expose cells to 5, 10, 12.5, 15, 17.5 and 27.5 J/m<sup>2</sup> UVC at a fluence rate of 1J/m<sup>2</sup>/s.

Immediately following VL or UVC exposure, PBS was aspirated from each well and cells were infected with 40 $\mu$ l of untreated AdCA17 virus in unsupplemented  $\alpha$ -MEM for 90

minutes at an MOI of 20 plaque forming units (pfu)/cell or overlaid with 40 $\mu$ l of media containing no virus for control. Following the viral adsorption period, the infection media was aspirated and cells were subsequently overlaid with 200 $\mu$ l of complete  $\alpha$ -MEM and incubated for a further 24 hours before harvesting for measuring  $\beta$ -gal activity. A single enhanced expression experiment consisted of triplicate wells for each treatment of the cells and triplicate wells of non-infected cells were used to obtain background levels of  $\beta$ -gal activity.  $\beta$ -gal activity was scored by measuring absorbance at 570nm as previously described (Pitsikas et al. 2005).

### *Immunoblotting*

20 $\mu$ g of protein from whole cell extracts (WCE) prepared from normal, CSA and CSB primary fibroblasts was separated by 8% SDS-polyacrylamide gel electrophoresis (PAGE) and transferred to a Hybond nitrocellulose membrane (Amersham Biosciences) in transfer buffer (25mM Tris, 0.2mM glycine, 15% Methanol, 0.01% SDS) for 2 hours. Following transfer, the membrane was blocked for 1 hour in TBST (10mM Tris pH 8.00, 15mM NaCl, 0.05% tween 20) plus 20% nonfat dry milk at room temperature. The membrane was then incubated at room temperature for 2 hours in TBST plus 5% nonfat dry milk and the primary antibody at a concentration of 1:1000 (Anti-CSB antibody, Bethyl Laboratories Inc. A301-345A). Following incubation with the primary antibody the membrane was washed 3 times for 10 min in TBST and then incubated for 1 hour at room temperature with a 1:5000 dilution of the HRP conjugated secondary antibody (Amersham anti-rabbit NA934). The membrane was then washed 3 times for 10 min in TBST and then chemiluminescent detection was performed using the ECL Plus<sup>TM</sup> Western Blotting Detection System (GE Healthcare) and Amersham Hyperfilm ECL. The anti-

CSB primary antibody used for detection of CSB recognizes an N-terminal region between residue 1 and 50 of the human CSB protein.

### *Graphing and Statistical Analysis*

The  $\beta$ -gal expression curves were plotted using Origin Lab software. Each point on the graphs represents an arithmetic mean  $\pm$  SE of the  $\beta$ -gal activity at each MB+VL dose to cells relative to the untreated control calculated by pooling data obtained from multiple independent experiments. Statistical analysis of enhanced expression experiments was done using a two sample independent t-test with a confidence interval of 0.05.

## **Results**

### *Enhanced expression of the CMV driven $\beta$ -galactosidase reporter gene in primary human fibroblasts following cellular pre-treatment with methylene blue plus visible light. .*

In order to determine the best approach to cellular treatment with MB+VL we used two MB+VL pre-treatment protocols to examine the expression of the undamaged reporter gene in AdCA17 for normal, CSA and CSB primary fibroblasts. Primary fibroblasts were either (A) incubated in increasing concentrations of MB and exposed to 10 min VL or (B) incubated in 15  $\mu$ g/ml MB and exposed to increasing amounts of VL prior to infection with undamaged AdCA17. Initial experiments which examined the time course of  $\beta$ -gal expression indicated that scoring at 24 h after infection resulted in readily detectable differences in  $\beta$ -gal expression levels between the CS and normal fibroblasts (data not shown, see Appendix II). Consequently, scoring for  $\beta$ -gal was carried out at 24h after infection for either protocol. Results of representative experiments are shown in Figure 1. It can be seen that for pre-treatment with increasing

concentrations of MB plus 10 min VL (Fig. 1A, left panel), decreased expression from undamaged AdCA17 was observed for the normal primary fibroblasts GM9503 and GM38A, while an increase in reporter gene expression was observed for both CSA (CS3BE) and CSB (CS1AN) primary fibroblasts. For exposure to increasing amounts of VL following incubation in 15 µg/ml MB (Fig. 1B, right panel) a large increase in expression was observed for the CSA (CS3BE) fibroblast, while the CSB (CS1AN) and normal (GM38A) showed a decrease in expression. Expression from AdCA17 in GM9503 did not appear to increase or decrease. A comparison of the 15 µg/ml exposure (Figure 1A) with the 10 min of VL exposure (Figure 1B), which represents the same MB+VL treatment, shows similar results, suggesting that the difference observed between the two curves is the result of different amounts of damage induced by the two methods. In order to maximize our ability to detect differences in enhanced expression of the reporter gene at low MB+VL treatment levels to cells subsequent experiments were performed using protocol A.

Expression of the undamaged AdCA17 reporter construct was examined next in a panel of normal, CSA and CSB primary fibroblasts using protocol A. Figure 2A shows the results for three normal primary fibroblasts, GM9503, GM38A and GM969C as well as for the average normal. No significant difference was observed for any of the doses examined for GM9503, GM38A or GM969C compared to the average normal (two-sample independent t-test; table 1 top row). Figure 2 A and B shows expression of β-gal from AdCA17 in several CSA and CSB primary fibroblasts compared to GM9503 and the average of all normal fibroblasts. For all CS fibroblasts examined, a significant enhancement in reporter gene expression compared to the average normal was observed at multiple MB pretreatment doses. While all CS fibroblasts

examined demonstrated enhanced expression, the degree of enhancement at each dose and the resulting profile of the curve varied.

*Enhanced expression of the AdCA35 reporter in primary human fibroblasts from patients with Cockayne syndrome following cellular pre-treatment with UVC*

We have reported previously that pre-treatment of cells with UVC irradiation leads to enhanced expression from the human cytomegalovirus immediate-early promoter of a  $\beta$ -gal reporter gene at lower UV fluences and to higher levels in several TCR-deficient cells (CS and XP) compared to TCR-proficient cells (normal and XPC) (Francis and Rainbow 2000; Zagal et al. 2005). In the present work, we examined expression from the murine cytomegalovirus immediate early (MCMV IE) promoter of the reporter gene following pre-treatment of cells with UVC for several additional TCR-deficient CS cells not included in our previous studies. Figure 3 shows the results for the 6 additional CS cell strains and an obligate CS heterozygote. Each panel shows the results for 2 of the additional CS strains together with the GM9503 normal and the CS1AN CSB cell strain, both of which were examined in previous reports (Francis and Rainbow 2000; Zagal et al. 2005). It can be seen that enhanced expression of the reporter gene was detected at lower UV fluences and to higher levels in all the CS cell strains tested compared to the normal and the obligate heterozygote cell strain. In addition, these results demonstrate that the response of the  $\beta$ -gal reporter gene in the recombinant AdCA35 is similar to that in Ad5HCMVSp1lacZ following cellular pretreatment with UVC.

*Western blot analysis of CSB expression in human primary skin fibroblasts from normal and Cockayne syndrome individuals.*

While all CS fibroblasts examined in this study had increased expression of the undamaged reporter compared to normal, the degree of increase at the different doses varied among CS cells. CSB protein expression was examined by western blot analysis to determine if the observed variability was associated with differences in protein expression, or the presence of truncated CSB proteins (Figure 4). For all primary normal and CS skin fibroblast examined here, the CSB-PGBD3 fusion protein was detected. All normal and CSA primary fibroblasts showed expression of CSB, while expression of full length CSB or any smaller truncation products were not detected in any of the CSB primary fibroblasts

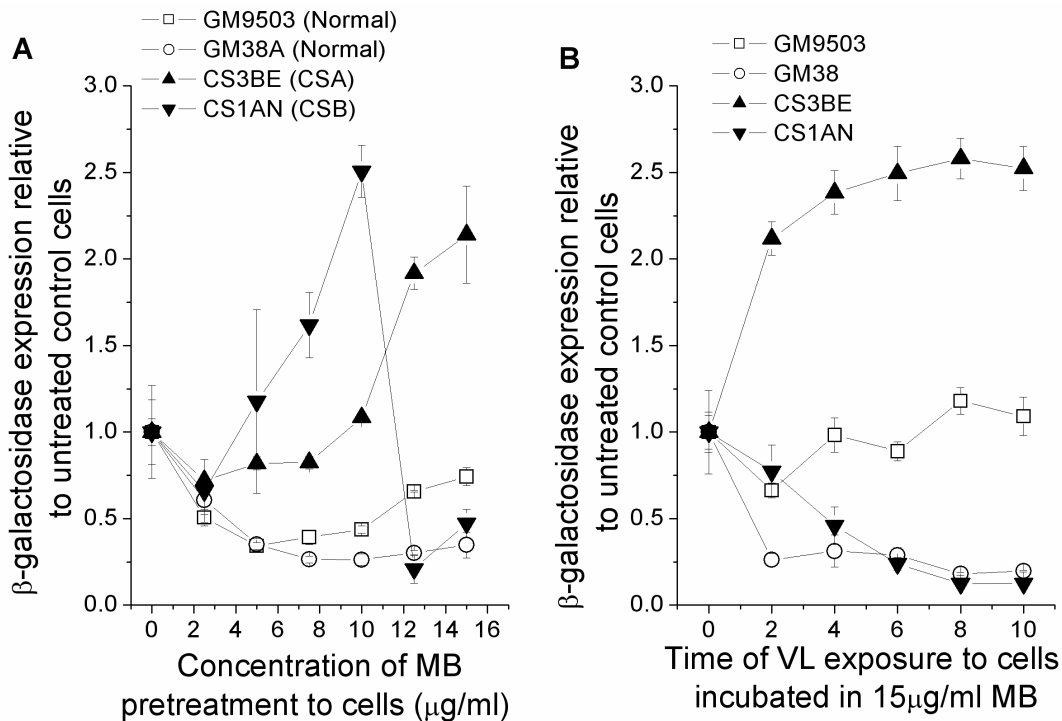


**Figure 1:** Expression of the undamaged reporter gene in normal and CS primary fibroblasts pretreated with MB+VL. For both A and B, cells were infected with untreated AdCA17 (MOI 20) and  $\beta$ -gal expression was scored 24 hours after infection. A) Cells were incubated in increasing concentrations of MB, exposed to 10 min VL and immediately infected with untreated AdCA17 (protocol A). B) Cells were incubated in media containing 15mg/ml MB (6 hours), exposed to increasing amounts of MB and immediately infected with untreated AdCA17 (protocol B). The above graphs are the result of a single experiment. Each data point is the average ( $\pm$  SE) of triplicate determinations for  $\beta$ -gal expression relative to the untreated control cells.

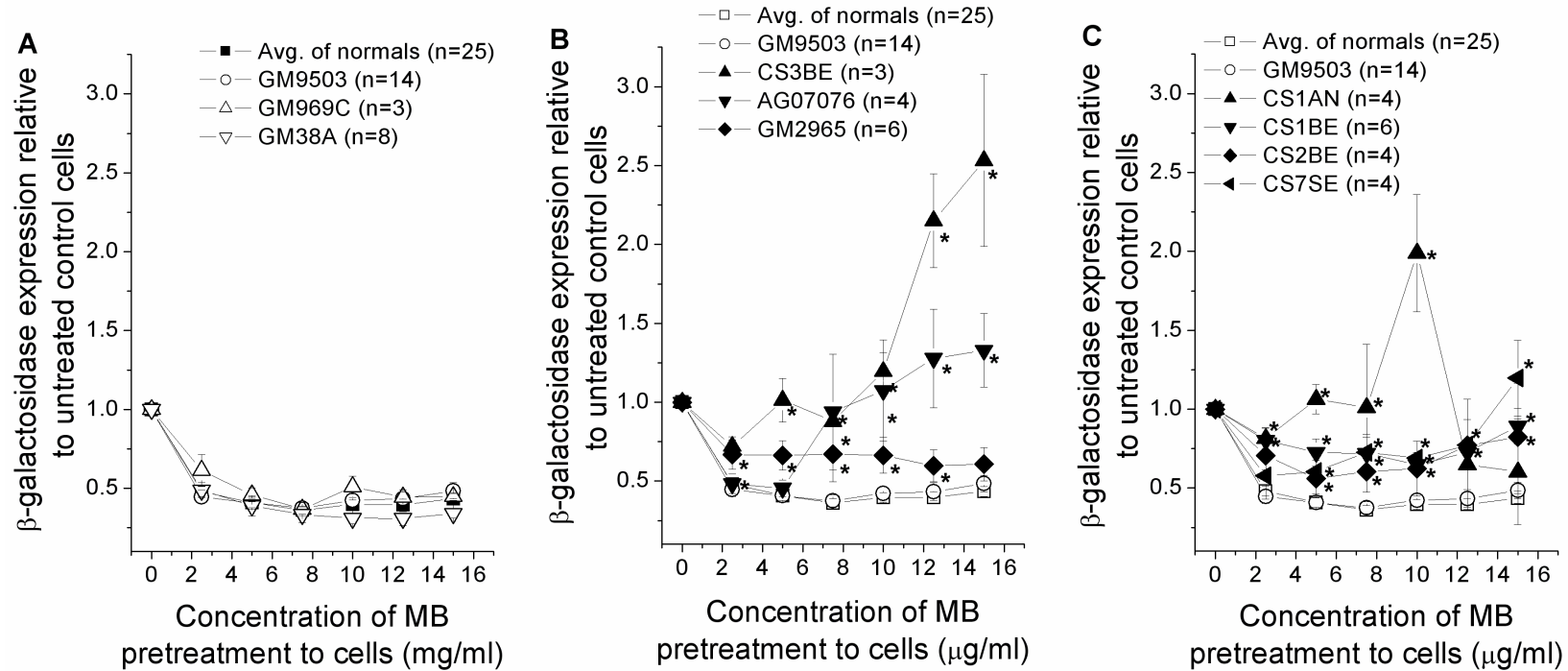


**Figure 2:** Expression of the undamaged reporter gene in normal primary fibroblasts pre-treated with increasing concentrations of MB plus 10 min VL (protocol A).  $\beta$ -gal expression was scored 24 hours after infection with undamaged AdCA17 (MOI 20). For each cell line, expression at each dose was normalized to expression in untreated control cells. Each point on the above curve is the average ( $\pm$  SE)  $\beta$ -gal expression from a number of experiments (n is indicated in the figure legends) each done in triplicate determinations. A) Expression of the undamaged reporter in normal primary fibroblasts pretreated with MB+VL. Also shown is the average of all normals. No significant differences were observed between any of the normal primary fibroblasts (two sample independent t-test). B) CSA and C) CSB primary fibroblasts pre-treated with MB+VL. Both curves show expression from GM9503 as well as the average of all normal fibroblasts. Expression from CS primary fibroblasts significantly different from the average normal are indicated by an asterisk ( $p < 0.05$  by two sample independent t-test).

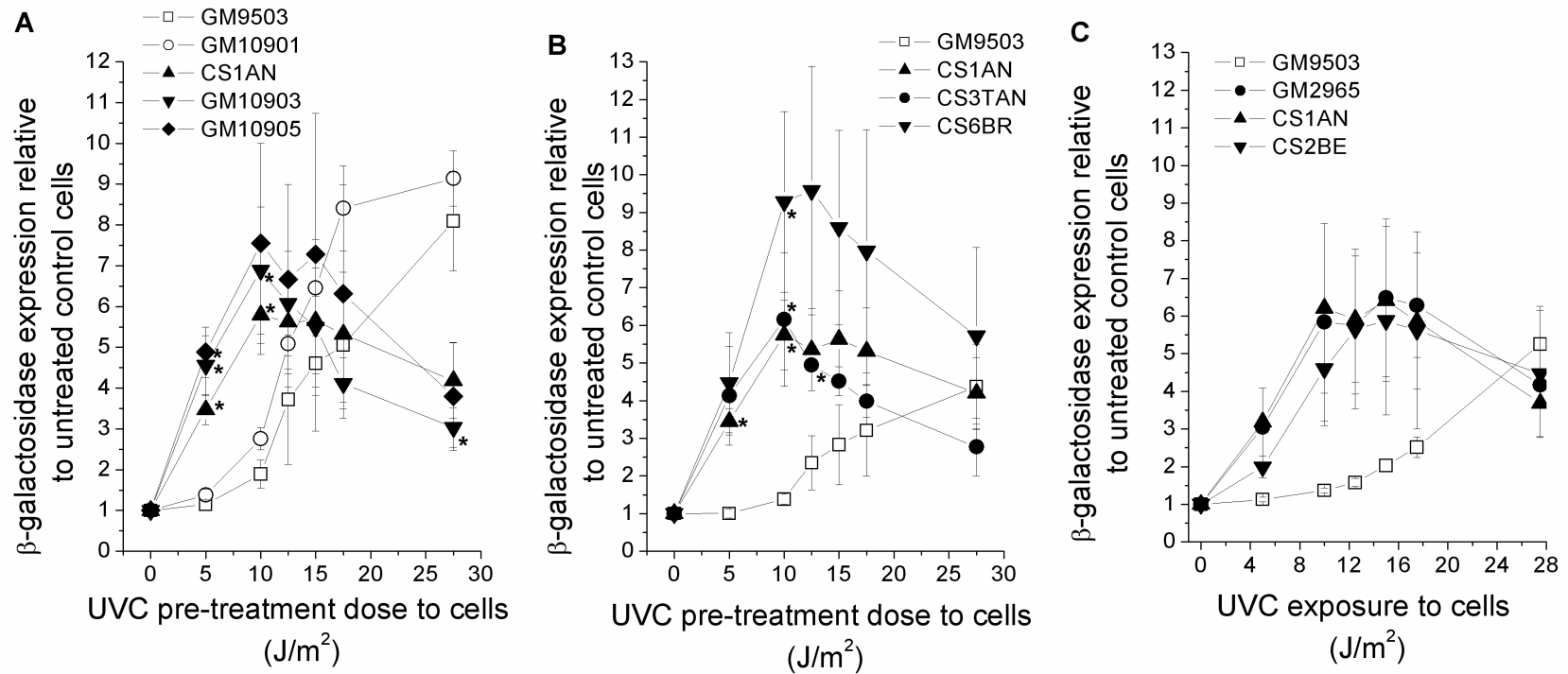


**Figure 3:** Enhanced expression of the undamaged AdCA35 reporter following cellular pretreatment with UVC.  $\beta$ -gal expression from untreated AdCA35 (MOI 20) was scored 24 hours after infection of normal and CS primary fibroblasts pretreated with increasing fluences of UVC. All curves show expression from GM9503 as well as a number of CS primary fibroblasts (CSA: CS6BR, GM2965 CSB: GM10903, GM10905, CS1AN, CS3TAN, CS2BE). A) GM10903 and GM10905 are fibroblasts from CS affected siblings and GM10901 are fibroblasts isolated from the unaffected mother of the siblings. Each point on the above curves is the average ( $\pm$  SE)  $\beta$ -gal expression from 3 (panel A and B) or 2 (panel C) independent experiments each done in triplicate determinations normalized to expression in untreated control cells. Expression from CS primary fibroblasts significantly different from GM9503 are indicated by an asterisk ( $p < 0.05$  by two sample independent t-test).

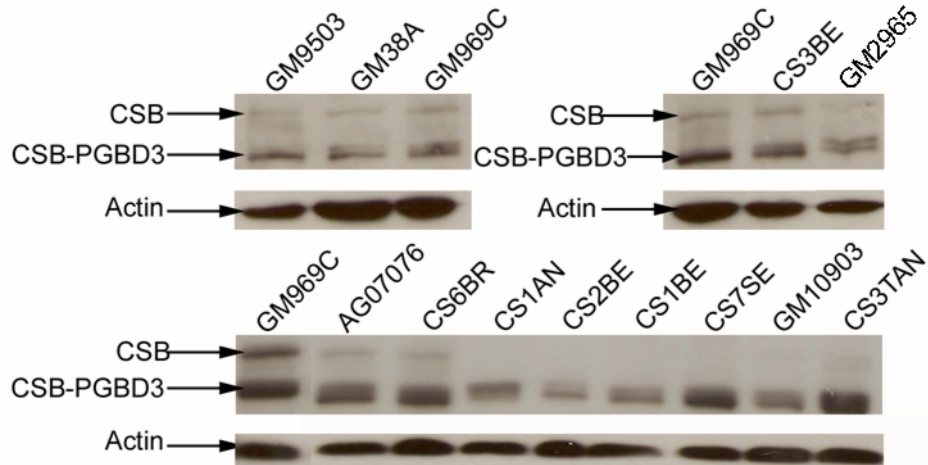


**Figure 4:** Western Blot analysis of CSB expression in normal, CSA and CSB primary fibroblasts. 20 $\mu$ g of protein from whole cell extracts were separated by 8% SDS-PAGE, transferred to a nitrocellulose membrane and probed with an anti-CSB antibody specific to the N-terminal region of CSB. The top band, seen in all normal and CSA fibroblasts, but not in CSB mutant fibroblasts corresponds to full length CSB. The lower band seen in all cell lines corresponds to the CSB-PGBD3 fusion protein derived from the first 5 exons of *CSB* and the *PGBD3* exon found in intron 5 of *CSB* (Newman et al. 2008).

## Discussion

The importance of the CSA and CSB proteins in normal growth and development, neurodegenerative processes and in cellular functions associated with aging is reflected in the severe phenotype of CS patients (Nance and Berry 1992; Natale 2011). Mutations in the CS genes have long been known to abolish the TCR sub-pathway of NER (Venema et al. 1990), the repair pathway responsible for removing bulky lesions induced by exposure to UV light (Li and Roberts 2001; van Hoffen et al. 2003). The GGR sub-pathway of NER, when eliminated by mutations in XP genes leads to the clinically distinct disorder XP (de Boer and Hoeijmakers 2000). TCR- and GGR-NER differ only in the initial lesion recognition step, after which the two sub-pathways converge and share all subsequent steps (Friedberg et al. 1995). CS patients have a normal skin cancer incidence rate compared to XP patients, who have an increased incidence rate of squamous cell carcinomas and malignant melanomas (Lehmann 2003). Another contrasting feature of the two disorders is neurodegeneration, which is considered a hallmark symptom of CS (Nance and Berry 1992; Natale 2011), while only 20% of XP patients display neurological abnormalities that are often less severe (Lehmann 2003). The striking difference between neurodegeneration, mental development and capacity to function in these two disorders led to the suggestion that the CS proteins are involved in processes unrelated to NER.

The *CSA* gene encodes a 396 amino acid protein whose sequence and predicted structure indicate it is a WD40 repeat protein. WD40-repeat proteins form stable  $\beta$ -propeller platforms that serve as rigid scaffolds to which other proteins can bind to in a stable or reversible manner (Li and Roberts 2001). A common function found in WD40-repeat proteins is co-ordination of multi-protein complex assemblies (Li and Roberts 2001). The *CSB* gene, which is mutated in approximately 80% of all characterized CS cases, encodes a 1493 amino acid protein that

belongs to the SWI/SNF2 family of DNA dependent ATPases (Laine and Egly 2006). CSB contains 7 conserved DNA helicase domains and has chromatin remodeling capabilities thought to be involved in increasing accessibility of repair factors to lesions and/or transcriptional regulation (Laine and Egly 2006). In an attempt to explain the CS phenotype non-NER functions of the CS proteins were investigated and there now exists a large amount of evidence demonstrating their involvement in BER of oxidative DNA damage (Francis et al. 1997; Dianov et al. 1999; Osterod et al. 2002; de Waard et al. 2003; de Waard et al. 2004; Spivak and Hanawalt 2006; D'Errico et al. 2007; Gorgels et al. 2007).

The results of the work presented here support the involvement of the CSA and CSB proteins in the repair of MB+VL induced 8-oxoG lesions. An enhancement of expression from the undamaged reporter was observed in CSA and CSB primary fibroblasts compared to normal primary fibroblasts (Figure 2). This observation suggests MB+VL induced damage persists to a greater extent in the genomic DNA of CS compared to normal fibroblasts, supporting a role for CSA and CSB in the removal of MB+VL induced 8-oxoG lesions. A number of other *in vitro* and *in vivo* studies provide evidence that processing of the oxidative lesion, 8-oxoG is defective in CS patients. Following exposure to IR, CS primary fibroblasts were found to accumulate significantly higher levels of 8-oxoG and 8-oxoadenine (8-oxoA) than normal primary fibroblasts with no significant difference in background levels observed prior to treatment (Tuo et al. 2003). Cellular extracts from these cells also showed a reduced ability to incise an oligonucleotide containing a single 8-oxoG or 8-oxoA (Tuo et al. 2003). Expression of *E. coli* formamidopyrimidine DNA glycosylase (FPG), a glycosylase that recognizes 8-oxoG (Meira et al. 2000), compliments the 8-oxoG incision defect in CS cells (Ropolo et al. 2007).

Previous reports have shown a good correlation between the sun sensitivity of CS patients and cellular sensitivity of RNA synthesis to UVC (Lehmann et al. 1993). However, to date no significant associations have been made between the severity of CS symptoms and the location of the mutations in either gene (Lehmann et al. 1993; Stefanini et al. 1996; Mallery et al. 1998; Laugel et al. 2008). Adding a further complication is the fact that specific mutations in CSB can lead to the development of two other disorders: the severe neurodegenerative disorder cerebro-oculo-facioskeletal syndrome (COFS) (Meira et al. 2000) and UV sensitive syndrome (UV<sup>S</sup>S) which is characterized by UV sensitivity with developmental and neurological defects being absent (Horibata et al. 2004). One study showed a complete absence of the CSB protein in a patient diagnosed with UV<sup>S</sup>S (Horibata et al. 2004) suggesting that it is not the absence of CSB that causes the severe CS phenotype but possibly the presence of a mutant/truncated protein. However, this conclusion has been recently challenged as Laugel et al. have shown a severe case of CS in which the CSB protein was not detected (Laugel et al. 2008). The patients from which fibroblasts were isolated in this studied varied in their clinical presentation of CS (mild to severe) and we were unable to detect the CSB protein, providing additional support for the latter observation.

We have reported previously that expression from the human cytomegalovirus immediate early (HCMV IE) promoter of the  $\beta$ -gal reporter gene is induced by cellular pretreatment with UVC, MB+VL and other DNA damaging agents (Francis and Rainbow 2000; Zacal et al. 2005; Pitsikas et al. 2007). While details of the molecular mechanism leading to enhanced expression of the reporter gene are not presently known, our laboratory has previously published data indicating that persistent DNA damage in active genes induces the cellular response leading to enhanced expression of CMV driven genes (Francis and Rainbow 2000). Stalling of RNA polII

at the site of these lesions is thought to be the initial signal leading to enhanced expression from the reporter gene. This work shows enhanced expression of the undamaged reporter gene following MB+VL pre-treatment in CSA and CSB primary fibroblasts. Studies have found the ability of 8-oxoG lesions to impede the progression of RNA polII to be weak or non-existent (Tornaletti et al. 2001; Larsen et al. 2004). However, CSB has been reported to stimulate RNA polII bypass of 8-oxoG (Charlet-Berguerand et al. 2006). The ability to detect bypass stimulation of 8-oxoG suggests, at the very least, that there is a transient stalling of RNA polII at the lesion. Regardless of the exact mechanism leading to enhanced expression, the data presented here demonstrate increased  $\beta$ -gal expression following MB+VL pretreatment in primary CS fibroblasts. Mutations in either the CSA (CS3BE, AG07076, CS6BR) or the CSB (CS1AN, CS1BE, CS7SE, CS2BE) gene lead to significantly enhanced expression of the undamaged reporter gene following MB+VL pretreatment when compared to normal primary fibroblasts. It has been proposed that CS may be a transcriptional disorder (Friedberg 1996) and a mild or less severe manifestation of CS symptoms may result from a loss or decrease in CS related transcriptional activity alone with the more severe presentation of the disease found in patients who have mutations that in addition abolish lesion bypass activity. The burden of a transcriptional deficit combined with the sequestering of transcription factors at RNA polII stall sites due to reduced or absent bypass activity could reduce transcription to a level that would not allow cells to meet their metabolic needs. Accumulation of oxidative DNA damage in neurons which eventually triggers apoptosis is often used as an explanation for neurodegeneration in CS. Neurons are post-mitotic cells with high metabolic activity and the type of damage most likely to occur in neurons is oxidative damage caused by ROS (Fishel et al. 2007). A reduced or abolished ability of CS proteins to stimulate bypass of oxidative lesions could result in an apoptotic signal

resulting in neuronal cell death. Neuronal cell death may also be explained by decreased levels of transcription resulting from stalled transcription complexes resulting in the inability of neurons to meet their high metabolic requirement, ultimately leading to their death. Individuals who retain bypass activity may have absent or mild retinal and/or neurodegeneration while still presenting other major symptoms of CS caused by the loss of other cellular processes associated with the CS proteins.

In this and previous work from our lab we have used the enhanced expression assay and UVC pre-treatment to demonstrate the TCR-NER defect in all CS cell strains examined (Figure 3, (Francis and Rainbow 2000; Zagal et al. 2005)). While pre-treatment of the primary fibroblasts with MB+VL resulted in significantly greater expression from the undamaged reporter gene at most doses in all CS fibroblasts examined, expression was greater than control for some doses in some CS fibroblasts (Figure 2 B and C). In contrast, MB+VL pre-treatment consistently led to a downregulation of reporter expression in normal primary fibroblasts (Figure 2A). These results demonstrate a very different response to oxidative damage in normal compared to repair deficient CS fibroblasts. Overall, these results support the conclusion that 8-oxoG lesions inhibit progression of actively transcribing RNA polIII and that CSA and CSB fibroblasts are defective in BER of MB+VL induced 8-oxoG lesions.

While certain CS characteristics are considered to be hallmarks of the disorder, there is a wide variation in the presence and severity of additional CS characteristics. This includes the severity of neurodegeneration and premature aging as well as the presence/severity of retinal degeneration. The phenotypes are often associated with damage caused by ROS and defective/reduced repair of this damage. It is tempting to speculate that the variation in response following cellular pretreatment with MB+VL reflects the clinical variability of the individuals

from which the cells in this study were obtained. GM2965, isolated from an atypical CSA patient with a mild CS phenotype shows a much lower enhancement of reporter gene expression compared to the other CSA fibroblasts, CS3BE and AG07076, both considered to be severe/classic CS. In contrast, CS2BE fibroblasts, isolated from an atypical CSB patients with mild symptoms, show expression similar to CS1BE and CS7SE which were isolated from patients classified as severe/classic CS. In addition, CS2BE was shown to accumulate greater levels of 8-oxoG following IR treatment compared to other CSB fibroblasts, suggesting these cells do not repair the lesion as well as other CS fibroblasts. Considering this, it is difficult to use the data to make correlations between the readout of enhanced expression and the clinical manifestation of CS in these individuals. Enhanced expression of the reporter gene indicates persistent lesions, and the difference in the level of expression may also reflect the difference in genetic background of the cells examined.

Our results provide further evidence that, while loss of TCR-NER of UVC induced damage is a molecular characteristic of CS cells, other functions of the CS proteins also play a major role in the pathogenesis of CS. These results provide additional support for the body of evidence demonstrating defective removal of 8-oxoG in the absence of the CS proteins as well as evidence that MB+VL induced 8-oxoG inhibits RNA polIII progression. In addition, the results provide further support for the theory that a decline in DNA repair capacity and the accumulation of oxidative DNA damage over time play a major role in human aging (Wilson et al. 2008).

### **Acknowledgements**

This work was supported by an operating grant from the National Cancer Institute of Canada with funds from the Canadian Cancer Society.

## **Chapter 6:**

**TRF2 interacts with the Cockayne syndrome group B protein and over expression of TRF2 reduces the repair of UV damaged DNA.**

## **Preface**

The work presented in this Chapter forms the beginning of a collaborative project between the laboratories of Dr. A.J. Rainbow and Dr. X-D. Zhu (Department of Biology, McMaster University, Hamilton, Ontario). Two manuscripts of the current work have been prepared from the collaborative effort and have been submitted for peer review to two journals, *Molecular and Cellular Biology* (American Society for Microbiology) and *Human Molecular Genetics* (Oxford Journals). Both of the prepared manuscripts had an author list of Batenberg, N., Mitchell, T.R.H., Leach, D.M., Rainbow, A.J., and Zhu X-D. Unfortunately, Dr. X-D Zhu and Taylor Mitchell have not allowed me to include any figures in full or in part from any manuscripts prepared as a result of this collaborative effort. They did give me permission to include figures from work I have done entirely alone or for a small number of figures for which the work was completed jointly between the two labs (Figures 5 and 6). My contributions to this collaborative work include my initial discussions with T.R.H Mitchell that lead to the idea that CSB may interact with some of the shelterin proteins and our initiative to carry out experiments on coimmunoprecipitation (coIP) of CSB and TRF2. This lead to our identification of an interaction between CSB and TRF2 and subsequent initial FISH experiments demonstrating potential telomere dysfunction in CSB fibroblasts (with Taylor Mitchell). Further contributions to the collaborative project done by me but not included in this work/Chapter include additional figures in the appendix,, critical insight and experimental design throughout the collaborative project as well as critical insight into the manuscripts both written entirely by Dr. X-D Zhu. For the work presented in this Chapter I did the experiments for and constructed Figure 4; conducted the experiments (with Taylor Mitchell) and generated Figures 5 and 6. For Figures 1, 2 and 3, cells overexpressing components of the shelterin complex were generated in Dr. X-D Zhu's lab

by Kim Glenfield Staples and the HCR experiments were conducted by Natalie Zacal. Figures 1 and 2 were constructed by Natalie Zacal and me. Some of the results generated as a result of this collaborative work between the laboratories of Dr. A.J. Rainbow and Dr. X-D. Zhu was also presented at a scientific meeting (shown below).

The following is the abstract for a poster presented by Nicole Batenburg (Officially by Dr. X-D Zhu when referring to the conference program) at the Canadian Cancer Research Conference (CCRC) in Toronto, Ontario Canada, November 27<sup>th</sup>-30<sup>th</sup>, 2011. (Batenburg et al. 2011)

**Characterization of the Role of CSB in Telomere Maintenance Associated with Tumourigenesis**

Batenburg NL, Mitchell TRH, Leach DM, Rainbow AJ, Zhu XD

Department of Biology, McMaster University, Hamilton, ON

Telomeres, the heterochromatic structure found at the ends of eukaryotic linear chromosomes, function to protect natural chromosome ends from being recognized as damaged DNA. Disruption in either telomere length or structure can lead to an induction of dysfunctional telomeres, leading to chromosome instability, an underlying hallmark of cancers. CSB is a multifunctional protein implicated in repair, transcription and chromatin remodelling. Germ-line mutations in CSB have been shown to give rise to Cockayne syndrome (CS) characterized by severe postnatal growth failure, progressive neurological degeneration and segmental premature ageing. While CS patients do not exhibit an increased risk for cancer, somatic mutations of CSB are found in a number of tumour types including colon, lung, ovarian and breast cancers, suggesting for a role of CSB in tumourigenesis. However whether and how CSB may contribute to tumourigenesis has not been fully understood. In this study we examined the role of CSB in telomere maintenance, which is implicated in tumourigenesis. We show that CSB is associated with a subset of human telomeres. Loss of CSB promotes the accumulation of dysfunctional telomeres and telomere shortening, suggesting CSB is required for maintaining telomere length and stability. The effect of cancer-associated CSB mutations on telomere integrity will also be discussed.

## **Abstract**

Cockayne syndrome (CS) is a segmental progeroid syndrome characterized by premature ageing and severe neurodegeneration. CS is caused by mutations in the CSA and CSB proteins which play a role in both nucleotide excision repair (NER) and base excision repair (BER). CSB also has functions in general transcription and chromosome remodeling. Telomeres are the nucleoprotein complex that protects the end of eukaryotic linear chromosomes from degradation and recognition as DNA double strand (ds) breaks. A six protein complex containing TRF1, TRF2, TIN2, POT1, Rap1 and TPP1, known as shelterin makes up the protein component of telomeres and regulates the DNA damage response. Telomeres have long been considered to be the cells mitotic clock and are strongly associated with cancer and ageing. Overexpression of TRF2 in the skin of mice leads to premature skin deterioration, hyperpigmentation and increased incidence of cancer. In addition, a number of cancer cells have been identified that have elevated levels of TRF2 expression. In this study we examined the effect of overexpressing TRF1, TRF2, TIN2, Rap1 and POT1 on DNA repair using an adenovirus based host cell reactivation (HCR) technique. We demonstrate that overexpression of TRF2 in human primary fibroblasts significantly reduces NER of UVC induced DNA damage by a mechanism that requires CSB. The reduction in HCR is specific to UVC induced lesions and has no effect on oxidative DNA damage caused by methylene blue plus visible light (MB+VL). Furthermore, we demonstrate a physical interaction between TRF2 and CSB by co-immunoprecipitation experiments and show that CSB deficient fibroblasts have increased telomere dysfunction by fluorescence *in situ* hybridization (FISH). The data presented here shows that a telomere associated protein can negatively affect NER in non-telomeric DNA and suggests that defects in telomere metabolism may play a role in the pathology of CS.

## Introduction

Telomeres are the heterochromatic ends of eukaryotic linear chromosomes that function to protect loss of coding regions from erosion by the end replication problem and were long considered to be transcriptionally inactive regions of the genome (Blasco 2007; Ottaviani et al. 2008). Telomeres are now known to be transcribed into telomeric repeat-containing RNA (TERRA) (Azzalin et al. 2007). The terminal ends of telomeres are not blunt ended, but rather have a 3' stretch of single stranded G rich DNA, known as the 3' overhang (Makarov et al. 1997; McElligott and Wellinger 1997). This overhang is thought to be generated by resection of the C rich strand by a still unidentified nuclease (Makarov et al. 1997). While telomeres act to protect the coding regions of the genome from erosion, they themselves require protection from being recognized by the cell as DNA damage, specifically as double strand (ds) DNA breaks (Palm and de Lange 2008). Improper processing of telomere ends as dsDNA breaks can lead to dysfunctional telomeres and induce cell cycle arrest or senescence (d'Adda di Fagagna et al. 2004; Palm and de Lange 2008). In mammals, telomere protection is achieved by physical seclusion of the free single stranded end and by the direct association of a six protein complex known as shelterin (de Lange 2005). Structural protection of the free end is achieved by strand invasion of the 3' overhang in upstream telomeric DNA to form T- and D- loop structures hiding it from detection as DNA damage (Griffith et al. 1999). The shelterin complex is made up of Telomere Repeat Binding Factor 1 and 2 (TRF1 and TRF2), Protection of Telomeres 1 (POT1), TRF1-Interacting Nuclear Protein 2 (TIN2), Rap1 (the human ortholog of the yeast repressor/activator protein 1) and TPP1 (for a review of the shelterin complex and its functions see Palm and de Lange 2008). Shelterin specifically associates with the TTAGGG telomere repeats through the binding activity of TRF1 and TRF2 and acts to cap the chromosome ends

and regulate the DNA damage response (Palm and de Lange 2008). Disruption of the function of shelterin components can lead to telomere abnormalities including telomere end-to-end fusions, telomere loss and telomere doublets/fragile telomeres (de Lange 2005; Palm and de Lange 2008; Martinez et al. 2009; Mitchell et al. 2009; Sfeir et al. 2009).

TRF2 function is necessary for telomere maintenance and cell cycle progression and it acts as a hub for the interaction of multiple proteins required in these cellular processes (Kim et al. 2009). TRF2 also interacts with base excision repair (BER) proteins (BER is discussed in more detail in Chapters 1-5) and stimulates repair synthesis by DNA polymerase  $\beta$  (Muftuoglu et al. 2006). TRF2 plays a vital role in telomere protection and removal of TRF2 from telomeres by conditional knockout or overexpression of a dominant-negative allele of TRF2 leads to telomere end-to-end fusions (van Steensel et al. 1998; Celli and de Lange 2005). Overexpression of TRF2 in human primary fibroblasts leads to accelerated telomere shortening (Karlseder et al. 2002) and overexpression in the skin of mice produces a severe phenotype in response to light including XP associated features such as premature skin deterioration, hyperpigmentation and increased skin cancer (Munoz et al. 2005). Skin cells isolated from these mice exhibited telomere abnormalities and general chromosome instability (Munoz et al. 2005) which was later shown to be mediated by the structure specific nucleotide excision repair (NER) nuclease XPF (Munoz et al. 2005; Wu et al. 2007; Wu et al. 2008). Furthermore, a number of human skin tumors have been identified with increased/elevated levels of TRF2 expression (Munoz et al. 2005; Wu et al. 2007; Wu et al. 2008). These findings suggested that TRF2 may function in excision repair of DNA base damage, implicating telomere maintenance and genome stability mediated by TRF2 in the processes of cancer and ageing.

The TTAGGG sequence of the mammalian telomere repeat renders them highly susceptible to guanine oxidation and the formation of thymine dimers (Rochette and Brash 2010; Wang et al. 2010). 7,8-dihydro-8-oxoguanine (8-oxoG) is one of the most predominantly formed oxidative base lesions and its' repair is initiated by a number of DNA glycosylases including OGG1. OGG1 is required for repair of 8-oxoG found in telomeres of yeast and mice and in the absence of OGG1 mediated repair, telomere length homeostasis is affected (Wang et al. 2010; Lutzelberger and Kjems 2011). Shortening of telomeres is associated with in vitro cellular aging and critically short telomeres can lead to senescence (Harley et al. 1990; de Lange 2002; Munoz et al. 2005).

Cockayne syndrome (CS) has been described and discussed in detail in Chapters 1, 2 and 5. Briefly the difficulty in explaining CS pathology through a defect in the transcription coupled repair (TCR) subpathway of NER led to the hypothesis that the CS proteins have additional functions, specifically that they were involved in the BER of oxidative DNA damage. Although a substantial amount of evidence supports a role for the CS proteins in repair of oxidative DNA damage (Francis et al. 1997; Dianov et al. 1999; Osterod et al. 2002; de Waard et al. 2003; de Waard et al. 2004; Spivak and Hanawalt 2006; D'Errico et al. 2007; Gorgels et al. 2007), the mechanism of their involvement is not fully understood. Defective BER provides a better explanation of the degenerative features of CS; however associations between the capacity of CS fibroblasts to respond to oxidative damage and the clinical phenotype of the donor have not been made (Natale 2011, Nance and Berry 1992, this work). In addition to the role CSB has been found to play in repair of oxidative DNA damage, further functions have been discovered including the ability to actively wrap DNA resulting in local topological changes in chromatin (Beerens et al. 2005), general chromatin remodeling capabilities (Newman et al. 2006), strand

exchange capabilities (Muftuoglu et al. 2006), strand annealing (Muftuoglu et al. 2006; Berquist and Wilson 2009) and a role in general transcription (Licht et al. 2003).

In the present work we have used an adenovirus based host cell reactivation (HCR) technique to demonstrate that overexpression of TRF2 negatively effects NER of UV-induced DNA damage in a process requiring CSB. We show that this effect of TRF2 overexpression is specific to lesions repaired via NER. In addition, we have identified an interaction between TRF2 and CSB by co-immunoprecipitation (coIP) and using fluorescence in situ hybridization demonstrate that loss of functional CSB leads to telomere dysfunction.

## **Materials and Methods**

### *Cell lines*

Normal primary fibroblast cell lines (IMR90, GM10901, GM38, GM9503 and GM8399), CSB-deficient primary fibroblast cell lines (GM10905, GM739, GM1428) were obtained from the NIGMS Human Genetic Cell Repository (Coriell Institute for Medical Research, Camden, NJ). Cells were grown in DMEM (or  $\alpha$ MEM) medium with 10% fetal bovine serum (FBS) for transformed cell lines HeLa, and 15% FBS for all primary fibroblasts, supplemented with non-essential amino acids, glutamine, 100 U/ml penicillin and 0.1 mg/ml streptomycin.

### *Host Cell Reactivation (HCR)*

HCR assays for UVC and MB+VL treated virus were performed as previously described (Leach and Rainbow 2011). The recombinant adenovirus Ad5HCMVSp1*lacZ* (Morsy et al.

1993) was obtained from the Robert E. Fitzhenry Vector Laboratory, McMaster University, Hamilton, Ontario and the virus was propagated, collected and tittered as previously described (Graham and Prevec 1991). Treatment of the virus with UV-irradiation was done as described (Bennett and Rainbow 1988).

Cells were seeded in triplicate for confluence (hTERT-immortalized GM10905 fibroblasts at  $1 \times 10^4$  cells per well; SV40 transformed GM16095 fibroblasts at  $3.5 \times 10^4$  cells per well) in 96-well plates. At 18-24 hours post seeding, cells were infected with 40  $\mu$ l of UVC or MB+VL treated or mock-treated virus at a multiplicity of infection of 40-100 plaque forming units (PFU)/cell (indicated in figure legends). Following a 90 min viral adsorption period the cells were re-fed 160 $\mu$ l warmed (37°C) growth media and the infected cells were harvested 24 hours post-infection for analysis of  $\beta$ -galactosidase activity. Following addition of the  $\beta$ -gal substrate the absorbance was measured at multiple times using a 96-well plate reader (Bio-Tek Instruments EL340 Bio Kinetics Reader) as described.

#### *Immunoblotting and immunoprecipitation*

Immunoblotting was carried out as previously described (Zhu et al. 2000; Mitchell et al. 2009). The TRF2 antibody was kindly provided by Dr. X-D Zhu (McMaster University, Hamilton, Ontario, Canada). Immunoprecipitation of endogenous CSB was performed essentially as described (Zhu et al. 2000; Mitchell et al. 2009). For immunoprecipitation of endogenous CSB, HeLa cells were collected and resuspended in ice-cold NP-40 buffer (1% NP-40, 0.15M NaCl, 0.01M sodium phosphate, pH 7.2). Following incubation on ice for 20 min, the supernatant was recovered by micro-centrifugation at 17 500g for 10 min. Protein extracts of 1.5

mg was mixed with 2  $\mu$ l mouse anti-CSB antibody (Abcam ab66598 and Bethyl A301-345A) and the mixture was incubated overnight at 4°C. Protein G-beads (30  $\mu$ l) was added to the mixture on the next day and the IP pellet was washed five times each with 1 ml of ice-cold NP-40 buffer containing 1 mM DTT, 1  $\mu$ g/ml aprotinin, 1  $\mu$ g/ml leupeptin, 10  $\mu$ g/ml pepstatin and 1 mM PMSF.

#### *Metaphase chromosome spreads and FISH*

Metaphase chromosome spreads were essentially prepared as described (van Steensel et al. 1998; Zhu et al. 2003). Cells were arrested at metaphase in nocodazole (0.1  $\mu$ g/ml) for 90-120 min. Following arrest, cells were harvested by trypsinization, incubated for 7 min at 37°C in 75 mM KCl, and fixed in freshly-made methanol/glacial acetic acid (3:1). Cells were stored overnight at 4°C, dropped onto slides and air-dried overnight in a chemical hood. FISH analysis on metaphase chromosome spreads was carried out essentially as described (Lansdorp et al. 1996; Zhu et al. 2003). Slides with chromosome spreads were incubated with 0.5  $\mu$ g/ml FITC-conjugated-(CCCTAA)<sub>3</sub> PNA probe (Biosynthesis Inc.) for 2 hr at room temperature. Following incubation, slides were washed, counter-stained with 0.2  $\mu$ g/ml DAPI, and embedded in 90% glycerol/10% PBS containing 1 mg/ml p-phenylene diamine (Sigma). All cell images were recorded on a Zeiss Axioplan 2 microscope with a Hamamatsu C4742-95 camera and processed in Open Lab.

## Results

### *Overexpression of the shelterin component TRF2 reduces HCR of the UVC treated reporter gene in primary fibroblasts*

TRF2 along with TRF1, Rap1, POT1, TPP1 and TIN2 (Palm and de Lange 2008) are components of the shelterin complex that function together to protect telomeres from the activity of DNA repair proteins (Palm and de Lange 2008). TRF2 binds to telomere DNA as a homodimer and is also found bound with its constitutive binding partner Rap1 in a 1:1 ratio (Zhu et al. 2000). The association of TRF2 overexpression with some cancers as well as XP like skin phenotypes such as skin deterioration, hyperpigmentation and increased skin cancer (Munoz et al. 2005) in mice overexpressing the protein led us to examine the effect of TRF2 overexpression on NER of UVC induced DNA damage. Similar to previous data demonstrated by Glenfield et al. we utilized the HCR assay to examine expression of the UVC treated  $\beta$ -gal reporter gene from Ad5HCMVSp1lacZ in IMR90 primary human fibroblasts overexpressing TRF2 or the empty vector as a control (Figure 1). In addition to TRF2 we also examined the effect of TRF1, Rap1, TIN2 and POT1 overexpression on HCR of the UVC treated reporter gene (Figure 1). Overexpression of TRF2, but not the other shelterin proteins examined led to a significant reduction in HCR of the UVC treated reporter gene compared to cells expressing the vector control. Overexpression of the shelterin proteins was confirmed by immunofluorescence (data not shown; Glenfield et al. 2007). These results are consistent with a negative regulation of NER by TRF2. (Glenfield et al. 2007)

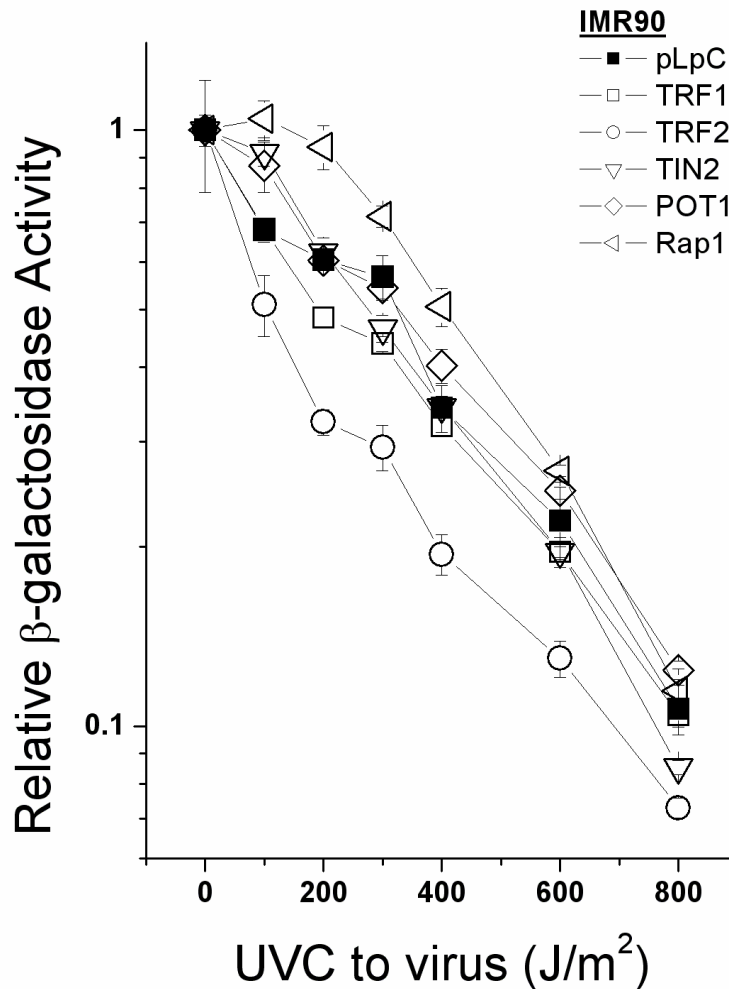


**Figure 1:** HCR of the UVC treated reporter gene in primary human fibroblasts overexpressing shelterin proteins. Shown above is a representative plot from a single independent experiment carried out with triplicate determinations. Each point on the above plot is the average relative  $\beta$ -gal activity  $\pm$ SE of the triplicate determinations at each UVC dose to the virus. IMR90 fibroblasts were seeded at a density of  $1.5 \times 10^4$  cells/well, infected with the UVC damaged virus (MOI 80) and harvested for  $\beta$ -gal scoring 24 hours later. Average relative  $D_{37}$  values (relative to IMR90pLpC) were calculated from 3-6 independent experiments and used for significance analysis by a one sample two tailed t-test (Rel  $D_{37}$  ( $\pm$ SE): TRF1-0.9745 $\pm$ 0.047; TRF2-0.559 $\pm$ 0.094; Rap1-1.01 $\pm$ 0.114; TIN2-1.017 $\pm$ 0.027; POT1-0.95 $\pm$ 0.088). HCR for the IMR90 fibroblasts overexpressing TRF2 showed a significant reduction ( $p=0.0423$ ) compared to the pLpC control. In contrast, overexpression for any of the other shelterin proteins examined here did not lead to a significant change in HCR capacity.

*Overexpression of TRF2 has no effect on HCR of the MB+VL treated reporter gene*

After detecting a significant difference in HCR of the UVC treated adenovirus reporter gene in IMR90 fibroblasts overexpressing TRF2 we examined reactivation of the MB+VL treated reporter gene in the same cells (Figure 2). Overexpression of TRF2 had no significant effect on HCR of the MB+VL treated reporter gene suggesting TRF2 specifically affects repair via NER.

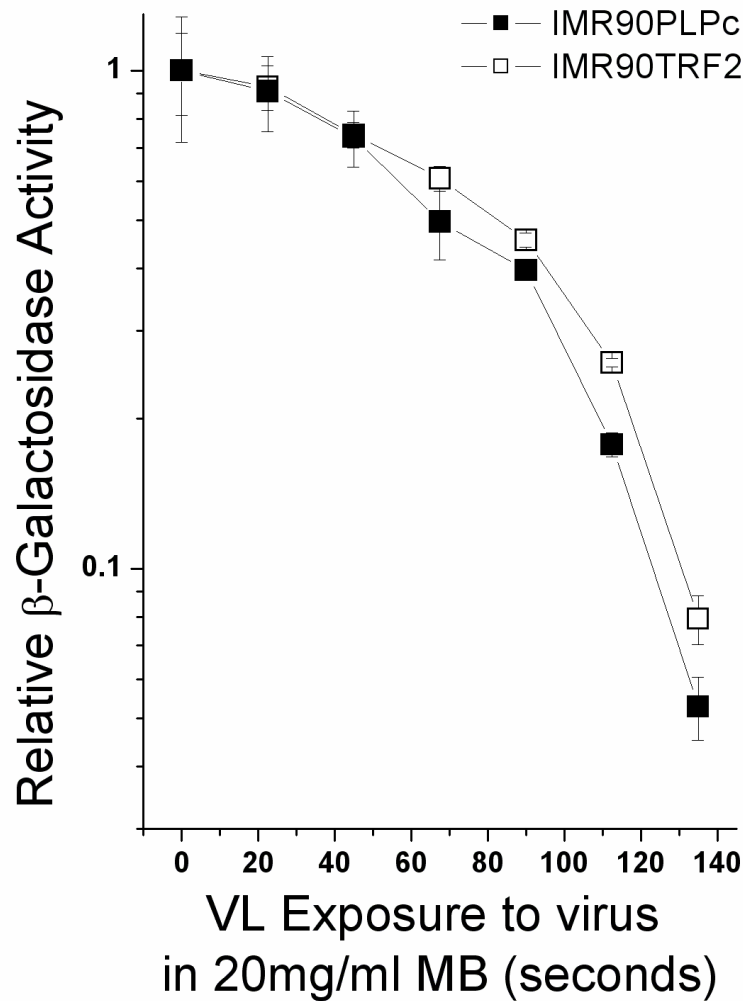


**Figure 2:** Normal HCR of the MB+VL treated reporter gene in IMR90 fibroblasts overexpressing TRF2. Shown above is a representative plot from a single independent experiment carried out with triplicate determinations. Each point on the above plot is the average relative  $\beta$ -gal activity  $\pm$ SE of the triplicate determinations at each VL dose to the virus. IMR90 fibroblasts were seeded at a density of  $1.5 \times 10^4$  cells/well, infected with the MB+VL damaged virus (MOI 80) and harvested for  $\beta$ -gal scoring 24 hours later. No significant difference in HCR capacity was observed for reactivation of the MB+VL treated Ad5HCMVSp1lacZ reporter for three independent experiments (Average absolute  $D_{37}$  ( $\pm$ SE): IMR90pLpC-84.55 $\pm$ 6.17s; IMR90TRF2-81.94 $\pm$ 8.18s; Relative  $D_{37}$  ( $\pm$ SE): IMR90TRF2 relative to control-0.97 $\pm$ 0.07s). HCR of the UVC treated reporter was included as a control and showed a reduction in HCR capacity consistent with Figure 1(data not shown).

*CSB is required for the TRF2 mediated decrease in HCR*

In untreated cells, a much greater reduction in HCR of the UVC treated reporter is observed in GGR-NER deficient XP cells from complementation group C compared to TCR-NER deficient CS cells (Francis and Rainbow 2000, discussed in Chapter 3) suggesting the majority of reporter gene reactivation occurs via GGR NER in untreated human cells. The percent reduction in HCR observed with TRF2 overexpression was consistent with the level of HCR reduction in TCR-NER deficient CS fibroblasts (Francis and Rainbow 2000). Together with the fact that telomeres are now known to be transcriptionally active we hypothesized that TRF2 may function in regulating TCR-NER through a process involving CSB. To examine this we performed HCR experiments in CS1AN CSB mutant cells overexpressing TRF2 (Figure 3). IMR90 fibroblasts overexpressing TRF2 were included as a control. In the absence of functional CSB, overexpression of TRF2 had no significant effect on HCR of the UVC treated reporter gene (one sample two tailed t-test), suggesting TRF2 may inhibit TCR-NER by negatively mediating the activity of CSB.

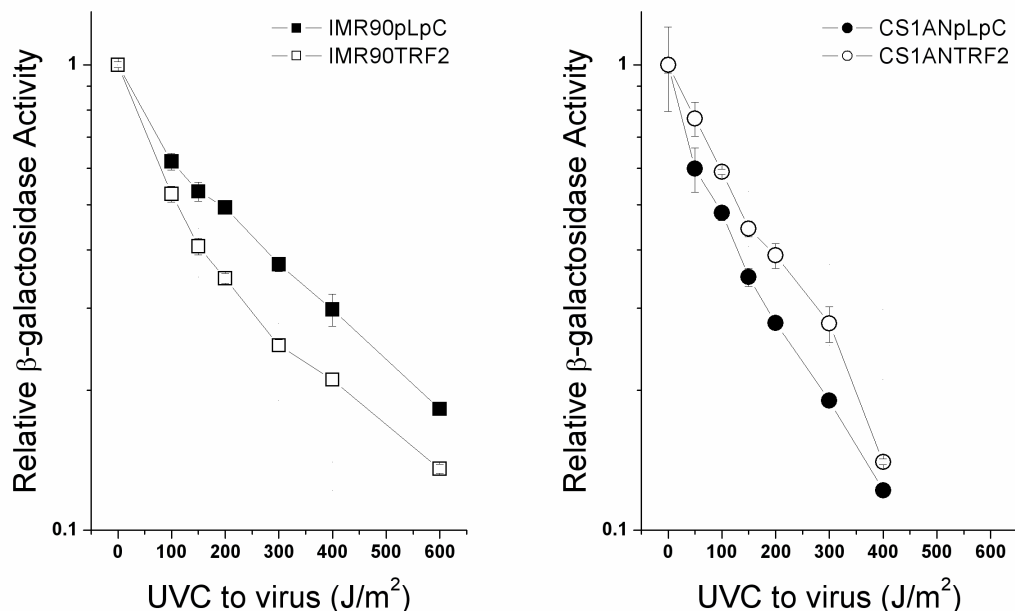


**Figure 3:** The TRF2 mediated decrease in HCR requires CSB. Shown above are representative plots from single independent experiments carried out with triplicate determinations. Each point on the above plot is the average relative  $\beta$ -gal activity  $\pm$ SE of the triplicate determinations at each UVC dose to the virus. Left panel: IMR90; Right panel CS1AN. Fibroblasts were seeded at a density of  $1.5 \times 10^4$  cells/well, infected with the UVC damaged virus (MOI 80) and harvested for  $\beta$ -gal scoring 24 hours later. Average relative  $D_{37}$  values (relative to IMR90pLpC) were calculated from 3 independent experiments and used for significance analysis by a one sample two tailed t-test. Consistent with the known defect in TCR-NER of CSB fibroblasts, CS1ANpLpC and CS1ANTRF2 both showed a significant decrease in HCR compared to IMR90pLpC ( $p=0.042$  and  $0.022$ , respectively). Similar to Figure 1, overexpression of TRF2 in IMR90 fibroblasts led to a decrease in HCR ( $p=0.032$ , all IMR90 TRF2 overexpression experiments combined;  $n=7$ ), while no significant difference was observed when overexpressed in the CSB mutant cell line CS1AN.

*The transcription coupled repair factor CSB interacts with TRF2*

After demonstrating that the TRF2 mediated reduction in HCR capacity required the presence of functional CSB we sought to determine if this was the result of a direct interaction between the two proteins. Analysis of the CSB amino acid sequence by Taylor Mitchell revealed the presence of a consensus YxLxP (amino acids 402-406) motif outside of the acidic region found in the N-terminal portion of the protein that can be recognized and bound by the TRF homology (TRFH) domain of TRF2 (Chen et al. 2008). Co-immunoprecipitation (CoIP) experiments using two different antibodies specific to CSB in whole cell extracts from HeLa cells revealed an interaction between endogenous CSB and TRF2 (Figure 4). Decreased HCR in the presence of overexpressed TRF2 suggests TRF2 may play a role in repair in non-telomeric regions or is capable of negatively regulating the activity of NER in non-telomeric DNA. Together, these data suggest that the interaction of TRF2 with CSB may negatively regulate its repair functions independent of the sequence context or genomic region.

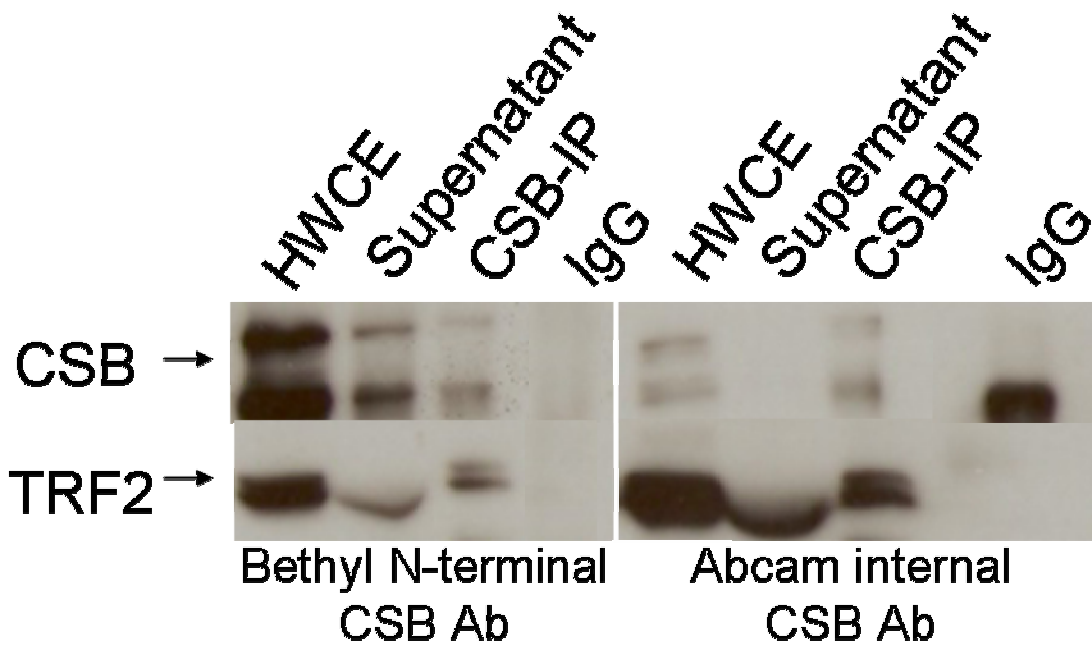


**Figure 4:** CSB interacts with TRF2 *in vivo*. Coimmunoprecipitation (coIP) of CSB from HeLa whole cell extracts (HWCE) using two different CSB antibodies. Anti-IgG was used as a negative control. Following IP with the anti-CSB antibodies, samples were separated on an 8% polyacrylamide gel by SDS-PAGE and transferred to a membrane where they were detected using an anti-TRF2 antibody. Both antibodies CoIPed CSB and TRF2 suggesting they interact either directly or are in complex *in vivo*.

*FISH analysis of metaphase cells lacking functional CSB suggests increased telomere instability*

Following the observation that CSB interacts with TRF2 we examined telomeres in CSA (CS3BE) and CSB (CS7SE) mutant primary fibroblasts by fluorescence *in situ* hybridization (FISH) (Figure 5 and 6). These initial experiments shown in Figures 5 and 6 suggested that CS mutant fibroblasts had a higher than normal number of dysfunctional telomeres (telomere loss and telomere doublets) leading to collaborative work that is not presented here but is discussed in more detail below.

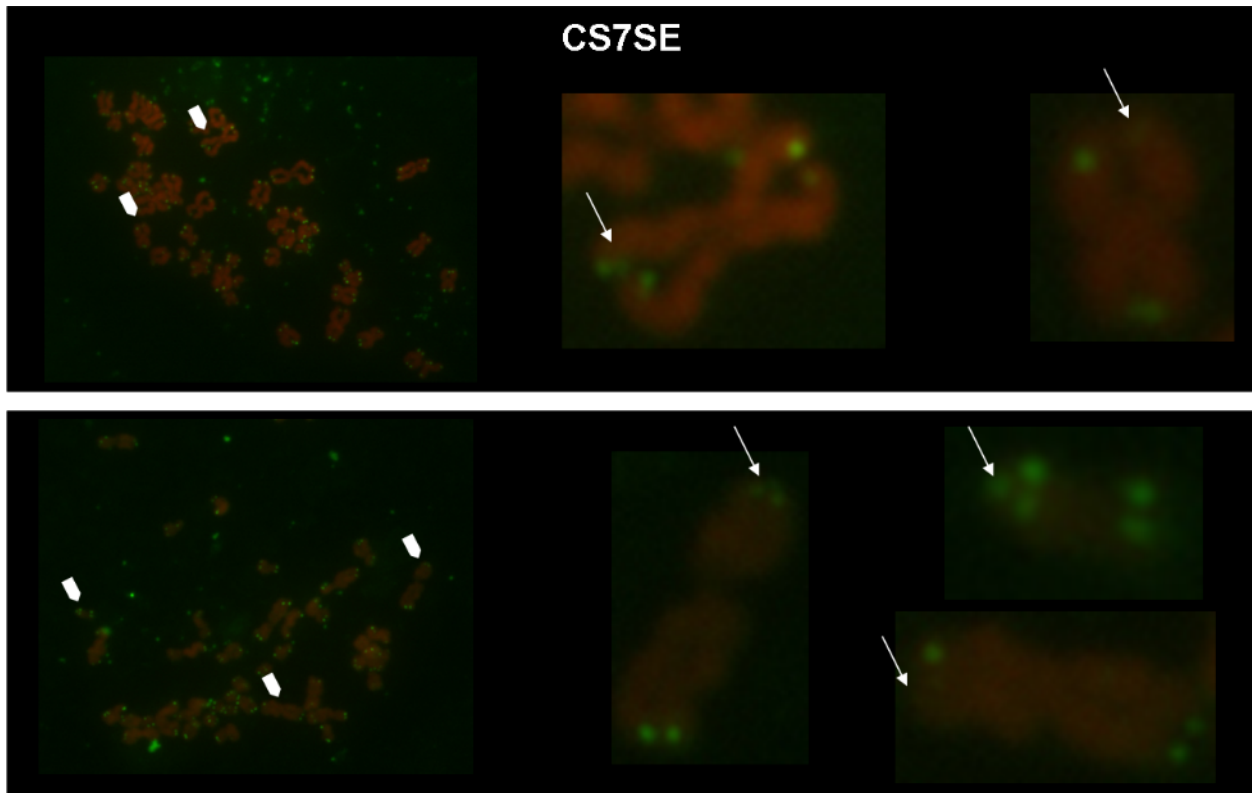


**Figure 5:** Analysis of metaphase chromosomes from CSB deficient CS7SE fibroblasts. Chromosomes were stained with DAPI and false coloured in red. Telomere DNA was detected by FISH using a FITC-conjugated  $(CCCTAA)_3$ -containing PNA probe (green). White arrows in the panels showing full spreads from a single cell indicate chromosomes with dysfunctional telomeres. Enlarged images of chromosomes with telomere loss and doublets are shown on the right. The experiment leading to this figure was carried out by myself and T.R.H. Mitchell. The figure was created by me.

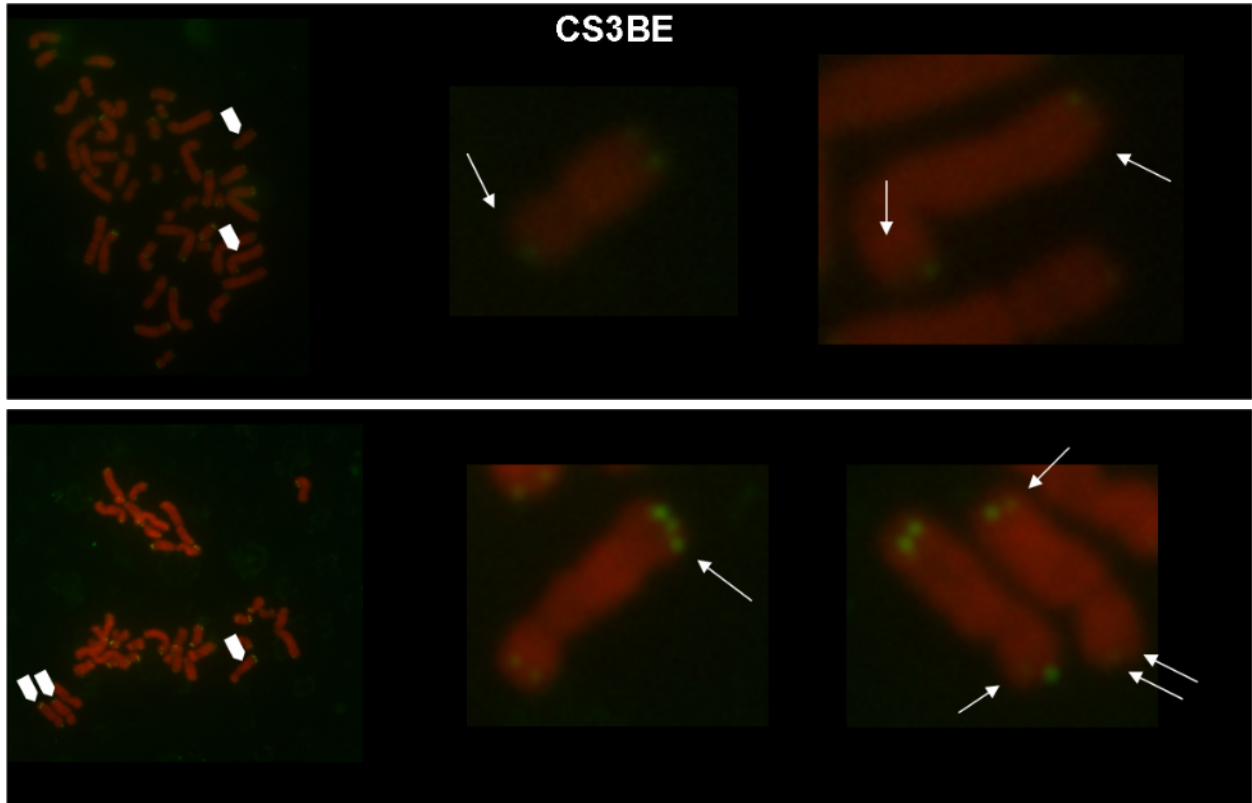


**Figure 6:** Analysis of metaphase chromosomes from CSA deficient CS3BE fibroblasts. Chromosomes were stained with DAPI and false coloured in red. Telomere DNA was detected by FISH using a FITC-conjugated  $(CCCTAA)_3$ -containing PNA probe (green). White arrows in the panels showing full spreads from a single cell indicate chromosomes with dysfunctional telomeres. Enlarged images of chromosomes with telomere loss and doublets are shown on the right. The experiment leading to this figure was carried out by myself and T.R.H. Mitchell. The figure was created by me.

## Discussion

CS is a complex segmental progeroid syndrome with a highly variable clinical presentation with the most notable features being premature ageing and neurodegeneration. A direct association between a molecular defect and the severity/presentation of CS has not yet been made. CSB is involved in repair of lesions through both NER and BER and the TTAGGG sequence of telomere repeats yields the chromosome end highly susceptible to lesions repaired via both pathways (Rochette and Brash 2010; Wang et al. 2010). Disruption of BER by removal of the major 8-oxoG glycosylase OGG1 in mice leads to persistent base damage in telomere DNA and an increase in telomere abnormalities (Wang et al. 2010). The exact role of CSB in BER of oxidative lesions such as 8-oxoG is not fully understood, but it has been shown to function as an elongation factor able to stimulate RNA polII bypass of the lesion (Charlet-Berguerand et al. 2006), to be in complex and functionally interact with OGG1 (Tuo et al. 2002a) and possibly to function in repair of the lesion throughout the genome independently of OGG1 (Osterod et al. 2002).

The data presented here demonstrate that TRF2 overexpression negatively effects NER of UVC induced damage by a mechanism involving CSB. Although HCR of the MB+VL treated reporter 24 hours after infection is unaffected by TRF2 overexpression, suggesting an NER specific effect, we cannot rule out potential differences at other time points. Together with the observed physical interaction between TRF2 and CSB this suggested that CSB may play an important role at telomeres. Following the identification of an interaction between CSB and TRF2 we examined telomeres in primary skin fibroblasts from two CS patients by telomere fluorescence *in situ* hybridization (Figures 5 and 6). These initial observations suggested an increased level of telomere abnormalities in cells from both CS complementation groups, leading

to further experiments carried out as a collaborative effort between our lab and Dr. X-D Zhu's lab (Department of Biology, McMaster University, Hamilton, Ontario, Canada).

Telomere integrity was examined by FISH in three additional cells from individuals with CS caused by mutations in CSB (CS1AN(GM739), GM1428(CS7SE), GM10905) as well as four fibroblasts from normal healthy individuals (GM38, GM9503, GM8399, GM10901; Note: GM10901 primary skin fibroblasts were isolated from the unaffected mother (obligate heterozygote) of the CS patient from which GM10905 primary fibroblasts were isolated). The results of these experiments demonstrated a significant increase in telomere dysfunction (telomere loss and telomere doublets) in CSB mutant cells CS1AN and CS7SE compared to the normal primary fibroblasts GM38, GM9503 and GM8399 (unpublished data, personal communication). Similar to CS1AN and CS7SE, FISH analysis of the fibroblasts from related individuals showed a significant increase in telomere loss and telomere doublets in GM10905 compared to the unaffected mother GM10901 (Batenburg et al. 2011). In addition, complementation of CSB deficient telomerase immortalized GM10905 fibroblasts by expression of the wild-type CSB gene led to a significant reduction in the number of telomere doublets per chromatid end compared to cells expressing the empty control vector (To facilitate introduction and expression of WT CSB in primary skin fibroblasts GM10901 and GM10905 primary fibroblasts were first immortalized with the catalytic subunit of telomerase (hTERT). Overexpression of hTERT in GM10905 (hTERT-GM10905) cells led to a substantial reduction in telomere loss while it had a negligible effect on the accumulation of telomere doublets (Batenburg et al. 2011)). Functional complementation of the NER defect associated with CS by introduction of WT CSB into hTERT-GM10905 (to generate hTERT-GM10905-CSB; control empty vector is referred to as hTERT-GM10905-vector) was confirmed by HCR of a UVC

damaged reporter gene as well as colony survival following cellular exposure to UVC (see Appendix III). These results demonstrated that functional CSB is important in the maintenance and stability of telomeres. In addition to dysfunctional telomeres, telomere length maintenance was affected by the absence of functional CSB. Telomere shortening was observed in CSB deficient fibroblasts while CSB complemented hTERT-GM10905 fibroblasts showed normal telomere maintenance (Batenburg et al. 2011). Taken together with the FISH, HCR and coIP data this suggests that TRF2 may play a role in regulating the function of CSB at telomeres. Telomere dysfunction and shortening are both associated with cancer, ageing and cellular senescence (Harley et al. 1990; de Lange 2002; Munoz et al. 2005) and may therefore play a role in the CS phenotype.

Loss of telomere repeats and/or loss of telomere protection by shelterin proteins are recognized by a number of DNA damage response factors including  $\gamma$ H2AX, ATM and 53BP1 (d'Adda di Fagagna et al. 2004; Palm and de Lange 2008) and form what is known as telomere dysfunction induced foci (TIF) (Takai et al. 2003). Using indirect immunofluorescence hTERT-GM10905-CSB and hTERT-GM10905-vector cells were examined for the presence of TIFs. Five or more TIFs per cell were observed in 18% of cells expressing vector alone with only 1% in cells complimented with CSB (Batenburg et al. 2011). These results suggest that in the absence of CSB a greater level of DNA damage may be present at telomeres, possibly playing a role in the downstream formation of telomere doublets and loss. The presence of a single 8-oxoG lesion impairs binding of TRF1 and TRF2 to TTAGGG repeats with greater amounts of the lesion or its repair intermediates (abasic sites or single nucleotide gaps) further decreasing their binding capacity (Opresko et al. 2005). Higher levels of 8-oxoG are known to accumulate in primary fibroblasts from CS patients (Tuo et al. 2003) presumably due to decreased BER activity

in CS fibroblasts which has been associated with a decrease in the transcription of *OGG1* and total protein levels (Dianov et al. 1999; Tuo et al. 2002b). It is therefore possible that the increase in TIFs observed in CS fibroblasts is a consequence of TRF1 and TRF2 binding being inhibited by 8-oxoG thereby deprotecting telomeres.

The transcription of telomeres into TERRA suggests a potential mechanism for regulating excision repair pathways involving CSB in telomeric DNA by coupling repair access to a regulated transcriptional program. The heterochromatic nature of telomeres appears to prevent repair of both BER and NER substrates (Rochette and Brash 2010; Rhee et al. 2011) possibly by inhibiting access of repair initiating proteins. Support for this comes from experiments comparing repair of oxidative base damage (Fpg sensitive sites) in telomeres and G rich minisatellite DNA showing complete repair 6 hours following damage induction in the latter with nearly a 2-fold increase in the number of oxidative lesions in telomere DNA over the same repair period (Rhee et al. 2011). This suggests that similar to the observed accumulation of thymine dimers in telomere DNA (Rochette and Brash 2010), telomeres are refractory to BER allowing oxidative base damage to accumulate. Knockout of *OGG1* in mouse embryonic fibroblasts (MEFs) leads to an increase in oxidative lesions in telomeres; demonstrating mammalian telomeres are accessible to the glycosylase at least part of the time (Wang et al. 2010). TERRA is transcribed in an RNA polIII dependent manner which could potentially facilitate TCR (Luke et al. 2008; Schoeftner and Blasco 2008). Although the majority of TERRA results from the transcription of the C-strand, small amounts of transcript from the G-strand are detectable (Azzalin et al. 2007) making it possible to couple repair of thymine dimers to transcription. TERRA levels are regulated in a cell cycle-dependent manner with the highest levels observed during G1 and the reaching lowest levels at the transition between late S and

early G2 in HeLa cells (Porro et al. 2010). A regulated transcription schedule, such as that observed with TERRA, may be a mechanism for “checking” and repairing telomeres prior to progression of the cell cycle. Only upon completion of transcription, which requires completion of repair (or transcriptional bypass of persistent damage) and reestablishing the heterochromatic state of the telomeres would the cell progress through the cell cycle. In cells with defective repair, such as CSB cells, TERRA transcription may still occur, but at lower rates, or by leaving unrepaired lesions that could lead to replication errors, deprotected/dysfunctional telomeres and ultimately telomere abnormalities. Additionally, improper TERRA transcription due to defective DNA repair at telomeres in the absence of CSB may also perturb the RPA to POT1 switch (Flynn et al. 2011), leading to improper telomere capping after DNA replication, potentially leading to telomere abnormalities.

While the majority of the work presented here focuses on TRF2 and CSB, the fact that loss of CSA suggests increased telomere instability (Figure 6) indicates that loss of a pathway such as TCR-NER or BER requiring both proteins acts upstream or in concert with the process(es) that generate abnormal telomeres. This is also supported by the observation that in CSA mutant cells, the interaction between CSB and TRF2 was not observed (Appendix III Figure 1) Detection of abnormal telomeres in CS fibroblasts may just be the result of a general deficit in repair, transcription and/or chromatin remodeling causing general genomic instability. Loss of CSB has been shown to cause metaphase fragility in the human U1 and U2 genes which are transcribed by RNA polII and the 5S gene which is transcribed by polIII (Kuhlman et al. 1999; Yu et al. 2000). Each of these three loci contain tandem repeats of short transcription units encoding highly structured RNA (Yu et al. 2000). TERRA is highly regulated, remains associated with telomeres (Azzalin et al. 2007; Schoeftner and Blasco 2008), has the potential to

form structured G-quadruplexes (Martadinata et al.) and is bound by a number of RNA binding proteins (Lopez de Silanes et al. 2010). It is possible that loss of CSB confers fragility on any repetitive sequence or genomic loci associated with the production of structured or complicated RNAs. The data presented here add a new aspect to the cellular and molecular defects associated with CS.

**Chapter 7**  
**Discussion**

Use of externally treated DNA to measure a host cell's ability to reactivate gene expression from a damaged template is a well established approach for examining repair of UVC induced DNA damage by NER. Controversy regarding the effects of 8-oxoG/oxidative damage within foreign DNA probes on gene expression questioned the use of the HCR assay to examine BER. This led us to examine the ability of cells to reactivate gene expression over time (Chapter 2) and to repair/remove 8-oxoG from the adenovirus encoded *lacZ* reporter gene (Chapter 3). The results of these experiments allowed us to demonstrate gene expression is reactivated over time in untreated mammalian cells and that this reactivation correlates with relative amounts of removal of MB+VL induced 8-oxoG lesions. The results of Chapters 2 and 3 validate the use of the HCR assay to examine BER using the MB+VL treated adenovirus reporter construct in untreated mammalian cells. We then employed the use of the adenovirus to examine BER in relation to ageing and neurodegeneration using human fibroblasts. Summarized below are the contributions of the Chapters contained in this work to the understanding of the relationship between oxidative DNA damage, ageing and neurodegeneration. The discussion sections of each Chapter contain significant information regarding certain theories and conclusions. The following section discusses specific aspects of the work; future directions of the work as well as connecting the data presented with the wider scope the DNA damage theory of ageing.

### **8-oxoG, transcription and repair**

As has been discussed throughout this work, the ability of 8-oxoG to inhibit transcription by RNA polIII is controversial, but likely varies depending on many factors. In Chapter 2 our data shows the presence of 8-oxoG lesions in the transcriptionally active  $\beta$ -gal gene leads to

decreased expression, consistent with RNA polIII inhibition. The data also demonstrate CSA and CSB are required for normal levels of gene reactivation. Southern blot experiments examining the removal of MB+VL induced 8-oxoG by the loss of Fpg sensitive sites demonstrated a relationship between the HCR assay and removal of lesions suggesting repair is being measured by reactivation rather than lesion bypass. The significantly decreased rate of 8-oxoG removal in CHO-AA8 cells compared to GM637F correlates with the reduction in HCR, providing further evidence that 8-oxoG in a transcribed gene is capable of impeding RNA polII progression.

Similar to decreased 8-oxoG incision in cells lacking functional CSB (Dianov et al. 1999; Tuo et al. 2001; Tuo et al. 2003; D'Errico et al. 2007), CSA fibroblasts are also defective in removal of 8-oxoG and lack of functional CSA does not have an effect on the 8-oxoG incision activity of cell extracts (D'Errico et al. 2007), suggesting that similar to NER, both CS proteins are required for stimulation of RNA polIII bypass activity or lesion removal for resumption of transcription. In Chapter 5 we used the enhanced expression assay to examine the persistence of MB+VL induced 8-oxoG in transcribed genes in normal and CS primary fibroblasts. Mutations in both CSA and CSB led to a significant increase in reporter gene expression compared to normal fibroblasts and it is believed that stalled RNA polIII complexes at sites of persistent DNA damage produce the signal for upregulated reporter gene expression (Francis and Rainbow 2000; Appendix II). These results support the conclusion that both proteins play a role in the response to stalled RNA polIII complexes at 8-oxoG lesions. CSB cells have reduced transcription of OGG1 resulting in an overall decrease of its protein levels in the cell (Dianov et al. 1999). OGG1 is found in complex with CSB, where it was thought CSB may function to stimulate OGG1 mediated BER of 8-oxoG (Tuo et al. 2002a). The presence of TCR-BER is somewhat controversial but is supported by some evidence such as experiments in wild-type MEFs

demonstrating that 8-oxoG is removed at a greater rate in the TS compared to NTS of a transfected plasmid (Le Page et al. 2000). Furthermore, In OGG1<sup>-/-</sup> MEFs, repair in the NTS is lost with no effect on removal of the lesion in the TS (Le Page et al. 2000; Osterod et al. 2002) and CSB<sup>-/-</sup> MEFs show no repair in the TS but wild-type levels in the NTS (Osterod et al. 2002) suggesting a role for CSB in TCR-BER. This idea is challenged by the fact that treatment of cells with  $\alpha$ -amanatin, which specifically inhibits RNA polII, does not affect CSB dependent repair (Osterod et al. 2002). OGG1 along with NTH1 (a DNA glycosylase that excises pyrimidine derived oxidized bases) constitute the majority of mammalian BER and when knocked out in mice do not result in an abnormal phenotypes (Minowa et al. 2000; Takao et al. 2002), which suggested redundancy in substrate recognition in, at the time, undiscovered glycosylases.

It is now known that OGG1 is only active within duplex DNA and has no incision activity in bubble or ssDNA structures, such as those found during transcription or replication (Dou et al. 2003). Three mammalian DNA glycosylases belonging to the *E. coli* MutM/Nei family, NEIL (Nei-like) 1-3 with incision activity in bubble and single stranded DNA have been identified and preferentially stimulate BER during transcription and replication (Dou et al. 2003; Hegde et al. 2012). NEIL2, which preferentially recognizes 5-hydroxyuracil (5-OHU), but can weakly incise 8-oxoG is expressed in a cell cycle independent manner (Hazra et al. 2002) and was recently shown to interact with RNA polII *in vivo* and initiate transcription-dependent BER of 5-OHU (Dou et al. 2003; Banerjee et al. 2011). NEIL1, which can stimulate incision of 8-oxoG in bubble or ssDNA but has higher excision activity when 8-oxoG is found in duplex DNA (Dou et al. 2003) is expressed during S-phase (Hazra et al. 2002) and has been shown to largely play a role in replication repair (Dou et al. 2008; Hegde et al. 2008; Theriot et al. 2010). While a lot is known regarding the function and substrate specificities of the different DNA glycosylases

capable of excising 8-oxoG, the mechanism(s) of preferential repair in TS of an active gene are still unclear, but the information discussed here suggests CSB plays a major role.

The ease with which damage can be introduced into the adenovirus' DNA which can then be easily delivered to the nucleus and subsequently re-isolated for analysis makes it an efficient tool for directly examining DNA repair. Our experiments in Chapter 3 examined removal of MB+VL induced 8-oxoG from the adenovirus encoded *lacZ* gene in a non-strand specific manner. The protocol could be adapted to examine repair in a strand specific manner by generation of single stranded RNA probes which would allow quick and direct examination of the repair rate of 8-oxoG in the TS and NTS. The advantage of using this system to study strand specific BER is that one can easily introduce the DNA into human primary fibroblasts without eliciting a DNA damage response (Blagosklonny and el-Deiry 1996) to measure repair of 8-oxoG in non-replicating but transcriptionally active DNA. This approach will allow us to gain a much better understanding of the repair processes and cellular responses occurring in cells associated with an age related decline in function such as in neurons.

In addition to facilitating the use of reporter genes, adenovirus DNA and plasmid DNA are used as probes to study repair kinetics of a given lesion because a large copy number can be easily introduced allowing for a more experimentally manageable number of cells to be used. Ultimately, it is necessary to show that repair of extrachromosomal viral DNA recapitulates repair in the genomic DNA of the cell. To achieve this I propose that cells be treated with MB+VL to induce 8-oxoG after being infected with undamaged viral DNA. Following periods of repair incubation, genomic DNA and viral DNA can be extracted, treated with Fpg and strand specific repair can be analysed by southern blotting with strand specific RNA probes. If this approach is not sensitive enough due to the low copy number of target genes in the host cell, a

strand-specific-PCR (An et al. 2011) could be used. Prior to extension of isolated Ad DNA by the procedure described by An et al. the DNA would be treated with Fpg to generate ssDNA breaks at sites of 8-oxoG. Defining a system for accurately studying BER in a strand specific manner in the non-replicating adenovirus would provide a powerful tool for analyzing BER process in the context of transcription. This information may provide us a better understanding of the repair processes occurring in post-mitotic neurons and how they play a role in natural ageing as well as neurodegenerative disorders.

### **MB increased BER capacity and Alzheimer's disease**

Clinical trials using MB to treat AD patients demonstrated it could improve cognitive function and slow disease progression (Gura 2008). Studies examining the potential mechanisms of MB's therapeutic action have shown it reduces A $\beta$  peptide levels (Medina et al. 2011), increase *in vitro* lifespan of human fibroblasts and boosts levels of cytochrome c (Atamna et al. 2008). The data presented in chapter 4 demonstrate that low levels of MB in tissue culture media increases BER of MB+VL 8-oxoG, which likely plays a role in extending the replicative lifespan of IMR90 *in vitro*. The ability of MB to restore cognitive function demonstrates that the cause of dysfunctional cells that leads to neurological impairment is not permanent and can be removed to restore proper function. We present a model for the action of MB (Chapter 4, Figure 5) suggesting MB reduces the level of oxidative stress and DNA damage within the cell by reducing A $\beta$  levels, increasing cytochrome c and stimulating BER. In neurons, which lack replication and its associated repair, mutagenic lesions such as 8-oxoG can lead to transcriptional mutagenesis. Over time as the frequency of a mutagenic lesion increases within the coding

region, the likelihood of a change in the resulting mRNA sequence increases as does the probability an improperly paired RNA base will lead to a codon/amino acid change and generate a mutant protein. In addition, transcription may be inhibited by lesions capable of inhibiting the progression of RNA polymerases leading to dysregulation of cellular function as more and more genes are improperly or fail to be transcribed. Because the DNA in neurons is not replicated, mutagenic lesions like 8-oxoG are not converted to permanent mutations and therefore any cellular dysfunction caused by their presence can be relieved by repair. The known cellular outcomes of MB treatment, increased BER (Chapter 4), decreased A $\beta$  levels (Medina et al. 2011) and increased cytochrome c levels (Atamna et al. 2008) suggest the therapeutic promise of MB is based on its' ability to restore function by removing DNA damage and relieving oxidative stress.

In the field of ageing research, processes that extend maximum longevity are of great interest. Whether it be the DNA damage theory of ageing or one of the many others, the core aspect of each is that a certain process leads to our progressive decline and eventual demise. In order for a specific theory to be true (not necessarily the sole factor of ageing but a significant contributor to the process), experiments must support it. Culturing of IMR90 fibroblasts in low levels of MB was shown to increase *in vitro* replicative life span (Atamna et al. 2008), in other words delay cellular senescence. The increase in the number of population doublings suggests that in the absence of MB in culture media, the Hayflick limit of these cells was not induced by critically shortened telomeres, but some other type of dysfunction, possibly accumulation of mutations and DNA damage. We showed that HCR of the MB+VL treated reporter decreases with increasing passage number, suggesting these cells leave a greater number of the mutagenic lesions unrepaired with each replication. We also showed that MB increases BER capacity in

primary human fibroblasts suggesting the increase in cellular lifespan was in part due to reduced levels of DNA damage in the cell. To explore this in more detail long term growth experiments in IMR90, GM9503 and GM8399 fibroblasts should be carried out without and without low levels of MB. At increasing passage numbers (until senescence), DNA would be isolated from the cells to measure the amount of 8-oxoG and G:C → A:T transversion. 8-oxoG content could be examined by alkaline pulsed field gel electrophoresis or the comet assay using DNA treated with Fpg. Mutation frequency can be done by measuring the loss of restriction sites, PCR or a combination of both. If a decrease in the genomic content of 8-oxoG and mutations is observed in cells cultured in MB, it would provide additional support for the DNA damage theory of ageing.

### **Oxidative DNA damage in telomeres**

The data shown in chapter 6 focused on repair of UVC induced damage, TRF2 and CSB with the majority of the discussion speculating on repair of oxidative base damage. Overexpression of TRF2 has no effect on HCR of the MB+VL treated reporter when examined at 24 hours. While overexpression of TRF1 did not have an effect on reactivation of the UVC treated reporter gene, like TRF2 it contains a TRFH domain that recognizes and binds YxLxP, such as that found in CSB, motifs in target proteins (Chen et al. 2008). TRF1 and TRF2 both bind telomeres in a sequence specific manner (Palm and de Lange 2008) and their binding is affected by the presence of 8-oxoG and its repair intermediates *in vitro* (Opresko et al. 2005). This suggests that accumulation of oxidative damage could cause deprotection of telomeres by shelterin *in vivo* thereby stimulating a repair response and allowing access of global repair proteins including OGG1 and CSB. Following oxidative stress BER complexes containing

OGG1 preferentially assemble in regions of open chromatin (Amouroux et al. 2010) and OGG1 knockout experiments demonstrated an increase in Fpg sensitive 8-oxoG lesions in telomeres supporting the idea that the glycosylase can access telomere repeats and stimulate repair of the lesion in telomeres at some point throughout the cell cycle (Wang et al. 2010). Deprotected telomeres trigger the DNA damage response and cell cycle arrest (Palm and de Lange 2008), therefore quick and efficient repair of these lesions would allow the cell to reestablish the proper state of the affected telomere(s) and cell cycle progression. TERRA levels are highest during G1 (Porro et al. 2010), suggesting transcription of telomeres is greatest prior to DNA synthesis. Relaxing telomere heterochromatin to facilitate access of the transcription machinery may provide the cell a mechanism for coordinating access of DNA repair proteins and/or coupling transcription to repair.

Evidence supports a role for CSB in OGG1 independent repair of 8-oxoG throughout the genome (Osterod et al. 2002) and the increased number of TIFs observed in CSB deficient cells (Batenburg et al. 2011) may indicate telomere deprotection resulting from inhibition of TRF1 and TRF2 binding by 8-oxoG. Examination of telomeres for the presence/amount of 8-oxoG in CSB deficient as well as CSB complemented fibroblasts by Fpg digestion and southern blotting using a probe specific to telomere repeats similar to that used by the Liu group (Lu and Liu 2009; Wang et al. 2010; Rhee et al. 2011) would help in understanding the nature of these TIFs. Loss of CSB would be expected to show increased oxidative damage at telomeres as increased steady state levels of 8-oxoG exist in CS cells (D'Errico et al. 2007), exposure of CS cells to ionizing radiation causes greater accumulation and persistence of 8-oxoG compared to controls (Tuo et al. 2003) and CS cells have lower OGG1 levels and incision activity (Dianov et al. 1999).

TRF1 does indeed physically interact with CSB and its protein levels are altered in CSB deficient cells (personal communication XDZ, unpublished data, data not shown). While the data presented in this work shows overexpression of TRF2 negatively effects reactivation of the UVC treated reporter in a CSB dependent manner, it had no effect on the MB+VL treated reporter. It is tempting to speculate that TRF1 and TRF2 function to mediate repair of different excision repair pathways at telomeres. *In vitro* incision assays show that overexpression of TRF1 can increase the incision activity of APE1 in telomere substrates containing a single 8-oxoG lesion while TRF2 has no effect (Rhee et al. 2011). Consistent with previous findings by Opresko et al., TRF1 and TRF2 exhibited a 40% decrease in binding ability to 8-oxoG containing telomere substrates prior to the addition of APE1 to the *in vitro* reaction mixtures (Rhee et al. 2011). Rhee et al.'s data demonstrate that in the presence of 8-oxoG and decreased TRF1 and TRF2 binding, APE1 can access telomere repeats and that TRF1 can stimulate its incision activity. Experiments examining HCR of the reporter gene containing MB+VL induced 8-oxoG lesions in normal and CSB deficient fibroblasts overexpressing TRF1 should be conducted. Based on the work presented by Rhee et al, one would predict that overexpression of TRF1 would increase HCR of the MB+VL treated reporter gene in normal fibroblasts, however the *in vitro* stimulation of APE1 incision activity by TRF1 may be specific to telomeres. If an effect of TRF1 overexpression is observed in normal fibroblasts it will be of great interest to see if CSB is required as was observed for TRF2 and HCR of the UVC treated reporter gene.

CS individuals appear normal at birth and show progressive neurodegeneration in early childhood. The nervous system is made up of post-mitotic neurons as well as mitotic astrocytes, neural stem cells and microglia. The function of neurons and their high metabolic demand subjects them to higher amounts of oxidative stress compared to other cell types. The fact that a

large number of human neurodegenerative disorders including CS, AD and AT show a DNA repair defect highlights the sensitivity of neurons to the DNA damage response. The high metabolic activity and lack of exposure to damage sources such as UVC suggests BER is likely the most important pathway in neurons.

Telomeres are considered to be the cell's mitotic clock due to their erosion with each subsequent cell division, which supports a major role for telomeres in cancer and ageing (Blackburn et al. 2006). While a lot is known about the role of telomeres and their associated proteins in mitotic cells, little is known regarding their role in non-dividing cells such as neurons. It is often asked if neurons are no longer dividing why it matters if the genome, including telomeres accumulates damage. DNA repair diseases with a neurodegenerative phenotype resulting from progressive neuronal cell death such as CS, Ataxia Telangiectasia, Werner's syndrome and Bloom's syndrome highlight the importance of functional DNA repair in the survival of neurons (McMurray 2005) and are often used to highlight the importance of telomeres in maintaining a healthy and functioning nervous system. Similar to CSB, these proteins do not only function at telomeres, but throughout the genome, which may indicate that it is not telomere stability per se that is maintaining cell survival but rather overall genome stability. In other words, observation of defective or damaged telomeres may just reflect the overall state of an unstable genome. As neurons are non-dividing cells, unrepaired DNA damage in their DNA likely results in reduced fidelity of information transferred from DNA to proteins and a progressive decline in cellular function (Taddei et al. 1997). In dividing cells, unrepaired damage persisting upon re-entering or continuing the cell cycle could lead to aberrant cell proliferation (cancer) or initiate an apoptotic response (Nospikel and Hanawalt 2003).

As mentioned previously, the TTAGGG sequence of telomeres leaves them highly susceptible to oxidative damage. Accumulation of damage in telomeres may act as a cellular sensor for the amount of unrepaired DNA damage in the cell. If deprotection of telomeres caused by decreased TRF1 and TRF2 binding affinity in the presence of oxidative damage reaches a certain threshold, the damage response would be activated potentially leading to cell cycle arrest. If the cell is able to repair the damage and restore the proper telomere state the cell cycle would resume. If damage remains unrepaired and the damage signal persists, cells may enter senescence or undergo apoptosis (Palm and de Lange 2008). The amount of oxidative damage in telomeres may act as an indicator of the state of the genome to the cell. In other words, high levels of unrepaired oxidative damage would lead to persistently uncapped telomeres. In addition to physically protecting genetic information, telomeres may act as damage sinks to monitor overall genome health and ultimately mediate the appropriate downstream cellular response such as cell cycle arrest or apoptosis. If this were the case, it would not matter if the cell was a post-mitotic cell such as a neuron as they still have telomeres that can be uncapped leading to a DNA damage response. It would be of interest to conduct experiments with CSB deficient and complemented cells grown in chronic oxidative stress to determine if CSB deficient cells show a greater accumulation of TIFs and if there is increased apoptosis. Depending on results for TRF1 and HCR of the MB+VL treated reporter, it would be interesting to examine the cellular localization of TRF1 in CSB deficient fibroblasts cultured under chronic oxidative stress. It is possible that dysfunctional telomeres caused by decreased repair capacity in neurons in CS individuals as well as with increasing age result in apoptotic signals leading to progressive neurodegeneration. Such a model would help to explain the neurodegenerative phenotype of CS

patients as well as connect decreased DNA repair observed with aging and the associated decline in neurological function.

### **Oxidative DNA damage and ageing**

Ageing is a nearly universal process that affects all but a very short list of species (Finch 2009). Every single human who is able to evade death by environmental causes long enough will eventually experience the progressive effects of this process and ultimately succumb to it. A major purpose for studying ageing is that it is the greatest risk factor for a number of degenerative processes and most types of cancer. Understanding these processes may allow us to develop strategies not only for extending our lifespan, but greatly improving our quality of life at the same time. Despite the vast amount of research devoted to uncovering the mechanisms of ageing, the underlying processes still largely remain a mystery. A major obstacle in ageing research has been the ability to demonstrate causal roles for observed changes such as increasing levels of oxidative DNA damage with increasing age and how these changes are manifested as ‘ageing phenotypes’. A number of different theories have been proposed to explain ageing including the DNA damage theory of ageing. DNA damage results in structural alteration of a DNA molecule and can affect gene expression, impair transcription, activate cell cycle check points leading to cell cycle arrest, senescence or even apoptosis (Hoeijmakers 2009). DNA damage can alter gene expression directly to cause cellular dysfunction or the DNA damage response can indirectly have an effect on gene expression by causing altered gene expression patterns (Seviour and Lin 2010).

The body of a fully developed and matured human being consists of mitotically active cells such as the skin epithelia, gut and adult stem cells while the majority of the tissues

including neurons are terminally differentiated and no longer replicate. Mitotically active cells accumulate additional DNA alterations associated with ageing including telomere shortening and replication associated DNA damage. In this work we have focused on DNA repair mechanisms as the cause of persistent DNA damage that can affect cellular function and lead to mutations in relation to ageing and neurodegeneration.

While the DNA damage theory of ageing is widely studied and supported by a large amount of association studies, it has yet to be proven. The problem has been with coupling increases in DNA damage and oxidative stress with increased phenotypic manifestation of increasing chronological age. Based on the principles of this theory, it would be expected that any alteration in a cell or organism that results in less DNA damage or decreased oxidative stress either by increased antioxidant defence mechanisms or more efficient mitochondrial respiration would produce a beneficial effect on the ageing process and lifespan.

While we do not demonstrate a causative link between DNA damage, repair and the processes of ageing and neurodegeneration, the data presented here are consistent with the DNA damage theory of ageing. In this work we show that the recombinant adenovirus is an excellent system for quick and efficient examination of repair in mammalian. Using this system we demonstrated an association between increased repair of oxidative DNA damage and cellular ageing. Increased BER was observed in IMR90 fibroblasts when cultured in MB, a condition that also extends lifespan of these cells. We also show that repair capacity is decreased during *in vitro* cellular ageing using the HCR assay. While we do not demonstrate a causative link between DNA damage, repair and the processes of ageing and neurodegeneration in humans, the data presented in this work are consistent with and provide additional support for the DNA damage theory of ageing.

## **Appendix I**

**Host cell reactivation of the MB+VL treater reporter gene in primary fibroblasts from patients with Alzheimer's disease.**

## Introduction

AD is a progressive age-related neurodegenerative disorder characterized by cognitive decline and behavioral changes. The etiology of AD is complicated and is thought to arise through complex interactions of genetic and environmental factors. The majority of AD cases are sporadic and display no identifiable relationship to genetic or environmental factors (Schellenberg, 1995). 15% of AD cases are inherited in an autosomal dependent manner and are referred to as Familial AD (FAD). The genes involved in FAD are *presenilin 1* (*PSEN1*, FAD III), *presenilin 2* (*PSEN2*) and *amyloid precursor protein* (*APP*) (Rosenberg, 2000). Presenilins are members of the transmembrane protein family and function as part of the gamma-secretase complex. While mutations in the *PSEN1* and *PSEN2* are known to cause AD in an autosomal dominant manner, the mechanisms of disease pathology are not well understood. There is evidence that decreased BER and increased oxidative DNA damage plays a role in AD pathology (For a discussion of oxidative DNA damage and AD see chapter 4 introduction and discussion). As discussed in Chapter 4, MB has shown promise as a therapeutic agent in treatment of AD and when present at low concentrations in growth media delays senescence of IMR90 primary skin fibroblasts *in vitro*. Here we have used the HCR assay to examine BER of MB+VL induced 8-oxoG in untreated AD primary skin fibroblasts as well as untreated age matched normal primary skin fibroblasts as a control. These experiments were conducted to determine if the HCR assay was capable of detecting an HCR defect in skin fibroblasts from AD patients.

## **Materials and Methods**

### *Host cell reactivation*

The HCR assay was conducted as described above in the chapter 4 materials and methods. The following are the specific details used here AD and normal control fibroblasts were seeded in 96 well plates at a density of  $1.0 \times 10^4$  cells/well. Following an incubation period of 18-20 hours, cells were infected with MB+VL treated AdCA35 (MOI 40).  $\beta$ -gal activity was scored 24 hours post-infection.

## **Results**

### *Normal HCR of the MB+VL treated reporter in AD primary fibroblasts*

The results for HCR of the MB+VL treated reporter in primary skin fibroblasts from patients affected with AD (Table A1-1 contains a list of the different AD primary fibroblasts used) are shown in Table A1-2a) and A1-2b). The relative  $D_{37}$  values for a number of AD cells compared to the appropriate age matched control as well as compared to a number of additional normal primary fibroblasts 24 hours after infection are shown. No significant difference were detected between an AD cell and its age matched control; between an AD cell strain and all normals; or between all AD cell strains as a group and all normal fibroblasts. We have only examined HCR of the MB+VL treated AdCA35 reporter gene 24 hours after infection.

**Table 1:** Age, race and sex of control cell lines isolated from apparently healthy individuals and from individuals affected with familial Alzheimer's disease Type III. Age refers to the age of the individual at the time of biopsy

<b>Cell Line</b>	<b>Group</b>	<b>Age</b>	<b>Race</b>	<b>Sex</b>
<b>GM00969</b>	Apparently Healthy	2	Caucasian	Female
<b>GM00038</b>	Apparently Healthy	9	Black	Female
<b>GM9503</b>	Apparently Healthy	10	Caucasian	Male
<b>GM00037</b>	Apparently Healthy	18	Caucasian	Female
<b>GM8399</b>	Apparently Healthy	19	-	Female
<b>GM08400</b>	Apparently Healthy	37	-	Female
<b>GM01863</b>	Apparently Healthy	46	Caucasian	Male
<b>AG02261B</b>	Apparently Healthy	61	Caucasian	Male
<b>GM02623D</b>	Apparently Healthy	61	Caucasian	Female
<b>GM00288</b>	Apparently Healthy	64	caucasian	Male
<b>GM01706A</b>	Apparently Healthy	82	Caucasian	Female
<b>Cell Line</b>	<b>Group</b>	<b>Age</b>	<b>Race</b>	<b>Sex</b>
<b>AG07768</b>	FAD III	31	Caucasian	Female
<b>AG08711</b>	FAD III (25% risk)	34	Caucasian	Female
<b>AG07671A</b>	FAD III	44	Caucasian	Male
<b>AG04159B</b>	FAD III	52	Caucasian	Female
<b>AG07629C</b>	FAD III	54	Caucasian	Male
<b>AG06848C</b>	FAD III	56	Caucasian	Femaile
<b>AG06840C</b>	FAD III	56	Caucasian	Male
<b>AG06844C</b>	FAD III	59	Caucasian	Male
<b>AG07613B</b>	FAD III	66	Caucasian	Male

**Table 2:** HCR capacity of AD primary skin fibroblasts measured by  $D_{37}$  relative to normal control primary fibroblasts. Scoring for  $\beta$ -gal activity from AdCA35 (MOI 40) was conducted 24 hours after infection. n= number of experiments. A one sample two tailed t-test was conducted to determine if any observed differences in the average relative  $D_{37}$  were significant ( $p \leq 0.05$ ) for the AD cell strain compared to the indicated normal. The  $D_{37}$  Values relative to normal for all AD cells were pooled to determine if the AD cells as a group showed any differences from all normal primary fibroblast (see bottom of table A4-2).

AD Cell line	(age)	Normal Control	(age)	Mean Rel		SE	n	p
				$D_{37}$	$\pm$			
<b>AG07671A</b>	<b>44</b>	GM1863	46	1.09	$\pm$	0.17	4	0.64
		GM38A	9	0.93	$\pm$	0.08	3	0.48
		GM9503	10	1.06	$\pm$	0.21	3	0.80
		Average		1.03	$\pm$	0.05	3	0.64
<b>AG06848C</b>	<b>56</b>	GM08400	37	0.69	$\pm$	0.25	2	0.42
		AG02261B	61	1.14	$\pm$	0.30	2	0.72
		GM9503	10	1.36	$\pm$	-	1	-
		GM8399	19	1.15	$\pm$	-	1	-
		GM1863	46	1.00	$\pm$	-	1	-
		GM02623D	61	0.44	$\pm$	-	1	-
Average		0.96	$\pm$	0.14	6	0.80		
<b>AG06840C</b>	<b>56</b>	GM08400	37	0.68	$\pm$	0.21	2	0.38
		AG02261B	61	1.14	$\pm$	0.24	2	0.67
		GM9503	10	1.31	$\pm$	-	1	-
		GM8399	19	1.11	$\pm$	-	1	-
		GM1863	46	0.96	$\pm$	-	1	-
		GM02623D	61	0.47	$\pm$	-	1	-
Average		0.95	$\pm$	0.13	6	0.69		

**Table 3:** HCR capacity of AD primary skin fibroblasts measured by  $D_{37}$  relative to normal control primary fibroblasts. Scoring for  $\beta$ -gal activity from AdCA35 (MOI 40) was conducted 24 hours after infection. n= number of experiments. A one sample two tailed t-test was conducted to determine if any observed differences in the average relative  $D_{37}$  were significant ( $p \leq 0.05$ ) for the AD cell strain compared to the indicated normal. The  $D_{37}$  Values relative to normal for all AD cells were pooled to determine if the AD cells as a group showed any differences from all normal primary fibroblast.

AD Cell line	(age)	Normal Control	(age)	Mean Rel $D_{37}$	+	SE	n	p
<b>AG04159B</b>	<b>52</b>	GM08400	37	0.81	+	-	1	-
		AG02261B	61	1.24	+	-	1	-
		GM9503	10	1.18	+	-	1	-
		GM8399	19	1.00	+	-	1	-
		GM1863	46	0.87	+	-	1	-
		Average		1.02	+	0.08	5	0.82
<b>GM08711</b>	<b>34</b>	GM08400	37	0.91	+	0.18	2	0.70
		AG02261B	61	1.54	+	0.14	2	0.16
		GM9503	10	1.59	+	-	1	-
		GM8399	19	1.35	+	-	1	-
		GM1863	46	1.17	+	-	1	-
		GM02623D	61	0.73	+	-	1	-
		Average		1.22	+	0.14	6	0.19
<b>AG06844D</b>	<b>59</b>	AG02261B	61	1.05	+	0.04	2	0.46
		GM00288	64	0.94	+	-	1	-
		GM08400	37	0.68	+	0.21	2	0.37
		GM1863	46	1.18	+	-	1	-
		GM9503	10	0.95	+	-	1	-
		GM38A	9	0.97	+	-	1	-
		GM37G	18	1.47	+	-	1	-
		GM969C	2	1.13	+	-	1	-
		GM01706A	82	0.93	+	-	1	-
		Average		1.03	-	0.07	9	0.66
<b>AG07768</b>	<b>31</b>	GM02623D	61	0.41	+	-	1	-
		AG02261B	61	0.78	+	-	1	-
		GM08400	37	0.40	+	-	1	-
		Average		0.53	+	0.13	3	0.06
<b>GM07613B</b>	<b>66</b>	AG02261B	61	0.77	+	-	1	-
		GM00288B	64	0.72	+	-	1	-
		GM1863	46	0.91	+	-	1	-
		GM01706A	82	0.72	+	-	1	-
		GM38A	9	0.74	+	-	1	-
		GM37G	18	1.13	+	-	1	-
		GM969C	2	0.87	+	-	1	-
		GM9503	10	0.73	+	-	1	-
		Average		0.82	+	0.05	8	0.01
Avg reduction of all AD cells comp to normals				0.96		0.04	53	0.35

## Discussion

The results presented here demonstrate no significant difference in repair of MB+VL induced oxidative DNA damage in untreated AD compared to untreated normal primary fibroblasts as measured by the HCR assay. In chapters 2 and 4 and appendix IV we show time courses for HCR of the MB+VL treated reporter gene and that different cells behave differently. It is possible that at earlier or later time points AD cells may show differences in expression of the MB+VL treated reporter. If differences exist at earlier time points it is of interest as repair immediately following introduction of DNA damage is critical as the longer damage remains undetected or unrepaired the greater the increase in genome instability. It is possible that AD cells show a different HCR time profile and if that is the case it may reveal potential pathogenic mechanisms of either disorder. In primary normal skin fibroblasts (Chapter 4 and appendix IV) reactivation of reporter gene expression reached a maximum from 12-24 hours. It is possible that in following defective recognition/repair of MB+VL induced 8-oxoG after infection, more efficient bypass mechanisms are stimulated. During this early period, normal fibroblasts may be repairing the DNA so that when we examine relative expression at 24 hours, we are unable to detect a difference. Conducting HCR time course experiments in AD fibroblasts could provide more useful/detailed information. In chapter 4, the effect of 100nM MB in culture media was examined using normal primary fibroblasts and demonstrated an increase in HCR capacity. We hypothesize that the therapeutic success of MB in treating AD patients is in part due to an increase in the capacity to repair oxidative DNA damage. We show that in normal primary lung fibroblasts from healthy donors HCR of the MB+VL treated reporter is increased. In conjunction with HCR time course experiments, it would be very interesting to examine the effect of 100nM MB in culture media on HCR in primary fibroblasts from AD patients.

We have also examined the effect of aluminum (Al) on HCR in fibroblasts from individuals with neurodegenerative disorders (See appendices IV and V). A debate regarding a role for Al in AD development and progression has existed for some time and evidence supports a role for Al in oxidative stress and damage (see appendix IV for a discussion). While we have not examined the effect of Al on AD fibroblasts, it would be of interest to conduct assays for cell survival and HCR using AD fibroblasts.

## **Appendix II**

### **Further examination of enhanced expression from the undamaged adenovirus based reporter construct in primary fibroblasts following cellular MB+VL treatment**

**MB+VL induced oxidative damage in a transcriptionally active gene leads to enhanced expression in normal primary fibroblasts.**

The data from our lab suggests the signal leading to enhanced expression of the undamaged reporter is the result of stalled RNA polII complexes at unrepaired lesions (Francis and Rainbow 2000). Here we have used two approaches to examine expression of the adenovirus reporter gene in the presence of MB+VL induced damage: cellular pre-treatment with MB+VL and pre-infection of cells with a luciferase expressing adenovirus reporter construct (AdCA18) damaged by MB+VL. Pre-infection of cells with the damaged AdCA18 virus introduces DNA containing damage in a transcriptionally active gene to the cell. The normal primary fibroblast GM9503 was used as a representative normal as we have shown little difference between a number of normal primary fibroblasts (see Chapter 6 Figure 2).  $\beta$ -gal expression from the undamaged reporter gene was scored 3, 6, 12, 24 and 44 hours after infection with undamaged AdCA35 (MOI 300). While normal BER exists in these cells, after a certain threshold level of damage is achieved, cellular repair machinery would not be capable of removing lesions at a rate fast enough to prevent RNA polII stalling and signaling the downstream signalling that results in upregulation of expression from the CMV promoter. For pre-infected cells, AdCA18 was treated with increasing VL doses in the presence of 20 $\mu$ g/ml MB. For cells receiving cellular pre-treatment, all cells were exposed to 10 min of VL in the presence of increasing concentrations of MB (0-60 $\mu$ g/ml). Figure 1 shows an increase in expression from the undamaged reporter in GM9503 normal primary fibroblasts at high doses for both cellular pre-treatment and pre-infection with MB+VL damaged AdCA18 44 hours post-infection. This data demonstrates the increased expression observed from the undamaged  $\beta$ -gal reporter gene is a result of MB+VL induced 8-oxoG in DNA rather than from other effects on the cell.

**Enhanced expression of the Ad5HCMVSp1LacZ reporter in primary human fibroblasts from patients with Cockayne syndrome following cellular pre-treatment with MB+VL.**

The HCMV IE enhancer/promoter is one of the most frequently used promoters to drive expression of transgenes inserted into viral vectors (Addison et al. 1997). Its use is based on the fact that it can drive high levels of transgene expression in a number of different types of cells (Boshart et al. 1985; Schmidt et al. 1990). The viral enhancer region contains a number of imperfect repeats that binds a number of different transcription factors including NF- $\kappa$ B, Ap1 and cAMP responsive binding (CREB) proteins. While the HCMV IE promoter is able to drive expression of transgenes in cells derived from both humans and mice, expression in mouse cells is 10-50 fold lower (Addison et al. 1995; Addison et al. 1995a). In addition to the AdCA17 virus, which drives expression of the transgene by insertion of the HCMV IE enhancer/promoter with *lacZ* in the rightward direction downstream of the E1a enhancer region remaining in the Ad backbone (Addison et al. 1997), we have examined expression of two additional viral constructs following cellular exposure to MB+VL. The Ad5HCMVSp1*lacZ* reporter construct, is similar to AdCA17 except the reporter cassette (HCMV IE upstream of the *lacZ* transcriptional start site) is inserted into the deleted E1 region in the opposite/leftward orientation (see chapter 2, Figure 8) resulting in a lower level of reporter gene expression, presumably by removing the effects of the E1a enhancer. Previous work from our lab has examined expression of the undamaged AdCA17 following cellular pretreatment with MB+VL (Pitsikas et al. 2007) and Ad5HCMVSp1*lacZ* following cellular pretreatment with UVC (Francis and Rainbow 2000). While we have observed increased expression from both of these constructs in repair deficient cells following cellular

pretreatment with a DNA damaging agent, it is of interest whether they behave similarly in the same cells following the same type of cellular pretreatment.

Similar to results observed with the AdCA17 construct, expression of the undamaged Ad5HCMVSp1*LacZ* reporter was increased in CS compared to normal primary fibroblasts. A dose of 40µg/ml MB and 10 min VL exposure to cells was used based on results observed with GM9503 (Figure 1). Following cellular pre-treatment, the primary fibroblasts were infected with undamaged Ad5HCMVSp1*lacZ* and β-gal expression was scored at 6, 12, 24 and 44 hours post-infection (Figure 2). Consistent with the results shown in Figure 1, expression of the reporter gene increased relative to the undamaged control in the normal primary fibroblasts, GM9503 at 44 hours. At 24 hours an increase in reporter gene expression was observed for all the CS lines examined compared to GM9503; consistent with a reduced ability of these cells to process 8-oxoG. At 6, 12 and 44 hours post-infection an increase in reporter gene expression was observed for the majority of CS fibroblasts examined. These results suggest that both AdCA17 and Ad5HCMVSp1*lacZ* behave in a similar manner following cellular pretreatment with MB+VL.

Reporter gene expression following multiple VL exposures to cells (0, 1, 5, 10, 15 and 20 min) incubated in the presence of 40µg/ml MB at 24 hours post-infection was examined. 24 hours was chosen as it is the time point for which a consistent increase in reporter gene expression was observed for all CS fibroblasts examined (see Figure 2). Figure 3 shows the average β-gal expression from a number of experiments following the indicated VL exposure times for each fibroblast strain compared control cells not exposed to VL. An increase in reporter gene expression in a number of CS fibroblasts compared to the normal primary fibroblast GM9503 was observed. A comparison of expression from the undamaged reporter in pooled

results for group CSA and CSB is shown in Figure 4. A consistent increase in reporter gene expression in CSA and CSB fibroblasts compared to GM9503 was observed.

While the conditions used to examine expression of Ad5HCMVSp1*lacZ* differed from those used with AdCA17, increased expression was observed in CS primary fibroblasts compared to the normal primary fibroblast GM9503. These results suggest that the cellular response to pretreatment with a DNA damaging agent that leads to changes in expression from the HCMV IE reporter construct occur mainly by changes in the activity/level of cellular transcription factors that bind the transgenic promoter rather than the E1a enhancer. Additionally, these results demonstrate the importance of optimizing pretreatment and  $\beta$ -gal scoring conditions when using the enhanced expression assay as a tool for detecting persistent DNA damage in the genomic DNA of primary fibroblasts.

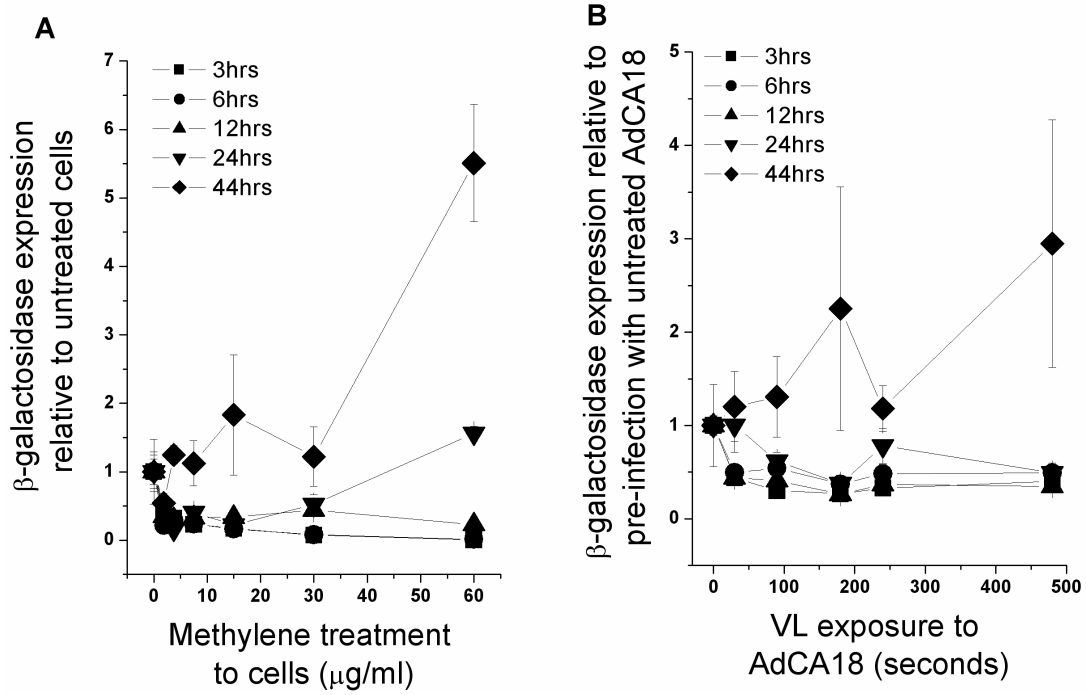


**Figure 1:** Enhanced expression of the undamaged  $\beta$ -gal reporter in normal primary fibroblasts. A) GM9503 normal primary fibroblasts overlaid with media containing increasing concentrations of MB (0-60 $\mu\text{g/ml}$ ) for 3 hours prior to cellular exposure to 10 min VL and followed by immediate infection with undamaged AdCA35 (MOI 300). B) GM9503 normal primary fibroblasts infected with MB+VL (20 $\mu\text{g/ml}$  MB in PBS) treated AdCA18 (luciferase) followed by immediate infection with undamaged AdCA35. Each point on the above curves is the average ( $\pm$  SE) of triplicate determinations from a single experiment. For each treatment condition  $\beta$ -gal expression was scored at 3, 6, 12, 24 and 44 hours after infection with the undamaged AdCA35.

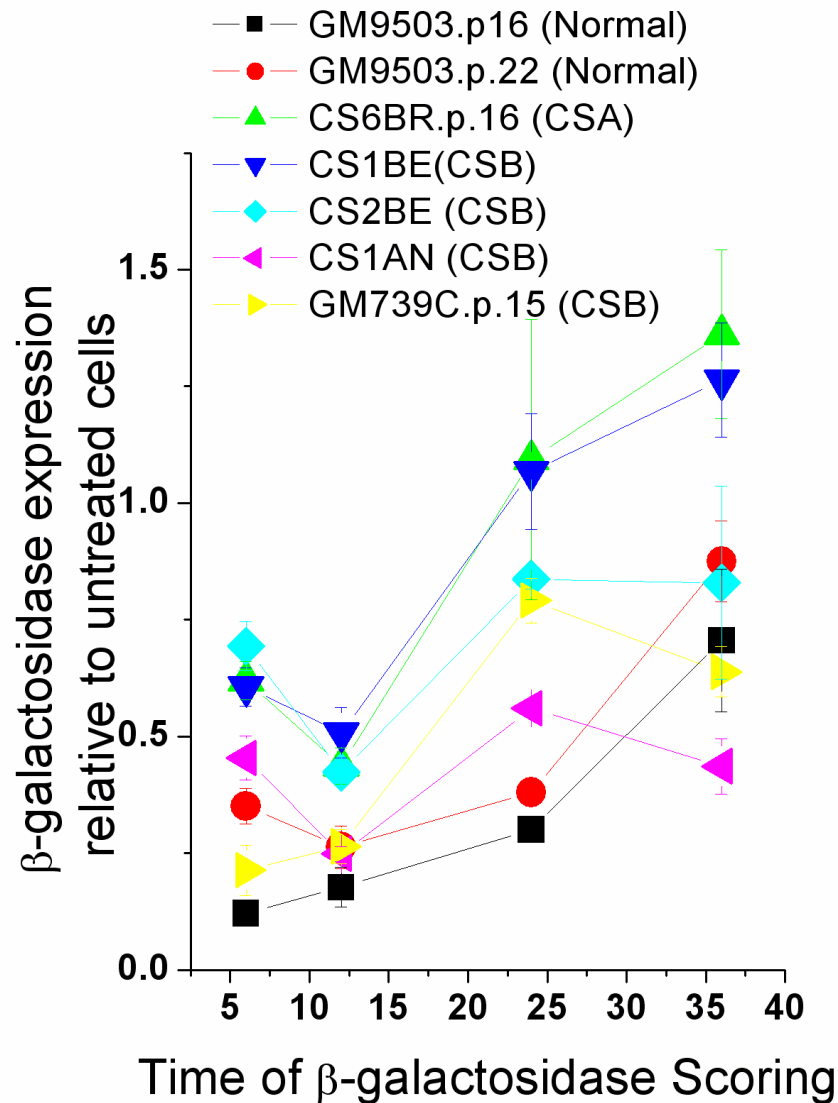


**Figure 2:** Time course for  $\beta$ -gal expression in normal and CS primary fibroblasts pre-treated with MB+VL. Cells were incubated in media containing 40mg/ml MB for 3 hours prior to 10 min VL exposure followed by immediate infection with undamaged Ad5HCMVSp1LacZ (MOI 250). B-gal expression was scored 6, 12, 24 and 44 hours post-infection. Each point on the above graph is the average ( $\pm$  SE) from a single experiment done in triplicate determinations.

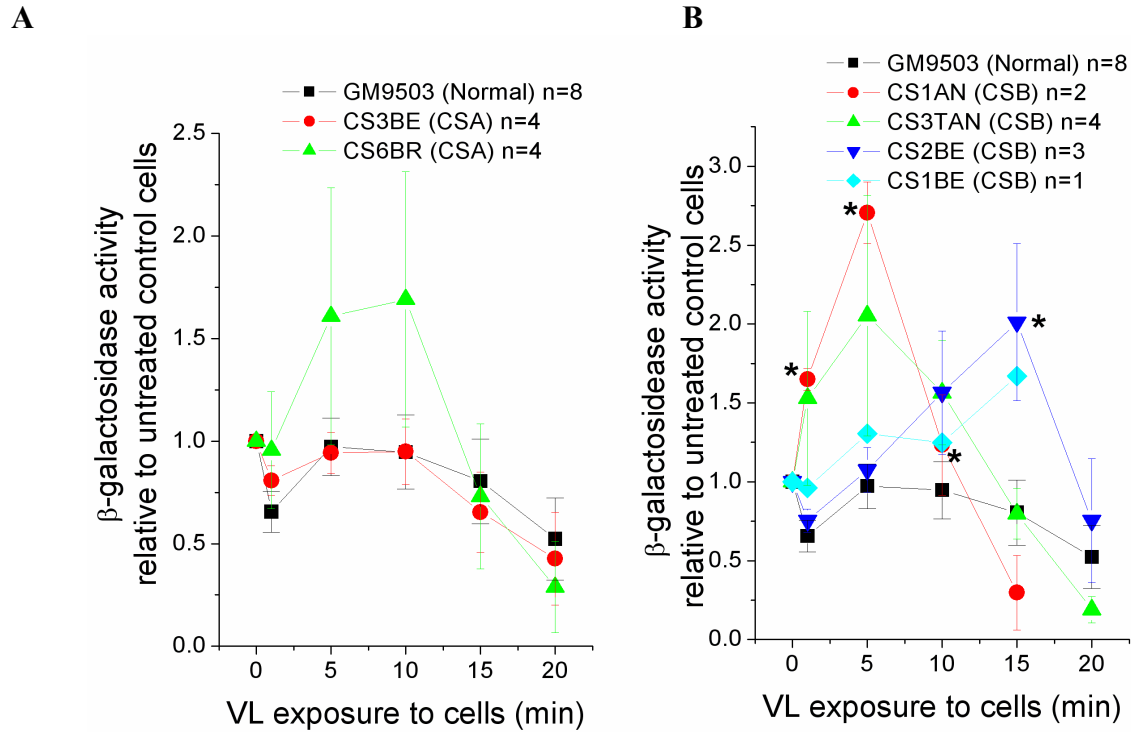


**Figure 3:** Enhanced expression of the undamaged reporter in normal and CS primary fibroblasts following pre-treatment with MB+VL. Cells were incubated in media containing 40 $\mu$ g/ml MB for 3 hours prior to VL exposure followed by immediate infection with undamaged Ad5HCMVSp1LacZ (MOI 250).  $\beta$ -gal expression was scored 24 hours after infection. Expression from undamaged Ad5HCMVSp1LacZ for CSA (A) and CSB (B) primary fibroblasts is shown compared to the normal primary fibroblast GM9503. Each point on the above curve is the average ( $\pm$  SE) of multiple experiments each carried out with triplicate determinations. Asterisks indicate points significantly different from GM9503 for a given VL exposure time (two sample independent t-test,  $p < 0.05$ ).

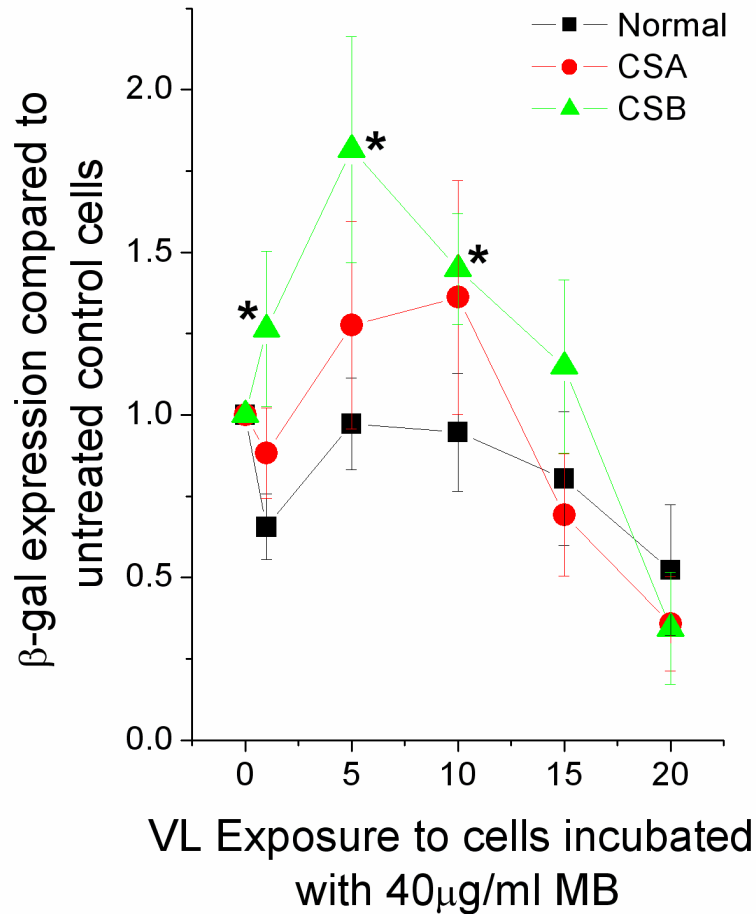


**Figure 4:** Enhanced expression of the undamaged reporter in CSA and CSB primary fibroblasts pre-treated with MB+VL. CS fibroblasts were grouped into CSA and CSB and expression of the undamaged reporter was compared to the normal primary fibroblast GM9503. Each point on the above graph is the average ( $\pm$  SE)  $\beta$ -gal expression compared to the undamaged control cells for all CSA and CSB fibroblasts (grouped accordingly) from each experiment. The same data used to construct the averaged graph shown in Figure 3 for individual cells was used to construct this curve. Asterisks indicate points significantly different from GM9503 for a given VL exposure time (two sample independent t-test,  $p < 0.05$ ).

**Table 1:** Summary of mutations, clinical symptoms and cellular characteristics of normal, CSA and CSB primary fibroblasts. For each cell line the mutation characterized at each allele is indicated, information regarding neurological and retinal abnormalities is given for those cell lines for which the information is available and the response of each cell line to in the HCR, colony survival (UVC only) and enhanced expression assay following UVC and MB+VL treatment. References are contained in the table as lowercase superscript letters and identified below the table (on the next page).

Cell Strain Information			Clinical Features		UVC Damage			MB+VL Damage	
Cell Strain	Age <sup>a</sup>	Mutation	Neurological Abnormalities	Retinal/Ocular Abnormalities	HCR	Survival	Enhanced Expression	HCR	Enhanced Expression
<b>Normal</b>									
GM9503	10	-	N	N	-	-	-	-	-
GM38A	9	-	N	N	-	-	-	-	-
GM969C	2	-	N	N	-	-	-	-	-
<b>CSA</b>									
CS3BE	13	37G>T (E13X) <sup>b</sup> 479C>T (A160V) <sup>b</sup>	Y <sup>i</sup>	Y <sup>i</sup>	D <sup>o</sup>	D <sup>p</sup>	I <sup>q</sup>	D <sup>s</sup>	I <sup>s</sup>
GM02965	25	Y322Stop <sup>c</sup> Y322Stop <sup>c</sup>	Mild <sup>j</sup>	N <sup>j</sup>	D <sup>o,r</sup>	-	I <sup>s</sup>	Normal <sup>o</sup>	Normal <sup>s</sup>
AG07076	11	37G>T(E13X) <sup>d</sup> 649G>C (A205P) <sup>d</sup>	Y <sup>d</sup>	Y <sup>d</sup>	-	-	I <sup>q</sup>	D <sup>s</sup>	I <sup>s</sup>
CS6BR	5	del 93aa (282-374) <sup>e</sup> del 27aa (348-374) <sup>e</sup>	Y <sup>k</sup>	Y <sup>k</sup>	-	-	I <sup>s</sup>	D <sup>s</sup>	I <sup>s</sup>
<b>CSB</b>									
CS1AN	3	K377amber <sup>f</sup> 858stop <sup>f</sup>	Y <sup>l</sup>	Y <sup>l</sup>	D <sup>o,r</sup>	D <sup>p,t</sup>	I <sup>q</sup>	D <sup>s</sup>	I <sup>s</sup>
CS1BE	10	R670W <sup>g</sup> -A3615 (Frameshift 1179- 1200stop) <sup>g</sup>	Y <sup>i</sup>	Y <sup>i</sup>	D <sup>o,r</sup>	D <sup>p</sup>	I <sup>q</sup>	D <sup>s</sup>	I <sup>s</sup>
CS7SE	8	- -	-	-	D <sup>s</sup>	D <sup>p,t,u</sup>	I <sup>q</sup>	D <sup>s</sup>	I <sup>s</sup>
CS2BE	21	-A3615 (Frameshift 1179- 1200stop) <sup>g</sup> deletion aa 665-723 <sup>g</sup>	Delayed <sup>i,m</sup>	Y <sup>i,m</sup>	D <sup>r</sup>	D <sup>p,u</sup>	I <sup>s</sup>	Normal <sup>s</sup>	Normal <sup>s</sup>
CS3TAN	2	(Trp851Arg) (W851R) <sup>g</sup> (Trp851Arg) (W851R) <sup>g</sup>	Y <sup>n</sup>	N <sup>n</sup>	-	-	I <sup>s</sup>	Normal <sup>s</sup>	Normal <sup>s</sup>
GM10903	9	R735opal <sup>h</sup> Gly917Silent <sup>h</sup>	Y <sup>h</sup>	Y <sup>h</sup>	-	-	I <sup>s</sup>	D <sup>s</sup>	I <sup>s</sup>

Y=yes; N=no; D-,Decreased; I – Increased; <sup>a</sup>indicates age at biopsy; <sup>b</sup>Ridley et al 2005; <sup>c</sup>McDaniel et al. 1997; <sup>d</sup>Cao et al. 2004; <sup>e</sup>Henning et al. 1995; <sup>f</sup>Troelstra et al. 1992; <sup>g</sup>Mallery et al. 1998; <sup>h</sup>Colella et al. 2000; <sup>i</sup>Brumback et al. 1978; <sup>j</sup>Kennedy et al. 1980; <sup>k</sup>Stefanini et al. 1996; <sup>l</sup>Scmickel et al. 1977; <sup>m</sup>Windmiller et al. 1963; <sup>n</sup>Lehmann et al. 1993; <sup>o</sup>Francis and Rainbow 1999; <sup>p</sup>Andrews et al. 1978; <sup>q</sup>Francis and Rainbow 2000; <sup>r</sup>Day et al 1981; <sup>s</sup>This paper; <sup>t</sup>Marshall et al. 1980; <sup>u</sup>Wade 1979;

## **Appendix III**

### **Examination of CSB deficient fibroblasts for complementation of UVC sensitivity after expression of recombinant wild type CSB**

## **Preface**

The work presented in this Appendix is an extension of Chapter 6 which demonstrated that TRF2 overexpression has an effect on NER of UVC induced DNA damage in the viral *lacZ* gene, that this effect requires CSB and that the two proteins interact. The data presented here were generated from experiments done to support the collaborative work between the laboratories of Dr. A.J. Rainbow and Dr. X-D Zhu (discussed in the preface to Chapter 6). These data demonstrate that the recombinant wild type CSB expressed in CSB mutant cell lines was functional so that conclusions could be made using data obtained through other experimental procedures such as FISH. The cell lines used in the experiments generating Figures 2 and 3 were generated in Dr. X-D Zhu's lab by Nicole Batenberg and the experiments and resulting figures were done by me. Figure 1 was constructed by me using data obtained by me.

To investigate the hypothesis that CSB plays a coordinated role at telomeres we began by performing reciprocal coimmunoprecipitation (coIP) experiments using anti-CSB and anti-TRF2 antibodies (Chapter 6; Figure 4). Reciprocal co-IP experiments demonstrated an interaction between CSB and TRF2 in HeLa cells, while experiments in SV40 transformed cells demonstrated a loss of TRF2 co-IP in both CSA and CSB mutant cells (Figure 1). Following the observation that CSB interacts with TRF2, a component of the telomere shelterin complex, we examined telomeres in CSA (CS3BE) and CSB (CS7SE) mutant primary fibroblasts by fluorescence *in situ* hybridization (FISH) (Chapter 6; Figures 5 and 6). These initial experiments suggested that CS mutant fibroblasts had a higher than normal number of dysfunctional telomeres (telomere loss and telomere doublets). The results of these initial experiments led to the collaborative project discussed in chapter 6.

To examine the function of the recombinant wild type CSB used to complement GM10905 and GM16095 (the same cell line designated CSB-SV40 in chapter 2), HCR of the UVC treated reporter was examined in GM10905 (Figure 2); and HCR and clonogenic survival of the SV40 transformed cells exposed to UVC-irradiation was examined (Figure 3A and 3B, respectively). It is characteristic of cells derived from CS individuals to demonstrate increased cell death in response to UV-irradiation in comparison to cells derived from normal individuals (Schmickel et al. 1977; Andrews et al. 1978). The CSB deficient SV40 transformed fibroblasts GM16095 expressing WT CSB, CSB with a mutation (R666C) or the vector alone (pLPC) (cells expressing these constructs were generated by Dr. Zhu's lab) were examined. Expression of WT CSB and the R666C mutant in GM16095 SV40 transformed fibroblasts led to a significant increase in clonogenic survival (as measured by differences in relative  $D_{10}$  values) compared to cells with the pLPC vector alone (Figure 3B). The R666C mutant performs as well as wild type

CSB for HCR complementation and better for clonogenic survival. The R666C mutation is within the CSB ATPase domain, which is required for WT recovery of RNA synthesis and survival following UVC exposure (Selzer et al. 2002). These results suggest that the mutation is silent. These experiments confirmed that the recombinant CSB used to complement GM10905 and GM16095 was functional.



**Figure 1:** Coimmunoprecipitation (coIP) of CSB and TRF2. CoIP in normal, CSA and CSB deficient SV40 transformed fibroblasts using the Bethyl CSB antibody. Anti-IgG was used as a negative control. See Chapter 6 for the CoIP protocol. Following IP with the anti-CSB antibody, samples were separated on an 8% polyacrylamide gel by SDS-PAGE and transferred to a membrane where they were detected using an anti-TRF2 antibody. I=input, s=supernatant, IP=immunoprecipitation. These data suggest the interaction between CSB and TRF2 requires the presence of CSA.

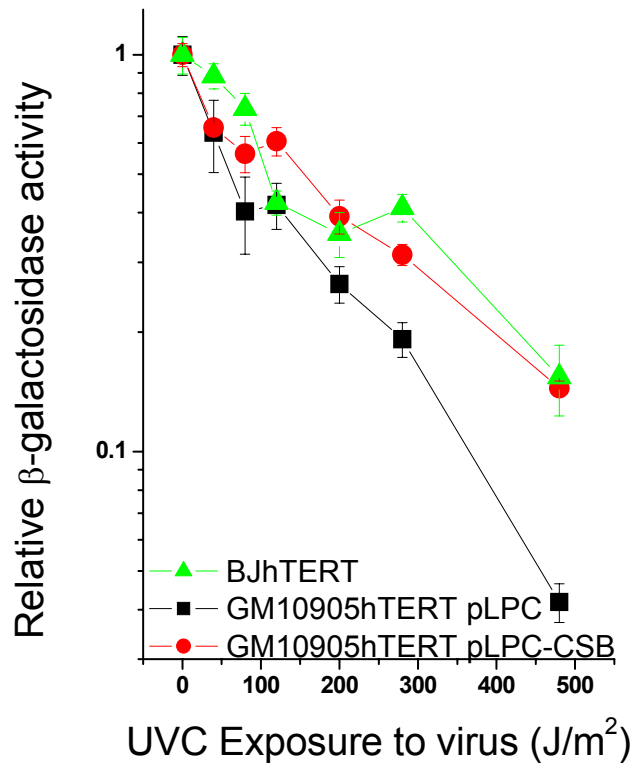


**Figure 2:** Expression of wild type CSB rescues the UV-repair defect in CSB deficient fibroblasts. capacity of hTERT immortalized GM10905 cells expressing WT CSB and vector control to reactivate expression of the UV-irradiated adenovirus reporter gene. Cells were infected with the UV-treated Ad5HCMVSp1*lacZ* reporter construct (MOI 100) and the ability to repair the UV-induced damage was examined 24 hours post-infection. Each data point on the above curve is the mean  $\pm$  S.E. of triplicate determinations from a single independent experiment. The level of reactivation in CSB complemented cells was similar to that seen in the repair proficient normal BJhTERT cells, both of which demonstrated an increase compared to cells with the vector alone.

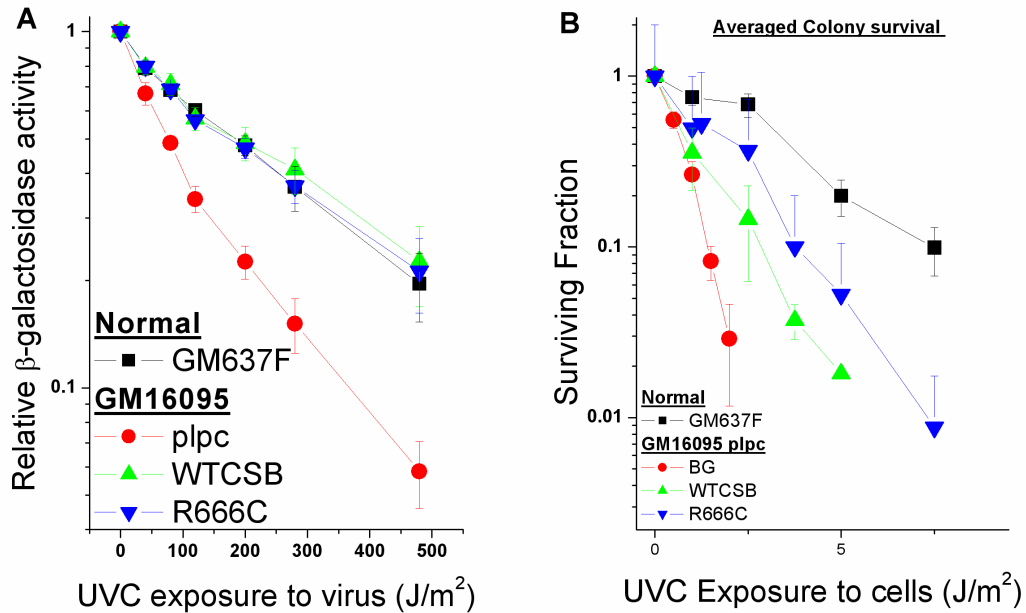


**Figure 3:** Complementation of the SV40 transformed GM16095 fibroblasts with WT and mutant CSB. A) Complementation of the UVC HCR defect in CSB mutant GM16095 fibroblasts by expression of WT CSB and CSB R666C. Each point on the above graph is the arithmetic mean ( $\pm$ SE) of 3 independent experiments. HCR of UVC treated Ad5HCMVSp1lacZ virus. A significant increase in HCR capacity as measured by absolute  $D_{37}$  was observed for GM637F, GM16095-WTCSB and GM16095-R666C compared to GM16095-plpc by two sample independent t-test ( $p < 0.05$ ). B) Clonogenic survival of GM16095 CSB deficient fibroblasts with WTCSB and mutant R666C. The repair proficient normal SV40 transformed fibroblast GM637F was used as a positive control. Each point on the above curve is the arithmetic mean average ( $\pm$ SE) surviving fraction at each dose of at least two experiments. Clonogenic survival was significantly measured by relative  $D_{10}$  values ( $n=4$ ) increased for GM637F, GM16095-WTCSB and GM16095-R666C compared to GM16095-plpc by one sample two tailed t-test ( $p < 0.05$ ).

## **Appendix IV**

**Examination of the response of primary fibroblasts from patients with Cockayne syndrome to oxidative damage and metal exposure.**

## **Introduction: Part I**

### ***Appendix IV Part I: HCR of the MB+VL treated reporter gene in primary fibroblasts from CS patients.***

In chapter 2 we show that expression from the MB+VL treated adenovirus (AdCA35) encoded  $\beta$ -gal reporter gene is reactivated to a maximum 12 hours after infection in the SV40 transformed normal skin fibroblast GM637F and that expression from the damaged reporter was significantly reduced in the CS-deficient CSA-SV40 (CS3BE.S3.G1) and CSB-SV40 (CS1AN.S3.G2) lines over the time course examined (Leach and Rainbow 2011). The SV40 large-T antigen (LT) binds and inactivates the function of p53 and pRb (Cheng et al. 2009) and we have shown that pRb status has an effect on  $\beta$ -gal expression from the viral reporter in the presence of DNA damage (Francis and Rainbow 2003). We have examined HCR of the MB+VL treated adenovirus reporter in primary human fibroblasts from a number of CS patients with varying degrees of disease severity in an attempt determine if a relationship exists between repair of oxidative DNA damage and the severity of the CS phenotype.

## **Results and Discussion**

The HCR time course was examined in the non-transformed normal primary skin fibroblasts GM9503, as well as the CS primary fibroblasts CS3BE (GM1856C/CSA) and CS1AN (GM739C/CSB), the non-transformed counterparts of CSA-SV40 and CSB-SV40 (respectively), to determine if primary and transformed fibroblasts behave similarly. Figure 1 shows pooled HCR curves and the gene reactivation time course for the MB+VL treated AdCA35 in GM9503, CS3BE and CS1AN. The data show a consistent reduction in gene reactivation in CS1AN compared to GM9503, while CS3BE showed decreased gene reactivation

between 3,12 and 24 hours but similar levels at 6 and 44 hours. Overall, these data show that the time course for gene reactivation in normal primary fibroblasts reaches a maximum by 12-24 hours similar to that in their SV40-transformed counterparts. Although there is an observable reduction in HCR in the primary CS skin fibroblasts CS3BE and CS1AN, no significant differences were observed compared to GM9503.

The ability of RNA polII to transcribe through 8-oxoG is controversial and it has been shown that a number of factors including CSB can stimulate bypass of the lesion by RNA polII (Charlet-Berguerand et al. 2006). In addition, transcription through 8-oxoG in normal and repair deficient mouse embryonic fibroblasts (MEFs) is dependent on promoter strength and the sequence context of the lesion (Pastoriza-Gallego et al. 2007). We hypothesized that the non-significant decrease in HCR observed in the primary CS fibroblasts resulted from the availability of WT p53 and pRb in primary and an increase in the ability to repair/bypass 8-oxoG lesions in primary fibroblasts. In an attempt to lessen the potential effect of transcriptional bypass through MB+VL induced 8-oxoG lesions in the adenovirus encoded  $\beta$ -gal reporter gene, we used the AdCA17 construct with the weaker HCMV IE promoter to examine HCR in various CS primary fibroblasts.

Based on the HCR time course for AdCA35 in primary fibroblasts (Figure 1C), we chose to examine HCR of MB+VL treated AdCA17 12 hours after infection in GM9503, CS3BE and CS1AN (Figure 2). We were able to detect a significant reduction in HCR at a number of MB+VL doses to AdCA17 in both CS3BE and CS1AN compared to GM9503. Bypass of 8-oxoG lesions by RNA polII is effected by promoter strength and is more efficient in the presence of a stronger promoter (Pastoriza-Gallego et al. 2007) The significant reduction seen using AdCA17 compared to the non-significant reduction from AdCA35 suggests the strength of the

CMV IE enhancer may be important when examining repair of MB+VL induced 8-oxoG in primary CS fibroblasts. The weaker HCMV promoter of AdCA17 may result in more RNA polII blocking/stalling compared to the MCMV promoter of AdCA35 that drives higher levels of  $\beta$ -gal expression (Addison et al. 1997).

We then examined HCR of the MB+VL treated reporter in a number of normal, CSA and CSB primary skin fibroblasts. While use of AdCA17 and scoring at 12 hours revealed a greater difference in HCR at 12hrs for CS1AN and CS3BE this was not the case for other CS lines. For a number of CS cell lines we were unable to detect a difference under those conditions (data not shown). As the CS cells being examined in this study were already shown to accumulate increased levels of 8-oxoG following IR exposure (Tuo et al. 2003), consistent with defective BER, we examined each cell line using different virus and  $\beta$ -gal scoring times. CS patients show high variability in the phenotypic presentation of the disorder (Nance and Berry 1992; Natale 2011) as well as varying degrees of 8-oxoG repair (Tuo et al. 2003) which may be caused by differences in genetic background. These differences in genetic background in the CS fibroblasts studied may have an effect on the general transcription deficit observed in CS cells (Balajee et al. 1997) as well as lesion bypass (Charlet-Berguerand et al. 2006) and OGG1 levels (Dianov et al. 1999) which may impact HCR of the MB+VL treated reporter gene. We examined HCR of the MB+VL treated reporter in AdCA17 and AdCA35 in a number of CS fibroblasts. If we were able to detect a difference in HCR capacity compared to normal repair proficient fibroblasts the conditions best demonstrating that difference are shown. Figure 3 (CSA) and 4 (CSB) show the averaged HCR curves for CSA and CSB primary fibroblasts (respectively) compared to the normal GM9503. For each CS cell type examined, the time point at which we were able to detect a difference in HCR is shown (if one was detectable). The results for HCR of the MB+VL

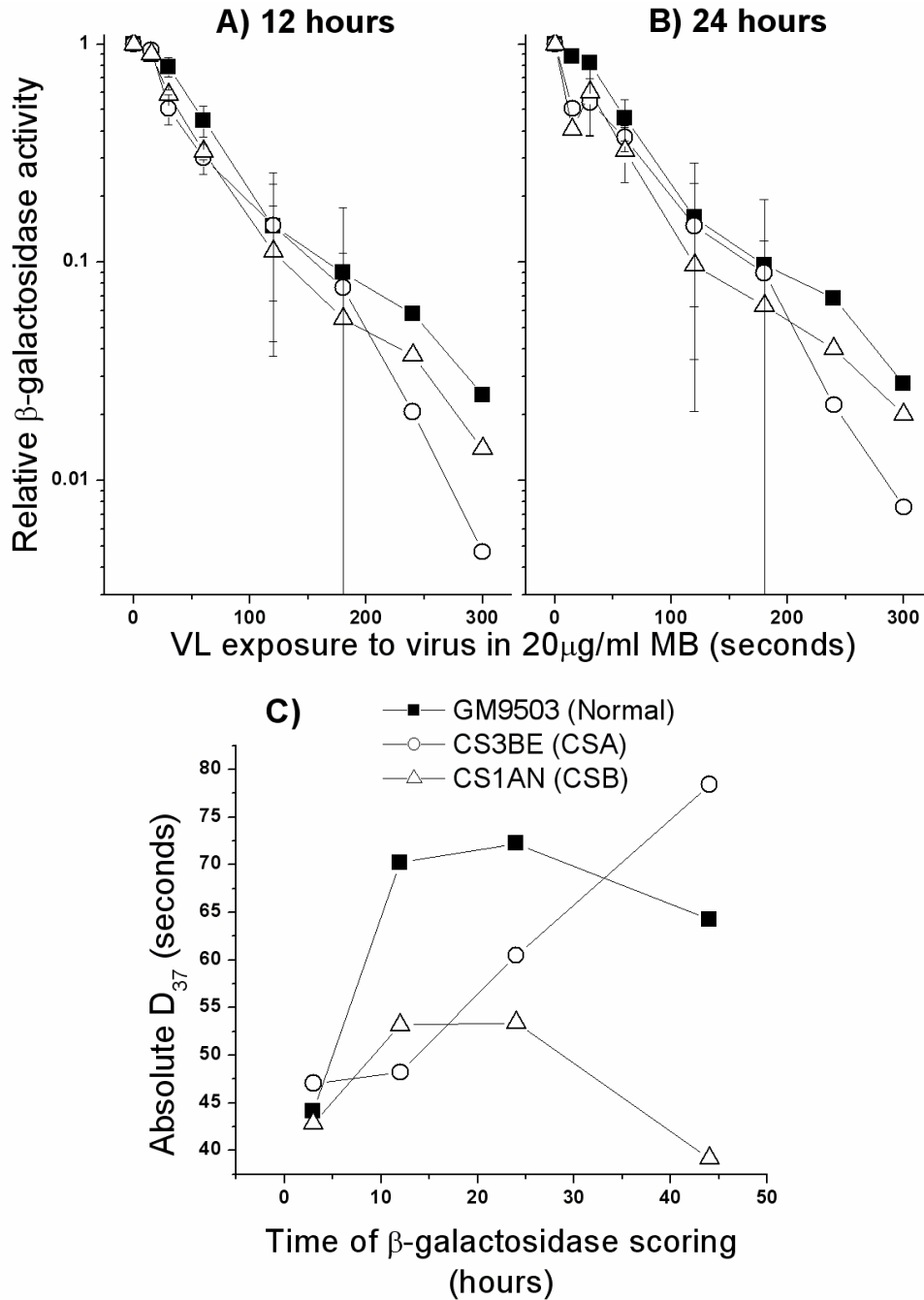
treated reporter was highly variable in CS primary fibroblasts demonstrating that use of the HCR assay alone to detect a repair deficiency in CS primary fibroblasts may yield false negative results.

Transformation of cells with the SV40 LT antigen leads to a number of changes within the cell (Agarwal et al. 1998) and is dependent on binding of SV40 LT proteins to pRb and p53 (Cheng et al. 2009). SV40 LT directly binds and inactivates pRb and two related proteins p130 and p107, whose functions are to repress transcription factors that regulate the expression of downstream factors involved in cell cycle entry and progression (Cheng et al. 2009). Binding of p53 by SV40 LT interferes with the tumor suppressors ability to function as a sequence specific transcription factor (Cheng et al. 2009). Treatment of primary fibroblasts with DNA damaging agents increases expression of the adenovirus encoded  $\beta$ -gal gene (Francis and Rainbow 2000; Francis and Rainbow 2003; Zacal et al. 2005) and pre-infection of cells with a damaged luciferase expressing adenovirus also results in upregulation of the reporter gene (Francis and Rainbow 2000, Appendix II). This damaged induced increase in CMV driven expression requires functional pRb (Francis and Rainbow 2003). It is possible that HCR of the MB+VL treated reporter gene is affected by enhanced expression making it difficult to draw conclusions.

In an attempt to understand the greater capacity of CS primary fibroblasts to reactivate expression of the MB+VL treated reporter relative to the normal primary control compared to SV40-transformed fibroblasts we examined the effect of expressing the human papillomavirus (HPV) E6 and E7 proteins. HPV E6 targets p53 for ubiquitin dependent degradation and E7 binds and inhibits the function of pRb. HCR of MB+VL treated AdCA17 was examined by pre-infection of cells with adenovirus constructs expressing either HPV E6 or E7, luciferase control (AdCA18) or no infection followed by infection with MB+VL treated AdCA17 24 hours later.

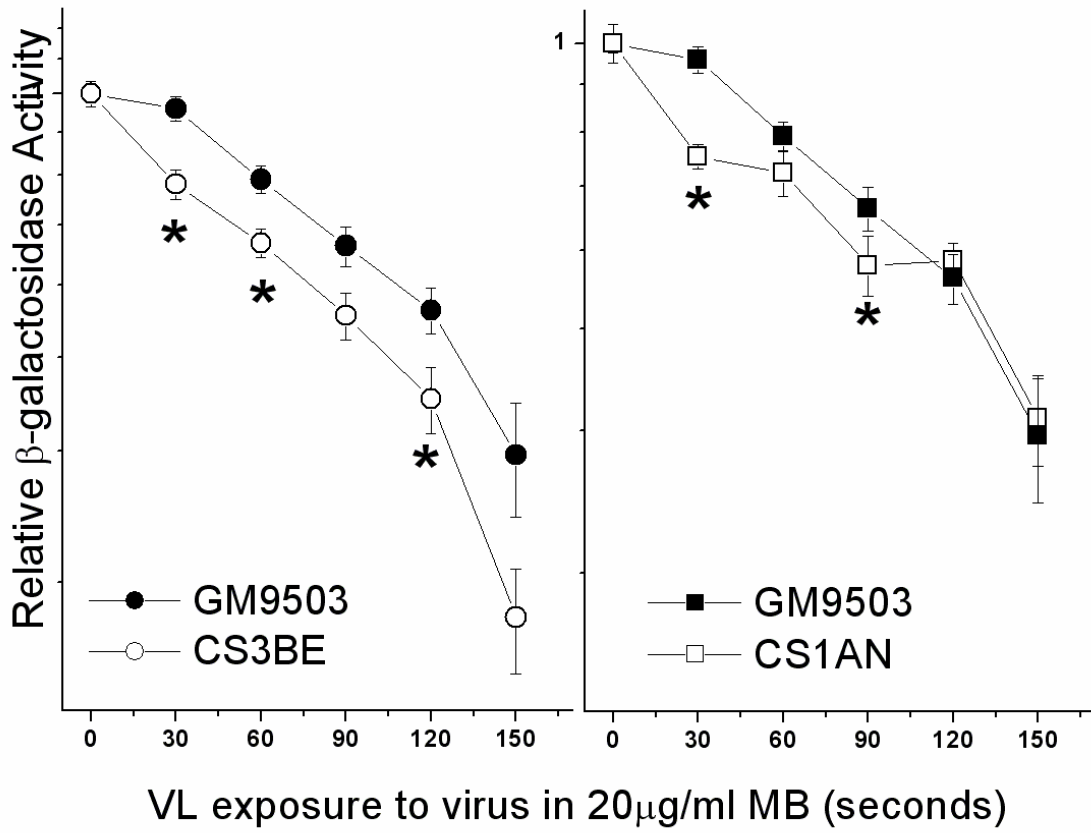
We did not observe a significant effect of any of these pre-infection conditions on HCR in the primary fibroblasts (data not shown). We also expressed the SV40 LT antigen in normal and CS primary fibroblasts by infection of cells with a retrovirus (data not shown). Using this approach we did not observe any changes in HCR in CS fibroblasts relative to normal fibroblasts. The inability to recapitulate the greater decrease in HCR from CS cells observed in SV40 transformed fibroblasts using these approaches may be due to the fact that in addition to the abrogation of p53 and pRb by SV40 LT, transformation of cells exiting crisis leads to many additional changes.

The variable results for CS primary fibroblasts demonstrated here suggest using the HCR assay to examine repair of MB+VL induced 8-oxoG compared to normal primary fibroblasts should be done with caution.



**Figure 1:** Normal and CS primary skin fibroblasts were infected with MB+VL treated AdCA35 (MOI 100) and  $\beta$ -gal was scored at 3, 12, 24 and 44 hours after infection. The HCR curves shown above for 12 hrs (A) and 24 hrs (B) are pooled curves from 3 independent experiments. Each point on the curves in A) and B) are the arithmetic mean ( $\pm$ SE) of  $\beta$ -gal expression from three independent experiments all done with triplicate determinations. HCR was decreased in CS primary fibroblasts compared to the normal fibroblast GM9503, however no significant differences were detected between any of the VL doses to the virus for CS fibroblasts compared to normal by two sample independent t-test. In addition, we were unable to detect any significant

differences between GM9503 and either CS cell type over any portion of the curve using the  $\chi^2$ -goodness of fit test. Absolute  $D_{37}$  values were extrapolated from the pooled HCR curves and used to plot the time course of gene reactivation from normal and CS fibroblasts (C). The time course for gene reactivation as measured by extrapolating the absolute  $D_{37}$  values from Figures A) and B) shows a decrease in CS1AN and a reduced rate of gene reactivation at early times in CS3BE. Overall, these data show that the time course for gene reactivation in normal primary fibroblasts reaches a maximum by 12-24 hours and that similar to their SV40-transformed counterparts, the primary skin CS fibroblasts GM1856C (CS3BE) and GM739C (CS1AN) demonstrate a reduction in the ability to reactivate reporter gene expression when compared to a normal primary skin fibroblast.



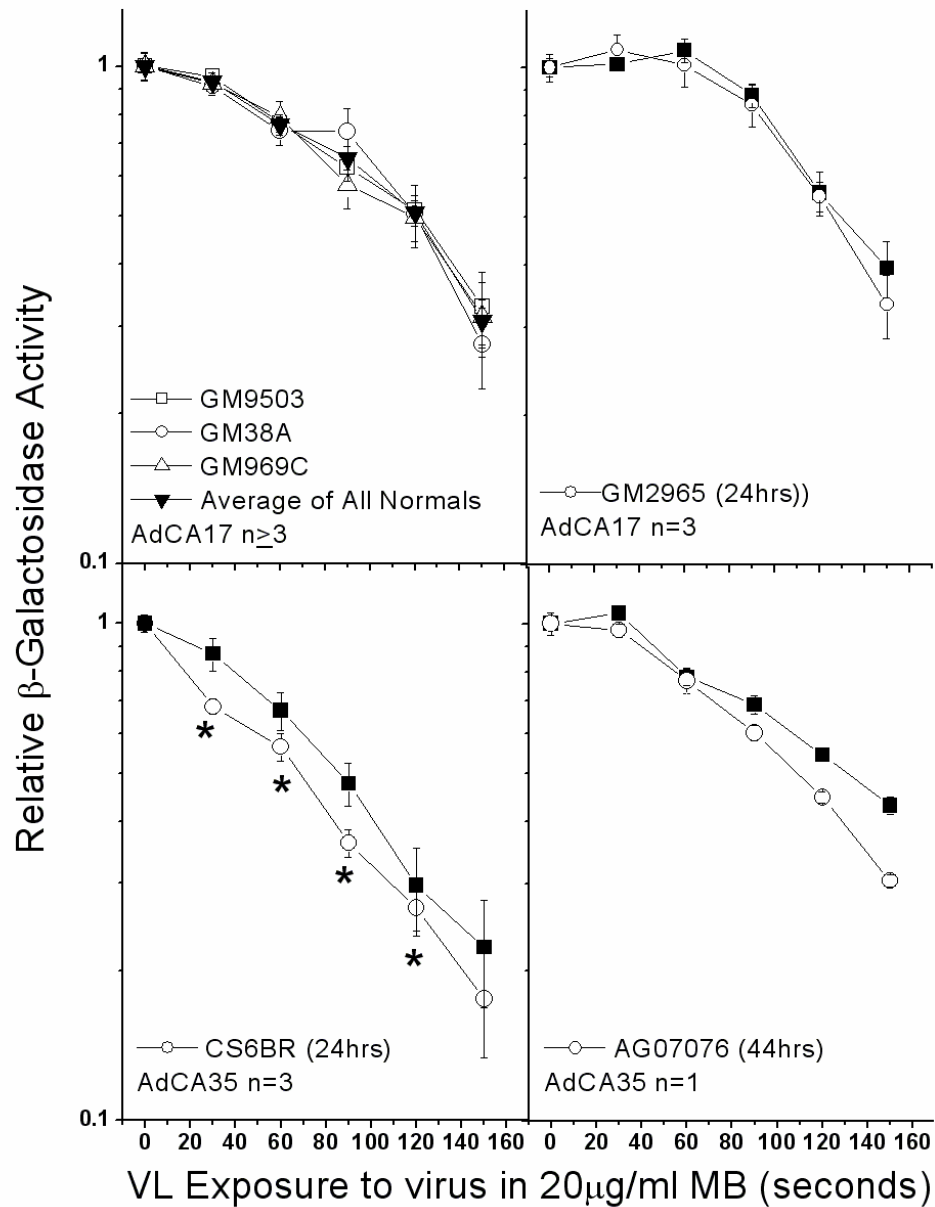


**Figure 3:** HCR of the MB+VL treated  $\beta$ -gal reporter in CSA primary fibroblasts compared to the normal primary fibroblast GM9503. The upper left panel shows the HCR survival curves for all normal primary fibroblasts examined. Cell strains, time of  $\beta$ -gal measurement and viral construct used (AdCA17 or AdCA35), number of experiments (n) are indicated within the Figure. Solid squares represent GM9503 and open circles represent CS fibroblasts. Each data point is the mean  $\beta$ -gal expression of experimental determinations from n independent experiments ( $\pm$  SE).  $\beta$ -gal expression in CS cell strains significantly different from GM9503 are indicated ( $p < 0.05$  by one sample two tailed t-test are marked with an asterisk).

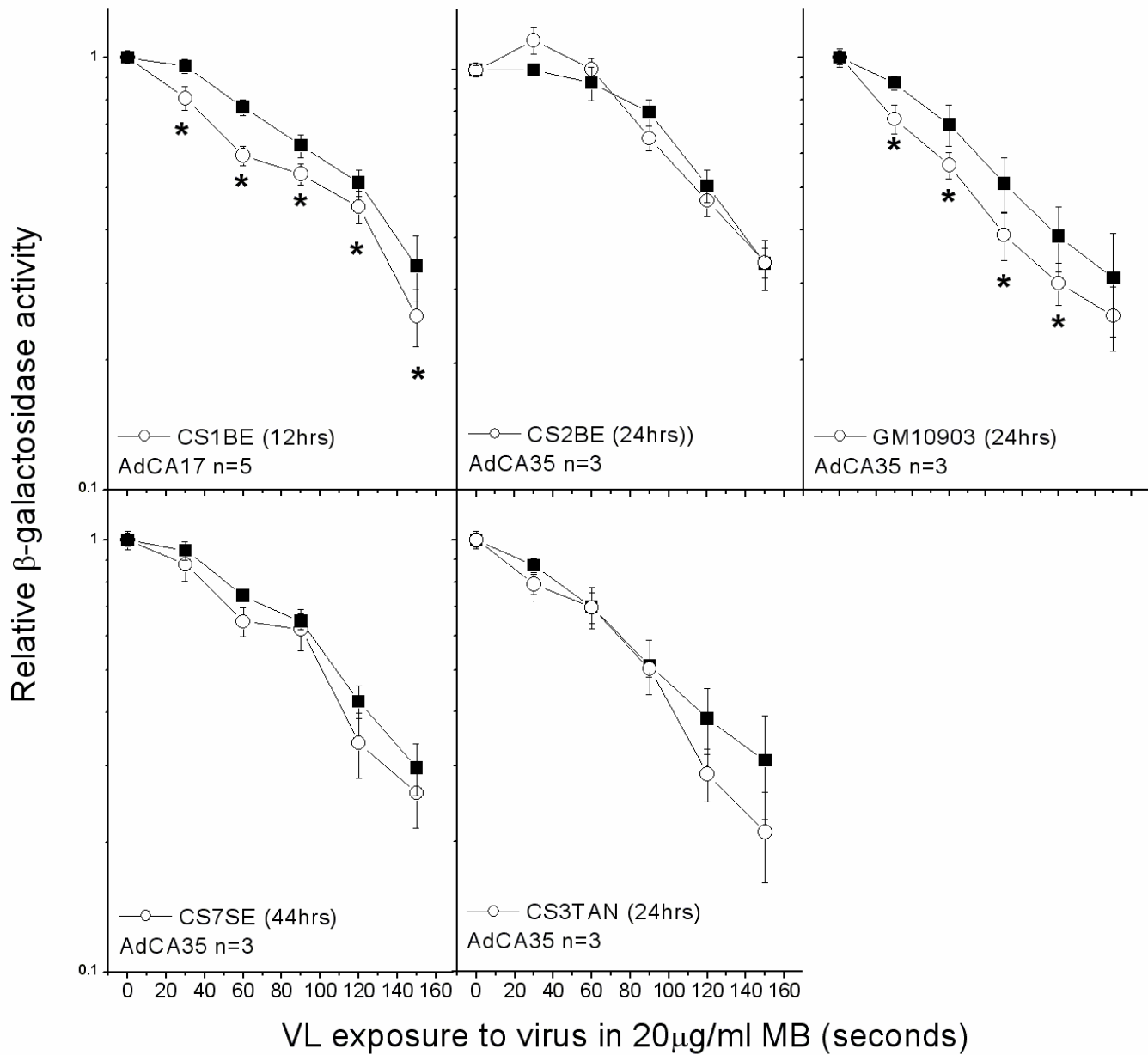


**Figure 4:** HCR of the MB+VL treated  $\beta$ -gal reporter in CSB primary fibroblasts compared to the normal primary fibroblast GM9503. The upper left panel shows the HCR survival curves for all normal primary fibroblasts examined. Cell strains, time of  $\beta$ -gal measurement and viral construct used (AdCA17 or AdCA35), number of experiments (n) are indicated within the figure. Solid squares represent GM9503 and open circles represent CS fibroblasts. Each data point is the mean  $\beta$ -gal expression of experimental determinations from n independent experiments ( $\pm$  SE).  $\beta$ -gal expression in CS cell strains significantly different from GM9503 are indicated (p < 0.05 by one sample two tailed t-test are marked with an asterisk).

## **Introduction: Part II**

### ***The effect of metals on repair of oxidative damage in primary fibroblasts from CS patients***

Heavy metals such as cadmium (Cd) and lead (Pb) can induce oxidative toxicity as well as have a negative biological effect by binding to proteins and effecting metal transport and protein function (Donna and Donma, 2005). Cd is a potent immunotoxic metal whose contamination poses a serious health threat throughout the world and has been classified as a human carcinogen by the International Agency for Research on Cancer (IARC, 1994). In human cells, Cd induces DNA strand breaks, sister chromatid exchanges and chromosomal aberrations (Stohs et al. 2001). Cd has been found to inhibit apoptosis caused by chromium exposure, a process which may play a role in Cd induced carcinogenesis (Shimada et al. 1998). Cellular exposure to Cd leads to increased oxidative stress by depletion of glutathione and protein bound sulfhydryl groups (Shimada et al. 1998; Stohs et al. 2001). Cd interferes with multiple DNA repair pathways and enhances the mutagenicity of other DNA damaging agents (Hartwig and Schwerdtle 2002) (Waisberg et al. 2003). Similar to Cd, Pb is also considered a potential human carcinogen (Donma and Metin Donma 2005). Pb can cause direct DNA damage, chromosomal disruption/breakage and inhibition of DNA synthesis and/or repair (Sibergeld et al. 2000). Pb may also generate ROS leading to oxidative DNA damage (Donma and Metin Donma 2005). Due to the chemical nature of Pb, it can substitute for zinc (Zn) in several proteins that act as transcriptional regulators and disrupt their proper functioning (Bellinger 2004).

Al is a non-redox trivalent cation with a high environmental abundance and although a definite biological function/effect of Al is not known, it has been implicated in neurodegeneration and AD and a number of studies suggest it could be involved in the formation of oxidative DNA damage. Al leads to impaired mitochondrial function as well as decreased antioxidant defense

mechanisms in cells isolated from the brain's of rats (Kumar et al. 2009). Consistent with this is the finding that aluminum chloride ( $\text{AlCl}_3$ ) led to increased oxidative damage in nDNA and mtDNA in brain tissue from mice (Rui and Yongjian 2010). Further more,  $\text{AlCl}_3$  treatment of root cells from the onion bulb *Allum cepa*, resulted in increased generation of reactive oxygen intermediates causing oxidative DNA damage and ultimately cell death (Achary et al. 2008). Based on these observations, we examined acute Al, Cd and Pb exposure on BER of the MB+VL treated reporter gene in CS fibroblasts.

## **Materials and Methods**

*Mitochondrial activity, The MTT (3-(4,5-dimethylthiazol-2yl)2,5-diphenyltetrazolium bromide) assay: Protocol*

Cells were seeded in 96 well plates at a density of  $1.2 \times 10^3$  cells/well for primary fibroblasts and  $3.5 \times 10^3$  cells/well for SV40 transformed fibroblasts. After seeding, cells were grown for 6-8hrs at  $37^\circ\text{C}$  in a humidified incubator (20%  $\text{O}_2$ , 5%  $\text{CO}_2$ ) and allowed to adhere. Following the 6-8 hour incubation period the overlaying media was aspirated and replaced with 200 $\mu\text{l}$  supplemented media ( $\alpha$ -MEM, 15% FBS for primary fibroblasts, 10% FBS for SV40 transformed fibroblasts) containing aluminum sulfate ( $\text{Al}_2(\text{SO}_4)_3$ ), cadmium chloride ( $\text{CdCl}_2$ ) or lead nitrate ( $\text{Pb}(\text{CH}_3\text{COO})_4$ ) at increasing concentrations. Media containing no metal was used as a control. The cells were then incubated at  $37^\circ\text{C}$  in a humidified incubator (20%  $\text{O}_2$ , 5%  $\text{CO}_2$ ) for a period of 10-14 days for primary fibroblasts or 5-7 days for SV40 transformed fibroblasts or until the untreated control cells were confluent. At this point 20 $\mu\text{l}$  of 5mg/ml 3-(4,5-dimethylthiazol-2yl)2,5-diphenyltetrazolium bromide (MTT) was added to each well of the 96 well plate and incubated for 4hrs or until black crystals (water insoluble formazan) had clearly

formed in the wells. Following the formation of the insoluble crystals the media was aspirated from each well with care taken not to disturb the crystals. MTT is converted to insoluble formazan by mitochondrial reductase which means the amount of crystals formed represents mitochondrial activity. Following the removal of media the formazan crystals were solubilized by the addition of 100µl of DMSO and incubation at 37°C for 10 min followed by measurement of the optical absorbance of the resulting solution at 570nm.

## **Results and discussion**

*Metabolic activity of Normal and CS fibroblasts in the presence of aluminum, cadmium and lead; the MTT assay.*

We examined the effect of aluminum sulfate ( $\text{Al}_2(\text{SO}_4)_3$ ), cadmium chloride ( $\text{CdCl}_2$ ) and lead nitrate ( $\text{Pb}(\text{CH}_3\text{COO})_4$ ) on cell metabolic activity/viability by measuring mitochondrial activity using the MTT assay; a readout for cell viability (Figure 5). The effect of Al, Cd and Pb on viability was examined in primary fibroblasts from normal (GM9503, GM38A) and CS (CS3BE (CSA), CS1AN (CSB)) in Figure 5. Compared to normal fibroblasts CS deficient fibroblasts demonstrated increased viability in the presence of increasing concentrations of  $\text{Al}_2(\text{SO}_4)_3$  (top left panel). For  $\text{CdCl}_2$  exposure CS fibroblasts, particularly CSA deficient fibroblasts demonstrated increased sensitivity. Finally, for lead exposure of CS primary fibroblasts showed an apparent increase in resistance to the toxic effects of exposure to  $\text{Pb}(\text{CH}_3\text{COO})_4$ .

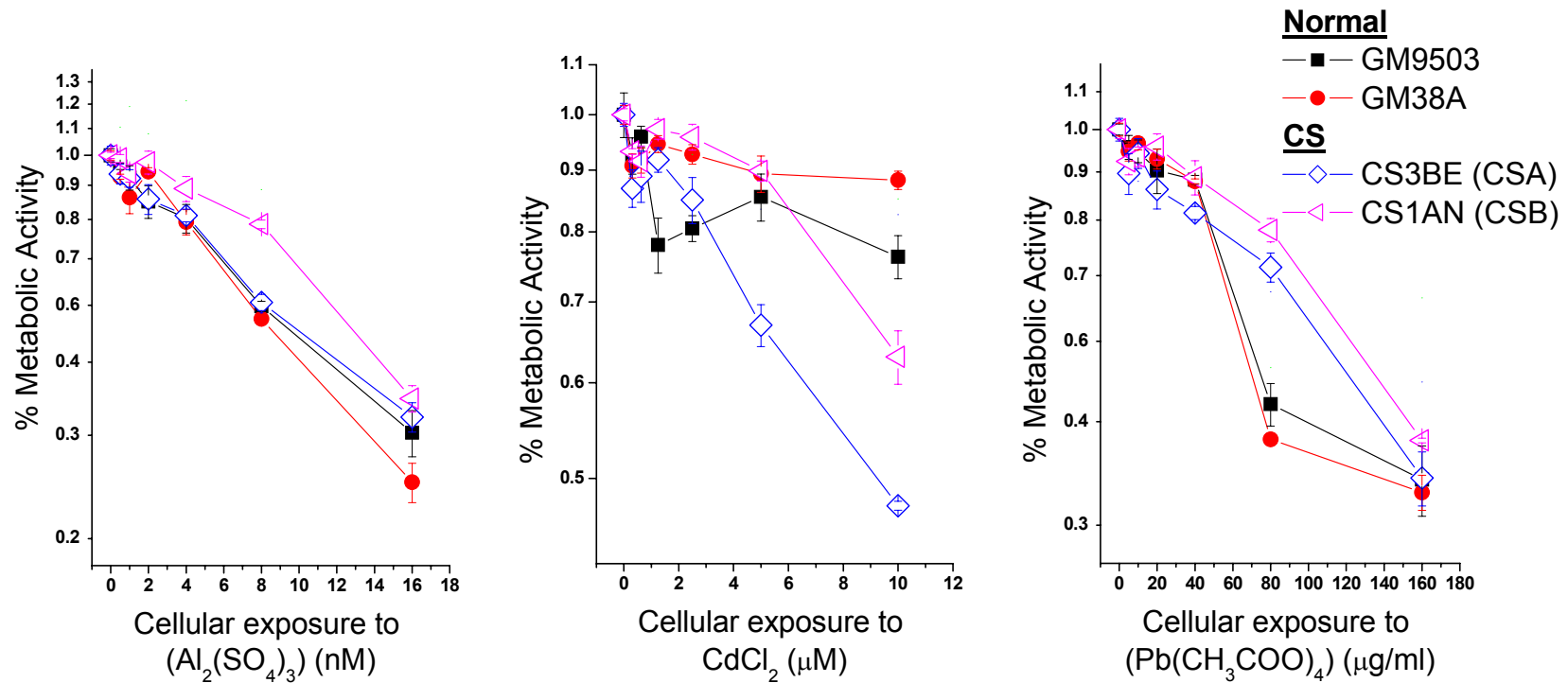


**Figure 5:** The effect of  $\text{Al}_2(\text{SO}_4)_3$  (left),  $\text{CdCl}_2$  (middle) and  $\text{Pb}(\text{CH}_3\text{COO})_4$  (left) on metabolic activity/cell viability in normal and CS deficient fibroblasts. The top row shows the effect of each metal on primary fibroblast strains from normal and CS individuals. The figure legend is contained within the leftmost plot. Each plot above is the result of a single experiment done in triplicate determinations ( $\pm$ SE).

*HCR of the MB+VL treated reporter in the presence of Al, Cd and Pb.*

The toxicity of each metal determined by the MTT assay allowed us to determine the appropriate doses of Al, Cd, and Pb to examine the effect of the presence of each of these metals on HCR of the MB+VL treated adenovirus reporter. The criteria used to determine the dose of each metal was i) a dose that demonstrated a difference in survival between normal and CS cells and ii) that the dose was not toxic to the point that it would result in a significant amount of cell death upon treatment of cells following infection with the damaged reporter. Based on these criteria HCR of the MB+VL treated reporter was examined in the presence of 4mM  $\text{Al}_2(\text{SO}_4)_3$ , 10 $\mu\text{M}$   $\text{CdCl}_2$ , and 50 $\mu\text{g/ml}$   $\text{Pb}(\text{CH}_3\text{COO})_4$ . In addition, we tested the effect of Al treatment at two additional doses, 8mM and 16mM and found no significant difference between the two higher doses and the 4mM treatment (data not shown). Figure 6 shows the effect of Al, Cd and Pb on HCR in primary fibroblasts from normal (GM9503), and CS (CS3BE/GM1856C and CS1AN/GM739C) individuals. The  $D_{37}$  values from the HCR curves in Figure 6 are shown in table 3. HCR capacity caused by the presence of 4mM  $\text{Al}_2(\text{SO}_4)_3$  in the CS fibroblasts CS3BE and CS1AN was reduced by 23% and 40% respectively. At high MB+VL doses (210s), treatment with 10 $\mu\text{M}$   $\text{CdCl}_2$  appears to result in a small reduction in HCR capacity in both CS3BE and CS1AN.

The observed reduction in HCR capacity observed for the CSA fibroblast CS3BE led us to further examine HCR in CS fibroblasts in the presence of 4mM Al (Table 2 summarizes the results). We were unable to detect a significant effect of Al on HCR capacity in CS fibroblasts, suggesting it does not play a role in repair of 8-oxoG lesions. It appears as though lead and cadmium may have an effect at higher doses, therefore further experiments examining these doses in a greater number of CS strains should be examined.

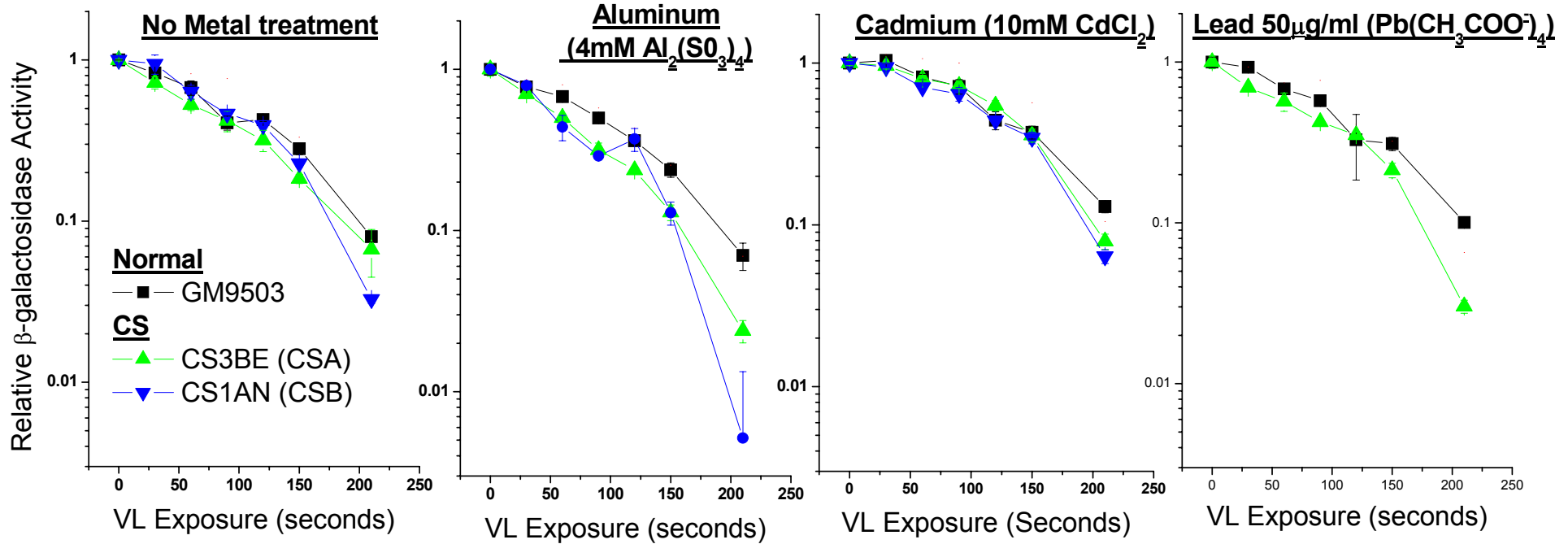


**Figure 6:** The effect of aluminum, cadmium and lead on HCR of the MB+VL treated AdCA35 reporter gene. The above metal treatments were done in parallel in the same experiment. Cells were infected with the MB+VL treated AdCA35 reporter gene at an MOI of 40. Following the 90 min viral absorption period the infection media was aspirated and replaced with 200 $\mu$ l of warmed supplemented media ( $\alpha$ -MEM, 15% FBS) containing the indicated concentration of each metal.  $\beta$ -gal scoring was carried out 24 hours following addition of the media containing the metals. Each point on the above plots is the result of a single experiment done in triplicate determinations ( $\pm$ SE).

**Table 1:** The effect of 4mM  $\text{Al}_2(\text{SO}_3)_4$  on HCR of the MB+VL treated reporter in normal and CS primary fibroblast strains. The  $D_{37}$  values were obtained from the HCR curves shown in Figure 2, which are the results of a single experiment. The top portion of the table shows the absolute  $D_{37}$  values under all 4 conditions (no treatment control, 4mM  $\text{Al}_2(\text{SO}_3)_4$ , 10mM  $\text{CdCl}_2$  and 50mg/ml  $\text{Pb}(\text{CH}_3\text{COO})_4$ ). The middle portion of the table shows the  $D_{37}$  values for each cell line relative to GM9503 under each treatment condition. The bottom portion of the table compared the  $D_{37}$  values for each metal treatment within each cell line compared to the no treatment control.

		<b>Absolute <math>D_{37}</math></b>			
<b>Cell Line</b>	<b>Group</b>	<b>No Treatment</b>	<b>4mM Aluminum</b>	<b>10mM Cadmium</b>	<b>50mg/ml lead</b>
<b>GM9503</b>	Normal	130.3	117.7	150.6	113.5
<b>GM1856C</b>	CSA	103.5	79.68	147.6	111.6
<b>GM739C</b>	CSb	123.2	74.26	141.5	-
		<b><math>D_{37}</math> Relative to GM9503</b>			
<b>Cell Line</b>	<b>Group</b>				
<b>GM9503</b>	Normal	1.00	1.00	1.00	1.00
<b>GM1856C</b>	CSA	0.79	0.68	0.98	0.98
<b>GM739C</b>	CSB	0.95	0.63	0.94	-
		<b><math>D_{37}</math> Relative to No Treatment control (within each cell line)</b>			
<b>Cell Line</b>	<b>Group</b>				
<b>GM9503</b>	Normal	1.00	0.90	1.16	0.87
<b>GM1856C</b>	CSA	1.00	0.77	1.43	1.08
<b>GM739C</b>	CSB	1.00	0.60	1.15	-

**Table 2:** The effect of 4mM Aluminum sulfate on HCR of the MB+VL treated reporter gene in normal and CS primary fibroblasts. The mean  $D_{37}$  represents the  $D_{37}$  of  $Al_2(SO_4)_3$  treated cells compared to control untreated cells. n=number of experiments. A one sample two tailed t-test was used to determine if a significant difference existed between control and HCR in the presence of Al.

Aluminum effect						
Cell Line	Group	Mean			n	p
		Rel $D_{37}$	±	SE		
<b>GM9503</b>	Normal	0.92524	±	0.028	5	0.05578
<b>GM38A</b>	Normal	1.05077	±	0.04137	2	0.43524
<b>AG07076</b>	CSA	1.15541	±	0.31004	2	0.70419
<b>CS3BE</b>	CSA	0.92934	±	0.06935	5	0.36585
<b>GM2965</b>	CSA	1.00253	±	0.03353	2	0.95202
<b>CS1AN</b>	CSB	0.93519	±	0.16684	3	0.73513
<b>CS7SE</b>	CSB	0.816076	±	-	1	-

## Discussion

The results presented here for examining the effect of Al, Pb and Cd on HCR of the MB+VL treated reporter in normal and CS deficient fibroblasts do not demonstrate a significant effect. The initial observation of a decrease in HCR capacity in the presence of 4mM Al in BER deficient CS primary fibroblasts (Figure 6; Table 1) was quite intriguing leading us to examine a number of additional CS and normal primary fibroblasts (Table 2). While we were again unable to detect a significant effect on HCR in the presence of 4mM Al when  $\beta$ -gal expression was measured at 24 hours after infection, it appears as though the presence of Al may have a negative effect on HCR capacity in both normal and CS primary fibroblasts. Al is a non-redox trivalent cation with a high environmental abundance and although a definite biological function/effect of Al is not known, it has been hypothesized to be involved in the etiology of AD. The Al hypothesis in AD development began in 1965 when it was shown that injection of Al salts into rabbit brains lead to the formation of neurofibrillary tangles (NFT), one of the neuropathological characteristics of AD (Klatzo et al. 1965), a result which was subsequently reproduced in cats (Crapper et al. 1973). Since then a large body of evidence has accumulated which supports a role for Al in the pathogenesis of AD as well as evidence supporting arguments against an Al involvement in the disease process. Some studies have demonstrated that Al may affect DNA segregation during mitosis such as the reported ability of Al to induce the formation of micronucleus (MN) *in vitro* in human lymphocytes and skin fibroblasts from normal individuals; however Al did not induce formation of MN in lymphocyte or skin fibroblasts cultures from patients with AD.(Trippi et al. 2001).

Similar to the suggestion for examining HCR of the MB+VL treated reporter in primary fibroblasts from AD patients (Appendix I), a full HCR time course should be done for each cell line as differences may not be readily detectable at 24 hours. Time course data for SV40-transformed (Chapter 2) and primary CS (Appendix IV; Figure 1) suggest the greatest differences in HCR capacity in the absence of Al or other metals is at 12 hours. As a result of this, strong conclusions regarding Al's affect should be avoided until all time points are examined. While we were unable to show a BER deficiency in primary skin fibroblasts from patients with AD (Appendix I), several lines of evidence support the conclusion that the pathway is in fact defective (Mecocci et al. 1994; Lyras et al. 1997; Gabbita et al. 1998; Lovell et al. 1999; Wang et al. 2005). The results of the data shown here together with the Al hypothesis and decreased BER in AD cells suggests examining the time course for HCR of the MB+VL treated reporter in primary skin fibroblasts from AD patients in the presence of 4mM  $Al_2(SO_3)_4$  may provide some interesting data regarding AD pathology.

The presence of Cd appears to have a stimulatory effect on HCR when compared to untreated control cells. In human cells Cd induces DNA strand breaks, sister chromatid exchanges and chromosomal aberrations (Stohs et al. 2001). Cellular exposure to Cd leads to increased oxidative stress by depletion of glutathione and protein bound sulfhydryl groups (Shimada et al. 1998; Stohs et al. 2001) and interferes with multiple DNA repair pathways and enhances the mutagenicity of other DNA damaging agents (Hartwig and Schwerdtle 2002) (Waisberg et al. 2003). While the data for HCR shown here is from a single experiment, it suggests the dose used in these experiments may be inducing BER by generating small, 'hormetic' levels of damage or stress in the cells, leading to greater b-gal reactivation. It would

be of interest to carry out further studies examining the effect of Cd on HCR as well as the associated cellular redox state and level of damage in genomic DNA.

## **Appendix V**

### **Examination of the response of fibroblasts from patients with Ataxia telangiectasia to oxidative damage and metal exposure**

## Introduction

### *Ataxia Telangiectasia (AT)*

AT is an autosomal recessive disorder characterized by progressive cerebellar ataxia with onset in early childhood. Additional symptoms of AT include oculocutaneous telangiectasia, immunodeficiency and chromosomal instability. AT patients have a predisposition to cancer, primarily lymphomas and acute lymphatic leukemia (Shiloh 1995; Lavin and Shiloh 1997). Cells from AT patients are hypersensitive to IR and radiomimetic chemicals and are defective in cell cycle checkpoints activated by DNA damage (Taylor et al. 1994). AT is caused by mutations in the *ATM* (AT-mutated) gene located on chromosome 11 at position q22-23 (Gatti et al. 1988). *ATM* encodes the large 350 kDa ATM protein which shares a region of homology with the phosphatidyl inositol-3 (PI3) kinase (Savitsky et al. 1995; Savitsky et al. 1995) which generally plays a role in DNA damage repair, recombination and cell cycle checkpoints. ATM is a protein kinase at the core of DNA damage signaling and together with the MRN complex (Mre11-Rad50-NBS1) senses double strand breaks (DSBs) (Kastan and Bartek 2004). Following activation by dsDNA breaks, ATM initiates a signaling cascade, including autophosphorylation and phosphorylation of the checkpoint kinase Chk2 which in turn initiates a secondary wave of phosphorylation that extends the signaling leading to the recruitment of repair factors and ultimately to resolution of the DSB. Since the discovery of the gene responsible for AT, a large number of mutations have been reported, the majority of which lead to a truncated protein, however, no mutational hotspots have been identified (Jiang et al. 2006). Protein kinases such as the ATM and the ATM and Rad3-related (ATR) proteins are molecular switches that function in coordinating and achieving the goal(s) of signal transduction pathway(s). A large-scale proteomic analysis revealed more than 700 proteins with over 900 regulated phosphorylation

sites with the consensus sequence recognized by ATM and/or ATR that are phosphorylated in response to DNA damage (Matsuoka et al. 2007). Included in the large list of targets are the excision repair proteins XPA, XPC, RPA1, CSB and components of the general transcription factor TFIIH ((Matsuoka et al. 2007). Additionally CSN1, COP3, and COP7A which are subunits of the COP9 signalosome (CSN), a regulator of cullin based ubiquitin ligases underwent phosphorylation (Matsuoka et al. 2007). This complex is important in SCF E3 ligase activity and alters its association with the repair protein CSA (Matsuoka et al. 2007). Although ATM is known to be involved in repair of DSBs, we examined HCR of the MB+VL treated adenovirus to determine if BER of oxidative damage is decreased in cells from an additional neurodegenerative disorder.

## **Results**

*Metabolic activity of Normal and AT cells in the presence of aluminum, cadmium and lead; the MTT assay.*

We examined the effect of aluminum sulfate ( $\text{Al}_2(\text{SO}_4)_3$ ), cadmium chloride ( $\text{CdCl}_2$ ) and lead nitrate ( $\text{Pb}(\text{CH}_3\text{COO})_4$ ) on cell metabolic activity/viability by measuring mitochondrial activity using the MTT assay (protocol described in appendix IV); a readout for cell viability (Figure 1). The effect of Al, Cd and Pb on viability was examined in primary fibroblasts from normal (GM9503, GM38A), and ataxia telangiectasia (AT) (GM05823E, GM01588A) individuals and is shown in Figure 1 (top row). Compared to normal fibroblasts, ATM deficient fibroblasts demonstrated increased viability in the presence of increasing concentrations of  $\text{Al}_2(\text{SO}_4)_3$  (top left panel). For  $\text{CdCl}_2$  exposure (top middle panel) AT and normal primary

fibroblasts displayed similar resistance. Finally, for lead exposure (top right panel) AT showed an apparent increased resistance to the toxic effects of exposure to  $\text{Pb}(\text{CH}_3\text{COO})_4$ . We also examined toxicity of Al, Cd and Pb on SV40 transformed normal (GM637F), AT (GM16666A) and AT deficient GM16666A transformed fibroblasts complemented with functional ATM fibroblasts (GM16667A) (Figure 1, bottom row). In contrast to the results obtained for metal toxicity for primary AT fibroblasts, SV40 transformed AT fibroblasts display increased sensitivity to Al and Pb (left and right panels, respectively). SV40 transformed AT fibroblasts demonstrated increased resistance to Cd compared to normal (middle panel) similar to the results observed for primary fibroblasts. ATM complementation (GM16667A) increased resistance to the toxic effects of all three metals (Al, Cd and Pb) on cell viability/metabolic activity.

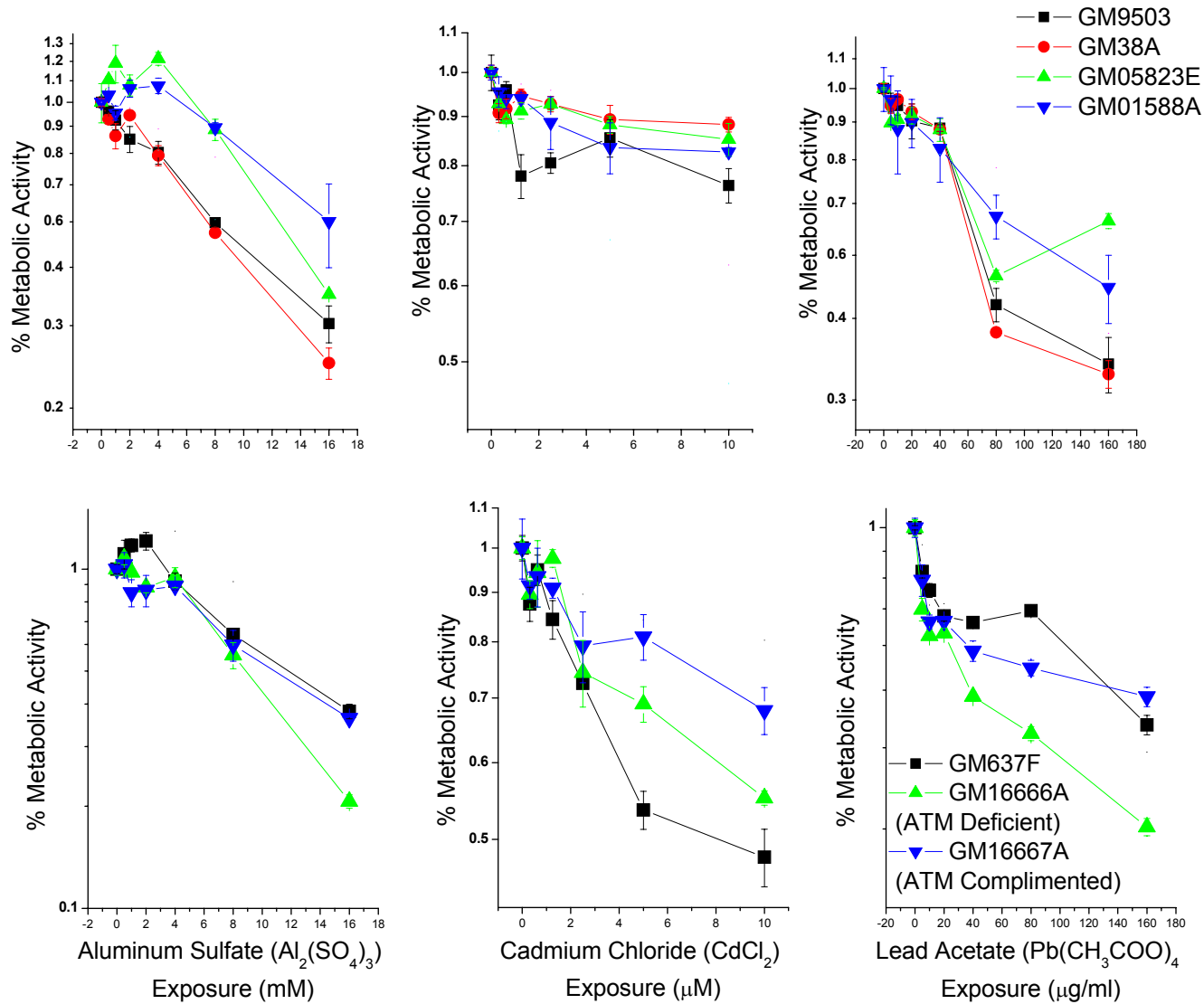


**Figure 1:** The effect of  $\text{Al}_2(\text{SO}_4)_3$  (left),  $\text{CdCl}_2$  (middle) and  $\text{Pb}(\text{CH}_3\text{COO})_4$  (left) on metabolic activity/cell viability in normal AT and fibroblasts. The top row shows the effect of each metal on primary fibroblast strains from each group and the bottom row shows

the effect of each metal on SV40 transformed normal, ATM deficient and ATM complemented fibroblasts. The figure legend is contained within the leftmost plot of each row. Metal treatment is indicated at the bottom of each column. Each plot above is the result of a single experiment done in triplicate determinations ( $\pm$ SE).

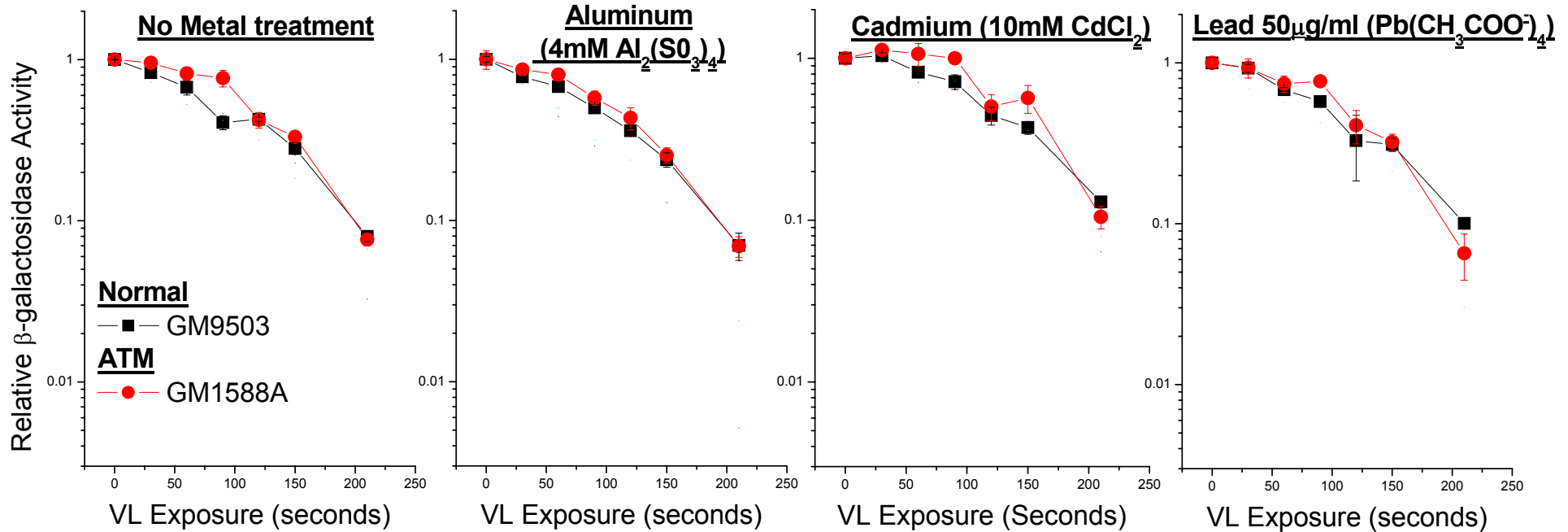


**Figure 2:** The effect of aluminum, cadmium and lead on HCR of the MB+VL treated AdCA35 reporter gene in ATM deficient human primary skin fibroblasts. The above metal treatments were done in parallel in the same experiment. Cells were infected with the MB+VL treated AdCA35 reporter gene at an MOI of 40. Following the 90 min viral absorption period the infection media was aspirated and replaced with 200  $\mu$ l of warmed supplemented media ( $\alpha$ -MEM, 15% FBS) containing the indicated concentration of each metal.  $\beta$ -gal scoring was carried out 24 hours following addition of the media containing the metals. Each point on the above plots is the result of a single experiment done in triplicate determinations ( $\pm$ SE).

**Table 1:** The effect of 4mM  $\text{Al}_2(\text{SO}_3)_4$  on HCR of the MB+VL treated reporter in normal and AT primary fibroblast strains. The  $D_{37}$  values were obtained from the HCR curves shown in Figure 2, which are the results of a single experiment. The top portion of the table shows the absolute  $D_{37}$  values under all 4 conditions (no treatment control, 4mM  $\text{Al}_2(\text{SO}_3)_4$ , 10mM  $\text{CdCl}_2$  and 50mg/ml  $\text{Pb}(\text{CH}_3\text{COO})_4$ ). The middle portion of the table shows the  $D_{37}$  values for each cell line relative to GM9503 under each treatment condition. The bottom portion of the table compared the  $D_{37}$  values for each metal treatment within each cell line compared to the no treatment control.

		<b>Absolute <math>D_{37}</math></b>			
<b>Cell Line</b>	<b>Group</b>	<b>No Treatment</b>	<b>4mM Aluminum</b>	<b>10mM Cadmium</b>	<b>50mg/ml lead</b>
<b>GM9503</b>	Normal	130.3	117.7	150.6	113.5
<b>GM1588A</b>	AT	136.5	128.9	165.2	132.6
		<b><math>D_{37}</math> Relative to GM9503</b>			
<b>Cell Line</b>	<b>Group</b>				
<b>GM9503</b>	Normal	1.00	1.00	1.00	1.00
<b>GM1588A</b>	AT	1.05	1.10	1.10	1.17
		<b><math>D_{37}</math> Relative to No Treatment control (within each cell line)</b>			
<b>Cell Line</b>	<b>Group</b>				
<b>GM9503</b>	Normal	1.00	0.90	1.16	0.87
<b>GM1588A</b>	AT	1.00	0.94	1.21	0.97

## **Discussion**

### *Metals and Ataxia Telangiectasia*

For both Al and Pb treatment, loss of functional ATM in the presence of functional p53/pRb (primary fibroblasts; GM05823E and GM01588A) we observed increased cell viability compared to normal primary fibroblasts (functional ATM, functional p53/pRb; GM9503 and GM38A). This result suggests that ATM functions upstream of p53/pRb in an apoptotic/cell cycle pathway in response to Al and Pb exposure. In the absence of p53/pRb (SV40 transformed fibroblasts), the loss of functional ATM (GM16666A) resulted in a decrease in cell survival/viability and the complementation of ATM deficient cells with functional (GM16667A) ATM resulted in increased resistance to Al and Pb toxicity. If the only ATM response to Al and Pb was to signal apoptosis/cell cycle arrest through p53/pRb, ATM status should not matter in SV40 transformed fibroblasts which lack p53/pRb. The fact that we observe an increase in cell viability when ATM deficient SV40 transformed fibroblasts are complemented with functional ATM indicates ATM is required in a p53/pRb independent pathway in response to Al and Pb. Taken together these data indicate that ATM may function in a p53 dependent apoptotic pathway as well as a p53 independent pro-survival pathway in response to Al and Pb treatment. To further address these possibilities it should be determined if the lower metabolic activity in normal primary fibroblasts is the result of reduced mitochondrial activity or apoptosis in the presence of Al and Pb and if there increased genomic instability/DNA damage in the AT fibroblasts that appear to survive better (ie. is damaged DNA going undetected). Al and Pb did not appear to have an effect on HCR of the MB+VL damaged reporter indicating these metals do not have an effect on reactivation of the MB+VL treated reporter. Further studies using the SV40 transformed ATM deficient GM16666A cell line and its ATM complemented isogenic

counterpart GM16667A to examine the effect of Al, Cd and Pb on repair of MB+VL induced oxidative DNA damage using both the HCR (time course) and MTT assay would be useful. It would also be interesting to examine the chromosomes of primary fibroblasts lacking ATM that appear to be more resistant to the metals. Chromosomal breaks may be going unnoticed in AT cells in the presence of the metals, allowing the cells to divide and produce daughter cells with abnormal chromosomes, potentially rendering AT individuals more susceptible to cancer.

For treatment with Cd, the MTT assay did not reveal any differences between normal and AT primary fibroblasts as viability of both AT fibroblast strains GM05823E and GM01588A were intermediate to the normal fibroblasts GM9503 and GM38A. In SV40 transformed fibroblasts, the AT deficient fibroblast line GM16666A demonstrated greater resistance to the toxic effects of Cd than the normal control GM637F. The addition of functional ATM to GM16666A (GM16667A) resulted in increased viability. GM16666A and GM16667A are isogenic cell lines and both displayed increased resistance to Cd compared to GM637F, I have chosen to ignore GM637F, stressing the importance of isogenic backgrounds when using the HCR assay. Similar to the results seen with Al and Pb, it appears as though in the absence of p53/pRb, ATM functions in a pathway that promotes cell survival/viability in the presence of Cd. In the absence of p53, cells can incur a greater level of DNA damage as apoptotic signaling by p53 is absent/reduced. Following cell division after a certain threshold of DNA damage, even in the absence of apoptosis, resulting daughter cells would likely be less viable. In the presence of functional ATM, DNA damage signaling and DSB repair can occur properly. It is likely that the observed increase in Cd resistance in SV40 transformed fibroblasts with functional ATM is the result of increased damage recognition and repair resulting in viable cells. To determine if this is the case apoptosis and chromosome structure in ATM deficient (GM16666A) and ATM

complemented (GM16667A) cells should be examined following exposure to Cd. The same should also be done for exposure to Al and Pb. Apoptosis can be measured using a  $\beta$ -galactosidase apoptosis kit and chromosome structure can be examined by FISH.

## References

- Achary, V. M., S. Jena, K. K. Panda and B. B. Panda (2008). "Aluminium induced oxidative stress and DNA damage in root cells of *Allium cepa* L." *Ecotoxicol Environ Saf* **70**(2): 300-10.
- Addison, C., J. Gauldie, W. Muller and F. Graham (1995). "An adenoviral vector expressing interleukin-4 modulates tumorigenicity and induces regression in a murine breast-cancer model." *Int J Oncol* **7**(6): 1253-60.
- Addison, C. L., T. Braciak, R. Ralston, W. J. Muller, J. Gauldie and F. L. Graham (1995a). "Intratumoral injection of an adenovirus expressing interleukin 2 induces regression and immunity in a murine breast cancer model." *Proc Natl Acad Sci U S A* **92**(18): 8522-6.
- Addison, C. L., M. Hitt, D. Kunsken and F. L. Graham (1997). "Comparison of the human versus murine cytomegalovirus immediate early gene promoters for transgene expression by adenoviral vectors." *J Gen Virol* **78** ( Pt 7): 1653-61.
- Adimoolam, S. and J. M. Ford (2002). "p53 and DNA damage-inducible expression of the xeroderma pigmentosum group C gene." *Proc Natl Acad Sci U S A* **99**(20): 12985-90.
- Agarwal, M. L., W. R. Taylor, M. V. Chernov, O. B. Chernova and G. R. Stark (1998). "The p53 network." *J Biol Chem* **273**(1): 1-4.
- Ames, B. N. (1989). "Endogenous DNA damage as related to cancer and aging." *Mutat Res* **214**(1): 41-6.
- Amouroux, R., A. Campalans, B. Epe and J. P. Radicella (2010). "Oxidative stress triggers the preferential assembly of base excision repair complexes on open chromatin regions." *Nucleic Acids Res* **38**(9): 2878-90.
- An, J., T. Yang, Y. Huang, F. Liu, J. Sun, Y. Wang, Q. Xu, D. Wu and P. Zhou (2011). "Strand-specific PCR of UV radiation-damaged genomic DNA revealed an essential role of DNA-PKcs in the transcription-coupled repair." *BMC Biochem* **12**: 2.
- Andrews, A. D., S. F. Barrett, F. W. Yoder and J. H. Robbins (1978). "Cockayne's syndrome fibroblasts have increased sensitivity to ultraviolet light but normal rates of unscheduled DNA synthesis." *J Invest Dermatol* **70**(5): 237-9.
- Arking, R. (2006). *The Biology of Aging: Observations and Principles* Oxford, U.K. , Oxford University Press
- Atamna, H., A. Nguyen, C. Schultz, K. Boyle, J. Newberry, H. Kato and B. N. Ames (2008). "Methylene blue delays cellular senescence and enhances key mitochondrial biochemical pathways." *Faseb J* **22**(3): 703-12.
- Atwood, C. S., R. N. Martins, M. A. Smith and G. Perry (2002). "Senile plaque composition and posttranslational modification of amyloid-beta peptide and associated proteins." *Peptides* **23**(7): 1343-50.
- Austad, S. N. (1989). "Life extension by dietary restriction in the bowl and doily spider, *Frontinella pyramitela*." *Exp Gerontol* **24**(1): 83-92.
- Azzalin, C. M., P. Reichenbach, L. Khoriavali, E. Giulotto and J. Lingner (2007). "Telomeric repeat containing RNA and RNA surveillance factors at mammalian chromosome ends." *Science* **318**(5851): 798-801.
- Balajee, A. S., A. May, G. L. Dianov, E. C. Friedberg and V. A. Bohr (1997). "Reduced RNA polymerase II transcription in intact and permeabilized Cockayne syndrome group B cells." *Proc Natl Acad Sci U S A* **94**(9): 4306-11.

- Banerjee, D., S. M. Mandal, A. Das, M. L. Hegde, S. Das, K. K. Bhakat, I. Boldogh, P. S. Sarkar, S. Mitra and T. K. Hazra (2011). "Preferential repair of oxidized base damage in the transcribed genes of mammalian cells." *J Biol Chem* **286**(8): 6006-16.
- Barnes, D. E. and T. Lindahl (2004). "Repair and genetic consequences of endogenous DNA base damage in mammalian cells." *Annu Rev Genet* **38**: 445-76.
- Bartek, J. and J. Lukas (2001). "Mammalian G1- and S-phase checkpoints in response to DNA damage." *Curr Opin Cell Biol* **13**(6): 738-47.
- Batenburg, N., T. R. Mitchell, D. M. Leach, A. J. Rainbow and X. D. Zhu (2011). Characterization of the Role of CSB in Telomere Maintenance Associated with Tumorigenesis The Canadian Cancer Research Conference, Toronto, Ontario, Canada.
- Beerens, N., J. H. Hoeijmakers, R. Kanaar, W. Vermeulen and C. Wyman (2005). "The CSB protein actively wraps DNA." *J Biol Chem* **280**(6): 4722-9.
- Behl, C., J. B. Davis, R. Lesley and D. Schubert (1994). "Hydrogen peroxide mediates amyloid beta protein toxicity." *Cell* **77**(6): 817-27.
- Bellinger, D. C. (2004). "Lead." *Pediatrics* **113**(4 Suppl): 1016-22.
- Bennett, C. B. and A. J. Rainbow (1988). "Enhanced reactivation and mutagenesis of UV-irradiated adenovirus in normal human fibroblasts." *Mutagenesis* **3**(2): 157-64.
- Bergelson, J. M., J. A. Cunningham, G. Droguett, E. A. Kurt-Jones, A. Krithivas, J. S. Hong, M. S. Horwitz, R. L. Crowell and R. W. Finberg (1997). "Isolation of a common receptor for Coxsackie B viruses and adenoviruses 2 and 5." *Science* **275**(5304): 1320-3.
- Berquist, B. R. and D. M. Wilson, 3rd (2009). "Nucleic acid binding activity of human Cockayne syndrome B protein and identification of Ca(2+) as a novel metal cofactor." *J Mol Biol* **391**(5): 820-32.
- Blackburn, E. H., C. W. Greider and J. W. Szostak (2006). "Telomeres and telomerase: the path from maize, Tetrahymena and yeast to human cancer and aging." *Nat Med* **12**(10): 1133-8.
- Blagosklonny, M. V. and W. S. el-Deiry (1996). "In vitro evaluation of a p53-expressing adenovirus as an anti-cancer drug." *Int J Cancer* **67**(3): 386-92.
- Blainey, P. C., A. M. van Oijen, A. Banerjee, G. L. Verdine and X. S. Xie (2006). "A base-excision DNA-repair protein finds intrahelical lesion bases by fast sliding in contact with DNA." *Proc Natl Acad Sci U S A* **103**(15): 5752-7.
- Blasco, M. A. (2007). "The epigenetic regulation of mammalian telomeres." *Nat Rev Genet* **8**(4): 299-309.
- Bodnar, J. W., P. I. Hanson, M. Polvino-Bodnar, W. Zempsky and D. C. Ward (1989). "The terminal regions of adenovirus and minute virus of mice DNAs are preferentially associated with the nuclear matrix in infected cells." *J Virol* **63**(10): 4344-53.
- Bohr, V., R. M. Anson, S. Mazur and G. Dianov (1998). "Oxidative DNA damage processing and changes with aging." *Toxicol Lett* **102-103**: 47-52.
- Boshart, M., F. Weber, G. Jahn, K. Dorsch-Hasler, B. Fleckenstein and W. Schaffner (1985). "A very strong enhancer is located upstream of an immediate early gene of human cytomegalovirus." *Cell* **41**(2): 521-30.
- Boszko, I. P. and A. J. Rainbow (1999). "Removal of UV photoproducts from an adenovirus-encoded reporter gene following infection of unirradiated and UV-irradiated human fibroblasts." *Somat Cell Mol Genet* **25**(5-6): 301-15.

- Bowman, K. K., D. M. Sicard, J. M. Ford and P. C. Hanawalt (2000). "Reduced global genomic repair of ultraviolet light-induced cyclobutane pyrimidine dimers in simian virus 40-transformed human cells." Mol Carcinog **29**(1): 17-24.
- Butterfield, D. A. (2002). "Amyloid beta-peptide (1-42)-induced oxidative stress and neurotoxicity: implications for neurodegeneration in Alzheimer's disease brain. A review." Free Radic Res **36**(12): 1307-13.
- Capell, B. C., B. E. Tloutan and S. J. Orlow (2009). "From the rarest to the most common: insights from progeroid syndromes into skin cancer and aging." J Invest Dermatol **129**(10): 2340-50.
- Celli, G. B. and T. de Lange (2005). "DNA processing is not required for ATM-mediated telomere damage response after TRF2 deletion." Nat Cell Biol **7**(7): 712-8.
- Chapman, T. and L. Partridge (1996). "Female fitness in *Drosophila melanogaster*: an interaction between the effect of nutrition and of encounter rate with males." Proc Biol Sci **263**(1371): 755-9.
- Charlet-Berguerand, N., S. Feuerhahn, S. E. Kong, H. Ziserman, J. W. Conaway, R. Conaway and J. M. Egly (2006). "RNA polymerase II bypass of oxidative DNA damage is regulated by transcription elongation factors." Embo J **25**(23): 5481-91.
- Chatterjee, P. K., M. E. Vayda and S. J. Flint (1986). "Identification of proteins and protein domains that contact DNA within adenovirus nucleoprotein cores by ultraviolet light crosslinking of oligonucleotides 32P-labelled in vivo." J Mol Biol **188**(1): 23-37.
- Chen, Y., Y. Yang, M. van Overbeek, J. R. Donigian, P. Baciú, T. de Lange and M. Lei (2008). "A shared docking motif in TRF1 and TRF2 used for differential recruitment of telomeric proteins." Science **319**(5866): 1092-6.
- Chen, Z. Y., C. Y. He, L. Meuse and M. A. Kay (2004). "Silencing of episomal transgene expression by plasmid bacterial DNA elements in vivo." Gene Ther **11**(10): 856-64.
- Cheng, J., J. A. DeCaprio, M. M. Fluck and B. S. Schaffhausen (2009). "Cellular transformation by Simian Virus 40 and Murine Polyoma Virus T antigens." Semin Cancer Biol **19**(4): 218-28.
- Cheng, K. C., D. S. Cahill, H. Kasai, S. Nishimura and L. A. Loeb (1992). "8-Hydroxyguanine, an abundant form of oxidative DNA damage, causes G----T and A----C substitutions." J Biol Chem **267**(1): 166-72.
- Chippindale, A. K., A. M. Leroi, S. B. Kim and M. R. Rose (1993). "Phenotypic plasticity and selection in *Drosophila* life-history evolution. I. Nutrition and the cost of reproduction." J. Evol. Biol. **6**: 171-193.
- Citterio, E., V. Van Den Boom, G. Schnitzler, R. Kanaar, E. Bonte, R. E. Kingston, J. H. Hoeijmakers and W. Vermeulen (2000). "ATP-dependent chromatin remodeling by the Cockayne syndrome B DNA repair-transcription-coupling factor." Mol Cell Biol **20**(20): 7643-53.
- Colicos, M. A., Y. Haj-Ahmad, K. Valerie, E. E. Henderson and A. J. Rainbow (1991). "Construction of a recombinant adenovirus containing the denV gene from bacteriophage T4 which can partially restore the DNA repair deficiency in xeroderma pigmentosum fibroblasts." Carcinogenesis **12**(2): 249-55.
- Coppede, F. and L. Migliore (2009). "DNA damage and repair in Alzheimer's disease." Curr Alzheimer Res **6**(1): 36-47.
- Cotten, M. and J. M. Weber (1995). "The adenovirus protease is required for virus entry into host cells." Virology **213**(2): 494-502.

- Crapper, D. R., S. S. Krishnan and A. J. Dalton (1973). "Brain aluminum distribution in Alzheimer's disease and experimental neurofibrillary degeneration." Science **180**(85): 511-3.
- Csaky, K. G. (2001). "Preparation of recombinant adenoviruses." Methods Mol Med **47**: 141-55.
- d'Adda di Fagagna, F., S. H. Teo and S. P. Jackson (2004). "Functional links between telomeres and proteins of the DNA-damage response." Genes Dev **18**(15): 1781-99.
- D'Errico, M., E. Parlanti, M. Teson, P. Degan, T. Lemma, A. Calcagnile, I. Iavarone, P. Jaruga, M. Ropolo, A. M. Pedrini, D. Orioli, G. Frosina, G. Zambruno, M. Dizdaroglu, M. Stefanini and E. Dogliotti (2007). "The role of CSA in the response to oxidative DNA damage in human cells." Oncogene **26**(30): 4336-43.
- David, S. S., V. L. O'Shea and S. Kundu (2007). "Base-excision repair of oxidative DNA damage." Nature **447**(7147): 941-50.
- de Boer, J., J. O. Andressoo, J. de Wit, J. Huijman, R. B. Beems, H. van Steeg, G. Weeda, G. T. van der Horst, W. van Leeuwen, A. P. Themmen, M. Meradji and J. H. Hoeijmakers (2002). "Premature aging in mice deficient in DNA repair and transcription." Science **296**(5571): 1276-9.
- de Boer, J. and J. H. Hoeijmakers (2000). "Nucleotide excision repair and human syndromes." Carcinogenesis **21**(3): 453-60.
- de Lange, T. (2002). "Protection of mammalian telomeres." Oncogene **21**(4): 532-40.
- de Lange, T. (2005). "Shelterin: the protein complex that shapes and safeguards human telomeres." Genes Dev **19**(18): 2100-10.
- de Waard, H., J. de Wit, J. O. Andressoo, C. T. van Oostrom, B. Riis, A. Weimann, H. E. Poulsen, H. van Steeg, J. H. Hoeijmakers and G. T. van der Horst (2004). "Different effects of CSA and CSB deficiency on sensitivity to oxidative DNA damage." Mol Cell Biol **24**(18): 7941-8.
- de Waard, H., J. de Wit, T. G. Gorgels, G. van den Aardweg, J. O. Andressoo, M. Vermeij, H. van Steeg, J. H. Hoeijmakers and G. T. van der Horst (2003). "Cell type-specific hypersensitivity to oxidative damage in CSB and XPA mice." DNA Repair (Amst) **2**(1): 13-25.
- Demple, B. and L. Harrison (1994). "Repair of oxidative damage to DNA: enzymology and biology." Annu Rev Biochem **63**: 915-48.
- Dianov, G., C. Bischoff, J. Piotrowski and V. A. Bohr (1998). "Repair pathways for processing of 8-oxoguanine in DNA by mammalian cell extracts." J Biol Chem **273**(50): 33811-6.
- Dianov, G., C. Bischoff, M. Sunesen and V. A. Bohr (1999). "Repair of 8-oxoguanine in DNA is deficient in Cockayne syndrome group B cells." Nucleic Acids Res **27**(5): 1365-8.
- Dianov, G., A. Price and T. Lindahl (1992). "Generation of single-nucleotide repair patches following excision of uracil residues from DNA." Mol Cell Biol **12**(4): 1605-12.
- Dianov, G. L. (2011). "Base excision repair targets for cancer therapy." Am J Cancer Res **1**(7): 845-51.
- Dianov, G. L., N. Souza-Pinto, S. G. Nyaga, T. Thybo, T. Stevnsner and V. A. Bohr (2001). "Base excision repair in nuclear and mitochondrial DNA." Prog Nucleic Acid Res Mol Biol **68**: 285-97.
- Dianov, G. L., T. Thybo, Dianova, II, L. J. Lipinski and V. A. Bohr (2000). "Single nucleotide patch base excision repair is the major pathway for removal of thymine glycol from DNA in human cell extracts." J Biol Chem **275**(16): 11809-13.

- Dizdaroglu, M. (2003). "Substrate specificities and excision kinetics of DNA glycosylases involved in base-excision repair of oxidative DNA damage." Mutat Res **531**(1-2): 109-26.
- Dizdaroglu, M. (2005). "Base-excision repair of oxidative DNA damage by DNA glycosylases." Mutat Res **591**(1-2): 45-59.
- Donahue, B. A., S. Yin, J. S. Taylor, D. Reines and P. C. Hanawalt (1994). "Transcript cleavage by RNA polymerase II arrested by a cyclobutane pyrimidine dimer in the DNA template." Proc Natl Acad Sci U S A **91**(18): 8502-6.
- Donma, O. and M. Metin Donma (2005). "Cadmium, lead and phytochemicals." Med Hypotheses **65**(4): 699-702.
- Dou, H., S. Mitra and T. K. Hazra (2003). "Repair of oxidized bases in DNA bubble structures by human DNA glycosylases NEIL1 and NEIL2." J Biol Chem **278**(50): 49679-84.
- Dou, H., C. A. Theriot, A. Das, M. L. Hegde, Y. Matsumoto, I. Boldogh, T. K. Hazra, K. K. Bhakat and S. Mitra (2008). "Interaction of the human DNA glycosylase NEIL1 with proliferating cell nuclear antigen. The potential for replication-associated repair of oxidized bases in mammalian genomes." J Biol Chem **283**(6): 3130-40.
- Dregoes, D. and A. J. Rainbow (2009). "Differential effects of hypoxia and acidosis on p53 expression, repair of UVC-damaged DNA and viability after UVC in normal and tumor-derived human cells." DNA Repair (Amst) **8**(3): 370-82.
- Dregoes, D., A. P. Rybak and A. J. Rainbow (2007). "Increased expression of p53 enhances transcription-coupled repair and global genomic repair of a UVC-damaged reporter gene in human cells." DNA Repair (Amst) **6**(5): 588-601.
- Droge, W. (2002). "Free radicals in the physiological control of cell function." Physiol Rev **82**(1): 47-95.
- Du, H., L. Guo, S. Yan, A. A. Sosunov, G. M. McKhann and S. S. Yan "Early deficits in synaptic mitochondria in an Alzheimer's disease mouse model." Proc Natl Acad Sci U S A **107**(43): 18670-5.
- Epe, B., M. Pflaum and S. Boiteux (1993). "DNA damage induced by photosensitizers in cellular and cell-free systems." Mutat Res **299**(3-4): 135-45.
- Eveno, E., F. Bourre, X. Quilliet, O. Chevallier-Lagente, L. Roza, A. P. Eker, W. J. Kleijer, O. Nikaido, M. Stefanini, J. H. Hoeijmakers and et al. (1995). "Different removal of ultraviolet photoproducts in genetically related xeroderma pigmentosum and trichothiodystrophy diseases." Cancer Res **55**(19): 4325-32.
- Failla, G. (1958). "The aging process and cancerogenesis." Ann N Y Acad Sci **71**(6): 1124-40.
- Fickenscher, H., T. Stamminger, R. Ruger and B. Fleckenstein (1989). "The role of a repetitive palindromic sequence element in the human cytomegalovirus major immediate early enhancer." J Gen Virol **70 ( Pt 1)**: 107-23.
- Finch, C. E. (2009). "Update on slow aging and negligible senescence--a mini-review." Gerontology **55**(3): 307-13.
- Finkel, T. and N. J. Holbrook (2000). "Oxidants, oxidative stress and the biology of ageing." Nature **408**(6809): 239-47.
- Fishel, M. L., M. R. Vasko and M. R. Kelley (2007). "DNA repair in neurons: so if they don't divide what's to repair?" Mutat Res **614**(1-2): 24-36.
- Flint, J. and T. Shenk (1989). "Adenovirus E1A protein paradigm viral transactivator." Annu Rev Genet **23**: 141-61.

- Floyd, R. A., J. E. Schneider, Jr. and D. P. Dittmer (2004). "Methylene blue photoinactivation of RNA viruses." Antiviral Res **61**(3): 141-51.
- Floyd, R. A., M. S. West, K. L. Eneff and J. E. Schneider (1989). "Methylene blue plus light mediates 8-hydroxyguanine formation in DNA." Arch Biochem Biophys **273**(1): 106-11.
- Flynn, R. L., R. C. Centore, R. J. O'Sullivan, R. Rai, A. Tse, Z. Songyang, S. Chang, J. Karlseder and L. Zou (2011). "TERRA and hnRNPA1 orchestrate an RPA-to-POT1 switch on telomeric single-stranded DNA." Nature **471**(7339): 532-6.
- Foote, C. S. (1976). Photosensitized oxidation and singlet oxygen: consequences in biological systems Free Radicals in Biology. W. A. Pryor. Baton Rouge Academic Press: 85-124.
- Fraga, C. G., M. K. Shigenaga, J. W. Park, P. Degan and B. N. Ames (1990). "Oxidative damage to DNA during aging: 8-hydroxy-2'-deoxyguanosine in rat organ DNA and urine." Proc Natl Acad Sci U S A **87**(12): 4533-7.
- Francis, M. A., P. Bagga, R. Athwal and A. J. Rainbow (2000). "Partial complementation of the DNA repair defects in cells from xeroderma pigmentosum groups A, C, D and F but not G by the denV gene from bacteriophage T4." Photochem Photobiol **72**(3): 365-73.
- Francis, M. A., P. S. Bagga, R. S. Athwal and A. J. Rainbow (1997). "Incomplete complementation of the DNA repair defect in cockayne syndrome cells by the denV gene from bacteriophage T4 suggests a deficiency in base excision repair." Mutat Res **385**(1): 59-74.
- Francis, M. A. and A. J. Rainbow (1999). "UV-enhanced reactivation of a UV-damaged reporter gene suggests transcription-coupled repair is UV-inducible in human cells." Carcinogenesis **20**(1): 19-26.
- Francis, M. A. and A. J. Rainbow (2000). "UV-enhanced expression of a reporter gene is induced at lower UV fluences in transcription-coupled repair deficient compared to normal human fibroblasts, and is absent in SV40-transformed counterparts." Photochem Photobiol **72**(4): 554-61.
- Francis, M. A. and A. J. Rainbow (2003). "Role for retinoblastoma protein family members in UV-enhanced expression from the human cytomegalovirus immediate early promoters." Photochem Photobiol **77**(6): 621-7.
- Fredman, J. N. and J. A. Engler (1993). "Adenovirus precursor to terminal protein interacts with the nuclear matrix in vivo and in vitro." J Virol **67**(6): 3384-95.
- Friedberg, C. E., C. W. Graham and W. Siede (1995). DNA Repair and Mutagenesis Washington DC, ASM Press.
- Friedberg, E. C. (1996). "Cockayne syndrome--a primary defect in DNA repair, transcription, both or neither?" Bioessays **18**(9): 731-8.
- Frosina, G., P. Fortini, O. Rossi, F. Carrozzino, G. Raspaglio, L. S. Cox, D. P. Lane, A. Abbondandolo and E. Dogliotti (1996). "Two pathways for base excision repair in mammalian cells." J Biol Chem **271**(16): 9573-8.
- Gabbita, S. P., M. A. Lovell and W. R. Markesbery (1998). "Increased nuclear DNA oxidation in the brain in Alzheimer's disease." J Neurochem **71**(5): 2034-40.
- Ganesan, A. K., J. Hunt and P. C. Hanawalt (1999). "Expression and nucleotide excision repair of a UV-irradiated reporter gene in unirradiated human cells." Mutat Res **433**(2): 117-26.
- Gatti, R. A., I. Berkel, E. Boder, G. Braedt, P. Charmley, P. Concannon, F. Ersoy, T. Foroud, N. G. Jaspers, K. Lange and et al. (1988). "Localization of an ataxia-telangiectasia gene to chromosome 11q22-23." Nature **336**(6199): 577-80.

- Gedik, C. M. and A. Collins (2005). "Establishing the background level of base oxidation in human lymphocyte DNA: results of an interlaboratory validation study." Faseb J **19**(1): 82-4.
- Ghodgaonkar, M. M., N. Zagal, S. Kassam, A. J. Rainbow and G. M. Shah (2008). "Depletion of poly(ADP-ribose) polymerase-1 reduces host cell reactivation of a UV-damaged adenovirus-encoded reporter gene in human dermal fibroblasts." DNA Repair (Amst) **7**(4): 617-32.
- Glenfield, K., Y. Wu, N. Zagal, A. J. Rainbow and X. D. Zhu (2007). FUNCTIONAL ANALYSIS OF HUMAN TELOMERE DNA BINDING PROTEIN TRF2 IN THE DNA DAMAGE RESPONSE PATHWAY. W.I.S.E. McMaster University, Hamilton, Ontario, Canada
- Goncalves, M. A. and A. A. de Vries (2006). "Adenovirus: from foe to friend." Rev Med Virol **16**(3): 167-86.
- Gorgels, T. G., I. van der Pluijm, R. M. Brandt, G. A. Garinis, H. van Steeg, G. van den Aardweg, G. H. Jansen, J. M. Ruijter, A. A. Bergen, D. van Norren, J. H. Hoeijmakers and G. T. van der Horst (2007). "Retinal degeneration and ionizing radiation hypersensitivity in a mouse model for Cockayne syndrome." Mol Cell Biol **27**(4): 1433-41.
- Graham, F. L. and L. Prevec (1991). "Manipulation of adenovirus vectors." Methods in molecular biology **7**: 109-28.
- Graham, F. L. and L. Prevec (1991). "Manipulation of adenovirus vectors." Methods Mol Biol **7**: 109-28.
- Graham, F. L., J. Smiley, W. C. Russell and R. Nairn (1977). "Characteristics of a human cell line transformed by DNA from human adenovirus type 5." J Gen Virol **36**(1): 59-74.
- Greber, U. F., M. Suomalainen, R. P. Stidwill, K. Boucke, M. W. Ebersold and A. Helenius (1997). "The role of the nuclear pore complex in adenovirus DNA entry." Embo J **16**(19): 5998-6007.
- Griffith, J. D., L. Comeau, S. Rosenfield, R. M. Stansel, A. Bianchi, H. Moss and T. de Lange (1999). "Mammalian telomeres end in a large duplex loop." Cell **97**(4): 503-14.
- Griffiths, H. R. (2000). "Antioxidants and protein oxidation." Free Radic Res **33 Suppl**: S47-58.
- Gura, T. (2008). "Hope in Alzheimer's fight emerges from unexpected places." Nat Med **14**(9): 894.
- Haass, C. and D. J. Selkoe (2007). "Soluble protein oligomers in neurodegeneration: lessons from the Alzheimer's amyloid beta-peptide." Nat Rev Mol Cell Biol **8**(2): 101-12.
- Halliwell, B. (2006). "Oxidative stress and neurodegeneration: where are we now?" J Neurochem **97**(6): 1634-58.
- Halliwell, B. and J. M. C. Gutteridge (1989). Free Radicals in Biology and Medicine Oxford, U.K., Clarendon Press.
- Hamilton, M. L., Z. Guo, C. D. Fuller, H. Van Remmen, W. F. Ward, S. N. Austad, D. A. Troyer, I. Thompson and A. Richardson (2001). "A reliable assessment of 8-oxo-2-deoxyguanosine levels in nuclear and mitochondrial DNA using the sodium iodide method to isolate DNA." Nucleic Acids Res **29**(10): 2117-26.
- Hanawalt, P. C. (2008). "Emerging links between premature ageing and defective DNA repair." Mech Ageing Dev **129**(7-8): 503-5.
- Hardy, J. (2006). "Has the amyloid cascade hypothesis for Alzheimer's disease been proved?" Curr Alzheimer Res **3**(1): 71-3.

- Harley, C. B., A. B. Futcher and C. W. Greider (1990). "Telomeres shorten during ageing of human fibroblasts." Nature **345**(6274): 458-60.
- Harman, D. (1956). "Aging: a theory based on free radical and radiation chemistry." J Gerontol **11**(3): 298-300.
- Harman, D. (1981). "The aging process." Proc Natl Acad Sci U S A **78**(11): 7124-8.
- Hartwig, A. and T. Schwerdtle (2002). "Interactions by carcinogenic metal compounds with DNA repair processes: toxicological implications." Toxicol Lett **127**(1-3): 47-54.
- Haruki, H., M. Okuwaki, M. Miyagishi, K. Taira and K. Nagata (2006). "Involvement of template-activating factor I/SET in transcription of adenovirus early genes as a positive-acting factor." J Virol **80**(2): 794-801.
- Hasty, P., J. Campisi, J. Hoeijmakers, H. van Steeg and J. Vijg (2003). "Aging and genome maintenance: lessons from the mouse?" Science **299**(5611): 1355-9.
- Hasty, P. and J. Vijg (2004). "Rebuttal to Miller: 'Accelerated aging': a primrose path to insight?" Aging Cell **3**(2): 67-9.
- Hayes, J. D. and L. I. McLellan (1999). "Glutathione and glutathione-dependent enzymes represent a co-ordinately regulated defence against oxidative stress." Free Radic Res **31**(4): 273-300.
- Hayflick, L. and P. S. Moorhead (1961). "The serial cultivation of human diploid cell strains." Exp Cell Res **25**: 585-621.
- Hazra, T. K., J. W. Hill, T. Izumi and S. Mitra (2001). "Multiple DNA glycosylases for repair of 8-oxoguanine and their potential in vivo functions." Prog Nucleic Acid Res Mol Biol **68**: 193-205.
- Hazra, T. K., T. Izumi, I. Boldogh, B. Imhoff, Y. W. Kow, P. Jaruga, M. Dizdaroglu and S. Mitra (2002). "Identification and characterization of a human DNA glycosylase for repair of modified bases in oxidatively damaged DNA." Proc Natl Acad Sci U S A **99**(6): 3523-8.
- Hazra, T. K., Y. W. Kow, Z. Hatahet, B. Imhoff, I. Boldogh, S. K. Mokkaapati, S. Mitra and T. Izumi (2002). "Identification and characterization of a novel human DNA glycosylase for repair of cytosine-derived lesions." J Biol Chem **277**(34): 30417-20.
- Hegde, M. L., A. K. Mantha, T. K. Hazra, K. K. Bhakat, S. Mitra and B. Szczechesny (2012). "Oxidative genome damage and its repair: Implications in aging and neurodegenerative diseases." Mech Ageing Dev.
- Hegde, M. L., C. A. Theriot, A. Das, P. M. Hegde, Z. Guo, R. K. Gary, T. K. Hazra, B. Shen and S. Mitra (2008). "Physical and functional interaction between human oxidized base-specific DNA glycosylase NEIL1 and flap endonuclease 1." J Biol Chem **283**(40): 27028-37.
- Hennighausen, L. and B. Fleckenstein (1986). "Nuclear factor 1 interacts with five DNA elements in the promoter region of the human cytomegalovirus major immediate early gene." Embo J **5**(6): 1367-71.
- Henning, K. A., L. Li, N. Iyer, L. D. McDaniel, M. S. Reagan, R. Legerski, R. A. Schultz, M. Stefanini, A. R. Lehmann, L. V. Mayne and E. C. Friedberg (1995). "The Cockayne syndrome group A gene encodes a WD repeat protein that interacts with CSB protein and a subunit of RNA polymerase II TFIIF." Cell **82**(4): 555-64.
- Henry, L. J., D. Xia, M. E. Wilke, J. Deisenhofer and R. D. Gerard (1994). "Characterization of the knob domain of the adenovirus type 5 fiber protein expressed in Escherichia coli." J Virol **68**(8): 5239-46.

- Hensley, K., J. M. Carney, M. P. Mattson, M. Aksenova, M. Harris, J. F. Wu, R. A. Floyd and D. A. Butterfield (1994). "A model for beta-amyloid aggregation and neurotoxicity based on free radical generation by the peptide: relevance to Alzheimer disease." Proc Natl Acad Sci U S A **91**(8): 3270-4.
- Hensley, K., N. Hall, R. Subramaniam, P. Cole, M. Harris, M. Aksenov, M. Aksenova, S. P. Gabbita, J. F. Wu, J. M. Carney and et al. (1995). "Brain regional correspondence between Alzheimer's disease histopathology and biomarkers of protein oxidation." J Neurochem **65**(5): 2146-56.
- Hirt, B. (1967). "Selective extraction of polyoma DNA from infected mouse cell cultures." J Mol Biol **26**(2): 365-9.
- Hitt, M., R. J. Parks and G. F.L. (1999). Structure and genetic organisation of adenovirus vectors. The development of human gene therapy Cold Spring Harbor, Cold Spring Harbor Laboratory Press: 61-86.
- Hoeijmakers, J. H. (2001). "Genome maintenance mechanisms for preventing cancer." Nature **411**(6835): 366-74.
- Hoeijmakers, J. H. (2009). "DNA damage, aging, and cancer." N Engl J Med **361**(15): 1475-85.
- Horibata, K., Y. Iwamoto, I. Kuraoka, N. G. Jaspers, A. Kurimasa, M. Oshimura, M. Ichihashi and K. Tanaka (2004). "Complete absence of Cockayne syndrome group B gene product gives rise to UV-sensitive syndrome but not Cockayne syndrome." Proc Natl Acad Sci U S A **101**(43): 15410-5.
- Horwitz, M. S. (1990). Adenoviridae and their replication Virology. B. N. Fields and D. M. Knipe. New York, Raven Press. **2**: 1679-1721.
- Huffman, J. L., O. Sundheim and J. A. Tainer (2005). "DNA base damage recognition and removal: new twists and grooves." Mutat Res **577**(1-2): 55-76.
- Hussain, S. P. and C. C. Harris (1998). "Molecular epidemiology of human cancer: contribution of mutation spectra studies of tumor suppressor genes." Cancer Res **58**(18): 4023-37.
- Hwang, B. J., J. M. Ford, P. C. Hanawalt and G. Chu (1999). "Expression of the p48 xeroderma pigmentosum gene is p53-dependent and is involved in global genomic repair." Proc Natl Acad Sci U S A **96**(2): 424-8.
- Iida, T., A. Furuta, K. Nishioka, Y. Nakabeppu and T. Iwaki (2002). "Expression of 8-oxoguanine DNA glycosylase is reduced and associated with neurofibrillary tangles in Alzheimer's disease brain." Acta Neuropathol **103**(1): 20-5.
- Imam, S. Z., F. E. Indig, W. H. Cheng, S. P. Saxena, T. Stevnsner, D. Kufe and V. A. Bohr (2007). "Cockayne syndrome protein B interacts with and is phosphorylated by c-Abl tyrosine kinase." Nucleic Acids Res **35**(15): 4941-51.
- Itoh, T., Y. Fujiwara, T. Ono and M. Yamaizumi (1995). "UVs syndrome, a new general category of photosensitive disorder with defective DNA repair, is distinct from xeroderma pigmentosum variant and rodent complementation group I." Am J Hum Genet **56**(6): 1267-76.
- Jackson, S. P. and J. Bartek (2009). "The DNA-damage response in human biology and disease." Nature **461**(7267): 1071-8.
- Jiang, H., B. Tang, K. Xia, Z. Hu, L. Shen, J. Tang, G. Zhao, Y. Zhang, F. Cai, Q. Pan, Z. Long, G. Wang and H. Dai (2006). "Mutation analysis of the ATM gene in two Chinese patients with ataxia telangiectasia." J Neurol Sci **241**(1-2): 1-6.
- Johnson, J. M. and J. J. Latimer (2005). "Analysis of DNA repair using transfection-based host cell reactivation." Methods Mol Biol **291**: 321-35.

- Kadioglu, E., S. Sardas, S. Aslan, E. Isik and A. Esat Karakaya (2004). "Detection of oxidative DNA damage in lymphocytes of patients with Alzheimer's disease." *Biomarkers* **9**(2): 203-9.
- Kaneko, T., S. Tahara and M. Matsuo (1996). "Non-linear accumulation of 8-hydroxy-2'-deoxyguanosine, a marker of oxidized DNA damage, during aging." *Mutat Res* **316**(5-6): 277-85.
- Kang, J., H. G. Lemaire, A. Unterbeck, J. M. Salbaum, C. L. Masters, K. H. Grzeschik, G. Multhaup, K. Beyreuther and B. Muller-Hill (1987). "The precursor of Alzheimer's disease amyloid A4 protein resembles a cell-surface receptor." *Nature* **325**(6106): 733-6.
- Karen, K. A. and P. Hearing (2011). "Adenovirus core protein VII protects the viral genome from a DNA damage response at early times after infection." *J Virol* **85**(9): 4135-42.
- Karlseder, J., A. Smogorzewska and T. de Lange (2002). "Senescence induced by altered telomere state, not telomere loss." *Science* **295**(5564): 2446-9.
- Kasai, H. and S. Nishimura (1984). "Hydroxylation of deoxyguanosine at the C-8 position by ascorbic acid and other reducing agents." *Nucleic Acids Res* **12**(4): 2137-45.
- Kassam, S. N. and A. J. Rainbow (2007). "Deficient base excision repair of oxidative DNA damage induced by methylene blue plus visible light in xeroderma pigmentosum group C fibroblasts." *Biochem Biophys Res Commun* **359**(4): 1004-9.
- Kassam, S. N. and A. J. Rainbow (2009). "UV-inducible base excision repair of oxidative damaged DNA in human cells." *Mutagenesis* **24**(1): 75-83.
- Kastan, M. B. and J. Bartek (2004). "Cell-cycle checkpoints and cancer." *Nature* **432**(7015): 316-23.
- Kathe, S. D., G. P. Shen and S. S. Wallace (2004). "Single-stranded breaks in DNA but not oxidative DNA base damages block transcriptional elongation by RNA polymerase II in HeLa cell nuclear extracts." *J Biol Chem* **279**(18): 18511-20.
- Kelner, M. J., R. Bagnell, B. Hale and N. M. Alexander (1988). "Methylene blue competes with paraquat for reduction by flavo-enzymes resulting in decreased superoxide production in the presence of heme proteins." *Arch Biochem Biophys* **262**(2): 422-6.
- Kelner, M. J., R. Bagnell, B. Hale and N. M. Alexander (1988). "Potential of methylene blue to block oxygen radical generation in reperfusion injury." *Basic Life Sci* **49**: 895-8.
- Khobta, A., N. Kitsera, B. Speckmann and B. Epe (2009). "8-Oxoguanine DNA glycosylase (Ogg1) causes a transcriptional inactivation of damaged DNA in the absence of functional Cockayne syndrome B (Csb) protein." *DNA Repair (Amst)* **8**(3): 309-17.
- Kim, H., O. H. Lee, H. Xin, L. Y. Chen, J. Qin, H. K. Chae, S. Y. Lin, A. Safari, D. Liu and Z. Songyang (2009). "TRF2 functions as a protein hub and regulates telomere maintenance by recognizing specific peptide motifs." *Nat Struct Mol Biol* **16**(4): 372-9.
- Kirkwood, T. B. (2005). "Understanding the odd science of aging." *Cell* **120**(4): 437-47.
- Kirkwood, T. B. and S. N. Austad (2000). "Why do we age?" *Nature* **408**(6809): 233-8.
- Kitsera, N., D. Stathis, B. Luhnsdorf, H. Muller, T. Carell, B. Epe and A. Khobta "8-Oxo-7,8-dihydroguanine in DNA does not constitute a barrier to transcription, but is converted into transcription-blocking damage by OGG1." *Nucleic Acids Res.*
- Klass, M. R. (1977). "Aging in the nematode *Caenorhabditis elegans*: major biological and environmental factors influencing life span." *Mech Ageing Dev* **6**(6): 413-29.
- Klatzo, I., H. Wisniewski and E. Streicher (1965). "Experimental Production of Neurofibrillary Degeneration. I. Light Microscopic Observations." *J Neuropathol Exp Neurol* **24**: 187-99.

- Klaunig, J. E. and L. M. Kamendulis (2004). "The role of oxidative stress in carcinogenesis." Annu Rev Pharmacol Toxicol **44**: 239-67.
- Klungland, A. and S. Bjelland (2007). "Oxidative damage to purines in DNA: role of mammalian Ogg1." DNA Repair (Amst) **6**(4): 481-8.
- Komatsu, T., H. Haruki and K. Nagata (2011). "Cellular and viral chromatin proteins are positive factors in the regulation of adenovirus gene expression." Nucleic Acids Res **39**(3): 889-901.
- Kovacic, P. and J. D. Jacintho (2001). "Mechanisms of carcinogenesis: focus on oxidative stress and electron transfer." Curr Med Chem **8**(7): 773-96.
- Kovesdi, I., D. E. Brough, J. T. Bruder and T. J. Wickham (1997). "Adenoviral vectors for gene transfer." Curr Opin Biotechnol **8**(5): 583-9.
- Kraemer, K. H., M. M. Lee and J. Scotto (1987). "Xeroderma pigmentosum. Cutaneous, ocular, and neurologic abnormalities in 830 published cases." Arch Dermatol **123**(2): 241-50.
- Krahn, J. M., W. A. Beard, H. Miller, A. P. Grollman and S. H. Wilson (2003). "Structure of DNA polymerase beta with the mutagenic DNA lesion 8-oxodeoxyguanine reveals structural insights into its coding potential." Structure **11**(1): 121-7.
- Kuhlman, T. C., H. Cho, D. Reinberg and N. Hernandez (1999). "The general transcription factors IIA, IIB, IIF, and IIE are required for RNA polymerase II transcription from the human U1 small nuclear RNA promoter." Mol Cell Biol **19**(3): 2130-41.
- Kumar, V., A. Bal and K. D. Gill (2009). "Susceptibility of mitochondrial superoxide dismutase to aluminium induced oxidative damage." Toxicology **255**(3): 117-23.
- Kuraoka, I., M. Endou, Y. Yamaguchi, T. Wada, H. Handa and K. Tanaka (2003). "Effects of endogenous DNA base lesions on transcription elongation by mammalian RNA polymerase II. Implications for transcription-coupled DNA repair and transcriptional mutagenesis." J Biol Chem **278**(9): 7294-9.
- LaFerla, F. M., K. N. Green and S. Oddo (2007). "Intracellular amyloid-beta in Alzheimer's disease." Nat Rev Neurosci **8**(7): 499-509.
- Laine, J. P. and J. M. Egly (2006). "When transcription and repair meet: a complex system." Trends Genet **22**(8): 430-6.
- Lansdorp, P. M., N. P. Verwoerd, F. M. van de Rijke, V. Dragowska, M. T. Little, R. W. Dirks, A. K. Raap and H. J. Tanke (1996). "Heterogeneity in telomere length of human chromosomes." Hum Mol Genet **5**(5): 685-91.
- Larsen, E., K. Kwon, F. Coin, J. M. Egly and A. Klungland (2004). "Transcription activities at 8-oxoG lesions in DNA." DNA Repair (Amst) **3**(11): 1457-68.
- Laugel, V., C. Dalloz, A. Stary, V. Cormier-Daire, I. Desguerre, M. Renouil, A. Fourmaintraux, R. Velez-Cruz, J. M. Egly, A. Sarasin and H. Dollfus (2008). "Deletion of 5' sequences of the CSB gene provides insight into the pathophysiology of Cockayne syndrome." Eur J Hum Genet **16**(3): 320-7.
- Lavin, M. F. and Y. Shiloh (1997). "The genetic defect in ataxia-telangiectasia." Annu Rev Immunol **15**: 177-202.
- Le Page, F., A. Klungland, D. E. Barnes, A. Sarasin and S. Boiteux (2000). "Transcription coupled repair of 8-oxoguanine in murine cells: the ogg1 protein is required for repair in nontranscribed sequences but not in transcribed sequences." Proc Natl Acad Sci U S A **97**(15): 8397-402.

- Leach, D. M. and A. J. Rainbow (2011). "Early host cell reactivation of an oxidatively damaged adenovirus-encoded reporter gene requires the Cockayne syndrome proteins CSA and CSB." *Mutagenesis* **26**(2): 315-21.
- Lee, T. W., F. J. Lawrence, V. Dauksaite, G. Akusjarvi, G. E. Blair and D. A. Matthews (2004). "Precursor of human adenovirus core polypeptide Mu targets the nucleolus and modulates the expression of E2 proteins." *J Gen Virol* **85**(Pt 1): 185-96.
- Lehmann, A. R. (2003). "DNA repair-deficient diseases, xeroderma pigmentosum, Cockayne syndrome and trichothiodystrophy." *Biochimie* **85**(11): 1101-11.
- Lehmann, A. R., A. F. Thompson, S. A. Harcourt, M. Stefanini and P. G. Norris (1993). "Cockayne's syndrome: correlation of clinical features with cellular sensitivity of RNA synthesis to UV irradiation." *J Med Genet* **30**(8): 679-82.
- Levy, J. A., H. Fraenkel-Conrat and R. A. Owens (1994). Viruses with Medium and Large DNA genomes *Virology* Englewood Cliffs, New Jersey, Prentice Hall. **Third Edition** 185-191.
- Li, D. and R. Roberts (2001). "WD-repeat proteins: structure characteristics, biological function, and their involvement in human diseases." *Cell Mol Life Sci* **58**(14): 2085-97.
- Licht, C. L., T. Stevnsner and V. A. Bohr (2003). "Cockayne syndrome group B cellular and biochemical functions." *Am J Hum Genet* **73**(6): 1217-39.
- Lin, S. J., P. A. Defossez and L. Guarente (2000). "Requirement of NAD and SIR2 for life-span extension by calorie restriction in *Saccharomyces cerevisiae*." *Science* **289**(5487): 2126-8.
- Liu, J., E. Head, A. M. Gharib, W. Yuan, R. T. Ingersoll, T. M. Hagen, C. W. Cotman and B. N. Ames (2002). "Memory loss in old rats is associated with brain mitochondrial decay and RNA/DNA oxidation: partial reversal by feeding acetyl-L-carnitine and/or R-alpha - lipoic acid." *Proc Natl Acad Sci U S A* **99**(4): 2356-61.
- Lopes, J. P., C. R. Oliveira and P. Agostinho (2009). "Cell cycle re-entry in Alzheimer's disease: a major neuropathological characteristic?" *Curr Alzheimer Res* **6**(3): 205-12.
- Lopez de Silanes, I., M. Stagno d'Alcontres and M. A. Blasco (2010). "TERRA transcripts are bound by a complex array of RNA-binding proteins." *Nat Commun* **1**: 33.
- Lovell, M. A., S. P. Gabbita and W. R. Markesbery (1999). "Increased DNA oxidation and decreased levels of repair products in Alzheimer's disease ventricular CSF." *J Neurochem* **72**(2): 771-6.
- Lovell, M. A., C. Xie and W. R. Markesbery (2000). "Decreased base excision repair and increased helicase activity in Alzheimer's disease brain." *Brain Res* **855**(1): 116-23.
- Lu, J. and Y. Liu (2009). "Deletion of Ogg1 DNA glycosylase results in telomere base damage and length alteration in yeast." *Embo J* **29**(2): 398-409.
- Luke, B., A. Panza, S. Redon, N. Iglesias, Z. Li and J. Lingner (2008). "The Rat1p 5' to 3' exonuclease degrades telomeric repeat-containing RNA and promotes telomere elongation in *Saccharomyces cerevisiae*." *Mol Cell* **32**(4): 465-77.
- Lutzberger, M. and J. Kjems (2011). "S1 nuclease analysis of alternatively spliced mRNA." *Methods Mol Biol* **703**: 161-71.
- Lyras, L., N. J. Cairns, A. Jenner, P. Jenner and B. Halliwell (1997). "An assessment of oxidative damage to proteins, lipids, and DNA in brain from patients with Alzheimer's disease." *J Neurochem* **68**(5): 2061-9.
- Lytle, C. D., R. S. Day, 3rd, K. B. Hellman and L. E. Bockstahler (1976). "Infection of UV-irradiated xeroderma pigmentosum fibroblasts by herpes simplex virus: study of capacity and Weigle reactivation." *Mutat Res* **36**(3): 257-64.

- Makarov, V. L., Y. Hirose and J. P. Langmore (1997). "Long G tails at both ends of human chromosomes suggest a C strand degradation mechanism for telomere shortening." Cell **88**(5): 657-66.
- Mallery, D. L., B. Tanganelli, S. Colella, H. Steingrimsdottir, A. J. van Gool, C. Troelstra, M. Stefanini and A. R. Lehmann (1998). "Molecular analysis of mutations in the CSB (ERCC6) gene in patients with Cockayne syndrome." Am J Hum Genet **62**(1): 77-85.
- Mao, G., X. Pan, B. B. Zhu, Y. Zhang, F. Yuan, J. Huang, M. A. Lovell, M. P. Lee, W. R. Markesbery, G. M. Li and L. Gu (2007). "Identification and characterization of OGG1 mutations in patients with Alzheimer's disease." Nucleic Acids Res **35**(8): 2759-66.
- Mao, P. and P. H. Reddy (2011). "Aging and amyloid beta-induced oxidative DNA damage and mitochondrial dysfunction in Alzheimer's disease: implications for early intervention and therapeutics." Biochim Biophys Acta **1812**(11): 1359-70.
- Martadinata, H., B. Heddi, K. W. Lim and A. T. Phan "Structure of long human telomeric RNA (TERRA): G-quadruplexes formed by four and eight UUAGGG repeats are stable building blocks." Biochemistry **50**(29): 6455-61.
- Martin, G. M. (2005). "Genetic modulation of senescent phenotypes in Homo sapiens." Cell **120**(4): 523-32.
- Martin, G. M. and J. Oshima (2000). "Lessons from human progeroid syndromes." Nature **408**(6809): 263-6.
- Martinez, P., M. Thanasoula, P. Munoz, C. Liao, A. Tejera, C. McNees, J. M. Flores, O. Fernandez-Capetillo, M. Tarsounas and M. A. Blasco (2009). "Increased telomere fragility and fusions resulting from TRF1 deficiency lead to degenerative pathologies and increased cancer in mice." Genes Dev **23**(17): 2060-75.
- Masoro, E. J. (2005). "Overview of caloric restriction and ageing." Mech Ageing Dev **126**(9): 913-22.
- Matson, S. W., D. W. Bean and J. W. George (1994). "DNA helicases: enzymes with essential roles in all aspects of DNA metabolism." Bioessays **16**(1): 13-22.
- Matsuoka, S., B. A. Ballif, A. Smogorzewska, E. R. McDonald, 3rd, K. E. Hurov, J. Luo, C. E. Bakalarski, Z. Zhao, N. Solimini, Y. Lerenthal, Y. Shiloh, S. P. Gygi and S. J. Elledge (2007). "ATM and ATR substrate analysis reveals extensive protein networks responsive to DNA damage." Science **316**(5828): 1160-6.
- Mattson, M. P. (2004). "Pathways towards and away from Alzheimer's disease." Nature **430**(7000): 631-9.
- Maynard, S., S. H. Schurman, C. Harboe, N. C. de Souza-Pinto and V. A. Bohr (2009). "Base excision repair of oxidative DNA damage and association with cancer and aging." Carcinogenesis **30**(1): 2-10.
- Mayne, L. V. and A. R. Lehmann (1982). "Failure of RNA synthesis to recover after UV irradiation: an early defect in cells from individuals with Cockayne's syndrome and xeroderma pigmentosum." Cancer Res **42**(4): 1473-8.
- Mayr, G. A. and P. Freimuth (1997). "A single locus on human chromosome 21 directs the expression of a receptor for adenovirus type 2 in mouse A9 cells." J Virol **71**(1): 412-8.
- McCord, J. M. and I. Fridovich (1970). "The utility of superoxide dismutase in studying free radical reactions. II. The mechanism of the mediation of cytochrome c reduction by a variety of electron carriers." J Biol Chem **245**(6): 1374-7.
- McElligott, R. and R. J. Wellinger (1997). "The terminal DNA structure of mammalian chromosomes." Embo J **16**(12): 3705-14.

- McMurray, C. T. (2005). "To die or not to die: DNA repair in neurons." *Mutat Res* **577**(1-2): 260-74.
- Mecocci, P., U. MacGarvey and M. F. Beal (1994). "Oxidative damage to mitochondrial DNA is increased in Alzheimer's disease." *Ann Neurol* **36**(5): 747-51.
- Medina-Kauwe, L. K. (2003). "Endocytosis of adenovirus and adenovirus capsid proteins." *Adv Drug Deliv Rev* **55**(11): 1485-96.
- Medina, D. X., A. Caccamo and S. Oddo (2011). "Methylene blue reduces abeta levels and rescues early cognitive deficit by increasing proteasome activity." *Brain Pathol* **21**(2): 140-9.
- Meier, O. and U. F. Greber (2004). "Adenovirus endocytosis." *J Gene Med* **6 Suppl 1**: S152-63.
- Meira, L. B., J. M. Graham, Jr., C. R. Greenberg, D. B. Busch, A. T. Doughty, D. W. Ziffer, D. M. Coleman, I. Savre-Train and E. C. Friedberg (2000). "Manitoba aboriginal kindred with original cerebro-oculo- facio-skeletal syndrome has a mutation in the Cockayne syndrome group B (CSB) gene." *Am J Hum Genet* **66**(4): 1221-8.
- Mellon, I., G. Spivak and P. C. Hanawalt (1987). "Selective removal of transcription-blocking DNA damage from the transcribed strand of the mammalian DHFR gene." *Cell* **51**(2): 241-9.
- Migliore, L., I. Fontana, F. Trippi, R. Colognato, F. Coppede, G. Tognoni, B. Nucciarone and G. Siciliano (2005). "Oxidative DNA damage in peripheral leukocytes of mild cognitive impairment and AD patients." *Neurobiol Aging* **26**(5): 567-73.
- Miller, R. A. (2004). "'Accelerated aging': a primrose path to insight?" *Aging Cell* **3**(2): 47-51.
- Minowa, O., T. Arai, M. Hirano, Y. Monden, S. Nakai, M. Fukuda, M. Itoh, H. Takano, Y. Hippou, H. Aburatani, K. Masumura, T. Nohmi, S. Nishimura and T. Noda (2000). "Mmh/Ogg1 gene inactivation results in accumulation of 8-hydroxyguanine in mice." *Proc Natl Acad Sci U S A* **97**(8): 4156-61.
- Mitchell, T. R., K. Glenfield, K. Jeyanthan and X. D. Zhu (2009). "Arginine methylation regulates telomere length and stability." *Mol Cell Biol* **29**(18): 4918-34.
- Mori, T., T. L. Rinaldy, R. S. Athwal, G. P. Kaur, O. Nikaido, R. S. Lloyd and A. Rinaldy (1993). "A xeroderma pigmentosum complementation group A related gene: confirmation using monoclonal antibodies against the cyclobutane dimer and (6-4) photoproduct." *Mutat Res* **293**(2): 143-50.
- Moriya, M. (1993). "Single-stranded shuttle phagemid for mutagenesis studies in mammalian cells: 8-oxoguanine in DNA induces targeted G.C-->T.A transversions in simian kidney cells." *Proc Natl Acad Sci U S A* **90**(3): 1122-6.
- Morsy, M. A., E. L. Alford, A. Bett, F. L. Graham and C. T. Caskey (1993). "Efficient adenoviral-mediated ornithine transcarbamylase expression in deficient mouse and human hepatocytes." *J Clin Invest* **92**(3): 1580-6.
- Muftuoglu, M., S. Sharma, T. Thorslund, T. Stevnsner, M. M. Soerensen, R. M. Brosh, Jr. and V. A. Bohr (2006). "Cockayne syndrome group B protein has novel strand annealing and exchange activities." *Nucleic Acids Res* **34**(1): 295-304.
- Muftuoglu, M., H. K. Wong, S. Z. Imam, D. M. Wilson, 3rd, V. A. Bohr and P. L. Opresko (2006). "Telomere repeat binding factor 2 interacts with base excision repair proteins and stimulates DNA synthesis by DNA polymerase beta." *Cancer Res* **66**(1): 113-24.
- Munoz, P., R. Blanco, J. M. Flores and M. A. Blasco (2005). "XPF nuclease-dependent telomere loss and increased DNA damage in mice overexpressing TRF2 result in premature aging and cancer." *Nat Genet* **37**(10): 1063-71.

- Nance, M. A. and S. A. Berry (1992). "Cockayne syndrome: review of 140 cases." Am J Med Genet **42**(1): 68-84.
- Natale, V. (2011). "A comprehensive description of the severity groups in Cockayne syndrome." Am J Med Genet A **155A**(5): 1081-95.
- Neeley, W. L. and J. M. Essigmann (2006). "Mechanisms of formation, genotoxicity, and mutation of guanine oxidation products." Chem Res Toxicol **19**(4): 491-505.
- Newman, J. C., A. D. Bailey, H. Y. Fan, T. Pavelitz and A. M. Weiner (2008). "An abundant evolutionarily conserved CSB-PiggyBac fusion protein expressed in Cockayne syndrome." PLoS Genet **4**(3): e1000031.
- Newman, J. C., A. D. Bailey and A. M. Weiner (2006). "Cockayne syndrome group B protein (CSB) plays a general role in chromatin maintenance and remodeling." Proc Natl Acad Sci U S A **103**(25): 9613-8.
- Nguyen, T., P. J. Sherratt and C. B. Pickett (2003). "Regulatory mechanisms controlling gene expression mediated by the antioxidant response element." Annu Rev Pharmacol Toxicol **43**: 233-60.
- Niller, H. H. and L. Hennighausen (1991). "Formation of several specific nucleoprotein complexes on the human cytomegalovirus immediate early enhancer." Nucleic Acids Res **19**(13): 3715-21.
- Nouspikel, T. (2009). "DNA repair in mammalian cells : Nucleotide excision repair: variations on versatility." Cell Mol Life Sci **66**(6): 994-1009.
- Nouspikel, T. and P. C. Hanawalt (2003). "When parsimony backfires: neglecting DNA repair may doom neurons in Alzheimer's disease." Bioessays **25**(2): 168-73.
- Okumoto, D. S. and V. A. Bohr (1987). "DNA repair in the metallothionein gene increases with transcriptional activation." Nucleic Acids Res **15**(23): 10021-30.
- Opresko, P. L., J. Fan, S. Danzy, D. M. Wilson, 3rd and V. A. Bohr (2005). "Oxidative damage in telomeric DNA disrupts recognition by TRF1 and TRF2." Nucleic Acids Res **33**(4): 1230-9.
- Osborne, T. B., L. B. Mendel and E. L. Ferry (1917). "The Effect of Retardation of Growth Upon the Breeding Period and Duration of Life of Rats." Science **45**(1160): 294-5.
- Osterod, M., E. Larsen, F. Le Page, J. G. Hengstler, G. T. Van Der Horst, S. Boiteux, A. Klungland and B. Epe (2002). "A global DNA repair mechanism involving the Cockayne syndrome B (CSB) gene product can prevent the in vivo accumulation of endogenous oxidative DNA base damage." Oncogene **21**(54): 8232-9.
- Ottaviani, A., E. Gilson and F. Magdinier (2008). "Telomeric position effect: from the yeast paradigm to human pathologies?" Biochimie **90**(1): 93-107.
- Oz, M., D. E. Lorke, M. Hasan and G. A. Petroianu (2009). "Cellular and molecular actions of Methylene Blue in the nervous system." Med Res Rev **31**(1): 93-117.
- Palm, W. and T. de Lange (2008). "How shelterin protects mammalian telomeres." Annu Rev Genet **42**: 301-34.
- Palmer, D. J. and P. Ng (2005). "Helper-dependent adenoviral vectors for gene therapy." Hum Gene Ther **16**(1): 1-16.
- Park, E. M., M. K. Shigenaga, P. Degan, T. S. Korn, J. W. Kitzler, C. M. Wehr, P. Kolachana and B. N. Ames (1992). "Assay of excised oxidative DNA lesions: isolation of 8-oxoguanine and its nucleoside derivatives from biological fluids with a monoclonal antibody column." Proc Natl Acad Sci U S A **89**(8): 3375-9.

- Parker, W. D., Jr., C. M. Filley and J. K. Parks (1990). "Cytochrome oxidase deficiency in Alzheimer's disease." Neurology **40**(8): 1302-3.
- Pastoriza-Gallego, M., J. Armier and A. Sarasin (2007). "Transcription through 8-oxoguanine in DNA repair-proficient and Csb(-)/Ogg1(-) DNA repair-deficient mouse embryonic fibroblasts is dependent upon promoter strength and sequence context." Mutagenesis **22**(5): 343-51.
- Pesce, K. and M. J. Rothe (1996). "The premature aging syndromes." Clin Dermatol **14**(2): 161-70.
- Pitsikas, P., M. A. Francis and A. J. Rainbow (2005). "Enhanced host cell reactivation of a UV-damaged reporter gene in pre-UV-treated cells is delayed in Cockayne syndrome cells." J Photochem Photobiol B **81**(2): 89-97.
- Pitsikas, P., D. Lee and A. J. Rainbow (2007). "Reduced host cell reactivation of oxidative DNA damage in human cells deficient in the mismatch repair gene hMSH2." Mutagenesis **22**(3): 235-43.
- Porro, A., S. Feuerhahn, P. Reichenbach and J. Lingner (2010). "Molecular dissection of telomeric repeat-containing RNA biogenesis unveils the presence of distinct and multiple regulatory pathways." Mol Cell Biol **30**(20): 4808-17.
- Protic, M., E. Roilides, A. S. Levine and K. Dixon (1988). "Enhancement of DNA repair capacity of mammalian cells by carcinogen treatment." Somat Cell Mol Genet **14**(4): 351-7.
- Querfurth, H. W. and F. M. LaFerla "Alzheimer's disease." N Engl J Med **362**(4): 329-44.
- Rainbow, A. J. and S. Mak (1973). "DNA damage and biological function of human adenovirus after u.v.-irradiation." Int J Radiat Biol Relat Stud Phys Chem Med **24**(1): 59-72.
- Rainbow, A. J. and N. J. Zacal (2008). "Expression of an adenovirus encoded reporter gene and its reactivation following UVC and oxidative damage in cultured fish cells." Int J Radiat Biol **84**(6): 455-66.
- Rainbow, A. J., N. J. Zacal and D. M. Leach (2011). Reduced Repair of Oxidatively Damaged DNA in Ageing Human Fibroblasts (Poster). Canadian Cancer Research Conference. Toronto, Ontario, Canada.
- Rapin, I., Y. Lindenbaum, D. W. Dickson, K. H. Kraemer and J. H. Robbins (2000). "Cockayne syndrome and xeroderma pigmentosum." Neurology **55**(10): 1442-9.
- Reddy, P. H. and M. F. Beal (2008). "Amyloid beta, mitochondrial dysfunction and synaptic damage: implications for cognitive decline in aging and Alzheimer's disease." Trends Mol Med **14**(2): 45-53.
- Reddy, P. H., M. Manczak, P. Mao, M. J. Calkins, A. P. Reddy and U. Shirendeb "Amyloid-beta and mitochondria in aging and Alzheimer's disease: implications for synaptic damage and cognitive decline." J Alzheimers Dis **20 Suppl 2**: S499-512.
- Rhee, D. B., A. Ghosh, J. Lu, V. A. Bohr and Y. Liu (2011). "Factors that influence telomeric oxidative base damage and repair by DNA glycosylase OGG1." DNA Repair (Amst) **10**(1): 34-44.
- Riedel, W., U. Lang, U. Oetjen, U. Schlapp and M. Shibata (2003). "Inhibition of oxygen radical formation by methylene blue, aspirin, or alpha-lipoic acid, prevents bacterial-lipopolysaccharide-induced fever." Mol Cell Biochem **247**(1-2): 83-94.
- Rochette, P. J. and D. E. Brash (2010). "Human telomeres are hypersensitive to UV-induced DNA Damage and refractory to repair." PLoS Genet **6**(4): e1000926.

- Roelvink, P. W., A. Lizonova, J. G. Lee, Y. Li, J. M. Bergelson, R. W. Finberg, D. E. Brough, I. Kovesdi and T. J. Wickham (1998). "The coxsackievirus-adenovirus receptor protein can function as a cellular attachment protein for adenovirus serotypes from subgroups A, C, D, E, and F." *J Virol* **72**(10): 7909-15.
- Rolig, R. L. and P. J. McKinnon (2000). "Linking DNA damage and neurodegeneration." *Trends Neurosci* **23**(9): 417-24.
- Ropolo, M., P. Degan, M. Foresta, M. D'Errico, D. Lasiglie, E. Dogliotti, G. Casartelli, S. Zupo, A. Poggi and G. Frosina (2007). "Complementation of the oxidatively damaged DNA repair defect in Cockayne syndrome A and B cells by *Escherichia coli* formamidopyrimidine DNA glycosylase." *Free Radic Biol Med* **42**(12): 1807-17.
- Ross, P. J., M. A. Kennedy, C. Christou, M. Risco Quiroz, K. L. Poulin and R. J. Parks (2011). "Assembly of helper-dependent adenovirus DNA into chromatin promotes efficient gene expression." *J Virol* **85**(8): 3950-8.
- Ross, P. J., M. A. Kennedy and R. J. Parks (2009). "Host cell detection of noncoding stuffer DNA contained in helper-dependent adenovirus vectors leads to epigenetic repression of transgene expression." *J Virol* **83**(17): 8409-17.
- Rui, D. and Y. Yongjian (2010). "Aluminum chloride induced oxidative damage on cells derived from hippocampus and cortex of ICR mice." *Brain Res* **1324**: 96-102.
- Saban, S. D., M. Silvestry, G. R. Nemerow and P. L. Stewart (2006). "Visualization of alpha-helices in a 6-angstrom resolution cryoelectron microscopy structure of adenovirus allows refinement of capsid protein assignments." *J Virol* **80**(24): 12049-59.
- Salaris, S. C., C. F. Babbs and W. D. Voorhees, 3rd (1991). "Methylene blue as an inhibitor of superoxide generation by xanthine oxidase. A potential new drug for the attenuation of ischemia/reperfusion injury." *Biochem Pharmacol* **42**(3): 499-506.
- Salone, B., Y. Martina, S. Piersanti, E. Cundari, G. Cherubini, L. Franqueville, C. M. Failla, P. Boulanger and I. Saggio (2003). "Integrin alpha3beta1 is an alternative cellular receptor for adenovirus serotype 5." *J Virol* **77**(24): 13448-54.
- Sambucetti, L. C., J. M. Cherrington, G. W. Wilkinson and E. S. Mocarski (1989). "NF-kappa B activation of the cytomegalovirus enhancer is mediated by a viral transactivator and by T cell stimulation." *Embo J* **8**(13): 4251-8.
- San Martin, C. and R. M. Burnett (2003). "Structural studies on adenoviruses." *Curr Top Microbiol Immunol* **272**: 57-94.
- Savitsky, K., A. Bar-Shira, S. Gilad, G. Rotman, Y. Ziv, L. Vanagaite, D. A. Tagle, S. Smith, T. Uziel, S. Sfez, M. Ashkenazi, I. Pecker, M. Frydman, R. Harnik, S. R. Patanjali, A. Simmons, G. A. Clines, A. Sartiel, R. A. Gatti, L. Chessa, O. Sanal, M. F. Lavin, N. G. Jaspers, A. M. Taylor, C. F. Arlett, T. Miki, S. M. Weissman, M. Lovett, F. S. Collins and Y. Shiloh (1995). "A single ataxia telangiectasia gene with a product similar to PI-3 kinase." *Science* **268**(5218): 1749-53.
- Savitsky, K., S. Sfez, D. A. Tagle, Y. Ziv, A. Sartiel, F. S. Collins, Y. Shiloh and G. Rotman (1995). "The complete sequence of the coding region of the ATM gene reveals similarity to cell cycle regulators in different species." *Hum Mol Genet* **4**(11): 2025-32.
- Schaack, J., W. Y. Ho, P. Freimuth and T. Shenk (1990). "Adenovirus terminal protein mediates both nuclear matrix association and efficient transcription of adenovirus DNA." *Genes Dev* **4**(7): 1197-208.
- Schmickel, R. D., E. H. Chu, J. E. Trosko and C. C. Chang (1977). "Cockayne syndrome: a cellular sensitivity to ultraviolet light." *Pediatrics* **60**(2): 135-9.

- Schmidt, E. V., G. Christoph, R. Zeller and P. Leder (1990). "The cytomegalovirus enhancer: a pan-active control element in transgenic mice." *Mol Cell Biol* **10**(8): 4406-11.
- Schmitz, C., B. Axmacher, U. Zunker and H. Korr (1999). "Age-related changes of DNA repair and mitochondrial DNA synthesis in the mouse brain." *Acta Neuropathol* **97**(1): 71-81.
- Schoeftner, S. and M. A. Blasco (2008). "Developmentally regulated transcription of mammalian telomeres by DNA-dependent RNA polymerase II." *Nat Cell Biol* **10**(2): 228-36.
- Sedelnikova, O. A., I. Horikawa, D. B. Zimonjic, N. C. Popescu, W. M. Bonner and J. C. Barrett (2004). "Senescing human cells and ageing mice accumulate DNA lesions with unreparable double-strand breaks." *Nat Cell Biol* **6**(2): 168-70.
- Selby, C. P. and A. Sancar (1997). "Human transcription-repair coupling factor CSB/ERCC6 is a DNA-stimulated ATPase but is not a helicase and does not disrupt the ternary transcription complex of stalled RNA polymerase II." *J Biol Chem* **272**(3): 1885-90.
- Selkoe, D. J. (1994). "Normal and abnormal biology of the beta-amyloid precursor protein." *Annu Rev Neurosci* **17**: 489-517.
- Selkoe, D. J. (2001). "Alzheimer's disease: genes, proteins, and therapy." *Physiol Rev* **81**(2): 741-66.
- Selzer, R. R., S. Nyaga, J. Tuo, A. May, M. Muftuoglu, M. Christiansen, E. Citterio, R. M. Brosh, Jr. and V. A. Bohr (2002). "Differential requirement for the ATPase domain of the Cockayne syndrome group B gene in the processing of UV-induced DNA damage and 8-oxoguanine lesions in human cells." *Nucleic Acids Res* **30**(3): 782-93.
- Seviour, E. G. and S. Y. Lin (2010). "The DNA damage response: Balancing the scale between cancer and ageing." *Aging (Albany NY)* **2**(12): 900-7.
- Sfeir, A., S. T. Kosiyatrakul, D. Hockemeyer, S. L. MacRae, J. Karlseder, C. L. Schildkraut and T. de Lange (2009). "Mammalian telomeres resemble fragile sites and require TRF1 for efficient replication." *Cell* **138**(1): 90-103.
- Shao, C., S. Xiong, G. M. Li, L. Gu, G. Mao, W. R. Markesbery and M. A. Lovell (2008). "Altered 8-oxoguanine glycosylase in mild cognitive impairment and late-stage Alzheimer's disease brain." *Free Radic Biol Med* **45**(6): 813-9.
- Shenk, T. (1996). Adenoviridae: the viruses and their replication *Fields Virology* B. N. Fields, D. M. Knipe and P. M. Howley. Philadelphia, PA, Lippincott-Raven: 2111-2148.
- Shibutani, S., M. Takeshita and A. P. Grollman (1991). "Insertion of specific bases during DNA synthesis past the oxidation-damaged base 8-oxodG." *Nature* **349**(6308): 431-4.
- Shigenaga, M. K., C. J. Gimeno and B. N. Ames (1989). "Urinary 8-hydroxy-2'-deoxyguanosine as a biological marker of in vivo oxidative DNA damage." *Proc Natl Acad Sci U S A* **86**(24): 9697-701.
- Shiloh, Y. (1995). "Ataxia-telangiectasia: closer to unraveling the mystery." *Eur J Hum Genet* **3**(2): 116-38.
- Shimada, H., Y. H. Shiao, M. Shibata and M. P. Waalkes (1998). "Cadmium suppresses apoptosis induced by chromium." *J Toxicol Environ Health A* **54**(2): 159-68.
- Sidwell, R. U., A. Sandison, J. Wing, H. D. Fawcett, J. E. Seet, C. Fisher, T. Nardo, M. Stefanini, A. R. Lehmann and J. J. Cream (2006). "A novel mutation in the XPA gene associated with unusually mild clinical features in a patient who developed a spindle cell melanoma." *Br J Dermatol* **155**(1): 81-8.
- Slamenova, D., K. Kuboskova, E. Horvathova and S. Robichova (2002). "Rosemary-stimulated reduction of DNA strand breaks and FPG-sensitive sites in mammalian cells treated with H<sub>2</sub>O<sub>2</sub> or visible light-excited Methylene Blue." *Cancer Lett* **177**(2): 145-53.

- Slupphaug, G., B. Kavli and H. E. Krokan (2003). "The interacting pathways for prevention and repair of oxidative DNA damage." Mutat Res **531**(1-2): 231-51.
- Smith, M. L., I. T. Chen, Q. Zhan, P. M. O'Connor and A. J. Fornace, Jr. (1995). "Involvement of the p53 tumor suppressor in repair of u.v.-type DNA damage." Oncogene **10**(6): 1053-9.
- Smith, M. L., J. M. Ford, M. C. Hollander, R. A. Bortnick, S. A. Amundson, Y. R. Seo, C. X. Deng, P. C. Hanawalt and A. J. Fornace, Jr. (2000). "p53-mediated DNA repair responses to UV radiation: studies of mouse cells lacking p53, p21, and/or gadd45 genes." Mol Cell Biol **20**(10): 3705-14.
- Spivak, G. and P. C. Hanawalt (2006). "Host cell reactivation of plasmids containing oxidative DNA lesions is defective in Cockayne syndrome but normal in UV-sensitive syndrome fibroblasts." DNA Repair (Amst) **5**(1): 13-22.
- Spivak, G., G. P. Pfeifer and P. Hanawalt (2006). "In vivo assays for transcription-coupled repair." Methods Enzymol **408**: 223-46.
- Stamminger, T., H. Fickenscher and B. Fleckenstein (1990). "Cell type-specific induction of the major immediate early enhancer of human cytomegalovirus by cyclic AMP." J Gen Virol **71 ( Pt 1)**: 105-13.
- Stefanini, M., H. Fawcett, E. Botta, T. Nardo and A. R. Lehmann (1996). "Genetic analysis of twenty-two patients with Cockayne syndrome." Hum Genet **97**(4): 418-23.
- Stevnsner, T., S. Nyaga, N. C. de Souza-Pinto, G. T. van der Horst, T. G. Gorgels, B. A. Hogue, T. Thorslund and V. A. Bohr (2002). "Mitochondrial repair of 8-oxoguanine is deficient in Cockayne syndrome group B." Oncogene **21**(57): 8675-82.
- Stivers, J. T. and Y. L. Jiang (2003). "A mechanistic perspective on the chemistry of DNA repair glycosylases." Chem Rev **103**(7): 2729-59.
- Stohs, S. J., D. Bagchi, E. Hassoun and M. Bagchi (2001). "Oxidative mechanisms in the toxicity of chromium and cadmium ions." J Environ Pathol Toxicol Oncol **20**(2): 77-88.
- Sun, X., P. Majumder, H. Shioya, F. Wu, S. Kumar, R. Weichselbaum, S. Kharbanda and D. Kufe (2000). "Activation of the cytoplasmic c-Abl tyrosine kinase by reactive oxygen species." J Biol Chem **275**(23): 17237-40.
- Sun, X., F. Wu, R. Datta, S. Kharbanda and D. Kufe (2000). "Interaction between protein kinase C delta and the c-Abl tyrosine kinase in the cellular response to oxidative stress." J Biol Chem **275**(11): 7470-3.
- Suram, A., M. L. Hegde and K. S. Rao (2007). "A new evidence for DNA nicking property of amyloid beta-peptide (1-42): relevance to Alzheimer's disease." Arch Biochem Biophys **463**(2): 245-52.
- Swerdlow, R. H. and S. M. Khan (2009). "The Alzheimer's disease mitochondrial cascade hypothesis: an update." Exp Neurol **218**(2): 308-15.
- Szilard, L. (1959). "On the Nature of the Aging Process." Proc Natl Acad Sci U S A **45**(1): 30-45.
- Taddei, F., M. Vulic, M. Radman and I. Matic (1997). "Genetic variability and adaptation to stress." Exs **83**: 271-90.
- Takai, H., A. Smogorzewska and T. de Lange (2003). "DNA damage foci at dysfunctional telomeres." Curr Biol **13**(17): 1549-56.
- Takao, M., S. Kanno, T. Shiromoto, R. Hasegawa, H. Ide, S. Ikeda, A. H. Sarker, S. Seki, J. Z. Xing, X. C. Le, M. Weinfeld, K. Kobayashi, J. Miyazaki, M. Muijtjens, J. H. Hoeijmakers, G. van der Horst and A. Yasui (2002). "Novel nuclear and mitochondrial

- glycosylases revealed by disruption of the mouse *Nth1* gene encoding an endonuclease III homolog for repair of thymine glycols." *Embo J* **21**(13): 3486-93.
- Tan, T. and G. Chu (2002). "p53 Binds and activates the xeroderma pigmentosum DDB2 gene in humans but not mice." *Mol Cell Biol* **22**(10): 3247-54.
- Tatar, M. (2007). "Diet restriction in *Drosophila melanogaster*. Design and analysis." *Interdiscip Top Gerontol* **35**: 115-36.
- Taylor, A. M., P. J. Byrd, C. M. McConville and S. Thacker (1994). "Genetic and cellular features of ataxia telangiectasia." *Int J Radiat Biol* **65**(1): 65-70.
- Theriot, C. A., M. L. Hegde, T. K. Hazra and S. Mitra (2010). "RPA physically interacts with the human DNA glycosylase NEIL1 to regulate excision of oxidative DNA base damage in primer-template structures." *DNA Repair (Amst)* **9**(6): 643-52.
- Thies, W. and L. Bleiler (2011). "2011 Alzheimer's disease facts and figures." *Alzheimers Dement* **7**(2): 208-44.
- Tomkinson, A. E., L. Chen, Z. Dong, J. B. Leppard, D. S. Levin, Z. B. Mackey and T. A. Motycka (2001). "Completion of base excision repair by mammalian DNA ligases." *Prog Nucleic Acid Res Mol Biol* **68**: 151-64.
- Tomko, R. P., R. Xu and L. Philipson (1997). "HCAR and MCAR: the human and mouse cellular receptors for subgroup C adenoviruses and group B coxsackieviruses." *Proc Natl Acad Sci U S A* **94**(7): 3352-6.
- Tornaletti, S., L. S. Maeda, R. D. Kolodner and P. C. Hanawalt (2004). "Effect of 8-oxoguanine on transcription elongation by T7 RNA polymerase and mammalian RNA polymerase II." *DNA Repair (Amst)* **3**(5): 483-94.
- Tornaletti, S., L. S. Maeda, D. R. Lloyd, D. Reines and P. C. Hanawalt (2001). "Effect of thymine glycol on transcription elongation by T7 RNA polymerase and mammalian RNA polymerase II." *J Biol Chem* **276**(48): 45367-71.
- Trippi, F., N. Botto, R. Scarpato, L. Petrozzi, U. Bonuccelli, S. Latorraca, S. Sorbi and L. Migliore (2001). "Spontaneous and induced chromosome damage in somatic cells of sporadic and familial Alzheimer's disease patients." *Mutagenesis* **16**(4): 323-7.
- Troelstra, C., A. van Gool, J. de Wit, W. Vermeulen, D. Bootsma and J. H. Hoeijmakers (1992). "ERCC6, a member of a subfamily of putative helicases, is involved in Cockayne's syndrome and preferential repair of active genes." *Cell* **71**(6): 939-53.
- Trotman, L. C., N. Mosberger, M. Fornerod, R. P. Stidwill and U. F. Greber (2001). "Import of adenovirus DNA involves the nuclear pore complex receptor CAN/Nup214 and histone H1." *Nat Cell Biol* **3**(12): 1092-100.
- Tuite, E. M. and J. M. Kelly (1993). "Photochemical interactions of methylene blue and analogues with DNA and other biological substrates." *J Photochem Photobiol B* **21**(2-3): 103-24.
- Tuo, J., C. Chen, X. Zeng, M. Christiansen and V. A. Bohr (2002a). "Functional crosstalk between hOgg1 and the helicase domain of Cockayne syndrome group B protein." *DNA Repair (Amst)* **1**(11): 913-27.
- Tuo, J., P. Jaruga, H. Rodriguez, V. A. Bohr and M. Dizdaroglu (2003). "Primary fibroblasts of Cockayne syndrome patients are defective in cellular repair of 8-hydroxyguanine and 8-hydroxyadenine resulting from oxidative stress." *Faseb J* **17**(6): 668-74.
- Tuo, J., P. Jaruga, H. Rodriguez, M. Dizdaroglu and V. A. Bohr (2002b). "The cockayne syndrome group B gene product is involved in cellular repair of 8-hydroxyadenine in DNA." *J Biol Chem* **277**(34): 30832-7.

- Tuo, J., M. Muftuoglu, C. Chen, P. Jaruga, R. R. Selzer, R. M. Brosh, Jr., H. Rodriguez, M. Dizdaroglu and V. A. Bohr (2001). "The Cockayne Syndrome group B gene product is involved in general genome base excision repair of 8-hydroxyguanine in DNA." J Biol Chem **276**(49): 45772-9.
- Valerie, K. and A. Singhal (1995). "Host-cell reactivation of reporter genes introduced into cells by adenovirus as a convenient way to measure cellular DNA repair." Mutat Res **336**(1): 91-100.
- van Hoffen, A., A. S. Balajee, A. A. van Zeeland and L. H. Mullenders (2003). "Nucleotide excision repair and its interplay with transcription." Toxicology **193**(1-2): 79-90.
- van Steensel, B., A. Smogorzewska and T. de Lange (1998). "TRF2 protects human telomeres from end-to-end fusions." Cell **92**(3): 401-13.
- Varadarajan, S., S. Yatin, M. Aksenova and D. A. Butterfield (2000). "Review: Alzheimer's amyloid beta-peptide-associated free radical oxidative stress and neurotoxicity." J Struct Biol **130**(2-3): 184-208.
- Vellinga, J., S. Van der Heijdt and R. C. Hoeben (2005). "The adenovirus capsid: major progress in minor proteins." J Gen Virol **86**(Pt 6): 1581-8.
- Venema, J., L. H. Mullenders, A. T. Natarajan, A. A. van Zeeland and L. V. Mayne (1990). "The genetic defect in Cockayne syndrome is associated with a defect in repair of UV-induced DNA damage in transcriptionally active DNA." Proc Natl Acad Sci U S A **87**(12): 4707-11.
- von Figura, G., D. Hartmann, Z. Song and K. L. Rudolph (2009). "Role of telomere dysfunction in aging and its detection by biomarkers." J Mol Med (Berl) **87**(12): 1165-71.
- Vural, H., H. Demirin, Y. Kara, I. Eren and N. Delibas (2010). "Alterations of plasma magnesium, copper, zinc, iron and selenium concentrations and some related erythrocyte antioxidant enzyme activities in patients with Alzheimer's disease." J Trace Elem Med Biol **24**(3): 169-73.
- Wainwright, M. (2003). "The use of dyes in modern biomedicine." Biotech Histochem **78**(3-4): 147-55.
- Wang, J., W. R. Markesbery and M. A. Lovell (2006). "Increased oxidative damage in nuclear and mitochondrial DNA in mild cognitive impairment." J Neurochem **96**(3): 825-32.
- Wang, J., S. Xiong, C. Xie, W. R. Markesbery and M. A. Lovell (2005). "Increased oxidative damage in nuclear and mitochondrial DNA in Alzheimer's disease." J Neurochem **93**(4): 953-62.
- Wang, Y. and T. Schlick (2007). "Distinct energetics and closing pathways for DNA polymerase beta with 8-oxoG template and different incoming nucleotides." BMC Struct Biol **7**: 7.
- Wang, Z., D. B. Rhee, J. Lu, C. T. Bohr, F. Zhou, H. Vallabhaneni, N. C. de Souza-Pinto and Y. Liu (2010). "Characterization of oxidative guanine damage and repair in mammalian telomeres." PLoS Genet **6**(5): e1000951.
- Weindruch, R. H. and R. L. Walford (1988). The retardation of aging and disease by dietary restriction Springfield, Illinois, C.C. Thomas
- Weissman, L., D. G. Jo, M. M. Sorensen, N. C. de Souza-Pinto, W. R. Markesbery, M. P. Mattson and V. A. Bohr (2007). "Defective DNA base excision repair in brain from individuals with Alzheimer's disease and amnesic mild cognitive impairment." Nucleic Acids Res **35**(16): 5545-55.
- Wilson, D. M., 3rd and D. Barsky (2001). "The major human abasic endonuclease: formation, consequences and repair of abasic lesions in DNA." Mutat Res **485**(4): 283-307.

- Wilson, D. M., 3rd and V. A. Bohr (2007). "The mechanics of base excision repair, and its relationship to aging and disease." DNA Repair (Amst) **6**(4): 544-59.
- Wilson, D. M., 3rd, V. A. Bohr and P. J. McKinnon (2008). "DNA damage, DNA repair, ageing and age-related disease." Mech Ageing Dev **129**(7-8): 349-52.
- Wodrich, H., A. Cassany, M. A. D'Angelo, T. Guan, G. Nemerow and L. Gerace (2006). "Adenovirus core protein pVII is translocated into the nucleus by multiple import receptor pathways." J Virol **80**(19): 9608-18.
- Wu, Y., T. R. Mitchell and X. D. Zhu (2008). "Human XPF controls TRF2 and telomere length maintenance through distinctive mechanisms." Mech Ageing Dev **129**(10): 602-10.
- Wu, Y., N. J. Zagal, A. J. Rainbow and X. D. Zhu (2007). "XPF with mutations in its conserved nuclease domain is defective in DNA repair but functions in TRF2-mediated telomere shortening." DNA Repair (Amst) **6**(2): 157-66.
- Yagi, T., Y. Matsumura, M. Sato, C. Nishigori, T. Mori, A. M. Sijbers and H. Takebe (1998). "Complete restoration of normal DNA repair characteristics in group F xeroderma pigmentosum cells by over-expression of transfected XPF cDNA." Carcinogenesis **19**(1): 55-60.
- Yeh, P. and M. Perricaudet (1997). "Advances in adenoviral vectors: from genetic engineering to their biology." Faseb J **11**(8): 615-23.
- Yu, A., H. Y. Fan, D. Liao, A. D. Bailey and A. M. Weiner (2000). "Activation of p53 or loss of the Cockayne syndrome group B repair protein causes metaphase fragility of human U1, U2, and 5S genes." Mol Cell **5**(5): 801-10.
- Zagal, N. J., M. A. Francis and A. J. Rainbow (2005). "Enhanced expression from the human cytomegalovirus immediate-early promoter in a non-replicating adenovirus encoded reporter gene following cellular exposure to chemical DNA damaging agents." Biochem Biophys Res Commun **332**(2): 441-9.
- Zhang, Y. and J. M. Bergelson (2005). "Adenovirus receptors." J Virol **79**(19): 12125-31.
- Zhao, L. J. and R. Padmanabhan (1988). "Nuclear transport of adenovirus DNA polymerase is facilitated by interaction with preterminal protein." Cell **55**(6): 1005-15.
- Zhu, X. D., B. Kuster, M. Mann, J. H. Petrini and T. de Lange (2000). "Cell-cycle-regulated association of RAD50/MRE11/NBS1 with TRF2 and human telomeres." Nat Genet **25**(3): 347-52.
- Zhu, X. D., B. Kuster, M. Mann, J. H. Petrini and T. Lange (2000). "Cell-cycle-regulated association of RAD50/MRE11/NBS1 with TRF2 and human telomeres." Nat Genet **25**(3): 347-52.
- Zhu, X. D., L. Niedernhofer, B. Kuster, M. Mann, J. H. Hoeijmakers and T. de Lange (2003). "ERCC1/XPF removes the 3' overhang from uncapped telomeres and represses formation of telomeric DNA-containing double minute chromosomes." Mol Cell **12**(6): 1489-98.
- Zielinska, A., O. T. Davies, R. A. Meldrum and N. J. Hodges (2010). "Direct visualization of repair of oxidative damage by OGG1 in the nuclei of live cells." J Biochem Mol Toxicol **25**(1): 1-7.